THE SYNTHESIS AND CHARACTERISATION OF CHIRAL THIOPHENE-BASED LIQUID CRYSTALS

CHRISSIE GROVER

A thesis submitted in partial fulfilment of the
requirements of The Nottingham Trent University
for the degree of Doctor of Philosophy

January 2000

THE SYNTHESIS AND CHARACTERISATION OF CHIRAL THIOPHENE-BASED LIQUID CRYSTALS

Summary of a thesis submitted for the degree of
Doctor of Philosophy

Chrissie Grover

Abstract

To meet a global demand for compounds which exhibit ferro-, ferri- and antiferro-electricity and to gain an insight into structure-property relationships of non-linear liquid crystals, the synthesis and mesomorphic properties of a variety of novel thiophene-based chiral esters **[Series I-XIV]** is reported.

[Series I]	(*S*)-4-(1-methylheptyloxycarbonyl)phenyl 5-(4-n-alkoxyphenyl)thiophene-2-carboxylates.
[Series II]	(*S*)-4'-(1-methylheptyloxycarbonyl)biphenyl-4-yl 5-(4-n-alkoxyphenyl)thiophene-2-carboxylates.
[Series III]	(*S*)-4-(1-methylheptyloxycarbonyl)phenyl 5'-n-alkyl-2',2-bithienyl-5-carboxylates.
[Series IV]	(*S*)-4'-(1-methylheptyloxycarbonyl)biphenyl-4-yl 5'-n-alkyl-2',2-bithienyl-5-carboxylates.
[Series V]	(*S*)-4-(1-methylheptyloxycarbonyl)phenyl 4-(4-n-alkoxyphenyl)thiophene-2-carboxylates.
[Series VI]	(*S*)-4'-(1-methylheptyloxycarbonyl)biphenyl-4-yl 4-(4-n-alkoxyphenyl)thiophene-2-carboxylates.
[Series VII]	(*S*)-4-(1-methylheptyloxycarbonyl)phenyl 5'-n-alkyl-2',4-bithienyl-2-carboxylates.
[Series VIII]	(*S*)-4'-(1-methylheptyloxycarbonyl)biphenyl-4-yl 5'-n-alkyl-2',4-bithienyl-2-carboxylates.
[Series IX]	(*S*)-4-(1-methylheptyloxycarbonyl)phenyl 5"-n-alkyl-2",2':5',2-terthienyl-5-carboxylates.
[Series X]	(*S*)-4'-(1-methylheptyloxycarbonyl)biphenyl-4-yl 5"-n-alkyl-2",2':5',2-terthienyl-5-carboxylates.
[Series XI]	(*S*)-4-(1-methylheptyloxycarbonyl)phenyl 5'-(4-n-decyloxyphenyl)-2',2-bithienyl-5-carboxylate.
[Series XII]	(*S*)-4-(1-methylheptyloxycarbonyl)phenyl 5-(4'-n-decyloxybiphenyl-4-yl)thiophene-2-carboxylate.
[Series XIII]	(*S*)-4-(1-methylheptyloxycarbonyl)phenyl 5-(4'-n-decyloxy-3'-fluorobiphenyl-4-yl)thiophene-2-carboxylate.
[Series XIV]	(*S*)-4-(1-methylheptyloxycarbonyl)phenyl 4-(4'-n-decyloxybiphenyl-4-yl)thiophene-2-carboxylate.

Thiophene-based esters **[Series I-XIV]** were prepared from an appropriate thiophene-containing carboxylic acid and either (*S*)-1-methylheptyl 4-hydroxybenzoate or (*S*)-1-methylheptyl 4'-hydroxybiphenyl-4-carboxylate, as source of 'chiral phenol'. The latter were employed to ensure a strong possibility for the occurrence of the S_C*ferro-, ferri- and antiferro-electric phase types and, to this effect, certain members of **Series I-IV, VI** and **IX-XV** exhibit the aforementioned phase types. Results for the n=12 homologue of **Series IV** have been published (*Mol. Cryst. Liq. Cryst.*, 1999, **332**, 303) whereas results for the n=10 homologue of **Series II** have been accepted for publication (*J. Mater. Chem.*, 2000).

An in depth structure-property relationship which impinges on the aspects of molecular length and molecular geometry is discussed. Increasing the overall molecular length by increasing the number of aromatic rings, enhances mesophase thermal stability and mesophase type, *e.g.*: **Series I** (three-ring), S_A, S_C*ferro-, ferri- and antiferro-electric; **Series II** (four-ring), S_A, S_C*ferro-, ferri-, antiferro-electric and S_I*. Four-ring compounds containing three-rings in the molecular core are thermally more stable than their isomeric counterparts containing two rings in the core and two rings in the terminal chiral moiety. (*S*)-4-(1-Methylheptyloxycarbonyl)phenyl 4"-n-decyloxy-1",1':4',1-terphenyl-4-carboxylate **[Series XV]** was prepared to serve as a model compound for comparison with **Series IX, XI** and **XII**.

Either one-, two- or three-thiophene rings can be readily accommodated by the central molecular core but their disposition dictates liquid crystallinity. Unlike 2,5-disubstituted thiophene, 2,4-disubstitued thiophene is extremely poor at promoting liquid crystallinity, *e.g.*, members of **Series VII** are non-mesomorphic whereas **Series III** are mesomorphic.

A short study of the influence of lateral fluorination is also reported. As expected, the inclusion of a lateral fluoro-substituent lowers the mesophase thermal stability and eliminates high order smectic phase types when compared with its non-fluorinated counterpart.

For Mum and Dad

ACKNOWLEDGEMENTS

I would like to express my thanks to Dr. R.C. Wilson and especially Dr. A.S. Matharu for their advice, supervision and friendship, not only throughout my PhD but also through my undergraduate years. For without them, this thesis would not have been made possible.

I would also like to thank Mark Sladen and Dave Chambers-Asman for all their help and also for their friendship. I would like to thank Mick Wood for n.m.r. assistance, Jim Walters for MS and HPLC services and Dr. P. Huddleston for interesting discussions. Thanks are also duly noted to the EPSRC for the award of the studentship.

Finally, I would like to thank Stewart who has supported me every step of the way.

HOW TO USE THIS THESIS

This thesis is designed to cater for both undergraduates and experienced researchers in the area of liquid crystal chemistry. To this effect, it is divided into three main sections:

1. INTRODUCTION AND AIMS

This section provides a valuable insight into the area of thermotropic liquid crystals, especially for those new to the subject. It covers the history and development of liquid crystals and draws the attention of the reader to the latest books and review articles. The aims reflect on the introductory text and show a strong necessity for the proposed research plan.

2. EXPERIMENTAL

This section is written according to the format as specified by Journal of the Chemical Society. All major experimental procedures are written fully so that they may be repeated readily. A synthetic overview is provided for each reaction scheme followed by complete experimental details. All compounds, except those which are commercially available, are numbered sequentially.

3. DISCUSSION

This section is intended primarily for the experienced researcher, however, it includes sufficient detail, *e.g.*, transition temperature plots, miscibility plots and reference to photographic evidence, so that it may be understood by those new to liquid crystals. Mesomorphic data for each series is discussed and an in depth structure-property relationship is undertaken.

REAGENTS, SOLVENTS AND EQUIPMENT

Diethyl ether was dried over sodium wire. Acetone, chloroform and dichloromethane were dried over granular anhydrous calcium chloride. Ethanol and toluene were dried over molecular sieves. Tetrahydrofuran was dried by continuously heating the solvent under reflux with sodium metal and benzophenone until a dark blue coloration was achieved. *N*,*N*-Dimethylformamide was distilled from calcium hydride and stored over molecular sieves. Titanium(IV) chloride, 1,2-dimethoxyethane and 1.6M and 2.5M *n*-butyllithium (solution in hexane) were used as supplied. Commercial starting materials were obtained from the Aldrich Chemical Company Limited.

Structural confirmation of intermediates and products was obtained by infra-red spectroscopy (Perkin-Elmer FT 1605 spectrophotometer) and ^{1}H nuclear magnetic resonance spectroscopy (JEOL FX60Q 270 MHz spectrometer). Transition temperature measurements were made using an Olympus BH-2 polarising microscope in conjunction with a Mettler FP52 hot stage and FP5 control unit and were confirmed by thermal analysis on a Perkin-Elmer DSC7 differential scanning calorimeter at heating and cooling rates of 5 and 10°C min^{-1}. Instrumental accuracy was checked using an indium standard. The measured latent heat for indium of 28.37 J g^{-1} compared well with the standard value for indium of 28.45 J g^{-1}. Images of textures from sandwich cells were captured using a Mitsubishi CP50 B (H) colour video printer whereas free-standing film textures were recorded using a Sony Hyper HAF SSC-DC38P digital video camera interfaced to a computer. Mass spectra were obtained on a Perkin-Elmer 8500 GC-MS comprising a 30 m BP1 column connected to a Perkin-Elmer ion trap detector. HPLC was undertaken using reverse phase on a Perkin-Elmer Series 200 instrument connected to a Jasco 875 uv/vis detector fitted with a ODS 2 column (150 x 4 mm) eluting with 80% aqueous tetrahydrofuran. Elemental analyses were performed by the microanalysis department at The University of Canterbury, Kent, England.

The progress of reactions were monitored by thin layer chromatography (TLC) using silica gel coated on glass plates (silica gel 60, 250 μm layer thickness) and column chromatography was performed using silica gel (silica gel 60, 220-240 mesh size).

ABBREVIATIONS

n-BuLi	n-Butyllithium solution in hexane.
DCC	1,3-*N,N'*-Dicyclohexylcarbodiimide.
DCM	Dichloromethane.
DME	1,2-Dimethoxyethane.
DMF	*N,N*-Dimethylformamide.
DMAP	4-*N*-Dimethylaminopyridine.
THF	Tetrahydrofuran.
s	Singlet.
d	Doublet.
quint.	Quintet.
m	Multiplet.
m.p.	Melting point.
b.p.	Boiling point.
cl.p.	Clearing point.
lit.	Literature melting or boiling point.
K	Crystal.
S_A	Smectic A.
S_C*	Chiral smectic C.
N	Nematic.
I	Isotropic liquid.
□	Crystal to mesophase or crystal to isotropic liquid transition temperature.
●	Mesophase to mesophase or mesophase to isotropic transition temperature.
■	Mesophase to crystal transition temperature.

CONTENTS

APPENDICES

Appendix 1: Synthesis of (*S*)-1-methylheptyl 4-hydroxybenzoate (**25**) and (*S*)-1-methylheptyl 4'-hydroxybiphenyl-4-carboxylate (**26**)

Appendix 2: Copy of abstract of paper accepted for publication to Journal of Materials Chemistry

Appendix 3: Copy of abstract of manuscript published in Molecular Crystals and Liquid Crystals

INTRODUCTION

1. INTRODUCTION AND AIMS

The liquid crystalline phase or mesophase is an intermediate state of matter that exists between the crystalline solid and the isotropic liquid. Most crystalline solids on heating convert sharply to the isotropic liquid at their melting point and on cooling from the isotropic liquid return to the crystalline solid. However, certain substances on heating neither readily convert to the isotropic liquid nor on cooling do they revert back to the crystalline solid but exist in an intermediate state of matter which possesses characteristics of both the crystalline solid and the isotropic liquid. Compounds which exhibit this phenomenon are termed ***liquid crystals****,* ***mesogenic*** *or* ***mesomorphic*** *and the intermediate state of matter is termed either the* ***liquid crystalline phase*** *or* ***mesophase****.*

1.1 HISTORICAL REVIEW

The first reported observation of a liquid crystalline compound was made by Reinitzer[1] in 1888, who noted the unusual melting behaviour of a sample of cholesteryl benzoate (**1**). At 145.5°C, cholesteryl benzoate melted into an opaque, turbid liquid which then cleared to the isotropic liquid at the higher temperature of 178.5°C. However, at the time Reinitzer was unable to explain this unusual 'double melting' behaviour.

In 1890, Lehmann[2] viewed a sample of cholesteryl benzoate through a specially constructed light polarising microscope and, between the temperatures of 145.5°C and

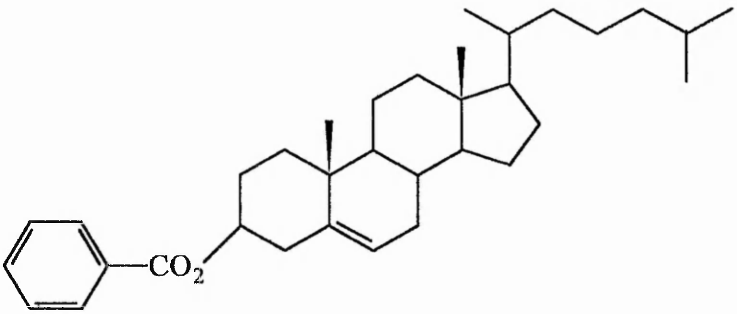

Cholesteryl benzoate (**1**)

178.5°C, he observed an iridescent colour effect, *i.e.*, a birefringent texture. Soon after this initial discovery, Lehmann also found similar effects in samples of ammonium oleate and *p*-azoxyanisole and he introduced the terms fliessende krystalle (fluid crystal) and flüssige krystalle (liquid crystal) to describe such compounds. However, Tammann[3] and Nernst[4] were sceptical of Lehmann's ideas and argued that either impurities or colloidal effects may be responsible for this unusual melting behaviour.

Soon after in 1900, Vorländer[5] attempted to establish a relationship between molecular structure and the occurrence of the liquid crystalline state by systematically synthesising numerous compounds. By 1908, he was able to conclude that compounds which exhibit liquid crystalline behaviour usually possess a predominantly linear molecular shape.

In 1922, Friedel[6] introduced the term ***mesophase*** (derived from the Greek words ***meso*** and ***phasis*** meaning intermediate and phase, respectively) to describe the intermediate state of matter. Furthermore, he was able to identify three different types of mesophase: smectic; nematic and; cholesteric. A description of these phases is given later in section 1.4.2, p. 14. It is important to note that Friedel did not realise the existence of different smectic phase types (smectic polymorphism) which were discovered earlier by Vorländer and Wilke[7] in 1906.

Apart from the advances in synthetic work, the early part of the twentieth century is also noted for numerous theoretical studies. For example, two mathematical theories for the nematic phase were proposed, namely the swarm theory and the continuum theory (also known as the distortion hypothesis). The swarm theory was initially proposed by Bose[8] in 1909 and was refined subsequently by Ornstein and Zernicke[9] in 1919. The theory states that molecules in the mesomorphic state do not orient in the same direction throughout the medium but are grouped in aggregates or swarms of 10^5 molecules which lie approximately parallel to one another. The swarm theory was able to explain many of the observations of the nematic phase, but was unable to explain the unusual results obtained from magnetic and electrical experiments performed by Zocher[10] in 1927. To this effect, Zocher then proposed the continuum theory, later refined by Oseen,[11] which envisages the liquid crystalline state as an anisotropic elastic medium with its own symmetry, viscosity and elasticity parameters.

The period from the mid 1930's to just after the Second World War, understandably produced very little progress both in synthetic and theoretical studies. However, interest was rekindled in 1957 by Brown[12] who published a review on liquid crystals. In 1962, Gray (now Professor Gray, CBE) investigated the relationship between molecular structure and mesomorphism and published his work in what is now regarded as an invaluable text, '**Molecular Structure and the Properties of Liquid Crystals**'.[13] In fact Professor Gray's outstanding contribution to the field of liquid crystals has been recognised internationally with the award of the Kyoto Prize for Advanced Technology by the Inamouri Foundation in 1995.

In the early 1970's the synthesis of the stable cyanobiphenyl compounds by Gray *et al.*[14] gave rise to the first commercially viable liquid crystal display, *i.e.*, TNLCD (Twisted Nematic Liquid Crystal Display).[15] The advantageous properties of liquid crystal displays, such as low power consumption, small size and portability compared with the relatively bulky and expensive Cathode Ray Tube (CRT) devices led to a tremendous increase in research activity. To this effect, soon after the faster switching Surface Stabilised Ferroelectric Liquid Crystal (SSFLC) display device was developed by Clark and Lagerwall[16] following the initial theoretical work of Meyer *et al.*[17]

To date, liquid crystal research continues to advance following the recent discovery of the ferri- and antiferro-electric phase types by Chandani *et al.*[18,19] in 1989. This has led to the development of an antiferroelectric display which has the ability to switch between two ferroelectric states and one antiferroelectric state, *i.e.*, exhibits tristate switching.

In the advancement of liquid crystal science, it is important to note that this is a multi-disciplinary subject involving collaboration between chemists, physicists, mathematicians and biologists. Hence, the author would like to draw the attention of the reader to two recent texts of particular interest: **'Handbook of Liquid Crystal Research'** edited by Collings and Patel[20] and; the **'Handbook of Liquid Crystals, Vols. I-IV'** edited by Demus *et al.*[21]

1.2 CLASSIFICATION AND MOLECULAR STRUCTURE OF LIQUID CRYSTALS

1.2.1 CLASSIFICATION

The simplest classification of liquid crystals is based on their mode of production. Compounds which exhibit liquid crystalline properties either due to the action of heat on the crystalline solid or by cooling the isotropic liquid are termed ***thermotropic liquid crystals***. Compounds that exhibit liquid crystalline phases due to the action of solvent (usually water) are termed ***lyotropic liquid crystals***. Although the latter are of great biological interest this thesis deals with thermotropic liquid crystals solely and lyotropic systems will not be dealt with further. However, for interest the author would like to draw the attention of the reader to the review article by Goodby[22] on lyotropic liquid crystals and their role in living systems.

However, the above classification is rather ambiguous since lyotropic liquid crystals can be affected by temperature and similarly thermotropic liquid crystals can be affected by the action of solvent. A more suitable classification is based on the structural integrity of the compound and classifies the compound as either ***amphiphilic*** or ***non-amphiphilic***.

Amphiphilic liquid crystals (**2-4**) are compounds which contain both lipophilic ('lipid-liking') and hydrophilic ('water-liking') groups and confer solubility in both organic and aqueous solvents.

Anionic amphiphile

$CH_3(CH_2)_nSO_4^-$---K^+/Na^+ **(2)**

Cationic amphiphile

$CH_3(CH_2)_nN^+Me_3$---Cl^-/Br^- **(3)**

Non-ionic amphiphile

n-$C_8H_{17}NH_2$ **(4)**

Mesophases formed by amphiphilic compounds arise via the production of multi-molecular units termed micelles or aggregates. The shape of the micelle is dependent on both the type of solvent and temperature.

Non-amphiphilic liquid crystals are predominantly non-polar or moderately polar compounds, *i.e.*, hydrophobic ('water-fearing') and confer solubility in organic solvents. Formation of mesophases in non-amphiphilic compounds is dependent on the arrangement of the individual lath- or disc-like molecules.

1.2.2 MOLECULAR STRUCTURE

The majority of low molecular mass (monomeric) compounds which exhibit liquid crystalline properties possess a characteristic elongated and lath-like structure (geometrically anisotropic) and are termed ***calamitic liquid crystals***. The general framework of a calamitic liquid crystal is shown in **Figure 1**.

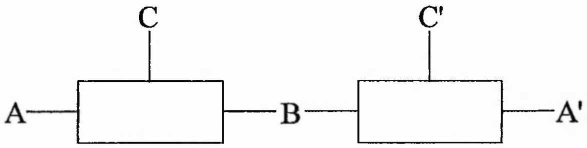

Figure 1 Schematic representation of a calamitic liquid crystal.

A and A' are terminal groups, usually either alkyl or alkoxy, which serve to extend the length of the molecule along the molecular long axis. The rectangles represent rigid polarisable units which are usually aromatic rings (1,4-phenyl, 2,5-pyrimidinyl, 2,6-naphthyl) but can also be alicyclic rings (*trans*-1,4-cyclohexyl). B is the central linking group (-CO_2-, -C≡C-, -CH=CH-) which serves to maintain linearity and also to extend conjugation between the adjacent polarisable units. C and C' are lateral substituents (F, Cl, CN, CH_3) which are present to extend the molecular breadth and play an important role in enhancing the physical properties of liquid crystals.

Recently, as shown in **Figure 2**, newer structures have been discovered which in some cases deviate drastically from the conventional lath-like or calamitic arrangement. In 1977, Chandrasekhar[23] synthesised disc-like liquid crystalline molecules, *e.g.*, compound (**5**), and disproved the general notion that only rod-like molecules were able to show such properties. Chandrasekhar described these disc-like compounds as ***discotic liquid crystals***. Other examples include swallow-tailed compounds[24] (**6**), biforked compounds[25] (**7**), phasmidic compounds[26] (**8**) and twin- or siamese twin-mesogens[27] (**9**).

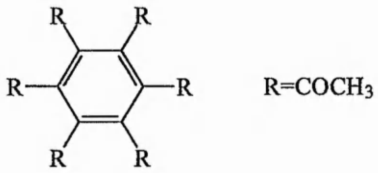

(5) DISCOTIC
K 288.0 DISCOTIC 292.8 I

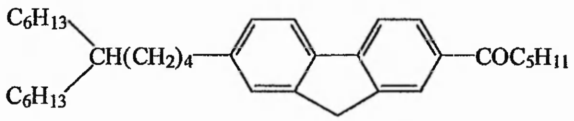

(6) SWALLOW-TAILED
K 36 S_A 52 I

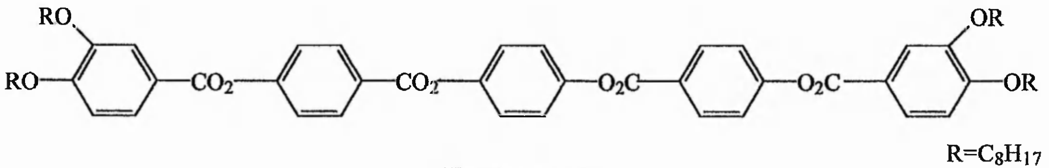

(7) BIFORKED
K 175 S_C 182.2 N 196.7 I

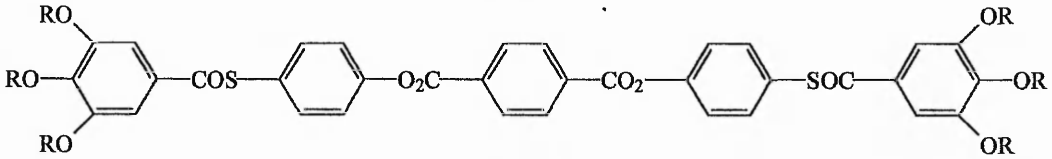

(8) PHASMIDIC
K 70 hexagonal columnar 81.5

R=$C_{12}H_{25}$

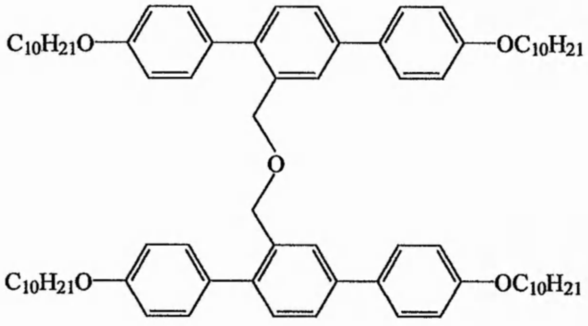

(9) SIAMESE TWIN
K 99 S_C 128 S_A 168 I

Figure 2 Structural variety of liquid crystalline molecules and their transition temperatures.

1.3 MESOPHASE FORMATION

Mesophase formation is dependent upon the magnitude of the anisotropy of intermolecular forces. Two intermolecular forces are present: lateral- and terminal-cohesive forces. The lateral forces are stronger than the terminal forces (anisotropy of intermolecular forces) and on heating these forces breakdown in a stepwise manner.

In 1933, Bernal and Crowfoot[28] examined the crystal structure of several known liquid crystalline compounds using X-ray crystallography. From their investigations they were able to deduce two different types of packing arrangement of the molecules within the crystal lattice:

i. layer lattice - the molecules are arranged with their long molecular axes parallel and with their ends lying in the same plane. The molecular long axes may be either orthogonal (perpendicular) or tilted with respect to the layer planes and;

ii. non-layer lattice - the molecules are aligned parallel with respect to each other. However, the ends of the molecules do not lie in the same plane but are interdigitated to give an imbricated structure.

The aspects of mesophase formation and the relevance of crystal structure is summarised in **Figure 3**. For example, on heating a crystal comprising a layer lattice structure, at temperature T_1, the weaker terminal cohesive forces break such that in-plane translational order is lost and the layers are free to slide and rotate over one another. This represents the formation of a smectic phase (a full description of smectic

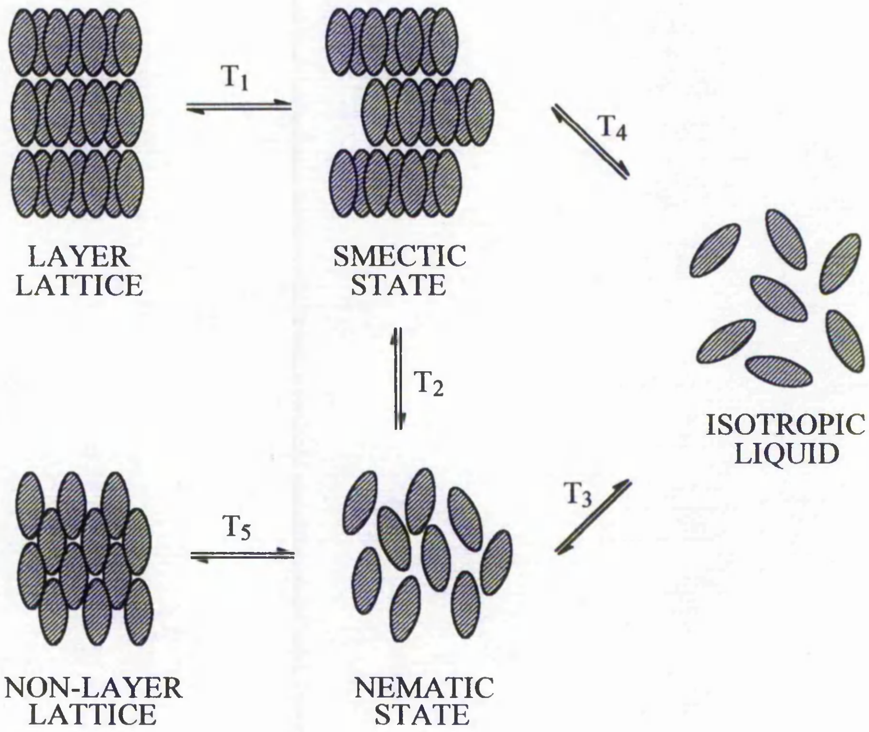

Figure 3 Diagrammatic representation of molecular rearrangements which may occur on heating a crystalline solid composed of either a layer- or non-layer-lattice.

phase types is given in section 1.4.2.3, p. 18). On heating to a higher temperature there are two further possibilities:

i. at T_2, the lateral cohesive forces may now weaken such that the molecules are no longer confined within layers and out of plane translational order is lost. The structure is stabilised by residual terminal- and lateral-cohesive forces and simulates the nematic phase (a full description of the nematic phase is given in section 1.4.2.1, p. 14). Thereafter, at a temperature, T_3, the nematic phase converts to the isotropic liquid as total order is lost;

ii. alternatively, the smectic phase may convert directly to the isotropic liquid at temperature, T_4, as a result of complete breakdown of both lateral- and terminal-cohesive forces.

However, for a non-layer lattice crystal structure it was initially assumed that due to its imbricated nature, only a nematic phase would be deemed possible on heating to a temperature, T_5. On further heating, at a temperature, T_3, the nematic phase would then convert to the isotropic liquid. However, Leadbetter *et al.*[29] showed that in certain members of an homologous series of 4'-n-alkyl- and 4'-n-alkoxy-4-cyanobiphenyls (K and M series), which possess a non-layer lattice, exhibit a smectic A mesophase type. The structure of this phase is described in more detail in section, 1.4.2.3, p. 21.

Mesophases observed above the melting point, *i.e.*, above T_1 and T_5, are stable and are termed ***enantiotropic***, whereas those phases that occur below the melting point *i.e.*, below T_1 and T_5, on supercooling the crystal are metastable and are called ***monotropic***.

1.4 OPTICAL CHARACTERISATION AND MESOPHASE TYPES

1.4.1 OPTICAL CHARACTERISATION

Thermal optical microscopy is the most widely used technique for liquid crystal identification. The visual characteristics or ***optical textures*** are observed by sandwiching a thin sample of the mesogenic material between two glass substrates (sandwich cell) and viewing the cell between cross polarisers. The resulting optical texture caused by the interaction of defects at the molecular level in the sample with polarised light, enables mesophase identification. An understanding of the molecular alignment of the sample with respect to the glass substrate assists mesophase identification and as shown in **Figure 4**, there are two types of alignment: homeotropic and homogeneous.

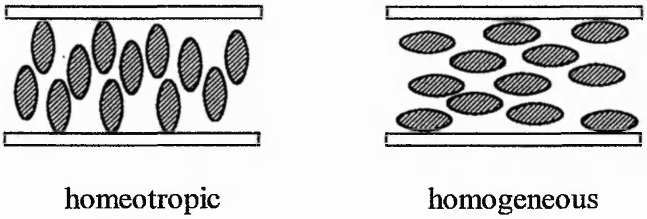

Figure 4 Homeotropic and homogeneous molecular alignments.

In the homeotropic alignment the molecules are arranged so that the molecular long axes lie normal (perpendicular) with respect to the glass substrate. The homeotropic alignment can be achieved by the use of surfactants such as lecithin. In the homogeneous alignment the molecules are arranged with their long axes parallel to the glass slide and may be achieved by rubbing the glass slide in a single direction.

However, for the identification of many optical textures it is desirable to have both homeotropic and homogeneous areas on the same glass slide.

Some mesophase types are difficult to distinguish using conventional sandwich cells (glass slide and coverslip) in which case free standing films may be employed. This technique involves drawing the mesogenic material (in either the S_A or S_C phase) over a small pre-drilled hole (1-2 mm diameter) in an aluminium plate. In this situation the smectic layers are perpendicular to the optic axis such that the S_A phase appears optically extinct between crossed polarisers. During a change in molecular alignment from perpendicular to tilted, the optical texture appears birefringent, *e.g.*, S_C phase.

1.4.2 MESOPHASE TYPES

In 1922, following extensive microscopic studies, Friedel identified three types of mesophase: nematic; smectic and; cholesteric. Subsequently, many new mesophase types have been discovered, *e.g.*, blue phases,[30] twist grain boundary phases[31] and recently, the ferri- and antiferro-electric phase types.[18,19] The following sections provide an insight to the structure and optical textures of each phase type.

1.4.2.1 THE NEMATIC PHASE (N)

The term nematic comes from the Greek word ***nematos*** meaning thread-like. This is due to the appearance of a characteristic thread-like texture when a thin sample of the nematic phase is viewed between cross polarisers. **Figure 5** depicts the general arrangement of the molecules in the nematic phase.

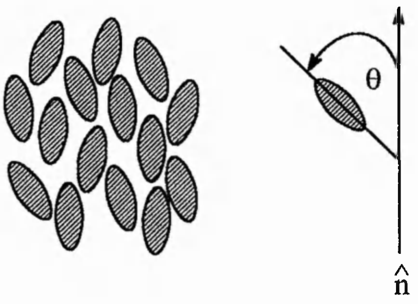

$$S=\frac{1}{2}(3\cos^2\theta-1)$$

Figure 5 Idealised nematic phase.

The molecules tend to lie approximately parallel to a common axis which is known as the director, $\hat{n}$, but are not fixed, *i.e.*, the molecules are free to rotate. The high mobility and low viscosity of the nematic phase means that it is very much 'fluid-like'. X-Ray diffraction studies by Hückel,[32] show a substantial resemblance to those for the isotropic liquid, *i.e.*, very weak and diffuse.

The degree of alignment of the molecules with respect to the director, $\hat{n}$, is termed the order parameter, S, where θ is the angle between the long axis of each individual rod-like molecule and the director. Typically for the nematic phase the order parameter, S, is in the region of 0.4-0.7 and is temperature dependent.

Optically the nematic phase is identified most readily on cooling from the isotropic liquid, where it appears in the form of highly coloured droplets known as ***nematic droplets*** which then coalesce to give predominantly thread- or marble-like textures. Brownian motion is also a strong characteristic of the nematic phase which is indicative of its high degree of disorder and mobility, *i.e.*, fluid-like.

The ***schlieren texture*** is sometimes observed which is identified by the appearance of dark brushes (two and four) emanating from point singularities. If the molecules adopt the homeotropic alignment then a dark field of view is observed, *i.e.*, optically extinct.

1.4.2.2 THE CHOLESTERIC PHASE (Ch or N*)

The designation cholesteric is used purely for historical reasons because this phase type was first observed in derivatives of cholesterol. However, it is now known that the cholesteric mesophase (Ch) appears in optically active compounds in place of the nematic phase and hence it may also be termed the chiral nematic phase (N*).

The structure of the cholesteric phase is regarded as a 'layered' nematic state in which the director, $\hat{n}$, of an individual layer is skewed slightly either clockwise or anti-clockwise with respect to the director in adjacent layers thus tracing the form of a helix **(Figure 6)**. The distance required for the director to complete one revolution (0-360°) is termed the pitch and is temperature dependent. At high temperatures the molecules have greater thermal energy causing the angle between successive layers to increase which results in a tighter or shorter pitch. At low temperatures, the angle between successive layers is smaller and hence the pitch is longer.

The cholesteric phase and the nematic phase are very similar except for:

i. the two phases do not normally co-exist, except in the unusual case of helical twist inversion;[33]

ii. mixing two cholesteric materials of opposite chirality gives rise to the nematic phase and;

iii. the addition of a chiral dopant to the nematic phase results in the appearance of the cholesteric phase.

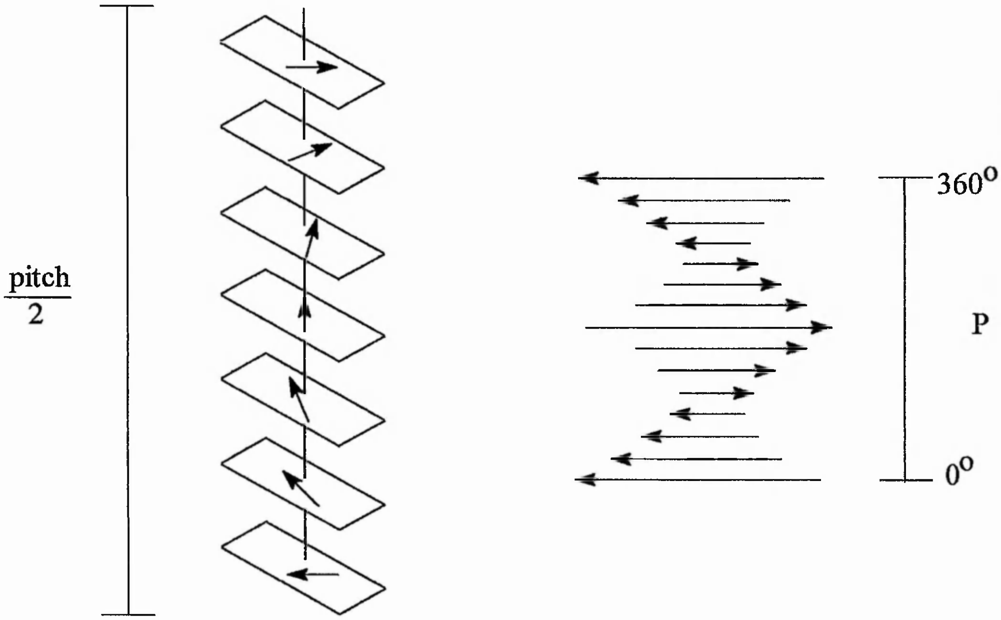

Figure 6 Diagrammatic representation of the cholesteric phase.

When the pitch length is equal to the wavelength of visible light, colours are selectively reflected (selective reflection). Since the pitch length is temperature dependent then a multitude of colours are possible. This simple principle forms the basis of many commercial thermochromic displays.

The examination of the cholesteric phase with a polarised microscope gives two distinct textures which are dependent upon the alignment of the helices on the supporting surfaces (**Figure** 7) with respect to the optical axis:

i. the focal-conic texture which forms upon cooling the isotropic liquid where there is no selective reflection and the helices lie perpendicular to the incident light and;

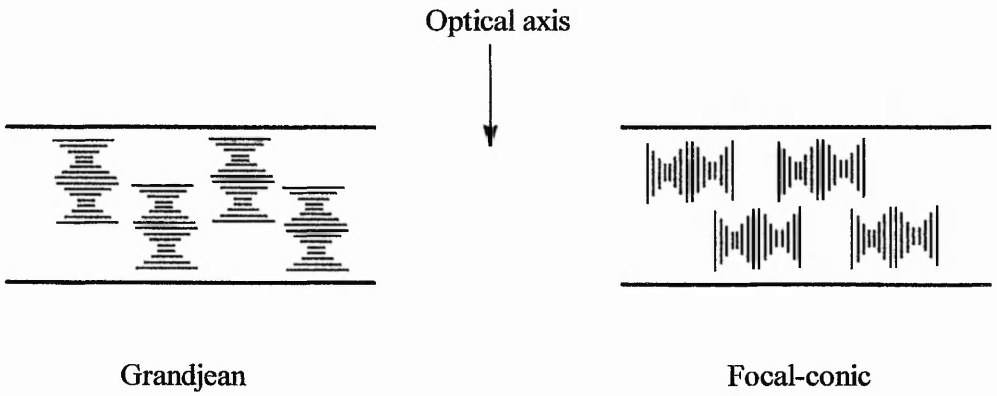

Figure 7 Helical orientation for Grandjean and focal-conic textures.

ii. the Grandjean texture which is obtained by mechanical shearing of the focal-conic texture. This texture contains oily streaks and often produces highly iridescent colours as the helical axes are parallel to the light path.

1.4.2.3 THE SMECTIC PHASE (S)

The name smectic is derived from the Greek word ***smectos*** meaning soap-like because such liquid crystalline phases were first observed in ammonium- and alkali-soaps. The molecules in a smectic phase are stratified and occur in layers. Within layers, the molecules may be situated either at right angles or tilted with respect to the layer planes. Unlike either the nematic or the cholesteric phase, the smectic phase possesses both positional and orientational order.

1.4.2.3.1 Smectic Polymorphism

Although Friedel[6] recognised the smectic phase, he did not however realise the existence of smectic polymorphism, *i.e.*, different smectic phase types. These arise due to differences in the amount of positional and orientational order within and between layers. Initially, Sackmann and Demus[34] classified seven different smectic polymorphs, which were designated using code letters S_A, S_B ..., S_G governed by the ***miscibility rule*** which states "Liquid crystalline modifications which exhibit an uninterrupted series of mixed crystals in binary systems without contradiction can be marked with the same symbol". To date, twelve different smectic phases types are known, which may be placed in an order of appearance (thermodynamic sequence) on cooling from the isotropic liquid as shown below.

$$\text{Isotropic liquid - N, } S_A, S_D, S_C, {S_B}^h, S_I, {S_B}^c, S_F, S_J, S_G, S_E, S_K, S_H \text{ – crystal} \xrightarrow[\text{decrease in temperature}]{}$$

The sequence overleaf has been refined recently such that it now distinguishes between *smectic liquid crystal phases* and *smectic crystal phases*. The latter possess strong 2-D order and resemble closely the crystalline solid. In addition there is the rather curious smectic D phase which is now designated solely as the D phase. Hence, the thermodynamic sequence of phases is now represented as shown below and is useful for the purpose of phase identification.

$$\xrightarrow[\text{decrease in temperature}]{\text{Isotropic liquid - N, } S_A\text{, D, } S_C\text{, } S_B\text{, } S_I\text{, CrB, } S_F\text{, CrJ, CrG, CrE, CrK, CrH - crystal}}$$

However, care must be exercised during phase identification as the above thermodynamic sequence does not always hold true due to the phenomenon of ***re-entrant*** phases.[35] This is where a phase reappears on cooling further down from its original position in the thermodynamic sequence. For example, Byron *et al.*[36] have reported a re-entrant S_A phase which reappears on cooling below the S_C phase.

The Smectic A Phase, S_A

This is the least ordered smectic polymorph. X-Ray diffraction studies[37] of the S_A phase show that the molecules are arranged with their molecular long axes perpendicular with respect to the *layer planes* (**Figure 8**). Within a *layer* there is zero positional order and the molecules are able to rotate freely along their long axes. In the classical S_A phase the layer spacing (d) is equal to the molecular length (l).

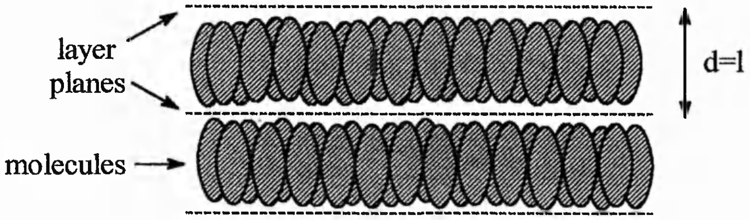

Figure 8 Idealised structure of the S_A phase.

However, as shown in **Figure 9**, in certain compounds that exhibit the S_A phase *e.g.*, the 4'-n-alkyl-4-cyanobiphenyls (K series), the layer spacing (d) is approximately 1.4 times greater than the molecular length (l). In this situation, the structure of the S_A phase is regarded as an interdigitated arrangement of molecules and termed S_Ad.

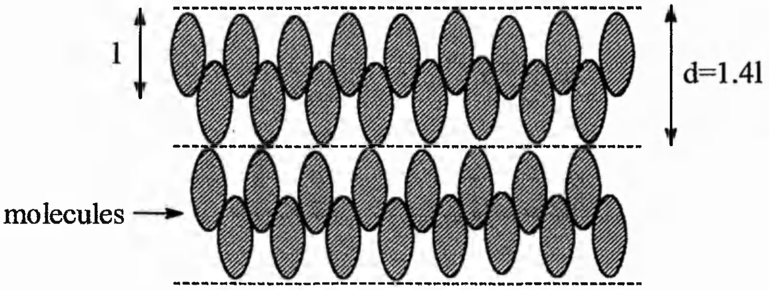

Figure 9 Interdigitated structure of the S_Ad phase.

Recently, the Twist Grain Boundary smectic A phase (TGBA) has been discovered[31] in chiral liquid crystalline materials and appears between the chiral nematic phase and the smectic A phase. Its structure possesses characteristics of both the chiral nematic phase and the smectic A phase, *i.e.*, comprises a layer arrangement (smectic A-like) consisting of screw dislocations which give rise to a helical structure (cholesteric-like). Due to its intermediate structure the TGBA phase is also termed a frustrated phase.

The Smectic B Phase, S_B and Crystal B Phase, CrB

In both the S_B and CrB phases the molecules are arranged in layers so that their long axes are situated orthogonal with respect to the layer planes. Unlike the S_A phase, the close packing arrangement of the molecules in hexagonal close-packed nets prevents free rotation (**Figure 10**). However, the molecules undergo co-operative rotation[38] in which the movement of one molecule influences the movement of the molecule adjacent to it.

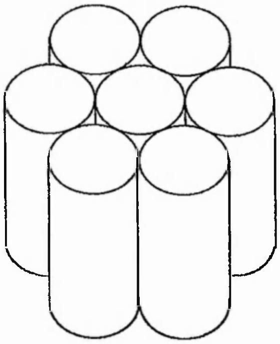

Figure 10 Hexagonal close-packed arrangement of the molecules in the B phase.

The difference between the S_B and CrB phases lies in the extent of inter-layer correlation of the hexagonal nets. In the S_B phase there is no inter-layer correlation of the molecules whereas in the CrB phase there is extensive long range inter-layer correlation. The latter gives a strong 3-D structure and hence the use of the term crystal. Goodby[39] has shown the existence of both types of B phase in 4-propionyl-4'-heptanoyloxyazobenzene (**10**).

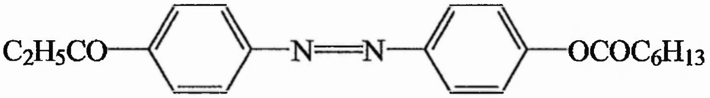

(10)

I 152.5°C N 141.7°C S_A 90.3°C S_B 86.0°C CrB

Two natural textures[†] (the homeotropic and mosaic texture) and one paramorphotic texture[‡] (the focal-conic fan texture) are exhibited by both types of B phase. The phase separates from the isotropic liquid in the form of either oblong sheets or platelets which have characteristic 'H'-shaped mosaic areas. In the paramorphotic fan texture of the CrB phase observed on cooling from the S_A phase, lines or ***transition bars***[40] appear briefly on the back of the S_A fans which then disappear to leave a smooth back.

The Smectic C Phase, S_C

In the smectic C phase, the molecules are arranged in layers and are tilted with respect to the layer planes. X-Ray studies reveal that the layer spacing (d) is less than the molecular length (l) which correlates well with the tilted arrangement of the molecules (**Figure 11**). The tilt angle, θ, defined as the angle between the molecule and the layer normal, is temperature dependent.

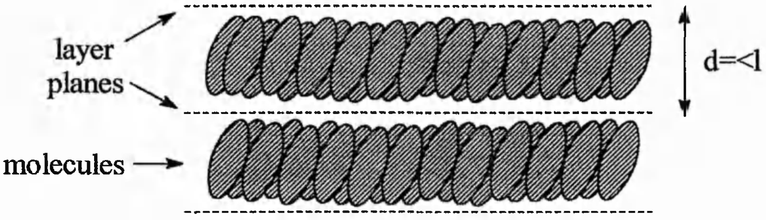

Figure 11 Idealised structure of the S_C phase.

[†] Natural textures appear on cooling from the isotropic liquid or nematic phase.
[‡] Paramorphotic textures appear on cooling from a previous smectic phase.

The smectic C phase exhibits two optical textures: the schlieren and the broken focal-conic fan texture. The schlieren texture is formed on cooling from either the isotropic liquid or the nematic phase and shows four point singularities (compared to two- and four-brush schlieren exhibited by the nematic phase). The fan texture is formed on cooling from the S_A phase where it is characterised by the shattering of the fans combined with the appearance of schlieren in the previously homeotropic region.

When the phase is composed of chiral compounds it becomes optically active due to the formation of a helix and is termed chiral smectic C (S_C*). The helix pitch length is temperature sensitive due to the dependence of tilt angle on temperature. When the pitch length of the helix is in the region of visible light, iridescent colours are observed (blue at lower temperatures and red at higher temperatures) and hence the S_C* phase can also be used as a temperature sensor. However, the main use of the S_C* phase is in the Surface Stabilised Ferroelectric Liquid Crystal (SSFLC) display.[16] Ferroelectric liquid crystals and the SSFLC device are described in more detail in section 1.6, p. 39.

The Crystal E Phase, CrE

The CrE phase is similar to the CrB phase with the molecules being arranged so that their long axes are perpendicular to the layer planes although the phase is more ordered. Within the layers of the CrE phase the molecules adopt a chevron-like or orthorhombic array (**Figure 12**). X-Ray data indicate that the distance between the molecules is such that they cannot undergo free rotation and instead the molecules oscillate through a restricted angle giving a ‘flapping’ motion.

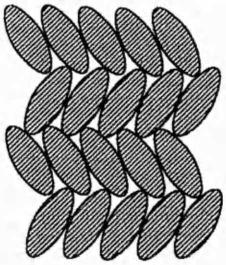

Figure 12 Cross-section of the CrE phase showing the chevron packing of the molecules.

The CrE phase is usually formed by cooling from either the S_A or S_B phase fan texture and is not normally observed in a phase sequence that contains ordered tilted smectic phases. The fan texture is recognised by clear, unbroken lines, almost parallel, across the fans coupled with a semi-transparent platelet texture which develops in the previously homeotropic areas. The natural mosaic texture of the CrE phase is not frequently observed.

The Smectic F Phase, S_F

In the smectic F phase the molecules are hexagonally close packed with respect to the director and they have short range positional ordering within the layers and long range bond orientational order in three dimensions. The ordering of the molecules within the layers is of a tilted nature with the molecules being tilted towards the edge of the hexagonal net (**Figure 13**). There is poor correlation between the layers, which allows the layers to slide over one another.

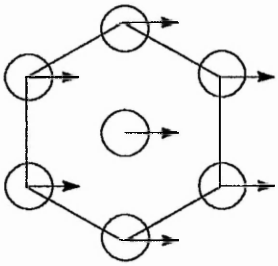

tilt to the side

Figure 13 Tilt direction in the S_F phase.

The S_F phase exhibits two main textures: the broken focal-conic fan and schlieren-mosaic textures. The broken focal-conic fan texture is almost identical to that of the S_I phase, however, the schlieren-mosaic texture allows the two textures to be distinguished. In the S_I phase the schlieren texture shows typical schlieren brushes arising from point singularities but for the S_F phase the schlieren areas are still retained but the texture is now crossed with fine mosaic lines giving a schlieren-mosaic texture. The S_F phase can also be brought readily into focus whereas the S_I phase appears as a blurred image.

When the smectic F phase is composed of optically active compounds, it exhibits a helical arrangement of the tilt orientational ordering on passing from one layer to the next. The pitch of the helix in this phase is temperature dependent and usually decreases with decreasing temperature. This effect is due to the tilt angle usually increasing with decreasing temperature which results in the pitch of the helix being shortened.

The Crystal G Phase, CrG

The crystal G phase has a high order crystal structure having a tilted pseudo-hexagonal arrangement of molecules with the molecules having an average tilt angle of 25-30° with respect to the layer normal. The phase is analogous with the S_F phase but differing in that it contains widespread inter-layer correlations.

The CrG phase exhibits one natural mosaic texture. The texture forms via dendritic growth of elongated splinters which coalesce to form the classical mosaic texture. A number of paramorphotic textures can be observed depending on the preceding phase. On cooling from the S_B phase an arced, broken, focal-conic texture is observed whereas upon cooling from the S_C or S_F phase, a broken fan texture is observed with a patchwork appearance.

When the phase is composed of chiral molecules the phase becomes ferroelectric. However, the spiralling of the tilt orientational ordering normal to the layer planes, observed for chiral smectic liquid crystal phases C*, I* and F* is not usually observed. The spiralling of the tilt may be present but it is very weak due to the crystallinic nature of the phase and cannot be detected over several hundred layers.

The Crystal H Phase, CrH

X-Ray diffraction data on the CrH phase indicate that this phase is equivalent to the CrE phase except that the molecules are tilted with respect to the layer planes. The molecules adopt an orthorhombic arrangement which is tilted to one side of the distorted hexagonal array with respect to the layer normal.

The CrH phase is most readily identified on cooling the mosaic texture of the CrG phase where at the CrG/H transition zigzag cross-hatched lines are seen within the mosaic regions which either disappear upon phase formation or may remain throughout the temperature range of the phase.

The phase becomes ferroelectric when composed of chiral molecules and as for the CrG* phase, a spiralling of the tilt orientational order to the layer planes is not seen.

The Smectic I Phase, S_I

The smectic I phase is almost identical to the smectic F phase except in the smectic I phase the molecules are tilted towards the apex of the hexagonal close packed net (**Figure 14**). The molecules are expected to be in dynamic motion about their long axes and the rotation is expected to be of a co-operative nature as the molecular centres are only separated by 0.4-0.5 nm.

When the phase is composed of optically active material there is spiralling of the tilt orientational order normal to the layer planes thus forming a macroscopic helix. The twist of the tilt direction between successive layers can either be right- or left-handed depending on the constituent molecules. The pitch of the helix, although temperature dependent, is usually greater for the S_I* phase than it is in the preceding S_C* phase for materials that contain both phases types.

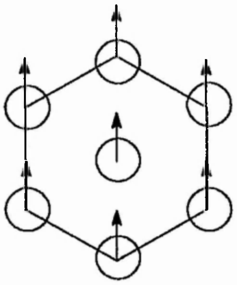

tilt to the apex

Figure 14 Tilt direction in the S_I phase.

The Crystal J Phase, CrJ and Crystal K Phase, CrK

The structures of the CrJ and CrK phases[41] are analogous to the CrG and CrH phases respectively, except for the tilt direction which is towards one apex of the hexagonal array (CrJ) or the orthorhombic array (CrK) as opposed to the side of the nets. Recently, the first observation of a natural texture of the CrK phase has been reported by Bowden *et al.*[42]

Both phases become ferroelectric when composed of chiral molecules. However, once again these phases do not form a helical distribution of the tilt about a direction normal to the layers as the helix is suppressed by crystallinic forces.

The D Phase, D

The D phase is rather an oddity in that it lies between two lamellar phases, *i.e.*, the S_A and S_C phases, although the D phase does not itself contain molecules which are arranged in layers. Although the D phase was detected in 1957 by Gray *et al.*,[43] to date there are relatively few materials which exhibit this phase. However, in general compounds which exhibit this phase have a dimeric structure composed of long terminal alkoxy chains and are capable of forming strong intermolecular interactions, *e.g.*, 4'-n-hexadecyloxy-3'-nitrobiphenyl-4-carboxylic acid (**11**).[44]

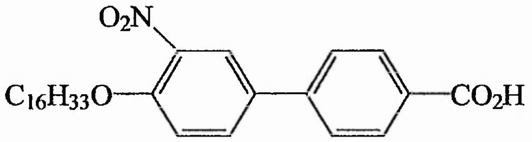

(11)

K 126.8°C S_C 171.0°C D 197.2°C S_A 201.9°C I

The structure of the D phase is thought to be a body centred cubic (BCC)[45] in which the aromatic cores of the molecules form spherical micelles which themselves form a lattice structure. However, an alternative model has been proposed[46] which suggests that the molecules may aggregate to form discs which may stack in a similar manner to discotic liquid crystals to form a columnar structure. Recently, investigations on the D phase of the 3'-substituted-4'-n-alkoxybiphenyl-4-carboxylic acids, carrying either a nitro- or cyano-group, have shown that the cubic structure varies with the lateral group substituted on the biphenyl ring.[47]

The D phase is optically isotropic and may be identified microscopically by the appearance of dark squares, hexagons and rectangles that nucleate in the S_C phase.

1.4.2.4 BLUE PHASES

The blue phases[48] appear in ultra-pure chiral compounds, in a narrow temperature interval (<1°C) between the cholesteric phase and the isotropic liquid. When viewed between cross polarisers they exhibit either a blue fog or blue-green mosaic texture and hence their name. Three different blue phases are known and are designated BPI, BPII and BPIII. Crystallographic studies show that BPI possesses a body centred cubic structure and BPII is a simple cubic. However, BPIII possesses poor structural symmetry and hence its structure has not been fully elucidated.[48,49]

1.5 THE RELATIONSHIP BETWEEN MOLECULAR STRUCTURE AND LIQUID CRYSTALLINE BEHAVIOUR

An understanding of the relationship between molecular structure and liquid crystalline behaviour plays an important role in the design and synthesis of liquid crystals for specific applications. As mentioned earlier (section 1.2.2, p. 7), calamitic liquid crystals are generally composed of rigid polarisable aromatic units connected together by a central linking group and outer terminal groups. By careful tailoring of these groups the mesophase thermal stability, *i.e.*, the temperature of transition: nematic to isotropic liquid (T_{N-I}); smectic to nematic (T_{S-N}) or; smectic to isotropic liquid (T_{S-I}) may be increased, reduced or completely eliminated.

At a simplistic level, the mesophase thermal stability may be related to the anisotropy of molecular polarisability, $\Delta\alpha$, which is defined as 'the difference in polarisability of the molecule along the long molecular axis with respect to the polarisability along the short molecular axis'. An increase in magnitude of $\Delta\alpha$ usually stabilises a particular mesophase whereas a decrease in its magnitude lowers the mesophase thermal stability.

An extensive study of structure-property relationships is outside the scope of this thesis and the author would like to draw the attention of the reader to the articles by Demus[21], Collings and Hird[50] and Toyne[51] for an in depth assessment of this subject. However, there now follows a brief assessment of structure-property relationships as applied to calamitic liquid crystals.

1.5.1 INFLUENCE OF TERMINAL GROUPS

Terminal substituents serve to extend the linearity of the molecule and increase the polarisability along the long molecular axis, which increases the magnitude of $\Delta\alpha$. The ability of many different terminal substituents to promote the thermal stability of the nematic phase was investigated by Gray *et al.*[52] who proposed the following average group efficiency order:

$$Ph > NHCOCH_3 > CN > OCH_3 > NO_2 > Cl > Br > N(CH_3)_2 > CH_3 > F > H$$

Group efficiency order

As can be seen from the above order, the replacement of the terminal hydrogen by any other substituent is beneficial to mesophase thermal stability.

1.5.1.1 HOMOLOGATION

The relationship between molecular structure and liquid crystallinity is more apparent for either an alkyl- or alkoxy-terminal substituent. Gray *et al.*[53] showed that when the transition temperatures for an homologous series are plotted against, n, the number of carbon atoms in the terminal chain, *i.e.*, transition temperature plot (**Figure 15**), several conclusions can be drawn from the data:

i. there is no correlation between melting point and length of the alkyl or alkoxy chain;

ii. early members of the series exhibit the nematic phase alone;

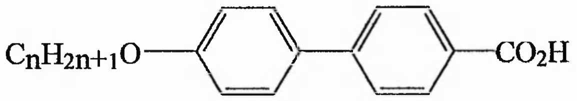

(12)

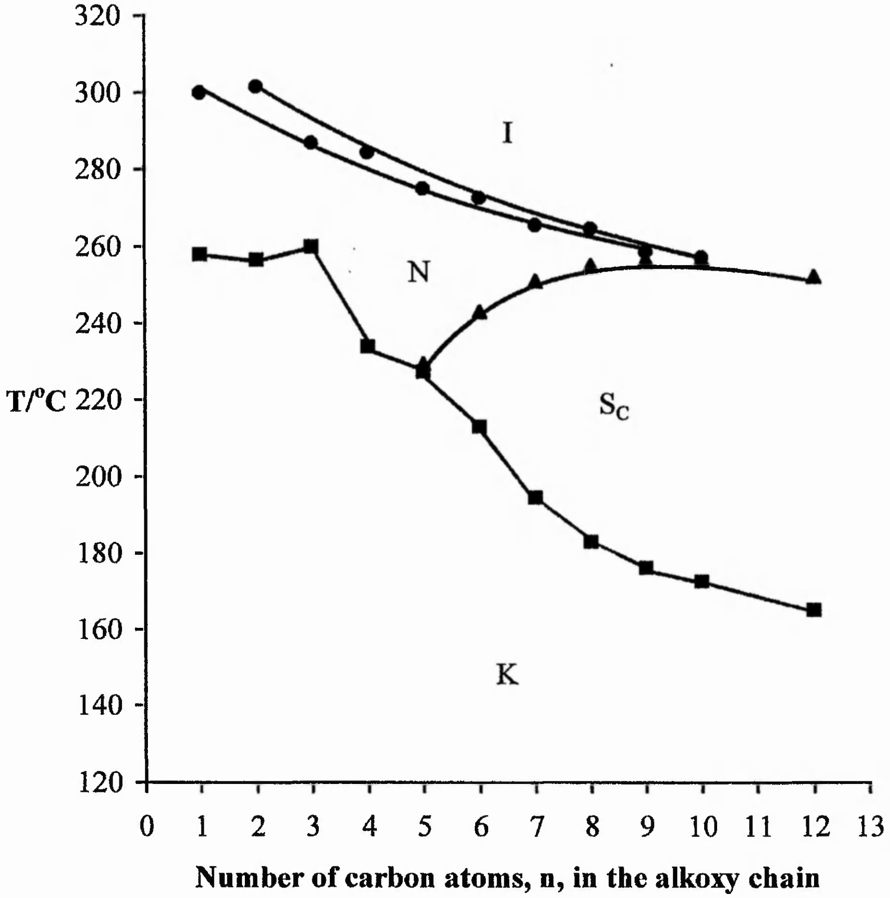

Figure 15 Plot of transition temperatures for an homologous series of 4'-n-alkoxybiphenyl-4-carboxylic acids (**12**).

iii. the nematic to isotropic liquid transition temperatures lie on two smooth decreasing curves. The points for the even-n homologues are correlated by one smooth curve whereas the point for the odd-n homologues are correlated by a second smooth curve. This alternation in the N-I transitions temperatures is known as the ***odd-even effect*** and may be explained by considering the number of C-C bonds directed along the long molecular axis with respect to the proportion directed along the short axis.

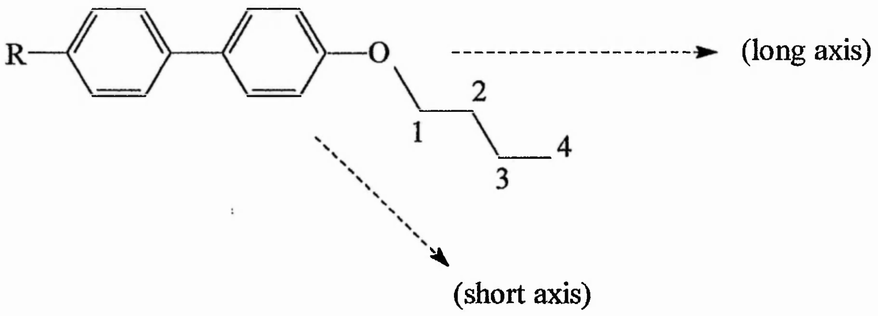

For compounds with a terminal alkoxy chain, the points for the N-I transition temperatures for even-n homologues lie on a smooth curve which is above that for the odd-n homologues. This is due to even members having more C-C bonds directed along the long molecular axis than across it. Therefore, the anisotropy of molecular polarisability, $\Delta\alpha$, is greater and the mesophase thermal stability is enhanced. For alkyl terminal chains, this trend is reversed, *i.e.*, the points for the odd-n homologues lie above the points for the even-n homologues and finally;

iv. for intermediate homologues both smectic and nematic phases may be observed. As the chain length increases smectic phases are more apparent at the expense of either the nematic or the cholesteric phase.

1.5.2 INFLUENCE OF THE CENTRAL LINKING GROUP

The purpose of the central linking group is to maintain the linearity of the molecule and also to extend conjugation between the adjacent aromatic fragments. A variety of central linking groups may be employed as shown below.

$-\overset{\overset{\displaystyle O}{\|}}{C}-O-$

ESTER

$-CH_2CH_2-$

DIMETHYLENE

$-C\equiv C-$

ALKYNE

$-CH=N-$

IMINE

$-CH=CH-$

ALKENE

$-N=N-$

AZO

Commonly, sp^2 hybridised groups are readily used as they have a flat, planar, geometry which enables close packing between adjacent molecules and allows conjugation between the aromatic moieties. However, when sp^3 hybridised groups are used to link the aromatic moieties, conjugation between the rings is prevented and as a result are thermally less stable. However, Gray and McDonnell[54] have shown that certain flexible central linking groups such as dimethylene and oxymethylene, which neither allow conjugation nor enhance rigidity, can be successfully employed to give mesogenic materials with low melting points and high clearing points.

1.5.3 INFLUENCE OF LATERAL SUBSTITUENTS

The introduction of a lateral substituent disrupts the close-packing arrangement of the molecules due to an increase in the molecular breadth of the compound. The molecular breadth may be described as ‘the diameter of the smallest cylinder through which the molecule may pass’.

The influence of lateral substituents and molecular broadening in mesophase thermal stability is best described with reference to the seminal work of Gray and Worrall.[55] They investigated the effect of introducing different lateral substituents in the 3'-position of a series of 3'-substituted 4'-n-alkoxybiphenyl-4-carboxylic acids (**13**) upon nematic thermal stability, concluding that as the size of the substituent increases the nematic mesophase thermal stability decreases.

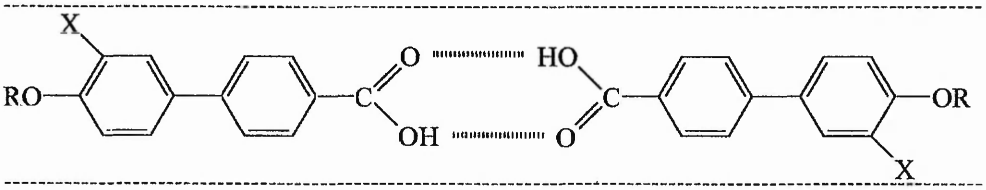

(**13**)

$X = H > F > CH_3 \approx Cl > Br > I \approx NO_2$
Nematic thermal stability

Also, if the substituent, X, is moved from the 3'-position to the 2'-position in compound (**13**), then the mesophase thermal stability is further reduced. In this situation, the two phenyl rings are no longer co-planar due to increased steric hindrance about the 1,1'-inter-ring bond which reduces inter-ring conjugation.

However, in certain compounds, the introduction of a lateral substituent has little or no effect on mesophase thermal stability. For example, the introduction of a lateral substituent, (X), in the 5-position of a series of 6-n-alkoxy-2-naphthoic acids (**14**),[56] results in an increase in the mesophase thermal stability. In this situation, the substituent is shielded by the overall molecular structure.

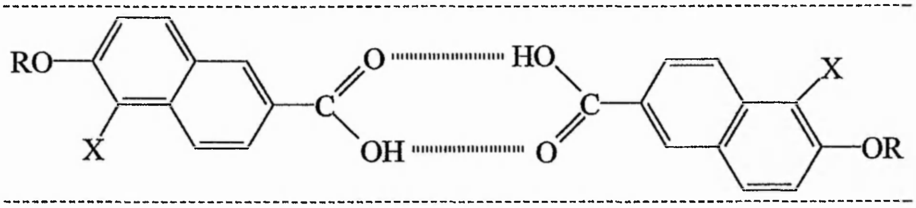

(14)

Although the introduction of lateral substituents is deemed detrimental to mesophase thermal stability, lateral substitution plays an important role in the design of low melting, room temperature liquid crystals for commercial applications. In particular, lateral fluoro-substituents[57-65] are commonly used because they impart the following advantages:

i. fluorine is the smallest substituent available (van der Waals radii of fluorine and hydrogen are 1.47Å and 1.2Å, respectively) which causes minimum disruption to the packing arrangement of the molecules;

ii. the introduction of a highly electronegative fluoro-substituent gives rise to a moderately polar C-F bond directed along the long molecular axis. This results in a lateral dipole which allows for the design of mesogenic materials with either a negative[57] or positive[63] dielectric anisotropy ($\Delta\varepsilon$), and;

iii. the lateral dipole produced by the C-F bond can either induce or stabilise the formation of tilted smectic phases.[57,64,65]

1.6 FERRO-, FERRI- AND ANTIFERRO-ELECTRIC LIQUID CRYSTALS

Chiral compounds which are exceptionally pure exhibit ferro-, ferri- and antiferroelectric phase types. The chiral smectic C phase (S_C* or S_C*ferroelectric) is relatively common, whereas the ferrielectric smectic C (S_C*ferrielectric) and antiferroelectric phase smectic C (S_C*antiferroelectric) have been discovered recently.[18,19] The S_C*ferro- and S_C*antiferro-electric phase types are of important commercial interest.

1.6.1 FERROELECTRICITY AND THE SURFACE STABILISED FERROELECTRIC LIQUID CRYSTAL (SSFLC) DISPLAY

The term ferroelectric refers to any system which possesses either a permanent or spontaneously polarised state. Valasek[66] first observed the ferroelectric effect in 1921 during experiments on crystals of Rochelle salt, which actually exhibits a piezoelectric effect, *i.e.*, induced polarisation resulting from a structural change in the crystal due to the application of mechanical stress.

Theoretical considerations by Meyer *et al.*[17] in 1975 postulated the following prerequisites for the existence of ferroelectricity in liquid crystals:

i. must possess laminar or layer-like structure;

ii. the molecules should be tilted with respect to the layer planes;

iii. the molecules should contain a strong transverse dipole moment and;

iv. the molecules should be chiral.

Meyer *et al.*[17] soon proved their theory of prerequisites by synthesising the first ferroelectric liquid crystal, namely (*S*)-4-n-decyloxybenzylidine-4'-amino-2-methylbutyl cinnamate **(15)**. Subsequently, Yoshino *et al.*[67] showed replacement of the 2-methylbutyl chiral unit with the isomeric 1-methylbutyl unit (DOBA-1-MBC) **(16)** causes a ten-fold increase in the value of the spontaneous polarisation. The two systems are directly comparable except that the chiral centre is positioned closer to the core in the DOBA-1-MBC.

DOBAMBC

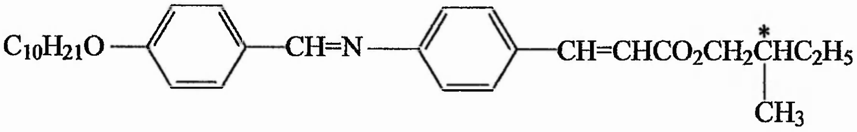

(15)

DOBA-1-MBC

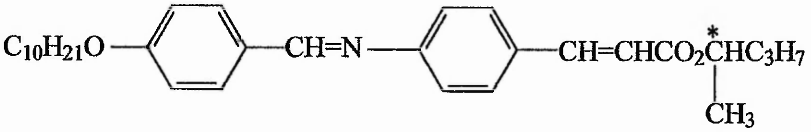

(16)

Although many chiral smectic phases (S_C*, S_F*, S_I*) meet the above requirements, the S_C* phase has been exploited in commercial applications and Clark and Lagerwall[15] in 1980 developed the Surface Stabilised Ferroelectric Liquid Crystal (SSFLC) display device.

In the achiral smectic C phase (S_C), the molecules occur in layers and are tilted with respect to the layer planes. The local symmetry elements consist of a centre of symmetry, a mirror plane and a C_2 axis parallel to the layer planes and normal to the tilt direction. This combination of elements gives C_{2h} symmetry.

In the case of the chiral smectic C phase (S_C*), the structure is similar to the achiral phase, *i.e.*, layers and tilt, except that the molecules spiral in a helical manner through the layers. Due to the chirality of the individual molecules, the centre of symmetry and mirror plane are lost and only the C_2 axis remains *i.e.*, reduced symmetry. As the molecules are polar, an imbalance arises with respect to the molecular dipoles along the C_2 axis. This imbalance occurs even though the molecules are undergoing rapid reorientational motion about their molecular long axes. The time-independent alignment of the dipoles along the C_2 axis causes the spontaneous polarisation to develop along this direction and parallel to the layer planes. Each individual layer therefore essentially has a spontaneous polarisation associated with it. However, due to the helical structure of the S_C* phase, there is cancellation of dipole moments within the helix and the magnitude of the overall dipole moment or spontaneous polarisation is zero. In this situation the phase is said to be *helielectric* (**Figure 16**).

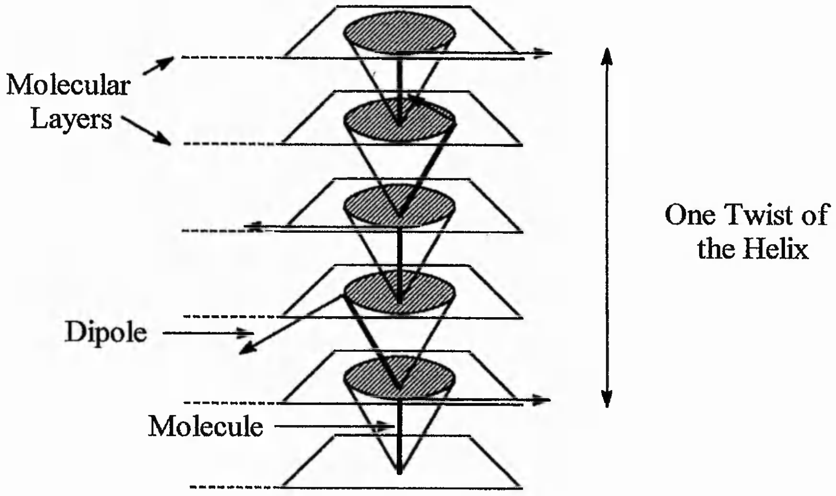

Figure 16 Helielectric structure of the S_C* phase.

In 1980, Clark and Lagerwall[16] proposed that if the helix could be suppressed, then all the dipole moments would align in the same direction thus giving rise to a spontaneously or permanently polarised state, *i.e.*, ferroelectric. To this effect, they developed the SSFLC display in which the helix is suppressed by confining the liquid crystal sample in an extremely thin cell and adopting the bookshelf geometry.

In the SSFLC display (**Figure 17**), the S_C* molecules are aligned parallel to the surfaces (bookshelf geometry) of a thin glass cell (1-2 μm) which causes the helix of the S_C* phase to unwind due to strong boundary forces (surface stabilisation). The direction of polarisation is perpendicular to the glass plates and on application of a small DC potential across the plates, the polarisation direction can be changed or switched. When the voltage is removed the position of the dipole moment remains unaltered and hence the ferroelectric device is said to be bistable. The optimum molecular tilt for this cell is 22.5° so that the change in angle described by the molecules as they undergo a directional change from one orientation to another, is ideally 45°. In comparison with the Twisted Nematic (TN) display,[15] which was developed ten years earlier, the SSFLC is commercially important as it confers the following advantages:

i. the ferroelectric device has a faster switching speed which is of the order of microseconds compared to milliseconds for the TN display;

ii. the ferroelectric states are bistable and have long term memory and;

iii. ferroelectric devices have high brightness and contrast ratios so that they may be used at low ambient light levels.

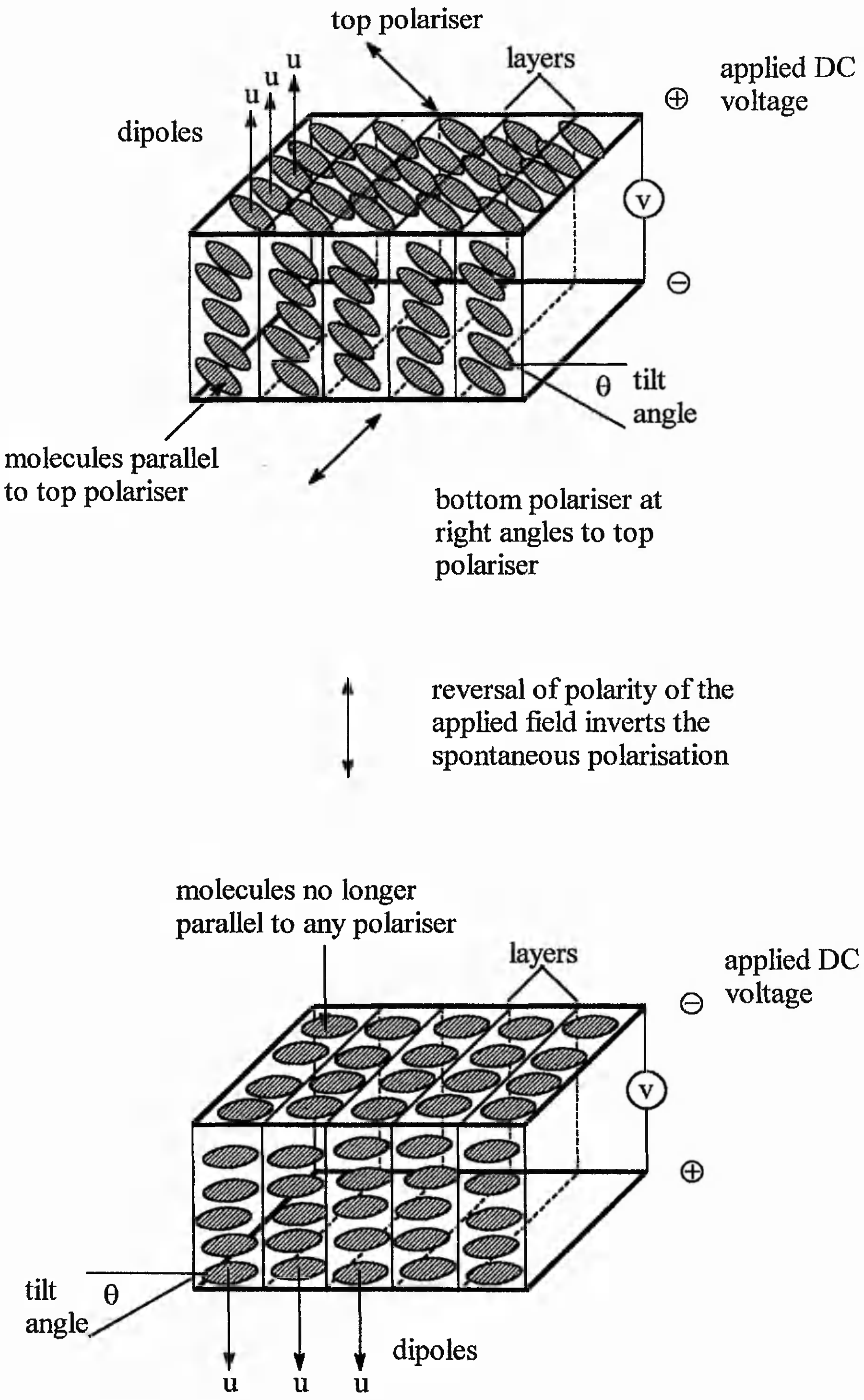

Figure 17 Optical transmission in the SSFLC display. The top cell demonstrates light transmission and the lower cell light extinction.

1.6.2 FERRI- AND ANTIFERRO-ELECTRICITY

In 1989, Chandani *et al.*[18,19] reported the occurrence of two new sub-phases of the S_C*ferroelectric phase, namely S_C*ferrielectric and S_C*antiferroelectric in a sample of 4-(1-methylheptyloxycarbonyl)phenyl 4'-octyloxybiphenyl-4-carboxylate (MHPOBC) (**16**).

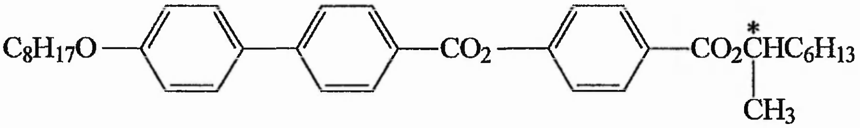

(16)

I 148°C S_A 120.9°C S_C* 119.2°C S_C*_{FERRI} 118.4°C S_C*_{ANTI} 64.0°C S_I*_{ANTI}

Initially it was presumed that for these new phases to be produced the molecule must contain a chiral centre, however, this has been recently been disproved by Nishiyama and co-workers[68,69] following the synthesis of the non-chiral swallow-tailed liquid crystals which exhibit an antiferroelectric-like phase. They proposed that either a bent or zigzag shaped dimer is formed due to the steric interaction between the swallow tails of a molecule and the single end chain of another molecule in adjacent layers. Thus the packing of these bent dimeric species gives rise to an antiferroelectric-like ordering.

Figure 18 shows the various structures of the ferro-, ferri- and antiferro-electric phase types. In the ferroelectric phase type the molecules tilt in the same direction in each layer and hence possess a strong permanent polarisation. On cooling from this phase, the ferrielectric phase (S_C*_γ or S_C*_{FERRI}) is formed. The structure of this phase is such that the ratio of the number of the right-tilting molecules to left-tilting molecules is unequal. The ratio of the number of right-tilting molecules to left-tilting molecules in the phase varies constantly from 2:1 to 3:2 with decreasing temperature. This change observed is known as the Devils staircase[70] and two types are known, either a temperature-induced or an applied field-induced Devils staircase. The ferrielectric phase therefore will have a measurable polarisation with many different layer combinations being possible.

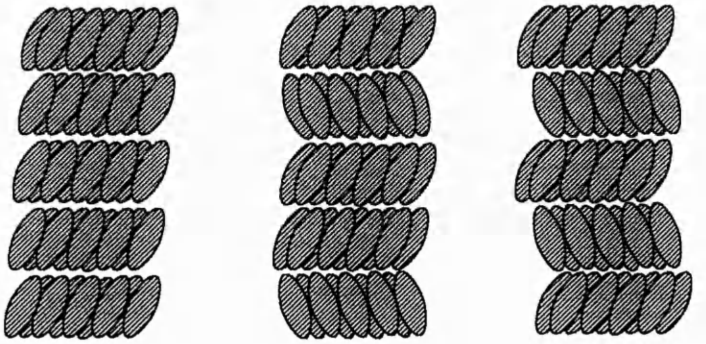

Figure 18 Structures of the ferro-, ferri- and antiferro-electric phase types.

On cooling from the ferrielectric phase, the antiferroelectric phase (S_C*_A or S_C*_{ANTI}) is formed. In this phase the number of left-tilting molecules to right-tilting molecules is equal and hence the phase possesses zero polarisation. Unlike the structure of the normal S_C* phase which is repeated every 360° rotation of the helix, the helical structure of the antiferroelectric phase repeats itself every 180° rotation. The phase therefore has a relatively short pitch and is temperature dependent.

1.6.2.1 ANTIFERROELECTRIC MATERIALS

From an in-depth review of the literature,[71-73] antiferroelectric behaviour is exhibited in compounds comprising a chiral centre near to the rigid aromatic core of the molecule, *e.g.*, MHPOBC (**16**) and TFMHPOBC (**17**). These types of compounds may be considered to consist of four sub-structures: the non-chiral chain; the central core; the connector and; the chiral chain (**Figure 19**).

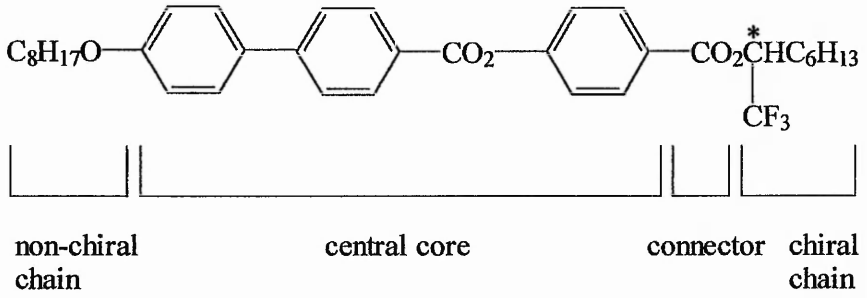

(**17**)

Figure 19 Structural formula of TFMHPOBC (**17**) with four sub-structures: non-chiral chain; central core; connector and; chiral chain.

The chiral chain plays a critical role in the formation of the antiferroelectric phase, however, the variety of the chiral chain is rather limited with the most common being $C^*H(CH_3)C_nH_{2n+1}$ and $C^*H(CF_3)C_nH_{2n+1}$. The latter stabilises the antiferroelectric phase more so than the former. A characteristic feature of the central core structure is that there are usually either three or more aromatic rings, of which at least two are not directly connected, but are separated by a central linking group. Some common linking groups include $-CO_2-$, $-OCH_2-$, $-CH_2O-$, $-CONH-$, however of these the ester linkage is by far the most common. The formation of the antiferroelectric phase is also influenced by the orientation of the ester groups within the molecule. For example, comparing compounds (**18**) and (**19**) shows how the reversal of an ester linkage can either induce or inhibit the formation of the antiferroelectric phase.[74,75]

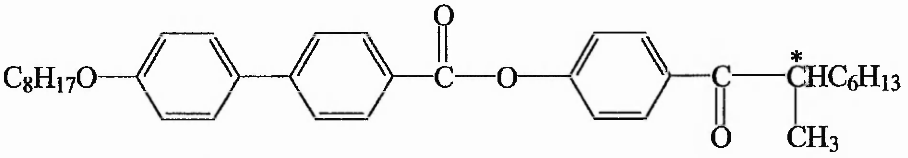 **(18)**

I 136°C S_A 108°C S_C* 49°C S_C*$_{ANTI}$

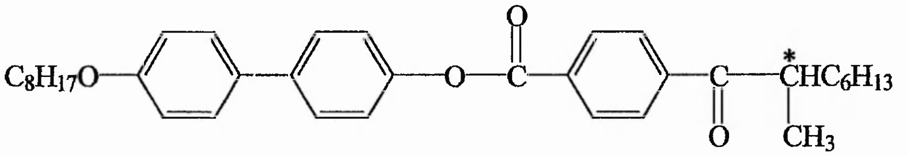 **(19)**

I 132°C S_A 100°C S_C* (no S_C*$_{ANTI}$)

1.6.2.2 DETECTION OF FERRI- AND ANTIFERRO-ELECTRIC PHASE TYPES

In the absence of elaborate electro-optical techniques, the simplest way of detecting the ferri- and antiferro-electric phase types is by thermal optical polarising microscopy. On cooling from the S_A phase, the S_C*$_{FERRO}$ phase is characterised by the appearance of arcs across the fans coupled with either an intense red or blue coloration in the previously homeotropic regions. The colours in this area are temperature dependent and related directly to changes in the pitch length of the S_C*$_{FERRO}$ phase. On further cooling of the S_C*$_{FERRO}$ phase the S_C*$_{FERRI}$ phase is observed, this is characterised by the appearance of an intense milky-white schlieren texture in the pseudohomeotropic region which is in constant motion. On cooling from the S_C*$_{FERRI}$ phase, the S_C*$_{ANTI}$ phase appears and is best characterised by the appearance of a second intense shimmering which sweeps across the plate to leave a translucent pseudohomeotropic area. Alternatively, observation of textures of free standing films of a compound which shows such phases is an excellent means of identification. Thereafter, final confirmation may be ascertained by undertaking rigorous miscibility studies with known materials.

Differential Scanning Calorimetry (DSC) may also be employed as a complimentary technique however, it is rather poor due to the very small enthalpy values associated with these phase changes.

1.6.2.3 APPLICATIONS OF ANTIFERROELECTRIC LIQUID CRYSTALS

The antiferroelectric phase is currently the subject of much research due to its great potential in display devices. The application of an electric field to an antiferroelectric material gives rise to a ferroelectric ordering which can be switched by a reverse pulse and which on removal from an electric field will revert back to the antiferroelectric phase. As shown in **Figure 20**, three states are produced in the switching of the antiferroelectric phase (tristate switching); one antiferroelectric and two ferrolelectric. Tristate switching from the antiferroelectric state to the ferroelectric states occurs at a defined electric field, where there is a sharp switching threshold that differs from normal ferroelectric switching. The presence of a sharp switching threshold in antiferroelectrics leads to improved contrast and multiplexing. Despite antiferroelectric research being in its infancy already a full colour display has been made using antiferroelectric technology.[19]

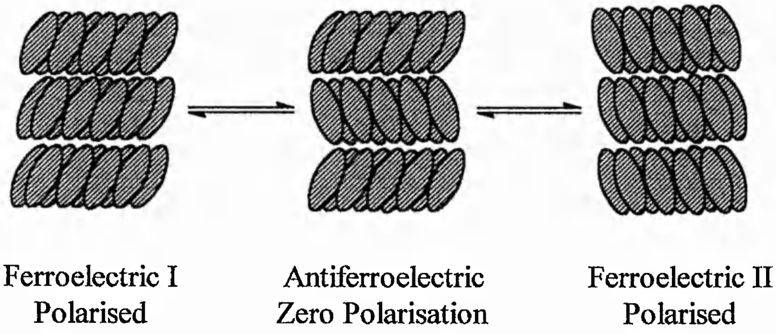

Figure 20 Antiferroelectric (tristate) switching.

1.7 AIMS OF THE PRESENT WORK

In general 1,4-disubstituted phenyl rings are readily employed in the synthesis of calamitic liquid crystals because they possess an exocyclic bond angle of 180° which is conducive for the generation of mesomorphic properties. In comparison compounds containing 1,3-disubstituted phenyl rings, where the exocyclic bond angle is 120°, are generally not liquid crystalline because their geometry severely disrupts the linear packing arrangement of the molecules.

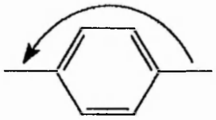

1,4-phenylene
Bond angle, 180°

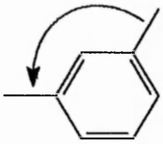

1,3-phenylene
Bond angle, 120°

Research at Nottingham Trent focuses on the synthesis and properties of either 'bent' or 'non-linear' shaped liquid crystalline molecules with particular expertise in thiophene-based liquid crystals.

Thiophene is a five membered heterocycle containing sulphur and is said to be π-excessive because it contains six pi-electrons spread over five nuclei. The chemistry of thiophene is dictated by its π-excessive nature and readily undergoes electrophilic aromatic substitution at the α-positions, *i.e.*, C2- and C5-positions, preferentially to the β-positions, *i.e.*, C3- and C4-positions. 2,5-Disubstitution of thiophene generates an exocyclic bond angle of 148° which is intermediate with respect to 1,4-phenylene (180°; mesomorphic) and 1,3-phenylene (120°; generally non-mesomorphic). Despite their non-linear geometry, suitably 2,5-disubstituted thiophenes are known to be liquid crystalline.[76-80]

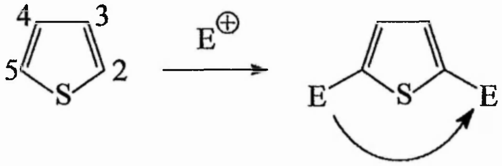

Bond angle = 148°

As discussed earlier there is a strong desire for compounds that exhibit the newly discovered ferri- and antiferro-electric phase types for potential use in novel fast-switching electro-optic display devices. The majority of compounds are composed of suitably substituted 1,4-phenylene rings, however, in 1996, Matharu *et al.*[81] reported the synthesis of a novel thiophene-based liquid crystal (**20**) which exhibits ferro-, ferri- and antiferro-electric properties.

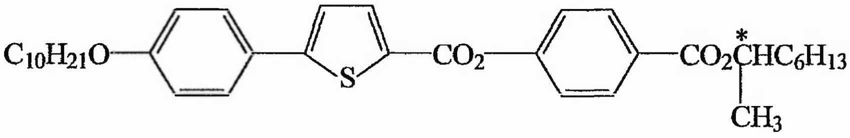

(**20**)

This particular result provided a strong incentive for the research programme because the area of chiral thiophene-based liquid crystals is relatively unexplored and it meets the desire of the liquid crystal community for more examples of ferri- and antiferro-electric compounds. Therefore, the main aim of this research was to synthesise and investigate the mesomorphic properties of a variety of novel thiophene-based esters containing the chiral 1-methylheptyl moiety as a terminal substituent.

The preliminary aim was to investigate the influence of increasing the overall molecular length of compound **(20)** by inserting an extra 1,4-phenylene ring into the chiral end group, *i.e.*, esters derived from 5-(4-n-alkoxyphenyl)thiophene-2-carboxylic acid and (*S*)-1-methylheptyl 4'-hydroxybiphenyl-4-carboxylate rather than (*S*)-1-methylheptyl 4-hydroxybenzoate. However, since it well known that the existence and properties of ferro-, ferri- and antiferro-electric phase types is dependent upon optical purity, it was essential to synthesise large quantities of both (*S*)-1-methylheptyl 4-hydroxybenzoate and (*S*)-1-methylheptyl 4'-hydroxybiphenyl-4-carboxylate from the same batch of *R*-(2)-octanol (Chiralselect grade, 99.9%). Hence compound **(20)** was re-synthesised together with its remaining homologues **[Series I]** and compared with its analogous counterparts **[Series II]** derived from (*S*)-1-methylheptyl 4'-hydroxybiphenyl-4-carboxylate.

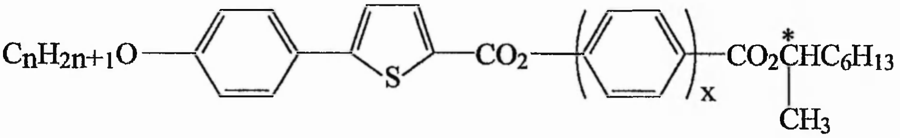

where: x=1, **Series I**
x=2, **Series II**

Series I and **II** were to serve as a useful reference point for the remainder of the research where it was envisaged to synthesise a variety of novel chiral thiophene-based liquid crystals in order to undertake an in depth structure-property relationship which pivoted on two key areas:

i. the influence of altering the central molecular core and;

ii. the influence of using either (*S*)-1-methylheptyl 4-hydroxybenzoate or (*S*)-1-methylheptyl 4'-hydroxybiphenyl-4-carboxylate.

The various proposed molecular architectures are summarised below.

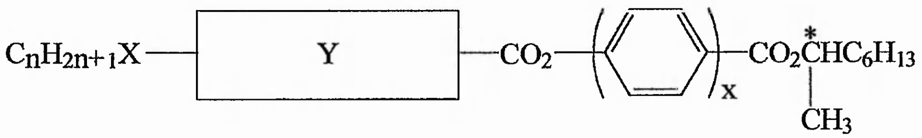

SERIES	X	Y	x
III and IV	-	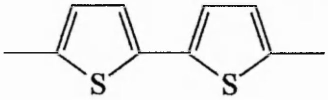	1,2
V and VI	O	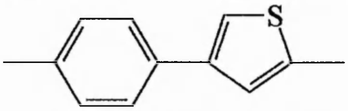	1,2
VII and VIII	-	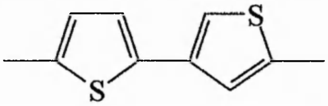	1,2
IX and X	-	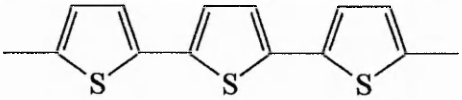	1,2
XI	O	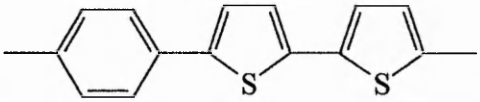	1
XII	O	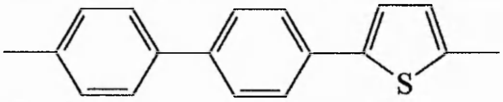	1
XIII	O	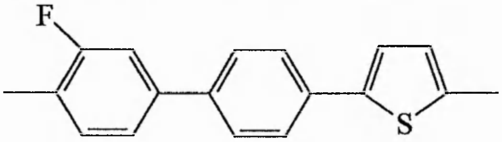	1
XIV	O	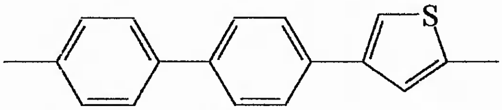	1
XV	O	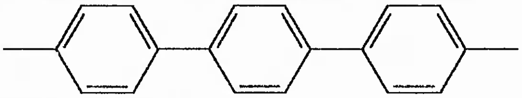	1

Altering the molecular core will obviously influence the molecular geometry and subsequently affect mesophase type and thermal stability. For example, replacement of the molecular core from 'phenyl-thiophene' [**Series I**] to 'thiophene-thiophene' [**Series III**] is expected to lower mesophase thermal stability because the latter is envisaged to possess a poor molecular geometry. However, altering the disposition of the two thiophene rings from 2',2- [**Series III**] to 2',4- [**Series VII**] may generate a structure which relieves geometrical strain and enhances stability.

Increasing the overall molecular geometry by either increasing the number of rings in the molecular core from two to three or using (*S*)-1-methylheptyl 4'-hydroxybiphenyl-4-carboxylate as the source of 'chiral phenol' is expected to enhance mesophase thermal stability. As the inclusion of an extra 1,4-phenylene ring produces compounds with high clearing points the synthesis of a lateral fluorinated compound [**Series XIII**] is expected to generate a low melting, low clearing material and may reduce the occurrence of high order smectic crystal phases. **Series XV** was synthesised to serve as a useful reference for comparison of the three-ring molecular core containing compounds.

EXPERIMENTAL

2. EXPERIMENTAL

2.1 SYNTHESIS OF ESTERS (27a-f) [Series I] AND (28a-i) [Series II] DERIVED FROM 5-(4-n-ALKOXYPHENYL)THIOPHENE-2-CARBOXYLIC ACIDS (24a-i) (Scheme 1)

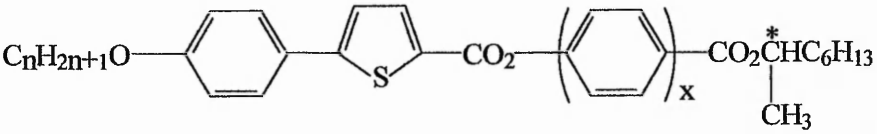

where: x=1, **(27a-f)** **[Series I]**; x=2, **(28a-i)** **[Series II]**

The preparative route leading to an homologous series of chiral thiophene-based esters [**Series I** and **Series II**], derived from 5-(4-n-alkoxyphenyl)thiophene-2-carboxylic acids **(24a-i)** and either (*S*)-1-methylheptyl 4-hydroxybenzoate **(25)** or (*S*)-1-methylheptyl 4'-hydroxybiphenyl-4-carboxylate **(26)**, is depicted in **Scheme 1**.

Commercial 4-bromophenol was alkylated with the appropriate 1-bromoalkane to afford a series of 4-n-alkoxy-1-bromobenzenes **(21a-i)**. This reaction is an example of the Williamson's ether synthesis where the phenolic proton of the 4-bromophenol is sufficiently acidic enough to be removed by a mild base such as potassium carbonate. The resultant phenoxide anion then participates in a nucleophilic substitution reaction with the 1-bromoalkane to afford compounds **(21a-i)**.

SCHEME 1

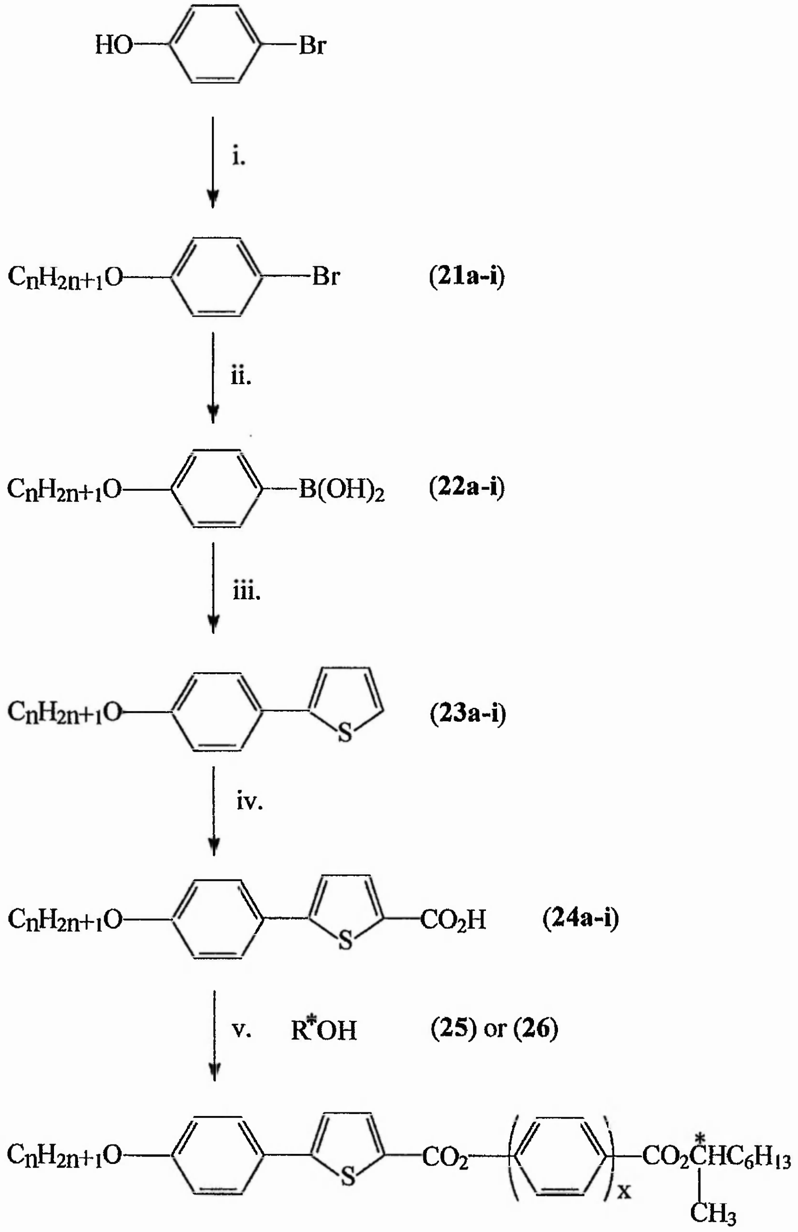

where: x=1, **(27a-f)** **[Series I]**
x=2, **(28a-i)** **[Series II]**

i. $C_nH_{2n+1}Br$, K_2CO_3, acetone, reflux.
ii. a) 1.6M n-BuLi, -78°C, N_2; b) $B(OMe)_3$; c) 4M HCl.
iii. 2-bromothiophene, $Pd(PPh_3)_4$, DME, Na_2CO_3, reflux.
iv. a) 1.6M n-BuLi, -78°C, N_2; b) CO_2, 4M HCl.
v. DCC, DCM, DMAP.

Low temperature (-78°C) lithiation of compounds (**21a-i**) with commercial 1.6M n-butyllithium followed by quenching with an excess of trimethyl borate gave the desired 4-n-alkoxyphenylboronic acids (**22a-i**) in excellent yield (74-91%).

Boronic acid synthesis and the use of boronic acids in the Suzuki coupling[82] reaction has revolutionised the synthesis of bi- and ter-aryls, many of which may have been inaccessible previously due to lengthy and expensive procedures. Boronic acids are particularly useful synthetic intermediates because they are: easy to prepare; usually crystalline; air-stable and; possess a long shelf-life.

Boronic acids may be prepared, as shown overleaf, either from Grignard or organolithium intermediates which have been quenched with trimethyl borate. Acid hydrolysis of the resultant intermediate boronate ester affords the desired boronic acid in good yield. However, the formation of borinic acids[83] is a common and undesirable problem because unlike the boronic acid itself, they are ineffective in the Suzuki coupling reaction. Fortunately, borinic acids may be easily removed by washing the crude boronic acid with hot petroleum ether. The borinic acid is readily soluble whereas the boronic acid is insoluble and hence can be isolated by filtration.

Spectral characterisation of boronic acids can sometimes give confusing results because they can adopt a variety of structures which include the monomer itself, ($ArB(OH)_2$), and di- and tri-meric anhydrides. Consequently, the m.p.s of boronic acids are not usually reproducible and ^1H n.m.r. and i.r. spectroscopic data do not always indicate the presence of the hydroxyl group. Fortunately, the anhydride forms are as equally reactive[84] as the monomeric form in the Suzuki coupling reaction.

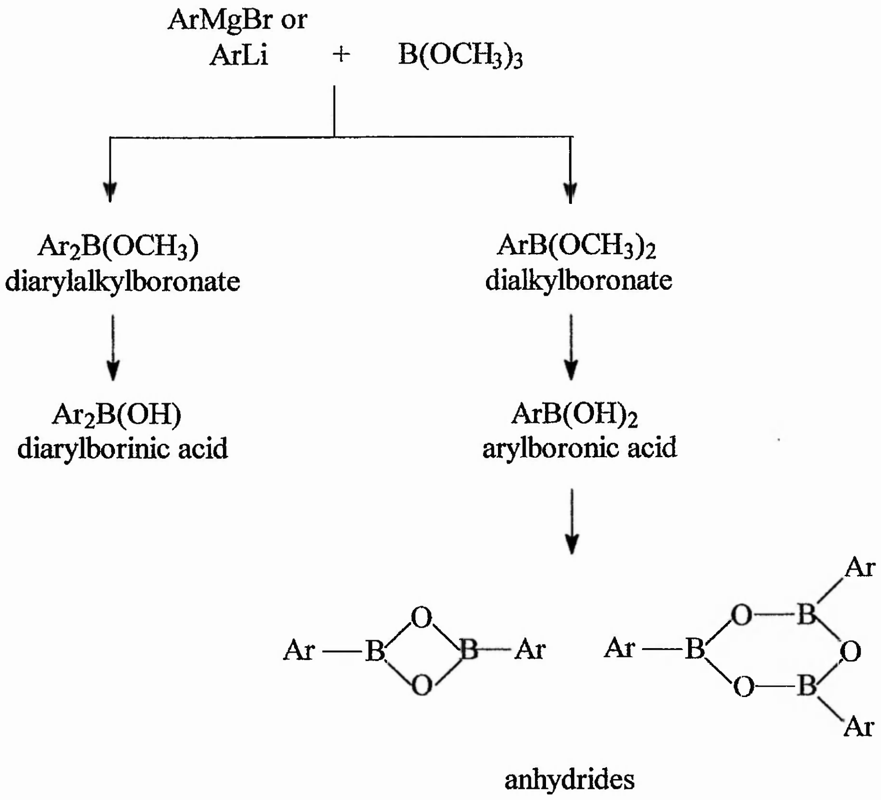

2-Bromothiophene was then cross-coupled with the appropriate boronic acid (**22a-i**) in the presence of a palladium catalyst (Suzuki coupling[82]) to afford the desired 2-(4-n-alkoxyphenyl)thiophenes (**23a-i**). The mechanism of the Suzuki coupling reaction is still unclear, however, Thompson and Gaudino[85] have proposed, as shown overleaf, that the arylboronate dianion (**a**) appears to be the reactive organometallic species which attacks the arylpalladium complex (**b**) to form the diarylpalladium complex (**c**) during the reaction.

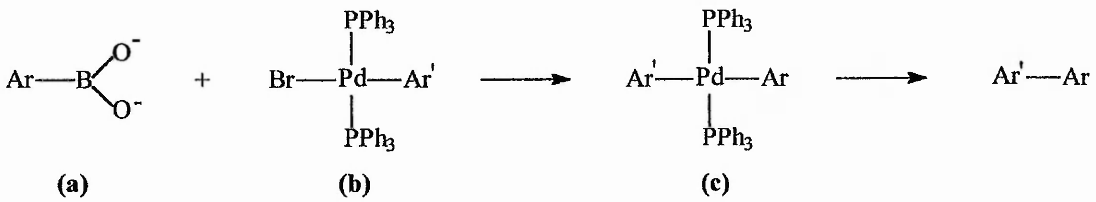

Recently, Martin and Yang[86] have proposed the following catalytic cycle for the Suzuki coupling reaction to show the role of the catalyst with respect to the other reagents.

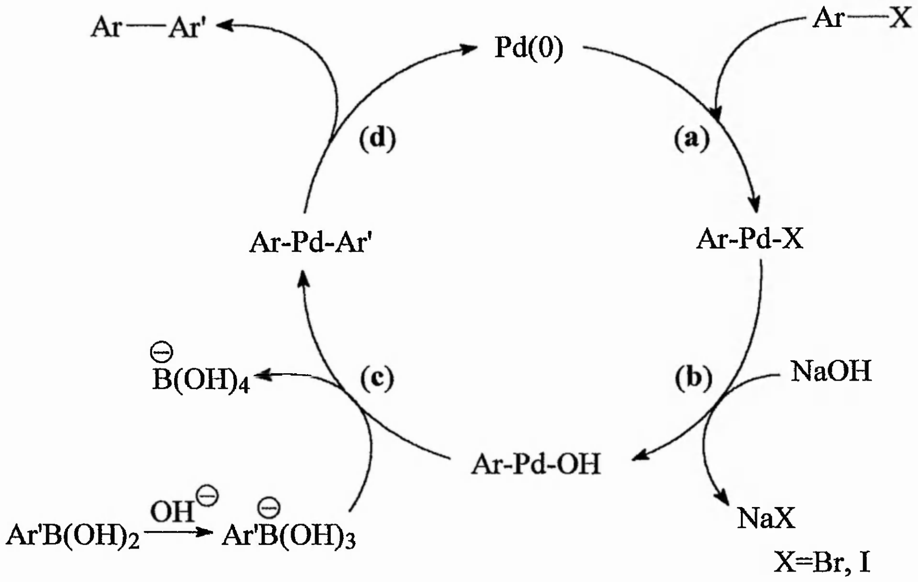

The above catalytic cycle shows the oxidative addition of the palladium(0) complex **(step a)** followed by the displacement of the halide ion from Ar-Pd-X by base **(step b)** to give the organopalladium hydroxide (Ar-Pd-OH) complex. This complex then reacts with the arylboronic acid to give the biaryl palladium complex **(step c)**. Reductive elimination of Ar-Pd-Ar' **(step d)** gives the desired biaryl (Ar-Ar') with regeneration of the catalyst (Pd(0)).

Lithiation and carbonation of compounds (**23a-i**) afforded the 5-(4-n-alkoxyphenyl)thiophene-2-carboxylic acids (**24a-i**). 1,3-*N,N'*-Dicyclohexyl-carbodiimide (DCC) esterification[87] of compounds (**24a-i**) with the appropriate chiral phenol[†] [(**25**) or (**26**)] in the presence of 4-*N*-dimethylaminopyridine (DMAP) as catalyst, furnished the desired chiral esters (**27a-f**) and (**28a-i**), *i.e.*, members of **Series I** and **Series II**, respectively.

DCC esterification[87] is a mild one-pot method which gives esters in high yield. As shown overleaf, the DCC (**b**) acts as a dehydrating agent and initially converts two equivalents of the carboxylic acid (**a**) into its corresponding anhydride (**c**) with the production of dicyclohexylurea (DCU) which precipitates as a white solid from the reaction solution. The anhydride (**c**) then reacts with the dimethylaminopyridine (DMAP) catalyst (**d**) to form a highly reactive acylpyridinium species (**e**) along with a carboxylate anion (**f**). Nucleophilic attack by the phenoxide anion (**h**), generated from the chiral phenol (**g**), on the acylpyridinium intermediate (**e**) affords the desired ester (**i**) with regeneration of DMAP (**d**) and hence the latter functions as a catalyst.

2.1.1 *4-n-Alkoxy-1-bromobenzenes* (**21a-i**)

The appropriate 1-bromoalkane (0.173 mol) was added to a rapidly stirred mixture of 4-bromophenol (15.0 g, 0.087 mol), anhydrous potassium carbonate (23.9 g, 0.173 mol) and dry acetone (200 ml). The reaction mixture was heated under reflux for 12

[†] Synthesised according to the methods of Chin *et al.*[88] and Booth *et al.*[89] as reported in Appendix 1.

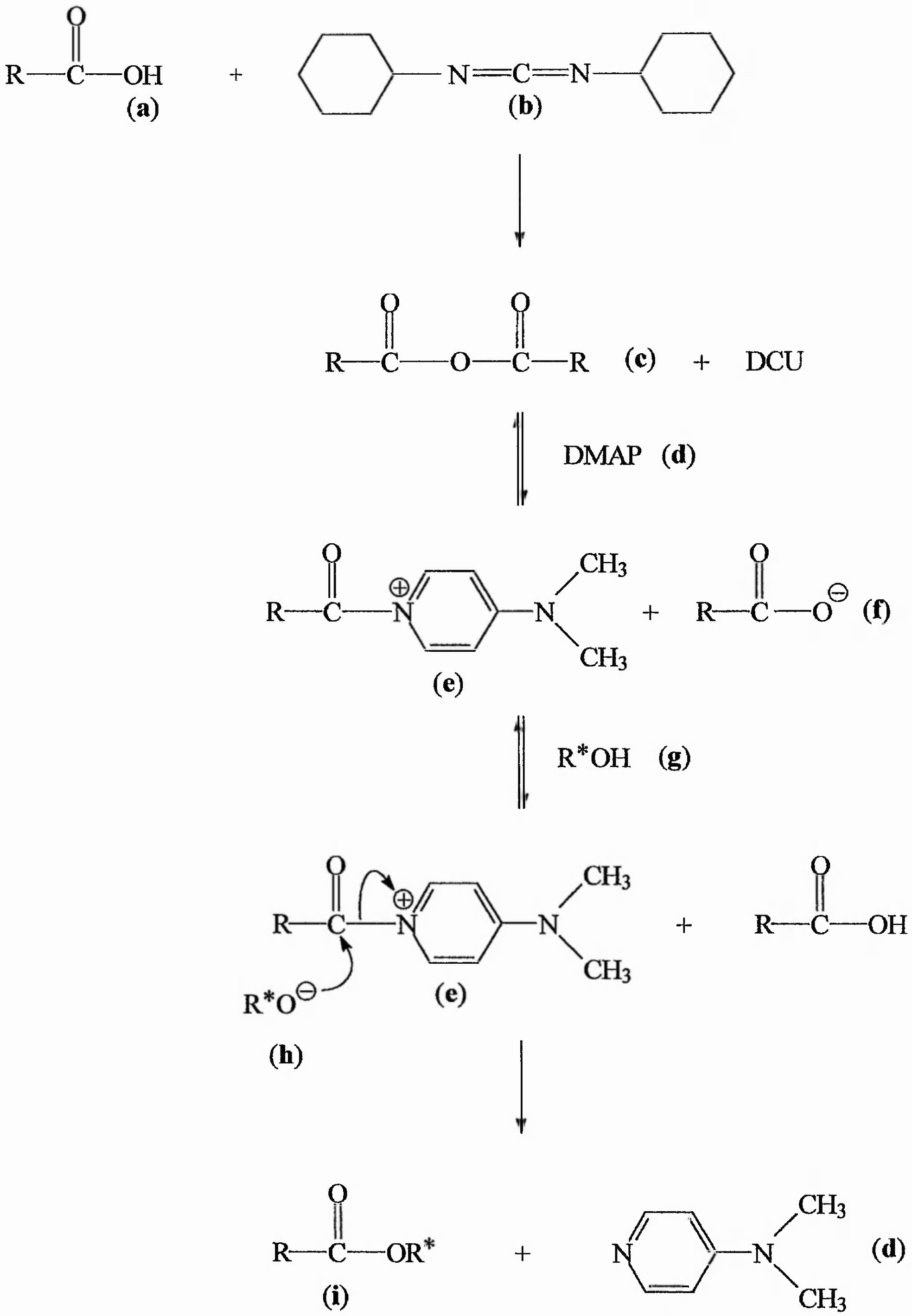

PROPOSED MECHANISM FOR DCC COUPLING

h., cooled and filtered to remove any insoluble material. The solvent was removed under reduced pressure and the crude residue was purified by vacuum distillation (Claisen) to yield the desired 4-n-alkoxy-1-bromobenzene (**21a-i**), (61-78%), as a colourless liquid. Purity of compounds was confirmed by TLC (silica gel, one spot). B.p.s: C_3H_7O (**21a**), 126-128°/1; C_4H_9O (**21b**), 124-126°/0.3; $C_5H_{11}O$ (**21c**), 146-148°/1; $C_6H_{13}O$ (**21d**), 122-124°/0.4; $C_7H_{15}O$ (**21e**), 164-166°/0.6; $C_8H_{17}O$ (**21f**), 160-162°/0.4; $C_9H_{19}O$ (**21g**), 172-174°/0.6; $C_{10}H_{21}O$ (**21h**), 176-178°/0.2; $C_{12}H_{25}O$ (**21i**), 200-202°C/0.25 mm Hg.

The following spectroscopic data refer to 4-n-nonyloxy-1-bromobenzene (**21g**) and are characteristic of the series:

^{1}H n.m.r. δ ($CDCl_3$): 0.9 (3H, t, CH_3), 1.2-1.4 (12H, m, alkyl), 1.7 (2H, quint., $ArOCH_2\underline{CH_2}$), 3.8 (2H, t, $ArO\underline{CH_2}$), 6.7 (2H, d, ArH, J=9Hz), 7.3 (2H, d, ArH, J=9Hz) ppm.

i.r. ν_{max} (Thin film): 2922, 2853, 1590, 1488, 1285, 1244, 1113, 1071, 821 cm^{-1}.

2.1.2 *4-n-Alkoxyphenylboronic acids* (**22a-i**)

In an atmosphere of nitrogen, commercial 1.6M n-BuLi (32.0 ml, 0.051 mol) was added to a stirred, cooled (-78°C) mixture of the appropriate 4-n-alkoxy-1-bromobenzene (**21a-i**) (0.047 mol) and dry THF (100 ml) at such a rate that the temperature did not exceed -65°C. After stirring for a further 2 h. at low temperature, trimethyl borate (22.9 ml, 0.204 mol) was injected and the reaction mixture allowed to warm to room temperature overnight. The reaction mixture was hydrolysed (4M HCl) and the crude product was extracted with diethyl ether (3 x 100 ml). The combined organic extract was dried ($MgSO_4$) and the solvent was removed under reduced pressure to yield the crude boronic acid (**22a-i**) (74-91%), as an off-white solid. The boronic acids (**22a-i**) were used in the next step of the reaction scheme without further purification.

For the purpose of spectroscopic characterisation, a small amount of 4-n-octyloxyphenylboronic acid (**22f**) was purified by washing the crude boronic acid with hot petroleum ether (b.p. 40-60°C) followed by recrystallisation from water. The following spectroscopic data refer to 4-n-octyloxyphenylboronic acid (**22f**) and are typical of the series:

^{1}H n.m.r. δ ($CDCl_3$): 0.9 (3H, t, CH_3), 1.2-1.5 (10H, m, alkyl), 1.8 (2H, quint., $ArOCH_2\underline{CH_2}$), 4.0 (2H, t, $ArO\underline{CH_2}$), 6.8 (2H, d, ArH, J=9Hz), 7.8 (2H, d, ArH, J=9Hz) ppm. No OH signal observed.

i.r. ν_{max} (KBr): 3400-3310 (O-H str.), 2920, 2850, 1605, 1510, 1465, 1251, 822 cm^{-1}.

2.1.3 *2-(4-n-Alkoxyphenyl)thiophenes* (**23a-i**)

A solution of 4-n-alkoxyphenylboronic acid (**22a-i**) (0.032 mol) dissolved in 1,2-dimethoxyethane (20 ml) was added to a vigorously stirred mixture of 2-bromothiophene (5.2 g, 0.032 mol), *tetrakis*(triphenylphosphine)palladium(0) (0.3 mol%), 2M aqueous sodium carbonate (30 ml) and 1,2-dimethoxyethane (30 ml) under dry nitrogen. The mixture was heated under reflux until all the 2-bromothiophene had been consumed (as indicated by TLC). The crude product was extracted with diethyl ether (2 x 100 ml), dried ($MgSO_4$) and the solvent was removed under reduced pressure to yield the crude product as a brown solid. Purification was achieved by flash chromatography on silica gel, eluting with 9:1 petroleum ether (b.p. 40-60°C):dichloromethane (DCM) to afford the desired 2-(4-n-alkoxyphenyl)thiophene **(23a-i)** (56-65%), as a pale yellow solid. Purity of product checked by TLC (silica gel, one spot). M.p.s: C_3H_7O **(23a)**, 81-83° [lit.[79] 77-78°]; C_4H_9O **(23b)**, 74-76° [lit.[79] 67-69°]; $C_5H_{11}O$ **(23c)**, 67-69° [lit.[79] 63-64°]; $C_6H_{13}O$ **(23d)**, 72-74° [lit.[79] 67-68°]; $C_7H_{15}O$ **(23e)**, 68-70° [lit.[79] 68-69°]; $C_8H_{17}O$ **(23f)**, 65-67° [lit.[79] 61-62°]; $C_9H_{19}O$ **(23g)**, 76-78° [lit.[79] 75-76°]; $C_{10}H_{21}O$ **(23h)**, 74-76° [lit.[79] 74-75°]; $C_{12}H_{25}O$ **(23i)**, 77-79°C.

The following spectroscopic data refer to 2-(4-n-nonyloxyphenyl)thiophene **(23g)** and are typical of the series:

^{1}H n.m.r. δ ($CDCl_3$): 0.9 (3H, t, CH_3), 1.2-1.4 (12H, m, alkyl), 1.8 (2H, quint., $ArOCH_2\underline{CH_2}$), 4.0 (2H, t, $ArO\underline{CH_2}$), 6.9 (2H, d, ArH, J=9Hz), 7.0 (1H, d, ThH, J=4Hz), 7.2 (2H, d, ThH, J=4Hz), 7.5 (2H, d, ArH, J=9Hz) ppm.

i.r. ν_{max} (KBr): 2954, 2918, 2848, 1606, 1501, 1262, 854, 681 cm^{-1}.

2.1.4 *5-(4-n-Alkoxyphenyl)thiophene-2-carboxylic acids* (24a-i)

In an atmosphere of nitrogen, 1.6M n-BuLi (12.0 ml, 0.019 mol) was added, dropwise, to a stirred, cooled (-78°C) solution of the appropriate 2-(4-n-alkoxyphenyl)thiophene **(23a-i)** (0.017 mol) in dry THF (50 ml) at such a rate that the temperature did not exceed -65°C. The resulting mixture was stirred for a further 2 h. at -78°C, then poured onto a large excess of solid carbon dioxide and allowed to warm to room temperature overnight. The resultant mixture was acidified (4M HCl), extracted (diethyl ether), dried ($MgSO_4$) and the solvent removed under reduced pressure to yield a green solid (55-59%). The 5-(4-n-alkoxyphenyl)thiophene-2-carboxylic acids (**24a-i**) were then used in the next step of the reaction without further purification.

The following spectroscopic data refer to crude 5-(4-n-octyloxyphenyl)thiophene-2-carboxylic acid (**24f**) and are typical of the series:

^{1}H n.m.r. δ ($CDCl_3$): 0.9 (3H, t, CH_3), 1.2-1.5 (10H, m, alkyl), 1.8 (2H, quint., $ArOCH_2\underline{CH_2}$), 4.0 (2H, t, $ArO\underline{CH_2}$), 4.5 (1H, s, CO_2H, disappears on D_2O shake), 6.9 (2H, d, ArH, J=9Hz), 7.2 (1H, d, ThH, J=4Hz), 7.6 (2H, d, ArH, J=9Hz), 7.8 (1H, d, ThH, J=4Hz) ppm.

i.r. ν_{max} (KBr): 3440-3310 (O-H str.), 2954, 1702 (C=O str.), 1459, 1253, 814 cm^{-1}.

2.1.5 (S)-*4-(1-Methylheptyloxycarbonyl)phenyl 5-(4-n-alkoxyphenyl)thiophene-2-carboxylates* (**27a-f**) **[Series I]**

1,3-*N,N'*-Dicyclohexylcarbodiimide (DCC) (0.37 g, 0.0018 mol) and (*S*)-1-methylheptyl 4-hydroxybenzoate (**25**) (0.38 g, 0.0015 mol) were added to the appropriate 5-(4-n-alkoxyphenyl)thiophene-2-carboxylic acid (**24d-i**) (0.0015 mol) in dry DCM (25 ml). 4-*N*-Dimethylaminopyridine (DMAP) (2-3 crystals) was added and the reaction mixture was left to stir for 2 h. at room temperature. The resultant white precipitate was removed by filtration and discarded. The filtrate was evaporated to dryness and subjected to flash chromatography on silica gel eluting with 1:1

DCM:petroleum ether (b.p. 40-60°C). The solvent was removed from the desired fractions and the crude product was further purified by repeated recrystallisation from ethanol to furnish the desired ester **(27a-f)** **[Series I]**, (46-48%), as a white crystalline solid. Purity of final compound confirmed by TLC (silica gel, one spot) and HPLC (>99%).

The melting points and transition temperatures of compounds **(27a-f)** are listed in **Table 1** (p. 141) of the results and discussion section. The following spectroscopic data refer to (*S*)-4-(1-methylheptyloxycarbonyl)phenyl 5-(4-n-nonyloxyphenyl)-thiophene-2-carboxylate **(27d)** and are typical of the series:

Found: C, 72.24; H, 7.93%. $C_{35}H_{46}O_5S$ requires C, 72.63; H, 8.01%.

MS (*m/z*) 578 (M+), 467, 361, 329.

^{1}H n.m.r. δ ($CDCl_3$): 0.9 (6H, t, 2 x CH_3), 1.2-1.4 (25H, m, alkyl + C*(H)$\underline{CH_3}$), 1.8 (2H, quint., $ArOCH_2\underline{CH_2}$), 4.0 (2H, t, $ArO\underline{CH_2}$), 5.1 (1H, sextet, $\underline{C^*(H)}CH_3$), 6.9 (2H, d, ArH, J=9Hz), 7.3 (1H, d, ThH, J=4Hz), 7.4 (2H, d, ArH, J=9Hz), 7.6 (2H, d, ArH. J=9Hz), 7.9 (1H, d, ThH, J=4Hz), 8.1 (2H, d, ArH, J=9Hz) ppm.

i.r. ν_{max} (KBr): 2954, 2924, 1722, (C=O str.), 1709 (C=O str.), 1605, 1271, 807 cm^{-1}.

2.1.6 (S)-*4'-(1-Methylheptyloxycarbonyl)biphenyl-4-yl 5-(4-n-alkoxyphenyl)-thiophene-2-carboxylates* **(28a-i)** **[Series II]**

Esters **(28a-i)** were prepared according to the method described previously on p. 65 for compounds **(27a-f)**. Quantities: (*S*)-1-methylheptyl 4'-hydroxybiphenyl-4-carboxylate **(26)** (0.49 g, 0.0015 mol); DCC (0.37 g, 0.0018 mol); 5-(4-n-alkoxyphenyl)thiophene-2-carboxylic acid **(24a-i)** (0.0015mol) and; DMAP (2-3 crystals). Yield, 50-64%. Product purity checked by TLC (silica gel, one spot) and HPLC (>99%).

The melting points and transition temperatures for compounds **(28a-i)** are listed in **Table 2** (p. 145) in the results and discussion section. The following spectroscopic data refer to (*S*)-4'-(1-methylheptyloxycarbonyl)biphenyl-4-yl 5-(4-n-nonyloxyphenyl)-thiophene-2-carboxylate **(28g)** and are typical of the series:

Found: C, 74.93; H, 7.55%. $C_{41}H_{50}O_5S$ requires C, 75.19; H, 7.70%.

MS (*m/z*) 654 (M+), 543, 361, 330, 329.

^{1}H n.m.r. δ ($CDCl_3$): 0.9 (6H, t, 2 x CH_3), 1.2-1.4 (25H, m, alkyl + $\mathrm{C^*(H)\underline{CH_3}}$), 1.8 (2H, quint., $\mathrm{ArOCH_2\underline{CH_2}}$), 4.0 (2H, t, $\mathrm{ArO\underline{CH_2}}$), 5.1 (1H, sextet, $\mathrm{\underline{C^*(H)}CH_3}$), 7.0 (2H, d, ArH, J=9Hz), 7.3 (1H, d, ThH, J=4Hz), 7.4 (2H, d, ArH, J=9Hz), 7.6 (6H, unresolved multiplet, ArH), 7.9 (1H, d, ThH, J=4Hz), 8.1 (2H, d, ArH, J=9Hz) ppm.

i.r. ν_{max} (KBr): 2954, 2924, 1722 (C=O str.), 1605, 1449, 1284, 807 cm^{-1}.

2.2 SYNTHESIS OF ESTERS (33a-f) [Series III] AND (34a-i) [Series IV] DERIVED FROM 5'-n-ALKYL-2',2-BITHIENYL-5-CARBOXYLIC ACIDS (32a-i) (Scheme 2)

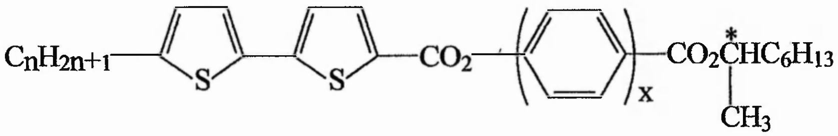

where: x=1, **(33a-f) [Series III]**; x=2, **(34a-i) [Series IV]**

Chiral thiophene esters [**Series III** and **IV**], derived from the 5'-n-alkyl-2',2-bithienyl-5-carboxylic acids (**32a-i**) and the appropriate chiral phenol (**25**) or (**26**), were prepared as outlined in **Scheme 2**.

Nickel-catalysed cross-coupling[90] of commercially available 2-bromothiophene with the Grignard reagent of 2-bromothiophene furnished 2,2'-bithienyl (**29**) in high yield (88%). Friedel-Crafts acylation of 2,2'-bithienyl (**29**) using the appropriate alkanoyl chloride, in the presence of titanium(IV) chloride as catalyst, afforded the intermediate 5-n-alkanoyl-2,2'-bithienyl (**30a-i**). Titanium(IV) chloride was chosen as catalyst in preference to aluminium(III) chloride since the latter causes thiophene to polymerise forming an intractable tar. No significant polymerisation occurs with titanium(IV) chloride and hence is described as a mild Lewis acid catalyst.

As expected, polyacylation was not detected since monoacylation reduces the reactivity of the resultant intermediate towards further electrophilic attack. The powerful –M

SCHEME 2

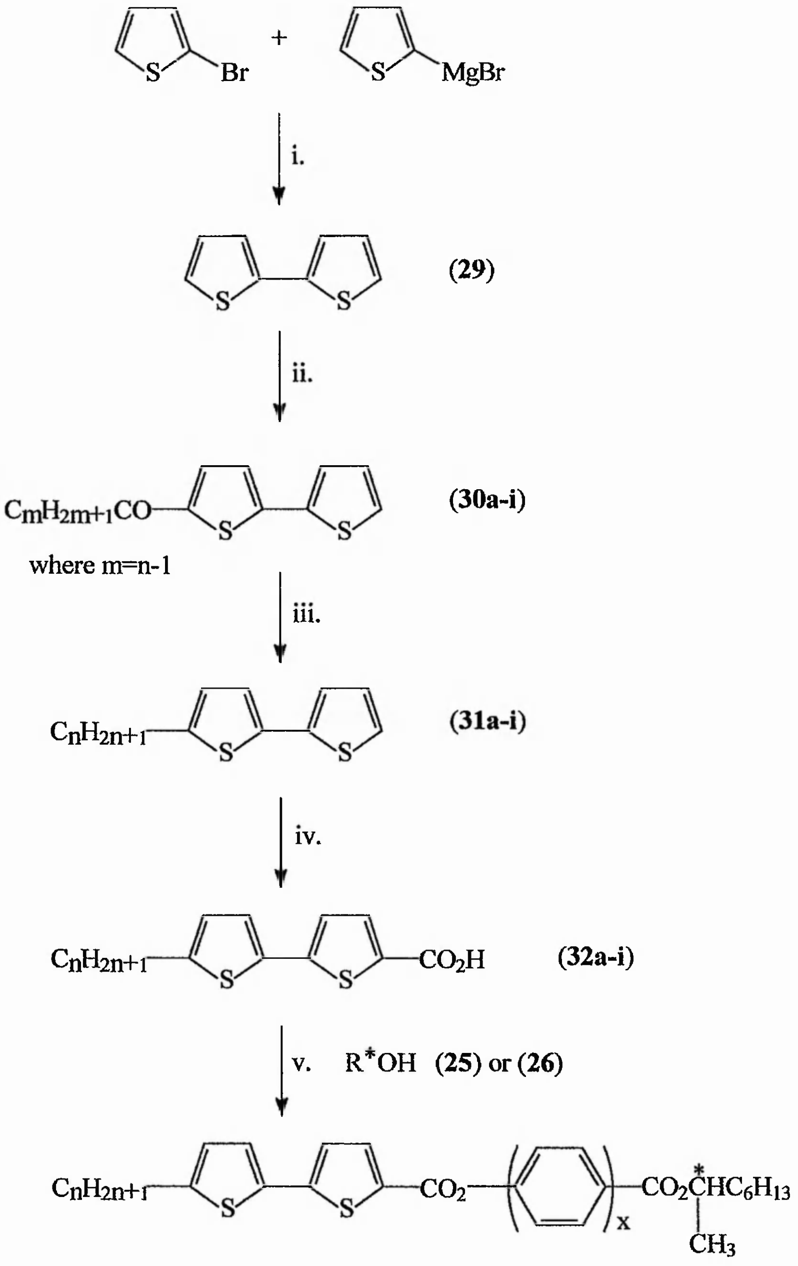

where: x=1, **(33a-f) [Series III]**
x=2, **(34a-i) [Series IV]**

- i. $[(C_6H_5)_2P(CH_2)_3P(C_6H_5)_2]NiCl_2$, diethyl ether.
- ii. $TiCl_4$, $C_mH_{2m+1}COCl$, DCM.
- iii. Hydrazine hydrate, diethylene glycol, KOH.
- iv. a) 1.6M n-BuLi, -78°C, N_2; b) CO_2, 4M HCl.
- v. DCC, DCM, DMAP.

effect of the carbonyl group withdraws electron density from the aromatic core rendering it electron deficient and hence resistant to further electrophilic attack.

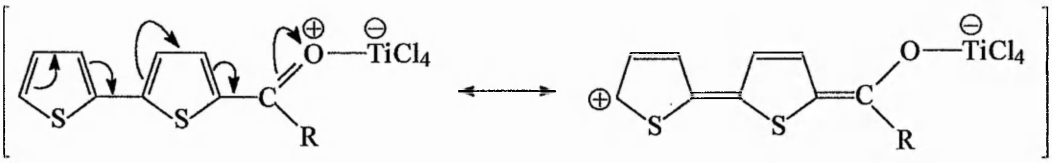

The intermediate ketones (**30a-i**) were reduced to the corresponding alkyl compounds (**31a-i**) using the Huang-Minlon[91] modification of the Wolff-Kishner reaction. The latter involves heating the appropriate ketone with hydrazine hydrate in the presence of a base (usually sodium- or potassium-hydroxide) and is therefore deemed very harsh. In the Huang-Minlon[91] modification the reaction employs a high boiling solvent (diethylene glycol) which moderates the reaction conditions. The mechanism, shown below, proceeds via the formation of a hydrazone intermediate (**a**) which subsequently undergoes reduction in the presence of the base. This results in the loss of nitrogen gas, (**b**) - (**d**), to give the desired alkane product (*e.g.*, **31a-i**).

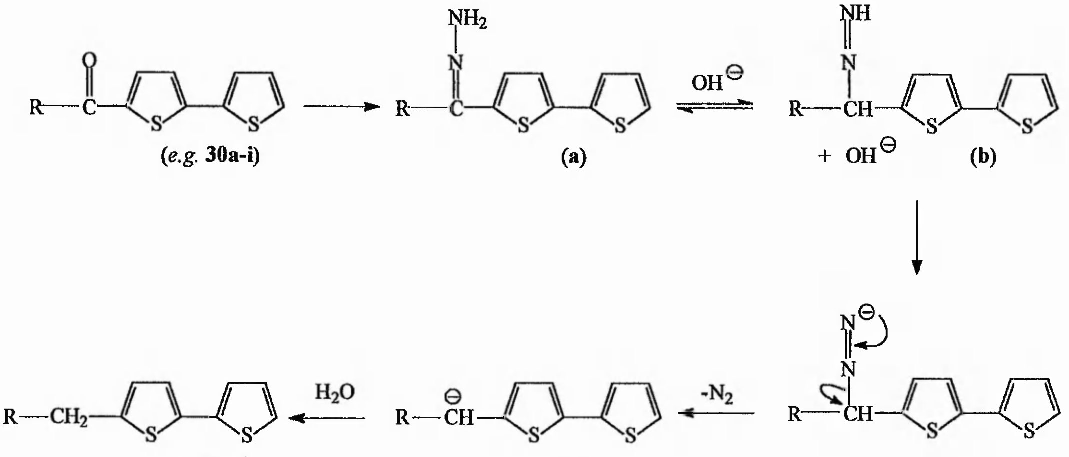

Subsequent treatment of compounds **(31a-i)** with 1.6M n-BuLi followed by quenching with solid carbon dioxide yielded the 5'-n-alkyl-2',2-bithienyl-5-carboxylic acids **(32a-i)**. Esterification of **(32a-i)** with the appropriate chiral phenol **(25)** or **(26)** afforded the desired chiral esters **(33a-f)** **[Series III]** and **(34a-i)** **[Series IV]**.

2.2.1 *2,2'-Bithienyl* **(29)**

In an atmosphere of nitrogen, a solution of 2-bromothiophene (40.0 g, 0.245 mol) dissolved in dry diethyl ether (200 ml) was added, dropwise, to a stirred suspension of magnesium turnings (7.1 g, 0.294 mol) in dry diethyl ether (50 ml) at such a rate that the diethyl ether boiled gently. When the addition was complete, the Grignard reagent was cooled to 0°C, transferred to a pressure-equalising funnel and added, dropwise, to a stirred mixture of 2-bromothiophene (33.0 g, 0.202 mol), [1,3-*bis*(diphenylphosphino)propane]nickel(II) chloride (1.1 g, 0.002 mol) and dry diethyl ether (100 ml) maintained in an inert atmosphere of nitrogen at 0 to -10°C. After the addition was complete, the reaction mixture was poured onto saturated ammonium carbonate solution, extracted with diethyl ether (4 x 150 ml), dried ($MgSO_4$) and the solvent removed *in vacuo*. Purification was achieved by vacuum distillation (Claisen) to afford the pure 2,2'-bithienyl **(29)** as a pale yellow liquid, 29.4 g (88%), which solidified on standing, b.p. 100-101°C/0.3 mm Hg, m.p. 33-34°C (lit.[92] m.p. 33°C). Product purity checked by TLC (silica gel, one spot).

^{1}H n.m.r. δ ($CDCl_3$): 6.9-7.1 (6H, unresolved multiplet, ThH) ppm.

i.r. ν_{max} (KBr): 3103, 3063, 1415, 1206, 1049, 828, 697 cm^{-1}.

2.2.2 *5-n-Alkanoyl-2,2'-bithienyls* (**30a-i**)

In an atmosphere of nitrogen, titanium(IV) chloride (2.96 ml, 0.027 mol) was added, dropwise, to a stirred, cooled (-10°C) solution of 2,2'-bithienyl (**29**) (4.5 g, 0.027 mol) and the appropriate alkanoyl chloride (0.027 mol) in dry DCM (100 ml). After the addition was complete, the reaction mixture was left to stir for 3 h. at room temperature. The reaction mixture was then hydrolysed with ice/concentrated hydrochloric acid (100 ml) and the crude product was extracted with DCM (2 x 100 ml). The combined organic extract was washed with saturated sodium hydrogen carbonate solution (2 x 80 ml), water (2 x 80 ml), dried ($MgSO_4$) and the solvent removed *in vacuo*. Purification was achieved by recrystallisation from ethanol to afford the desired 5-n-alkanoyl-2,2'-bithienyl (**30a-f**) as a green solid (64-84%). Product purity checked by TLC (silica gel, one spot). M.p.s: C_2H_5CO (**30a**), 88-90° [lit.[93] 91-92°]; C_3H_7CO (**30b**), 83-84° [lit.[93] 76-77°]; C_4H_9CO (**30c**), 84-86° [lit.[93] 85-86°]; $C_5H_{11}CO$ (**30d**), 79-81° [lit.[93] 75-76°]; $C_6H_{13}O$ (**30e**), 87-89° [lit.[93] 83-84°]; $C_7H_{15}CO$ (**30f**), 82-84° [lit.[93] 75-77°]; $C_8H_{17}CO$ (**30g**), 77-79° [lit.[93] 76-77°]; $C_9H_{19}CO$ (**30h**), 89-91° [lit.[93] 78-80°]; $C_{11}H_{23}CO$ (**30i**), 96-98° [lit.[93] 82-84°C].

The following data refer to 5-n-nonanoyl-2,2'-bithienyl (**30g**) and are typical of the series:

^1H n.m.r. δ ($CDCl_3$): 0.9 (3H, t, CH_3), 1.2-1.4 (10H, m, alkyl), 1.8 (2H, quint., $ThCOCH_2\underline{CH_2}$), 2.9 (2H, t, $ThCO\underline{CH_2}$), 7.0-7.6 (5H, unresolved multiplet, ThH) ppm.

i.r. ν_{max} (KBr): 2918, 2848, 1650 (C=O str.), 1451, 801, 696 cm^{-1}.

2.2.3 *5-n-Alkyl-2,2'-bithienyls* (**31a-i**)

A mixture of the appropriate 5-n-alkanoyl-2,2'-bithienyl (**30a-i**) (0.022 mol), diethylene glycol (150 ml) and hydrazine hydrate (21.3 ml, 0.44 mol) was heated slowly to reflux over a 2 h. period. The excess of hydrazine hydrate was then removed by atmospheric distillation and the internal temperature of the reaction mixture was raised to 210°C for 10 min. Potassium hydroxide (24.6 g, 0.44 mol) was added and the mixture was re-heated to reflux for a further 3 h. period. After cooling to room temperature the reaction mixture was quenched with 4M hydrochloric acid, extracted with diethyl ether, dried ($MgSO_4$) and the solvent removed *in vacuo* to yield the crude product as an orange liquid. Purification was achieved by vacuum distillation (Kugelrohr) to afford the pure 5-n-alkyl-2,2'-bithienyl (**31a-i**) as a clear yellow oil (67-88%) which solidified on standing. Product purity checked by TLC (silica gel, one spot). B.p.s: C_3H_7 (**31a**), 135°/0.2 [lit.[93] 125°/0.01]; C_4H_9 (**31b**), 135°/0.9 [lit.[93] 150°/0.4]; C_5H_{11} (**31c**), 115°/0.1 [lit.[93] 170°/0.1]; C_6H_{13} (**31d**), 180°/0.2 [lit.[93] 155°/0.02]; C_7H_{15} (**31e**), 190°/0.3 [lit.[93] 170°/0.05]; C_8H_{17} (**31f**), 205°/0.1 [lit.[93] 195°/0.05]; C_9H_{19} (**31g**), 180°/0.01 [lit.[93] 205°/0.05]; $C_{10}H_{21}$ (**31h**), 240°/0.5 [lit. [93] 210°C/0.3 mm Hg]; $C_{12}H_{25}$ (**31i**)[†].

The following data refer to 5-n-decyl-2,2'-bithienyl (**31h**) and are typical of the series:

[†] 5-n-dodecyl-2,2'-bithienyl purified by flash chromatography on silica gel eluting with 1:4 DCM:petroleum ether (b.p. 40-60°C).

^1H n.m.r. δ ($CDCl_3$): 0.9 (3H, t, CH_3), 1.2-1.4 (14H, m, alkyl), 1.8 (2H, quint., $ThCH_2\underline{CH_2}$), 2.8 (2H, t, $Th\underline{CH_2}$), 6.6-7.2 (5H, unresolved multiplet, ThH) ppm.

i.r. ν_{max} (KBr): 2949, 2925, 2920, 2848, 1466, 1426, 884, 800, 683 cm^{-1}.

2.2.4 *5'-n-Alkyl-2',2-bithienyl-5-carboxylic acids* (**32a-i**)

The 5'-n-alkyl-2',2-bithienyl-5-carboxylic acids (**32a-i**) were prepared according to the method described previously on p. 64 for compounds (**24a-i**). Quantities: 1.6M n-BuLi (5.0 ml, 0.008 mol); 5-n-alkyl-2,2'-bithienyl (**31a-i**) (0.007 mol) and; THF (25 ml). After work-up, the crude carboxylic acids were purified by recrystallisation from ethanol to afford the 5'-n-alkyl-2',2-bithienyl-5-carboxylic acids[†] (**32a-i**) (63-84%), as pale yellow solids. Product purity checked by TLC (silica gel, one spot). Melting points and transition temperatures: C_6H_{13} (**32d**), K-N 118.6°C; I 167.1° N 105.5° K; $C_{12}H_{25}$ (**32i**), K-N 106.7°C; I 149.4° N 140.4° S_C 100.1°C.

The following spectroscopic data refer to 5'-n-octyl-2',2-bithienyl-5-carboxylic acid (**32f**) and are typical of the series:

^1H n.m.r. δ ($CDCl_3$): 0.9 (3H, t, CH_3), 1.2-1.4 (10H, m, alkyl), 1.8 (2H, quint., ($ThCH_2\underline{CH_2}$), 2.8 (2H, t, $Th\underline{CH_2}$), 6.7 (1H, d, ThH, J=4Hz), 7.0 (2H, d, ThH, J=4Hz), 7.7 (1H, d, ThH, J=4Hz) ppm. No OH proton detected.

i.r. ν_{max} (KBr): 3443-3100 (O-H str.), 2922, 2851, 1690 (C=O str.), 1526, 769 cm^{-1}.

[†] The carboxylic acids are themselves liquid crystalline and homologues n=7-10 are reported in the thesis of SNR Shirazi.[78]

2.2.5 (S)*-4-(1-Methylheptyloxycarbonyl)phenyl 5'-n-alkyl-2',2-bithienyl-5-carboxylates* (33a-f) [Series III]

Esters **(33a-f)** **[Series III]** were prepared according to the procedure described on p. 65 for compounds **(27a-f)** by mixing (*S*)-1-methylheptyl 4-hydroxybenzoate **(25)** (0.38 g, 0.0015 mol) and 5'-n-alkyl-2',2-bithienyl-5-carboxylic acid **(32d-i)** (0.0015 mol) with DCC (0.37 g, 0.0018 mol) in the presence of DMAP (2-3 crystals). Purification was achieved by flash chromatography eluting with 7:3 chloroform:petroleum ether (b.p. 40-60°C) followed by repeated recrystallisation from ethanol to afford the desired carboxylates **(33a-f)** as white crystalline solids (50-71%). Product purity checked by TLC (silica gel, one spot) and HPLC (>99%).

The melting points and transition temperatures of compounds **(33a-f)** are listed in **Table 3** (p. 151) of the results and discussion section. The following data refer to the (*S*)-4-(1-methylheptyloxycarbonyl)phenyl 5'-n-dodecyl-2',2-bithienyl-5-carboxylate **(33f)** and are typical of the series:

Found: C, 70.62; H, 8.39%. $C_{36}H_{50}O_4S_2$ requires C, 70.78; H, 8.25%.

MS (*m/z*) 610 (M+), 499, 361.

^{1}H n.m.r. δ ($CDCl_3$): 0.9 (6H, t, 2 x CH_3), 1.2-1.4 (31H, m, alkyl + C*(H)$\underline{CH_3}$), 1.8 (2H, quint., Th$CH_2\underline{CH_2}$), 2.8 (2H, t, Th$\underline{CH_2}$), 5.2 (1H, sextet, $\underline{C*(H)}CH_3$), 6.7 (1H, d, ThH, J=4Hz), 7.2 (2H, d, ThH, J=4Hz), 7.3 (2H, d, ArH, J=9Hz), 7.9 (1H, d, ThH, J=4Hz), 8.1 (2H, d, ArH, J=9Hz) ppm.

i.r. ν_{max} (KBr): 2923, 2855, 1719 (C=O str.), 1603, 1273, 1075, 799 cm^{-1}.

2.2.6 (S)-*4'-(1-Methylheptyloxycarbonyl)biphenyl-4-yl 5'-n-alkyl-2',2-bithienyl-5-carboxylates* **(34a-i) [Series IV]**

Esters **(34a-i)** were prepared according to the procedure described on p. 65 for compounds **(27a-f)**. Quantities: DCC (0.25 g, 0.0012 mol); (*S*)-1-methylheptyl 4'-hydroxybiphenyl-4-carboxylate **(26)** (0.33 g, 0.001 mol); 5'-n-alkyl-2',2-bithienyl-5-carboxylic acid **(32a-i)** (0.001 mol) and; DMAP (2-3 crystals). Yield, 53-67%. Product purity confirmed by TLC (silica gel, one spot) and HPLC (>99%).

The melting points and transition temperatures of compounds **(34a-i)** are listed in **Table 4** (p. 155) of the results and discussion section. The following data refer to the (*S*)-4'-(1-methylheptyloxycarbonyl)biphenyl-4-yl 5'-n-dodecyl-2',2-bithienyl-5-carboxylate **(34i)** and are typical of the series:

Found: C, 73.38; H, 7.94%. $C_{42}H_{54}O_4S_2$ requires C, 73.43; H, 7.92%.

MS (*m/z*) 686 (M+), 363, 362, 361, 329.

^{1}H n.m.r. δ ($CDCl_3$): 0.9 (6H, t, 2 x CH_3), 1.2-1.4 (31H, m, alkyl + C*H($\underline{CH_3}$)), 1.8 (2H, quint., ThCH$_2\underline{CH_2}$), 2.8 (2H, t, Th$\underline{CH_2}$), 5.2 (1H, sextet, $\underline{C^*(H)}$CH$_3$), 6.8 (1H, d, ThH, J=4Hz), 7.2 (2H, unresolved multiplet, ThH), 7.3 (2H, d, ArH, J=9Hz), 7.7 (4H, unresolved multiplet, ArH), 7.9 (1H, d, ThH, J=4Hz), 8.1 (2H, d, ArH, J=9Hz) ppm.

i.r. ν_{max} (KBr): 2955, 2921, 2849, 1716 (C=O str.), 1282, 1189, 797 cm^{-1}.

2.3 SYNTHESIS OF ESTERS (40a-f) [Series V] AND (41a-f) [Series VI] DERIVED FROM 4-(4-n-ALKOXYPHENYL)THIOPHENE-2-CARBOXYLIC ACIDS (39a-f) (Scheme 3)

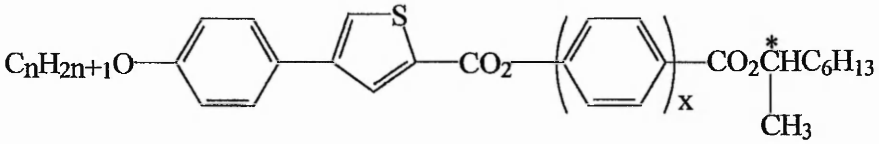

where: x=1, **(40a-f) [Series V]**; x=2, **(41a-f) [Series VI]**

The synthetic route leading to the preparation of the chiral thiophene-based esters **[Series V-VI]**, derived from the 4-(4-n-alkoxyphenyl)thiophene-2-carboxylic acids **(39a-f)** and the appropriate chiral phenol **(25)** or **(26)**, is depicted in **Scheme 3.**

The preparation of 4-bromothiophene-2-carboxaldehyde **(35)** was deemed as the key step in the synthesis. Substituted thiophenes may be easily brominated but, in many cases, isomers and polybrominated products are formed and the resultant mixture is extremely difficult to separate. To temper polybromination and control the position of substitution, 4-bromothiophene-2-carboxaldehyde **(35)** was prepared according to the methods reported by Goldfarb *et al.*[94] and Chadwick *et al.*[95] In these procedures, elemental bromine is added to a mixture of thiophene-2-carboxaldehyde in the presence of an excess of anhydrous aluminium(III) chloride. As shown on p. 79, the oxygen atom of the carbonyl group forms a complex with aluminium(III) chloride, which leaves a positive charge either on C-3 or C-5 of the thiophene ring. Hence, the C-4 position is accessible for electrophilic attack and thus the desired 4-bromothiophene-2-

SCHEME 3

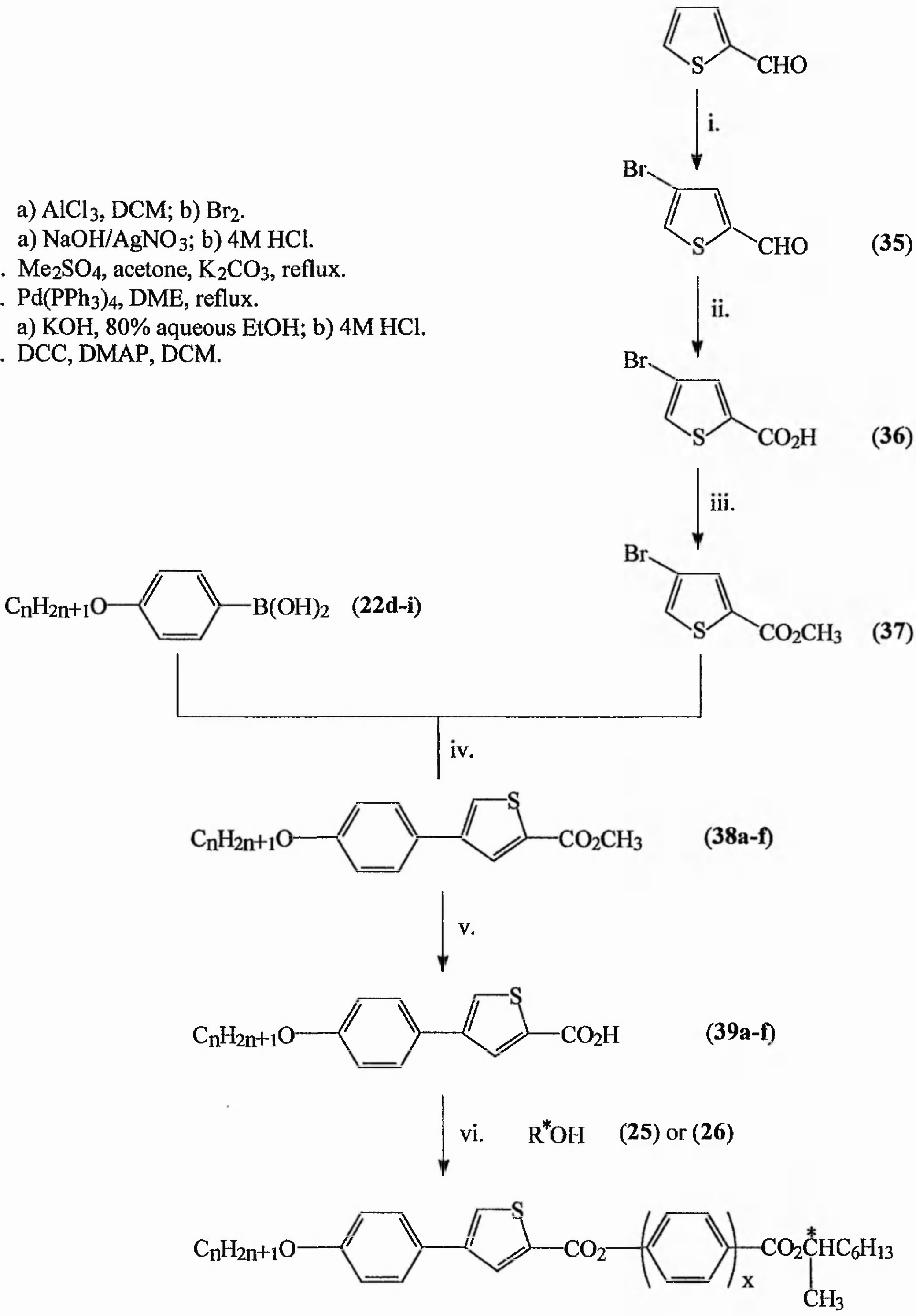

i. a) $AlCl_3$, DCM; b) Br_2.
ii. a) $NaOH/AgNO_3$; b) 4M HCl.
iii. Me_2SO_4, acetone, K_2CO_3, reflux.
iv. $Pd(PPh_3)_4$, DME, reflux.
v. a) KOH, 80% aqueous EtOH; b) 4M HCl.
vi. DCC, DMAP, DCM.

where: x=1, **(40a-f) [Series V]**
x=2, **(41a-f) [Series VI]**

carboxaldehyde (**35**) is formed. In the absence of $AlCl_3$, a mixture of both 4- and 5-bromothiophene-2-carboxaldehyde is formed which is difficult to purify.

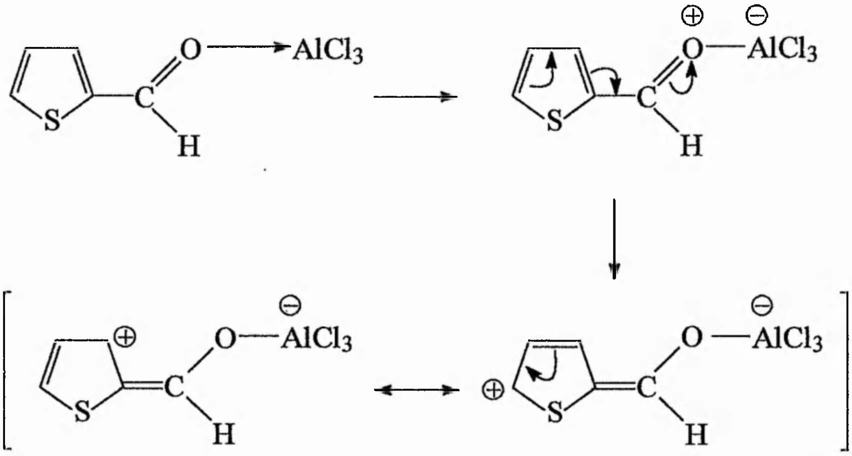

Oxidation of compound (**35**) using silver nitrate and sodium hydroxide afforded the intermediate 4-bromothiophene-2-carboxylic acid (**36**), which was subsequently converted into its methyl ester (**37**) in the presence of dimethyl sulphate in excellent yield (81%). Palladium-catalysed cross-coupling of (**37**) with the appropriate 4-n-alkoxyphenylboronic acid (**22a-f**) afforded the desired methyl 4-(4-n-alkoxyphenyl)thiophene-2-carboxylates (**38a-f**) in good yield (62-74%). Base hydrolysis (ethanolic potassium hydroxide) of compounds (**38a-f**) furnished the desired 4-(4-n-alkoxyphenyl)thiophene-2-carboxylic acids (**39a-f**) which were then esterified with the appropriate chiral phenol (**25**) or (**26**), to yield the desired chiral esters (**40a-f**) and (**41a-f**), *i.e.*, members of **Series V** and **VI**, respectively.

Ladd *et al.*[96] have reported an alternative route to the preparation of 4-bromothiophene-2-carboxylic acid (**36**) starting from 2,4,5-tribromothiophene.

Initially, 2,4,5-tribromothiophene is selectively lithiated (2.5M n-butyllithium) and quenched with water to afford 2,4-dibromothiophene. Thereafter, a second lithiation is then undertaken on 2,4,5-tribromothiophene which replaces the bromo-substituent at the C-2 position, followed by a carbon dioxide quench to furnish the desired 4-bromothiophene-2-carboxylic acid (**36**). Although this route reports similar yields to those reported by Goldfarb *et al.*[94] and Chadwick *et al.*[95] (~65%), it was not used because of the expensive nature of the 2,4,5-tribromothiophene starting material and possible troublesome purification.

2.3.1 *4-Bromothiophene-2-carboxaldehyde* (**35**)

Elemental bromine (8.8 ml, 0.17 mol) was added, dropwise, to a stirred mixture of freshly distilled thiophene-2-carboxaldehyde (13.1 ml, 0.14 mol) and anhydrous aluminium(III) chloride (37.3 g, 0.28 mol) maintained below 60°C. CAUTION - exercise extreme care on mixing due to the evolution of HBr gas. The reaction mixture was stirred overnight at room temperature, poured onto ice/concentrated hydrochloric acid (100 ml) and left to hydrolyse for 30 min. The crude product was extracted into dichloromethane (2 x 150 ml), washed with water (2 x 100 ml), brine (2 x 100 ml) and dried ($MgSO_4$). The solvent was removed *in vacuo* and the crude residue was recrystallised from aqueous methanol to yield the pure 4-bromothiophene-2-carboxaldehyde (**35**), 19.8 g (73%), m.p. 45-47°C, (lit.[94] 46.6-47.4°C) as a white crystalline solid. Product purity checked by TLC (silica gel, one spot).

^1H n.m.r. δ ($CDCl_3$): 7.6 (1H, d, ThH, J=2Hz), 7.7 (1H, d, ThH, J=2Hz), 9.8 (1H, s, CHO) ppm.

i.r. ν_{max} (KBr): 3096, 2923, 2852, 1667 (C=O str.), 1408, 1228, 1163, 783, 662 cm^{-1}.

2.3.2 *4-Bromothiophene-2-carboxylic acid* (**36**)

4-Bromothiophene-2-carboxaldehyde (**35**), (17.3 g, 0.091 mol) was added in one portion to a stirred mixture of aqueous silver nitrate solution (30.9 g, 0.182 mol in water (50 ml)) and aqueous sodium hydroxide (14.6 g, 0.364 mol in water (50 ml)). After stirring for 1 h., the inorganic salts were removed by filtration and discarded whereas the filtrate was acidified (4M HCl). The ensuing white precipitate was extracted with diethyl ether (2 x 100 ml), washed with water (2 x 100 ml) and dried ($MgSO_4$). The solvent was removed *in vacuo* and the crude residue was recrystallised from cyclohexane to yield the desired 4-bromothiophene-2-carboxylic acid (**36**), 14.9 g (80%), m.p. 122-124°C, (lit.[97] 122-122.5°C) as a white crystalline solid. Product purity checked by TLC (silica gel, one spot).

^1H n.m.r. δ ($CDCl_3$): 7.55 (1H, d, ThH, J=2Hz), 7.8 (1H, d, ThH, J=2Hz), 10.4 (1H, s, CO_2H, disappears on D_2O shake) ppm.

i.r. ν_{max} (KBr): 3449-3100 (O-H str.), 3086, 2917, 1675 (C=O str.), 1525, 748 cm^{-1}.

2.3.3 *Methyl 4-bromothiophene-2-carboxylate* (**37**)

4-Bromothiophene-2-carboxylic acid (14.6 g, 0.071 mol) (**36**) was added to a stirred mixture of anhydrous potassium carbonate (19.6 g, 0.142 mol), dimethyl sulphate (6.7 ml, 0.071 mol) and dry acetone (100 ml). The reaction mixture was heated under reflux for 4 h., cooled and filtered to remove any insoluble impurities. The filtrate was evaporated to dryness and the crude residue was purified by vacuum distillation

(Kugelrohr) to afford the desired methyl 4-bromothiophene-2-carboxylate (**37**), 12.6 g (81%), b.p. 95°C/0.02 mm Hg (lit.[98] 113-115/9 mm Hg) as a colourless oil. Product purity confirmed by TLC (silica gel, one spot).

^{1}H n.m.r. δ ($CDCl_3$): 4.0 (3H, s, CO_2CH_3), 7.4 (1H, d, ThH, J=2Hz), 7.7 (1H, d, ThH, J=2Hz) ppm.

i.r. ν_{max} (Thin film): 2953, 2870, 1716 (C=O str.), 1517, 1435, 1182, 1097, 769 cm^{-1}.

2.3.4 *Methyl 4-(4-n-alkoxyphenyl)thiophene-2-carboxylates* (**38a-f**)

Compounds (**38a-f**) were prepared according to the method described earlier on p. 63 for compound (**23a-i**). Quantities: methyl 4-bromothiophene-2-carboxylate (**37**) (1.5 g, 0.007 mol); 4-n-alkoxyphenylboronic acid (**22a-f**) (0.007 mol); 2M sodium carbonate (30 ml); *tetrakis*(triphenylphosphine)palladium(0) (0.3 mol%) and; 1,2-dimethoxyethane (30 ml). After work-up, purification of the crude product was achieved by flash chromatography, eluting with 2:1 petroleum ether (b.p. 40-60°C):dichloromethane, followed by recrystallisation from aqueous methanol to furnish the desired methyl 4-(4-n-alkoxyphenyl)thiophene-2-carboxylates (**38a-f**), (62-74%), as white crystalline solids. Product purity confirmed by TLC (silica gel, one spot). M.p.s: $C_6H_{13}O$ (**38a**), 74-76°; $C_7H_{15}O$ (**38b**) 79-81°; $C_8H_{17}O$ (**38c**), 84-86°; $C_9H_{19}O$ (**38d**), 88-90°; $C_{10}H_{21}O$ (**38e**) 82-84°, $C_{12}H_{25}O$ (**38f**), 88-90°C.

The following data refer to methyl 4-(4-n-decyloxyphenyl)thiophene-2-carboxylate (**38e**) and are typical of the series:

^1H n.m.r. δ ($CDCl_3$): 0.9 (3H, t, CH_3), 1.2-1.4 (14H, m, alkyl), 1.8 (2H, quint., $ArOCH_2\underline{CH_2}$), 3.9 (3H, s, CO_2CH_3), 4.0 (2H, t, $ArO\underline{CH_2}$), 6.9 (2H, d, ArH, J=9Hz), 7.5 (2H, d, ArH, J=9Hz), 7.55 (1H, d, ThH, J=2Hz), 8.0 (1H, d, ThH, J=2Hz) ppm.

i.r. ν_{max} (KBr): 2954, 2935, 2920, 2855, 1715 (C=O str.), 1512, 1297, 1086, 835, cm^{-1}.

2.3.5 *4-(4-n-Alkoxyphenyl)thiophene-2-carboxylic acids* (**39a-f**)

A mixture of the appropriate methyl 4-(4-n-alkoxyphenyl)thiophene-2-carboxylate (**38a-f**) (0.003 mol), potassium hydroxide (1.5 g, 0.027 mol) and 80%-aqueous ethanol (50ml) was heated under reflux for 2 h. period. After cooling to room temperature, the reaction mixture was acidified (4M HCl), extracted with diethyl ether (2 x 50 ml) and dried ($MgSO_4$). The solvent was removed using a rotary evaporator and the crude residue was purified by recrystallisation from aqueous methanol to afford the desired 4-(4-n-alkoxyphenyl)thiophene-2-carboxylic acids (**39a-f**), as white crystalline solids (78-92%). Product purity checked by TLC (silica gel, one spot). M.p.s. and transition temperatures[†]: $C_6H_{13}O$ (**39a**), K-I 124.7°; I-N/K 110.3°; $C_7H_{15}O$ (**39b**), K-I 133.1°; I-N/K 124.0°; $C_8H_{17}O$ (**39c**), K-I 111.0°; I-N/K 108.5°; $C_9H_{19}O$ (**39d**), K-I 114.7°; I-N/K 111.0°; $C_{10}H_{21}O$ (**39e**), K-I 112.3°; I-N/K 106.8°; $C_{12}H_{25}O$ (**39f**), K-I 116.6°; I-N/K 110.3°C.

The following spectroscopic data refer to the 4-(4-n-nonyloxyphenyl)thiophene-2-carboxylic acid (**39d**) and are typical of the series:

[†] I-N and N-K transition very close. Nematic phase observed in homologues n=6-12 in uncovered droplets. Melting points determined using an Mettler FP52 hot stage.

^{1}H n.m.r. δ ($CDCl_3$): 0.9 (3H, t, CH_3), 1.2-1.4 (12H, m, alkyl), 1.8 (2H, quint., $ArOCH_2\underline{CH_2}$), 4.0 (2H, t, $ArO\underline{CH_2}$), 6.95 (2H, d, ArH, J=9Hz), 7.5 (2H, d, ArH, J=9Hz), 7.55 (1H, d, ThH, J=2Hz), 8.1 (1H, d, ThH, J=2Hz) ppm. OH not detected.

i.r. ν_{max} (KBr): 3500-3300 (O-H str.), 2952, 2848, 1677 (C=O str.), 1258, 773 cm^{-1}.

2.3.6 (S)-*4-(1-Methylheptyloxycarbonyl)phenyl 4-(4-n-alkoxyphenyl)thiophene-2-carboxylates* **(46a-f) [Series V]**

The esters were prepared using the procedure outlined on p. 65 for compounds **(27a-f)** in which the appropriate 4-(4-n-alkoxyphenyl)thiophene-2-carboxylic acid **(45a-f)** (0.00064 mol) was reacted with (*S*)-1-methylheptyl 4-hydroxybenzoate **(25)** (0.16 g, 0.00064 mol) in the presence of DCC (0.16 g, 0.00077 mol) and DMAP (2-3 crystals). Purification was achieved using flash chromatography eluting with 1:1 DCM:petroleum ether (b.p. 40-60°C) followed by repeated recrystallisation from ethanol to give the desired carboxylate **(40a-f)**, (52-56%), as a white crystalline solid. Product purity confirmed by TLC (silica gel, one spot) and HPLC (>99%).

The melting points and transition temperatures of compounds **(40a-f)** are listed in **Table 5** (p. 161) of the results and discussion section. The following elemental and spectroscopic data refer to the (*S*)-4-(1-methylheptyloxycarbonyl)phenyl 4-(4-n-nonyloxyphenyl)thiophene-2-carboxylate **(40d)** and are typical of the series:

Found: C, 72.34; H, 7.96%. $C_{35}H_{46}O_5S$ requires C, 72.63; H, 8.01%.

MS (*m/z*) 578 (M+), 467, 341, 329.

^{1}H n.m.r. δ ($CDCl_3$): 0.9 (6H, t, CH_3), 1.2-1.5 (25H, m, alkyl + C*(H)CH_3), 1.8 (2H, quint., $ArOCH_2CH_2$), 4.0 (2H, t, $ArOCH_2$), 5.2 (1H, sextet, C*(H)CH_3), 7.0 (2H, d, ArH, J=9Hz), 7.3 (2H, d, ArH, J=9Hz), 7.5 (2H, d, ArH, J=9Hz), 7.7 (1H, d, ThH, J=2Hz), 8.1 (2H, d, ArH, J=9Hz), 8.2 (1H, d, ThH, J=2Hz) ppm.

i.r. ν_{max} (KBr): 2920, 2857, 1743 (C=O str.), 1714 (C=O str.), 1289, 1239, 777 cm^{-1}.

2.3.7 (S)-*4'-(1-Methylheptyloxycarbonyl)biphenyl-4-yl 4-(4-n-alkoxyphenyl)-thiophene-2-carboxylates* (**41a-f**) [**Series VI**]

The esters were prepared according to the method described on p. 65 for compounds (**27a-f**). Quantities: 4-(4-n-alkoxyphenyl)thiophene-2-carboxylic acid (**39a-f**) (0.00077 mol); (*S*)-1-methylheptyl 4'-hydroxybiphenyl-4-carboxylate (**26**) (0.25g, 0.00077 mol); DCC (0.19 g, 0.00092 mol) and; DMAP (2-3 crystals). Yield 52-60%. Product purity confirmed by TLC (silica gel, one spot) and HPLC (>99%).

The melting points and transition temperatures of the crystalline products are listed in **Table 6** (p. 164) of the results and discussion section. The following elemental and spectroscopic data refer to the (*S*)-4'-(1-methylheptyloxycarbonyl)biphenyl-4-yl 4-(4-n-hexyloxyphenyl)thiophene-2-carboxylate (**41a**) and are typical of the series:

Found: C, 74.24; H, 7.26%. $C_{38}H_{44}O_5S$ requires C, 74.48; H, 7.24%.

MS (*m/z*) 612 (M+), 501, 287.

^{1}H n.m.r. δ ($CDCl_3$): 0.9 (6H, t, 2 x CH_3), 1.2-1.5 (19H, m, alkyl + C*(H)CH_3), 1.8 (2H, quint., $ArOCH_2CH_2$), 4.0 (2H, t, $ArOCH_2$), 5.2 (1H, sextet, C*(H)CH_3), 7.0 (2H, d, ArH, J=9Hz), 7.3 (2H, d, ArH, J=9Hz), 7.6 (2H, d, ArH, J=9Hz), 7.7 (5H, unresolved multiplet, ArH/ThH), 8.1 (2H, d, ArH, J=9Hz), 8.2 (1H, d, ThH, J=2Hz) ppm.

i.r. ν_{max} (KBr): 2921, 2851, 1741 (C=O str.), 1716 (C=O str.), 1284, 1243, 766 cm^{-1}.

2.4 SYNTHESIS OF ESTERS (47a-f) [Series VII] AND (48a-f) [Series VIII] DERIVED FROM 5'-n-ALKYL-2',4-BITHIENYL-2-CARBOXYLIC ACIDS (46a-f) (Scheme 4)

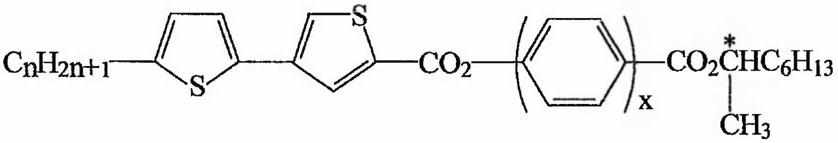

where: x=1, **(47a-f) [Series VII]**; x=2, **(48a-f) [Series VIII]**

The esters (**47a-f** and **48a-f**) derived from 5'-n-alkyl-2',4-bithienyl-2-carboxylic acids (**46a-f**) and the appropriate chiral phenol (**25**) or (**26**) were prepared as outlined in **Scheme 4.**

Initially it was envisaged to utilise the boronic acid cross-coupling methodology to synthesise compounds (**45a-f**) which were deemed as key intermediates. The proposed synthetic strategy, as shown on p. 89 (**Scheme 4a**), relied on the synthesis of 5-n-alkylthiophene-2-boronic acid from compounds (**43a-f**). Although Seed *et al.*[99] report the synthesis of thiophene-2-boronic acid in very high yields via low temperature lithiation, attempts to synthesise reasonable quantities of 5-n-alkylthiophene-2-boronic acids failed. Also, if reasonable quantities were to be prepared then problems at the coupling stage were expected. Gronowitz *et al.*[100] has reported poor coupling between thiophene-2-boronic acid and organic halides because of protodeboronation, *i.e.*, the boronic acid converts to the corresponding hydro-compound in the presence of aqueous basic conditions. In order to successfully prepare compounds (**45a-f**), the Stille[101,102] cross-coupling methodology was employed.

SCHEME 4

i. $TiCl_4$, $C_mH_{2m+1}COCl$, DCM.
ii. Hydrazine hydrate, diethylene glycol, KOH.
iii. a) 1.6M n-BuLi, -78°C, $Sn(Bu)_3$; b) H_2O.
iv. $Pd(PPh_3)_4$, DMF, 80°C.
v. KOH, 80% aq. EtOH, reflux.
vi. DCC, DCM, DMAP.

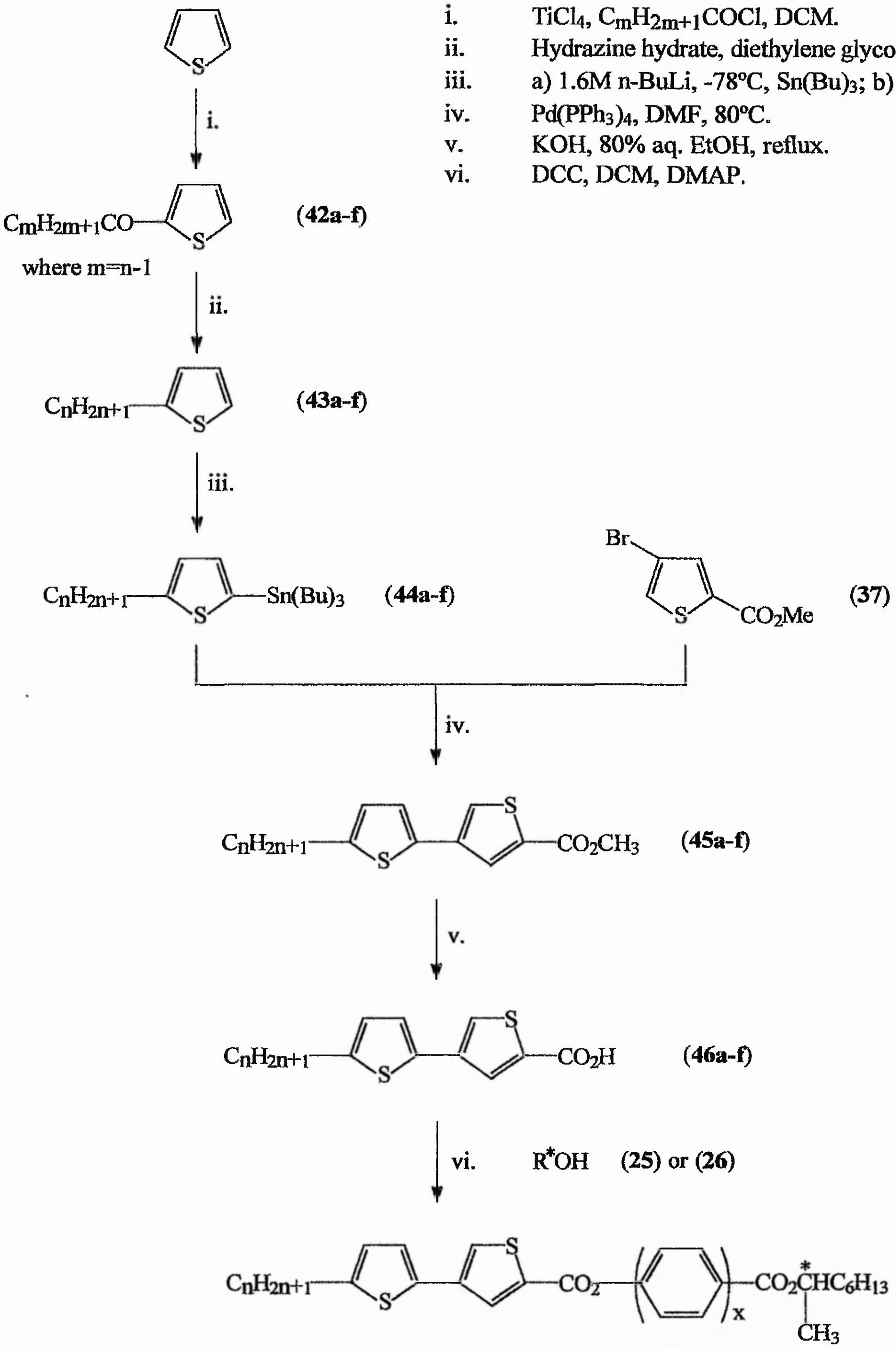

where: x=1, **(47a-f) [Series VII]**
x=2, **(48a-f) [Series VIII]**

SCHEME 4a

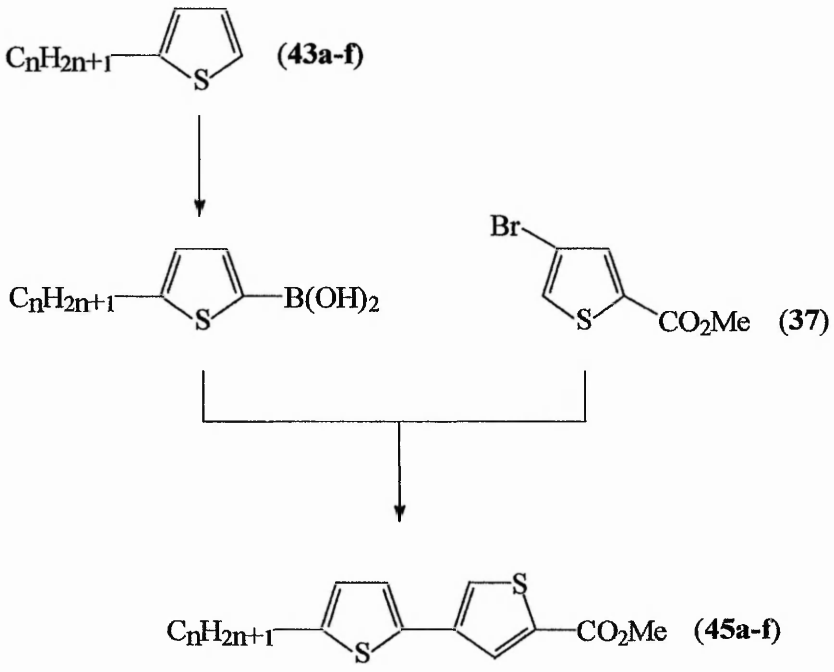

Titanium(IV) chloride mediated Friedel-Crafts acylation of thiophene with the appropriate alkanoyl chloride afforded the 5-n-alkanoylthiophenes (**42a-f**) in good yield (68-80%). Wolff-Kishner (Huang-Minlon[91] modification) reduction of compounds (**42a-f**) gave the corresponding 5-n-alkylthiophenes (**43a-f**). Lithiation (2.5M n-BuLi) of compounds (**43a-f**) at 0°C followed by the addition of tri-n-butyltin chloride at -78°C afforded the 2-(tri-n-butyltin)-5-n-alkylthiophenes (**44a-f**) in excellent yield (72-88%). Stille[101,102] coupling of compounds (**44a-f**) with methyl 4-bromothiophene-2-carboxylate (**37**) in the presence of *tetrakis*(triphenylphosphine)palladium(0) afforded the methyl 5'-n-alkyl-2',4-bithienyl-2-carboxylates (**45a-f**) in good yield (64-72%).

Stille coupling[101,102] is the reaction between either an organic halide or organic triflate with an organotin reagent to generate a carbon-carbon bond. The reaction is catalysed by transition metals, particularly nickel and palladium. The emergence of the Stille coupling reaction as a convenient method for C-C bond formation is largely due to the mildness of the reaction which allows the reaction to proceed even in the presence of many types of functional groups. There are several ways of producing the organotin reagent, which is readily isolable and is generally air stable.

$$\mathrm{R^1{-}Sn(alk)_3} + \mathrm{R^2{-}X} \xrightarrow{\mathrm{Pd(0)}} \mathrm{R^1{-}R^2} + \mathrm{XSn(alk)_3}$$

Subsequent hydrolysis of compounds **(45a-f)** in ethanolic potassium hydroxide afforded the desired 5'-n-alkyl-2',4-bithienyl-2-carboxylic acids **(46a-f)** which were then esterified with the appropriate chiral phenol, either **(25)** or **(26)**, to yield members of the series of chiral esters **(47a-f)** **[Series VII]** and **(48a-f)** **[Series VIII]**.

2.4.1 *5-n-Alkanoylthiophenes* (**42a-f**)

Friedel-Crafts acylation of thiophene (7.6 ml, 0.095 mol) using the appropriate alkanoyl chloride (0.095 mol) was carried out according to the procedure described on p. 72 for compounds **(30a-i)**. After work-up the crude product was purified using vacuum distillation (Kugelrohr) to afford the pure 5-n-alkanoylthiophenes **(42a-f)** (68-80%), as colourless liquids. Product purity confirmed by TLC (silica gel, one spot). B.p.s: $C_5H_{11}CO$ (**42a**), 95°/0.1 [lit.[77] 98-102°/0.5]; $C_6H_{13}CO$ (**42b**), 105°/0.1 [lit.[77] 121-129°/0.5]; $C_7H_{15}CO$ (**42c**), 150°/0.2 [lit.[77] 112-118°/0.3]; $C_8H_{17}CO$ (**42d**), 120°/0.1 [lit.[77] 110-115°/0.15]; $C_9H_{19}CO$ (**42e**), 170°/0.1 [lit.[77] 120-125°/0.4]; $C_{11}H_{23}CO$ (**42f**), 180°C/0.1 mm Hg.

The following data refer to the 5-n-heptanoylthiophene (**42b**) and are typical of the series:

^1H n.m.r. δ ($CDCl_3$): 0.9 (3H, t, CH_3), 1.2-1.4 (6H, m, alkyl), 1.8 (2H, quint., $ThCOCH_2\underline{CH_2}$), 2.9 (2H, t, $ThCO\underline{CH_2}$), 7.1 (1H, t, ThH), 7.6 (1H, d, ThH, J=4Hz), 7.7 (1H, d, ThH, J=4Hz) ppm.

i.r. ν_{max} (Thin film): 2923, 2852, 1664 (C=O str.), 1518, 1465, 1415 cm^{-1}.

2.4.2 *5-n-Alkylthiophenes* (**43a-f**)

The 5-n-alkylthiophenes (**43a-f**) were prepared using the method described on p. 73 for compounds (**31a-i**), from the appropriate ketone (**42a-f**) (0.05 mol) and hydrazine hydrate (24.2 ml, 0.5 mol) in diethylene glycol (150 ml), followed by the addition of potassium hydroxide (28.0 g, 0.5 mol). After work-up the crude product was purified by vacuum distillation (Kugelrohr) to give the desired 5-n-alkylthiophenes (**43a-f**), (78-88%), as colourless liquids. Product purity checked by TLC (silica gel, one spot). B.p.s: C_6H_{13} (**43a**), 75°/0.1 [lit.[77] 54°/0.1]; C_7H_{15} (**43b**), 110°/0.7 [lit.[77] 60°/0.1]; C_8H_{17} (**43c**), 105°/0.05 [lit.[77] 66°/0.1]; C_9H_{19} (**43d**), 120°/0.1 [lit.[77] 71°/0.1]; $C_{10}H_{21}CO$ (**43e**), 150°/0.1 [lit.[77] 88°/0.1]; $C_{12}H_{25}CO$ (**43f**), 150°C/0.02 mm Hg.

The following data refer to 5-n-octylthiophene (**43c**) and are typical of the series:

^{1}H n.m.r. δ ($CDCl_3$): 0.9 (3H, t, CH_3), 1.2-1.4 (10H, m, alkyl), 1.8 (2H, quint., $ThCH_2\underline{CH_2}$), 2.8 (2H, t, $Th\underline{CH_2}$), 7.1 (1H, t, ThH), 7.6 (1H, d, ThH, J=4Hz), 7.7 (1H, d, ThH, J=4Hz) ppm.

i.r. ν_{max} (Thin film): 3044, 2925, 2851, 1465, 850, 689 cm^{-1}.

2.4.3 *2-(Tri-n-butyltin)-5-n-alkylthiophenes* (**44a-f**)

In an atmosphere of nitrogen, 2.5M n-BuLi (21.0 ml, 0.053 mol) was added, dropwise, to a stirred, cooled (-78°C) solution of the appropriate 5-n-alkylthiophene (**43a-f**) (0.048 mol) at such a rate that the temperature did not exceed -70°C. After the addition was complete, the solution was stirred at -78°C for a further 1 h. Tri-n-butyltin chloride (14.4 ml, 0.053 mol) was injected, dropwise, and the reaction mixture was allowed to warm to room temperature overnight. The reaction mixture was quenched with water and the product extracted with diethyl ether (2 x 100 ml). The combined organic extract was washed with water (2 x 100 ml), dried ($MgSO_4$) and the solvent removed *in vacuo*. The resultant crude residue was then purified by vacuum distillation (Kugelrohr) to afford the desired 2-(tri-n-butyltin)-5-n-alkylthiophenes (**44a-f**), (72-88%), as pale yellow oils. B.p.s: C_6H_{13} (**44a**), 180°/0.5; C_7H_{15} (**44b**), 190°/0.5; C_8H_{17} (**44c**), 200°/0.5; C_9H_{19} (**44d**), 180°/0.1; $C_{10}H_{21}$ (**44e**), 210°/0.1; $C_{12}H_{25}$ (**44f**), 250°C/0.05 mm Hg.

The following spectroscopic data refer to 2-(tri-n-butyltin)-5-n-octylthiophene (**44c**) and is typical of the series:

^{1}H n.m.r. δ ($CDCl_3$): 0.9 (12H, t, 4 x CH_3), 1.0 (6H, t, 3 x $SnCH_2CH_2\underline{CH_2}$), 1.2-1.4 (16H, m, alkyl), 1.6 (6H, quint., 3 x $Sn\underline{CH_2}$), 1.8 (2H, quint., $ThCH_2\underline{CH_2}$), 2.9 (2H, t, $Th\underline{CH_2}$), 6.9 (1H, d, ThH, J=3Hz), 7.0 (1H, d, ThH, J=3Hz) ppm.

i.r. ν_{max} (Thin film): 2954, 2922, 2851, 1463, 1376, 1072, 935, 795, 690, 665 cm^{-1}.

2.4.4 *Methyl 5'-n-alkyl-2',4-bithienyl-2-carboxylates* (**45a-f**)

In an atmosphere of nitrogen, methyl 4-bromothiophene-2-carboxylate (**37**) (2.0 g, 0.009 mol) was added in one portion to a stirred mixture of the appropriate 2-(tri-n-butyltin)-5-n-alkylthiophene (**44a-f**) (0.01 mol) and *tetrakis*(triphenylphosphine)-palladium(0) (0.5 g, 0.0004 mol) in dry *N,N*-dimethylformamide (DMF) (40 ml). The reaction mixture was heated at 80°C for 2 h. and then cooled to room temperature. Water was added and the crude product extracted with diethyl ether (3 x 50 ml), dried ($MgSO_4$) and the solvent removed in vacuo.† The resulting white solid was purified by flash chromatography on silica gel eluting with 1:1 DCM:petroleum ether (b.p. 40-60°C) to yield the desired methyl 5'-n-alkyl-2',4-bithienyl-2-carboxylates (**45a-f**), (64-72%), as white crystalline solids. Product purity checked by TLC (silica gel, one spot). M.p.s: C_6H_{13} (**45a**), 47-49°; C_7H_{15} (**45b**), 53-55°; C_8H_{17} (**45c**), 57-59°; C_9H_{19} (**45d**), 52-54°; $C_{10}H_{21}$ (**45e**) 58-60°, $C_{12}H_{25}$ (**45f**), 60-62°C.

The following data refer to the methyl 5'-n-octyl-2',4-bithienyl-2-carboxylate (**45c**) and are typical of the series:

---

† High vacuum is required to remove both DMF and the tri-n-butyltin bromide by-product.

^1H n.m.r. δ ($CDCl_3$): 0.9 (3H, t, CH_3), 1.2-1.4 (10H, m, alkyl), 1.8 (2H, quint., $ThCH_2\underline{CH_2}$), 2.8 (2H, t, $Th\underline{CH_2}$), 3.9 (3H, s, CO_2CH_3), 6.7 (1H, d, ThH, J=4Hz), 7.0 (1H, d, ThH, J=4Hz), 7.4 (1H, d, ThH, J=2Hz), 8.0 (1H, d, ThH, J=2Hz) ppm.

i.r. ν_{max} (KBr): 2954, 2920, 2855, 1715 (C=O str.), 1512, 1297, 1086, 771 cm^{-1}.

2.4.5 *5'-n-Alkyl-2',4-bithienyl-2-carboxylic acids* (**46a-f**)

The 5'-n-alkyl-2',4-bithienyl-2-carboxylic acids (**46a-f**) were prepared according to the method described on p. 83 for compounds (**39a-f**). Quantities: methyl 5'-n-alkyl-2',4-bithienyl-2-carboxylates (**45a-f**) (0.006 mol); potassium hydroxide (3.0 g, 0.054 mol) and; 80%-aqueous ethanol (50 ml). Purification was achieved by repeated recrystallisation from aqueous methanol to afford the 5'-n-alkyl-2',4-bithienyl-2-carboxylic acids, (**46a-f**) (84-92%), as white crystalline solids. Product purity confirmed by TLC (silica gel, one spot). M.p.s: $C_6H_{13}O$ (**46a**), 115.8°; $C_7H_{15}O$ (**46b**), 115.1°; $C_8H_{17}O$ (**46c**), 109.9°; $C_9H_{19}O$ (**46d**), 101.6°; $C_{10}H_{21}O$ (**46e**), 107.9°; $C_{12}H_{25}O$ (**46f**), 103.9°C[†].

The following spectroscopic data refer to the 5'-n-nonyl-2',4-bithienyl-2-carboxylic acid (**46d**) and are typical of the series:

^1H n.m.r. δ ($CDCl_3$): 0.9 (3H, t, CH_3), 1.2-1.4 (12H, m alkyl), 1.8 (2H, quint., $ThCH_2\underline{CH_2}$), 2.8 (2H, t, $Th\underline{CH_2}$), 4.0 (1H, s, CO_2H, disappears on D_2O shake), 6.7

[†] Melting points determined using an Mettler FP52 hot stage. No liquid crystal mesophases observed prior to crystallisation.

(1H, d, ThH, J=4Hz), 7.0 (1H, d, ThH, J=4Hz), 7.5 (1H, d, ThH, J=2Hz), 8.0 (1H, d, ThH, J=2Hz) ppm.

i.r. ν_{max} (KBr): 3400-3310 (O-H str.), 2954, 1677 (C=O str.), 1446, 1257, 773 cm^{-1}.

2.4.6 (S)-*4-(1-Methylheptyloxycarbonyl)phenyl 5'-n-alkyl-2',4-bithienyl-2-carboxylates* (**47a-f**) **[Series VII]**

The esters were prepared, using the procedure described on p. 65 for compounds (**27a-f**). Quantities: 5'-n-alkyl-2',4-bithienyl-2-carboxylic acid (**46a-f**) (0.00088 mol); (*S*)-1-methylheptyl 4-hydroxybenzoate (**25**) (0.22 g, 0.00088mol); DCC (0.22 g, 0.0011 mol) and; DMAP (2-3 crystals). The crude residue was purified by flash chromatography eluting with 1:1 DCM:petroleum ether (b.p. 40-60°C), followed by recrystallisation from ethanol to afford the desired esters (**47a-f**), (48-54%), as white crystalline solids. Product purity confirmed by TLC (silica gel, one spot) and HPLC (>99%).

The melting points of compounds (**47a-f**) are listed in **Table 7** (p. 166) of the results and discussion section. The following spectroscopic data refer to the (*S*)-4-(1-methylheptyloxycarbonyl)phenyl 5'-n-dodecyl-2',4-bithienyl-2-carboxylate (**47f**) and are typical of the series:

Found: C, 70.56; H, 8.10%. $C_{36}H_{50}O_4S_2$ requires C, 70.78; H, 8.25%.

MS (*m/z*) 610 (M+), 499, 361.

^{1}H n.m.r. δ ($CDCl_3$): 0.9 (3H, t, CH_3), 1.2-1.5 (34H, m, alkyl + C*(H)$\underline{CH_3}$), 1.8 (2H, quint., $ThCH_2\underline{CH_2}$), 2.8 (2H, t, Th$\underline{CH_2}$), 5.2 (1H, sextet, $\underline{C^*(H)}CH_3$), 6.7 (1H, d, ThH, J=4Hz), 7.1 (1H, d, ThH, J=4Hz), 7.3 (2H, d, ArH, J=9Hz), 7.6 (1H, d, ThH, J=2Hz), 8.1 (3H, m, ThH/ArH) ppm.

i.r. ν_{max} (KBr): 2920, 2855, 1739 (C=O str.), 1715 (C=O str.), 1284, 1037, 767 cm^{-1}.

2.4.7 (S)-*4'-(1-Methylheptyloxycarbonyl)biphenyl-4-yl 5'-n-alkyl-2',4-bithienyl-2-carboxylates* (**48a-f**) **[Series VIII]**

The esters were prepared according to the procedure outlined on p. 65 for compounds (**27a-f**). Quantities: 5'-n-alkyl-2',4-bithienyl-2-carboxylic acid (**46a-f**) (0.00086 mol); (*S*)-1-methylheptyl 4'-hydroxybiphenyl-4-carboxylate (**26**) (0.28 g, 0.00086 mol); DCC (0.21 g, 0.001 mol) and; DMAP (2-3 crystals). Yield 46-56%. Product purity checked by TLC (silica gel, one spot) and HPLC (>99%).

The melting points and transition temperatures are reported in **Table 8** (p. 168) in the results and discussion section. The following data refer to the (*S*)-4'-(1-methylheptyloxycarbonyl)biphenyl-4-yl 5'-n-octyl-2',4-bithienyl-2-carboxylate (**48c**) and are typical of the series:

Found: C, 72.16; H, 7.37%. $C_{38}H_{46}O_4S_2$ requires C, 72.34; H, 7.35%.

MS (*m/z*) 630 (M+), 391, 305.

^{1}H n.m.r. δ ($CDCl_3$): 0.9 (6H, t, 2 x CH_3), 1.2-1.4 (23H, m, alkyl + $C^*(H)\underline{CH_3}$), 1.8 (2H, quint., $ThCH_2\underline{CH_2}$), 2.8 (2H, t, $Th\underline{CH_2}$), 5.2 (1H, sextet, $\underline{C^*(H)}CH_3$), 6.7 (1H, d, ThH, J=4Hz), 7.1 (1H, d, ThH, J=4Hz), 7.3 (2H, d, ArH, J=9Hz), 7.6 (1H, d, ThH, J=2Hz), 7.7 (4H, unresolved multiplet, ArH), 8.1 (3H, d, ThH/ArH) ppm.

i.r. ν_{max} (KBr): 2923, 2854, 1741 (C=O str.), 1713 (C=O str.), 1285, 1053, 774 cm^{-1}.

2.5 SYNTHESIS OF ESTERS (53a-f) [Series IX] AND (54a-f) [Series X] DERIVED FROM 5"-n-ALKYL-2",2':5',2-TERTHIENYL-5-CARBOXYLIC ACIDS (52a-f) (Scheme 5)

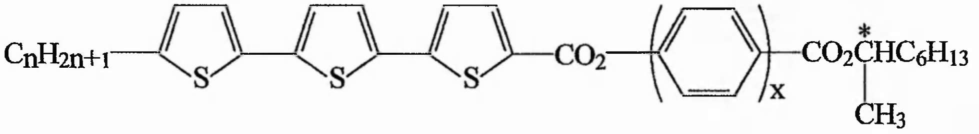

where: x=1, **(53a-f) [Series IX]**; x=2, **(54a-f) [Series X]**

The esters **[Series IX-X]** derived from the 5"-n-alkyl-2",2':5',2-terthienyl-5-carboxylic acids **(52a-f)** and the appropriate chiral phenols, either **(25)** or **(26)**, were prepared as shown in **Scheme 5.**

Although 2,2':5',2"-terthienyl **(49)** may be prepared via several methods,[103-107] the nickel-catalysed cross-coupling methodology reported by Tamao *et al.*[90] was employed due to its high yield and ease of purification. Hence, the Grignard reagent of 2-bromothiophene was cross-coupled with 2,5-dibromothiophene to afford 2,2':5',2"-terthienyl **(49)** in high yield (78%). Friedel-Crafts acylation followed by Huang-Minlon[91] reduction of the intermediate ketone **(50a-f)** afforded the 5-n-alkyl-2,2':5',2"-terthienyls **(51a-f)** in good yield (70-78%). Compounds **(51a-f)** were subsequently lithiated and added to an excess of solid carbon dioxide to furnish the 5"-n-alkyl-2",2':5',2-terthienyl-5-carboxylic acids **(52a-f)**. Esterification of **(52a-f)** with the appropriate chiral phenol **(25)** or **(26)** yielded the desired chiral esters **(53a-f) [Series IX]** and **(54a-f) [Series X]**.

SCHEME 5

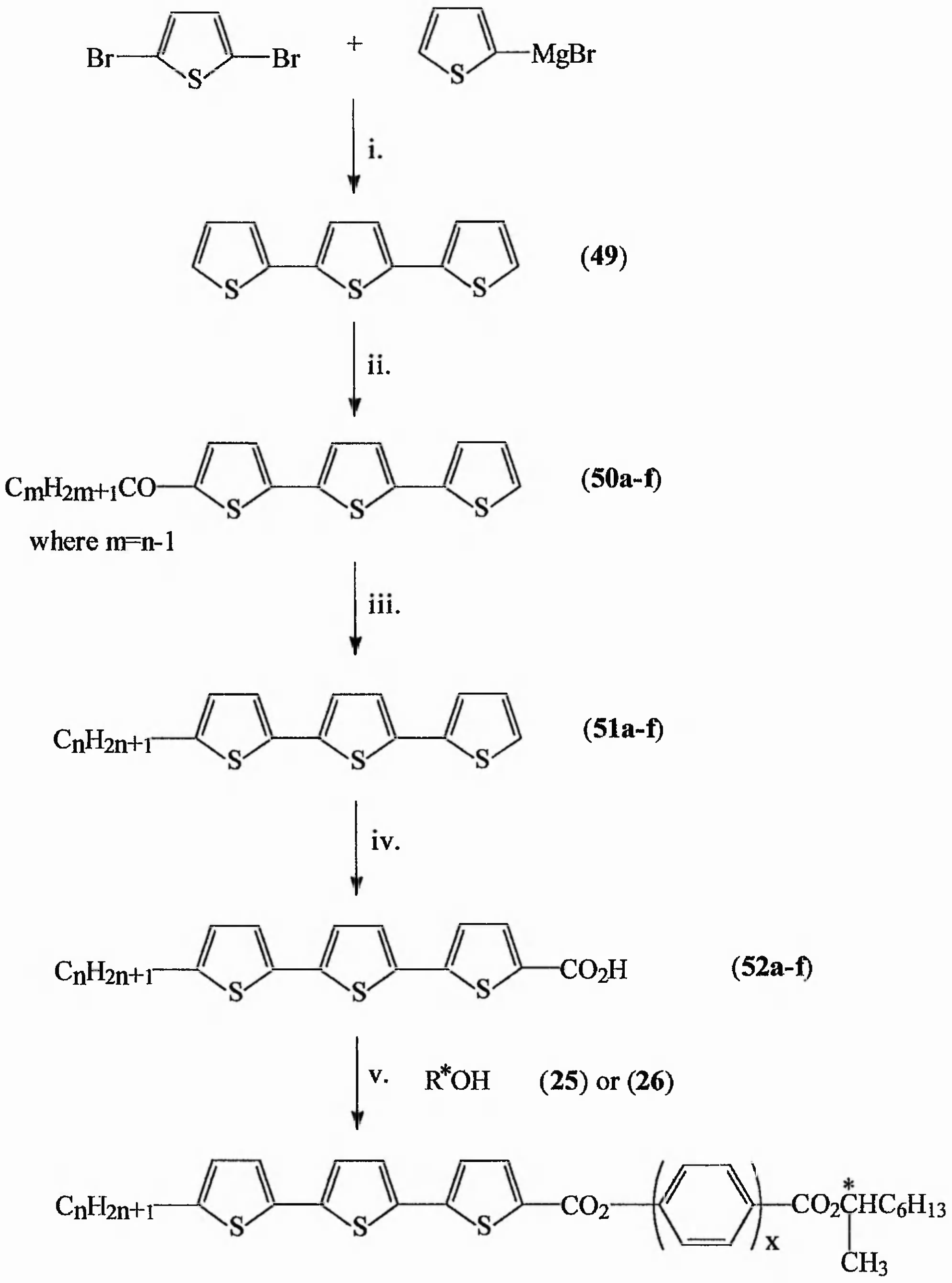

where: x=1, **(53a-f) [Series IX]**
x=2, **(54a-f) [Series X]**

i. $[(C_6H_5)_2P(CH_2)_3P(C_6H_5)_2]NiCl_2$, diethyl ether.
ii. $TiCl_4$, $C_mH_{2m+1}COCl$, DCM.
iii. Hydrazine hydrate, diethylene glycol, KOH.
iv. a) 1.6M n-BuLi, -78°C, N_2; b) CO_2, 4M HCl.
v. DCC, DCM, DMAP.

2.5.1 *2,2':5',2"-Terthienyl* (**49**)

In an atmosphere of nitrogen, 2-bromothiophene (60.0 g, 0.368 mol) in dry diethyl ether (200 ml) was added, dropwise, to magnesium turnings (9.7 g, 0.405 mol) in dry diethyl ether (50 ml) under dry nitrogen at such a rate that the solvent boiled gently. The reaction mixture was heated under reflux for 1 h., cooled to 0°C and added, dropwise, to a stirred, cooled (0°C), mixture of 2,5-dibromothiophene (44.2 g, 0.184 mol) and [1,3-*bis*(diphenylphosphino)propane]nickel(II) chloride (1.0 g, 0.0018 mol) in dry diethyl ether (150 ml). The reaction mixture was then stirred under reflux for 10 h., cooled and poured onto saturated ammonium chloride solution (200 ml). The crude product was extracted with diethyl ether (4 x 150 ml), washed with water (2 x 100 ml), dried ($MgSO_4$) and the solvent removed under reduced pressure. Purification was achieved by recrystallisation from ethanol to afford the desired 2,2':5',2"-terthienyl (**49**), 28.6 g (78%), m.p. 94-96°C (lit.[90] 93-95°C), as a yellow solid. Product purity checked by TLC (silica gel, one spot).

^{1}H n.m.r. δ ($CDCl_3$): 7.0-7.3 (8H, m, ThH) ppm.

i.r. ν_{max} (KBr): 3063, 1422, 796, 685 cm^{-1}.

2.5.2 *5-n-Alkanoyl-2,2':5',2"-terthienyls* (**50a-f**)

Friedel-Crafts acylation of 2,2':5',2"-terthienyl (**49**) (5.0 g, 0.02 mol) with the appropriate alkanoyl chloride (0.02 mol) in the presence of titanium(IV) chloride (2.2 ml, 0.02 mol) in dry DCM (100 ml) was carried out according to the method described on p. 72 for compounds (**30a-i**). After work-up, purification was achieved by flash chromatography on silica gel eluting with 4:1 chloroform:petroleum ether (b.p. 40-

60°C), followed by recrystallisation from ethanol to afford the desired 5-n-alkanoyl-2,2':5',2"-terthienyls **(50a-f)** (54-62%), as pale yellow solids. Product purity confirmed by TLC (silica gel, one spot). M.p.s: $C_5H_{11}CO$ **(50a)**, 134-136° [Lit.[93] 133-134°]; $C_6H_{13}CO$ **(50b)**, 126-128° [Lit.[93] 128-129°]; $C_7H_{15}CO$ **(50c)**, 133-135° [Lit.[93] 131-132°]; $C_8H_{17}CO$ **(50d)**, 128-130° [Lit.[93] 127-128°]; $C_9H_{19}CO$ **(50e)**, 133-135° [Lit.[93] 130-131°]; $C_{11}H_{23}CO$ **(50f)**, 129-131°C.

The following spectroscopic data refer to the 5-n-decanoyl-2,2':5',2"-terthienyl **(50e)** and are typical of the series:

^{1}H n.m.r. δ ($CDCl_3$): 0.9 (3H, t, CH_3), 1.2-1.4 (12H, m, alkyl), 1.8 (2H, quint., $ThCOCH_2\underline{CH_2}$), 2.8 (2H, t, $ThCO\underline{CH_2}$), 6.0-7.6 (7H, m, ThH) ppm.

i.r. ν_{max} (KBr): 2914, 2848, 1655 (C=O str.), 1460, 1443, 793 cm^{-1}.

2.5.3 *5-n-Alkyl-2,2':5',2"-terthienyls* (51a-f)

The 5-n-alkyl-2,2':5',2"-terthienyls **(51a-f)** were prepared by the method described on p. 73 for compounds **(31a-i)**, from the appropriate ketone **(50a-f)** (0.078 mol) and hydrazine hydrate (18.9 ml, 0.39 mol) in diethylene glycol (100 ml), followed by the addition of potassium hydroxide (21.8 g, 0.39 mol). Following work-up, the crude product was purified by flash chromatography on silica gel eluting with 1:6 chloroform:petroleum ether (b.p. 40-60°C) to furnish the desired 5-n-alkyl-2,2':5',2"-terthienyls **(51a-f)**, (70-78%), as pale yellow solids. Product purity confirmed by TLC (silica gel, one spot). M.p.s: C_6H_{13} **(51a)**, 62-64° [Lit.[93] 61-63°]; C_7H_{15} **(51b)**, 73-75°

[Lit.[93] 73-74°]; C_8H_{17} (**51c**), 76-78° [Lit.[93] 74-75°]; C_9H_{19} (**51d**), 75-77° [Lit.[93] 74-75°]; $C_{10}H_{21}$ (**51e**), 69-71° [Lit.[93] 70-71°]; $C_{12}H_{25}$ (**51f**), 75-77°C.

The following spectroscopic data refer to 5-n-heptyl-2,2':5',2"-terthienyl (**51b**) and is typical of the series:

^{1}H n.m.r. δ ($CDCl_3$): 0.9 (3H, t, CH_3), 1.2-1.6 (8H, m, alkyl), 1.8 (2H, quint., $ThCH_2\underline{CH_2}$), 2.8 (2H, t, $Th\underline{CH_2}$), 6.7-7.2 (7H, m, ThH) ppm.

i.r. ν_{max} (KBr): 3069, 2922, 2845, 1509, 1469, 1425, 791 cm^{-1}.

2.5.4 *5"-n-Alkyl-2",2':5',2-terthienyl-5-carboxylic acids* (**52a-f**)

The 5"-n-alkyl-2",2':5',2-terthienyl-5-carboxylic acids (**52a-f**) were prepared according to the method described on p. 64 for compounds (**24a-i**), from the appropriate 5-n-alkyl-2,2':5',2"-terthienyl (**51a-f**) (0.0044 mol) and 1.6M n-BuLi (3.0 ml, 0.0048 mol). After work-up, the crude 5"-n-alkyl-2",2':5',2-terthienyl-5-carboxylic acid (**52a-f**) was obtained as a yellow solid which was used in the next stage of the reaction without purification.

The following spectroscopic data refer to the crude 5"-n-hexyl-2",2':5',2-terthienyl-5-carboxylic acid (**52a**) and are typical of the series:

^{1}H n.m.r. δ ($CDCl_3$): 0.9 (3H, t, CH_3), 1.2-1.4 (6H, m, alkyl), 1.7 (2H, quint., $ThCH_2\underline{CH_2}$), 2.8 (2H, t, $Th\underline{CH_2}$), 6.7-7.7 (6H, m, ThH) ppm. No OH proton observed.

i.r. ν_{max} (KBr): 3440-3300 (O-H str.), 2954, 2921, 1661 (C=O str.), 1453, 795 cm^{-1}.

2.5.5 (S)-*4-(1-Methylheptyloxycarbonyl)phenyl 5"-n-alkyl-2",2':5',2-terthienyl-5-carboxylates* **(53a-f) [Series IX]**

Esters **(53a-f)** **[Series IX]** were prepared, by the method described on p. 65 for compounds **(27a-f)**, using the appropriate 5"-n-alkyl-2",2':5',2-terthienyl-5-carboxylic acid **(52a-f)** (0.001 mol) and (*S*)-1-methylheptyl 4-hydroxybenzoate **(25)** (0.25 g, 0.001 mol) in the presence of DCC (0.25 g, 0.0012 mol) and DMAP (2-3 crystals). After work-up, the crude esters were purified by flash chromatography eluting with 1:2 DCM:petroleum ether (b.p.40-60°C), followed by repeated recrystallisation from ethanol, to yield the yellow crystalline products **(53a-f)**, (62-70%). Product purity confirmed by TLC (silica gel, one spot) and HPLC (>99%).

The melting points and transition temperatures of compounds **(53a-f)** are listed in **Table 12** (p. 180) of the results and discussion section. The following data refer to the (*S*)-4-(1-methylheptyloxycarbonyl)phenyl 5"-n-nonyl-2",2':5',2-terthienyl-5-carboxylate **(53d)** and are typical of the series:

Found: C, 68.24; H, 7.09. $C_{37}H_{46}O_4S_3$ requires C, 68.27; H, 7.12%.

MS (*m/z*) 650 (M+), 610, 401.

^{1}H n.m.r. δ ($CDCl_3$): 0.9 (6H, t, 2 x CH_3), 1.2-1.4 (25H, m, alkyl + $C^*(H)\underline{CH_3}$), 1.8 (2H, quint., $ThCH_2\underline{CH_2}$), 2.8 (2H, t, $Th\underline{CH_2}$), 5.2 (1H, sextet, $\underline{C^*(H)}CH_3$), 6.7 (1H, d, ThH, J=4Hz), 7.0-7.2 (4H, unresolved multiplet, ThH), 7.3 (2H, d, ArH, J=9Hz), 7.9 (1H, d, ThH, J=4Hz), 8.1 (2H, d, ArH, J=9Hz) ppm.

i.r. ν_{max} (KBr): 2955, 2925, 1715 (C=O str.), 1603, 1273, 794 cm^{-1}.

2.5.6 (S)-*4'-(1-Methylheptyloxycarbonyl)biphenyl-4-yl 5"-n-alkyl-2",2':5',2-terthienyl-5-carboxylates* (**54a-f**) **[Series X]**

Esters (**54a-f**) **[Series X]** were prepared according to the procedure outlined on p. 65 for compounds (**27a-f**). Quantities: 5"-n-alkyl-2",2':5',2-terthienyl-5-carboxylic acid (**52a-f**) (0.001 mol); (*S*)-1-methylheptyl 4'-hydroxybiphenyl-4-carboxylate (**26**) (0.33g, 0.001 mol); DCC (0.25 g, 0.0012 mol) and; DMAP (2-3 crystals). Yield (52-60%). Product purity confirmed by TLC (silica gel, one spot) and HPLC (>99%).

The melting points and transition temperatures for the esters are reported in **Table 13** of the results section (p. 184). The following data refer to the (*S*)-4'-(1-methylheptyloxycarbonyl)biphenyl-4-yl 5"-n-heptyl-2",2':5',2-terthienyl-5-carboxylate (**54b**) and are typical of the series:

Found: C, 70.36; H, 6.62%. $C_{41}H_{46}O_4S_3$ requires C, 70.45; H, 6.63%.

MS (*m/z*) 698 (M+), 658, 657, 373.

^{1}H n.m.r. δ ($CDCl_3$): 0.9 (6H, t, 2 x CH_3), 1.2-1.5 (21H, m, alkyl + C*(H)$\underline{CH_3}$), 1.8 (2H, quint., ThCH$_2\underline{CH_2}$), 2.8 (2H, t, Th$\underline{CH_2}$), 5.2 (1H, sextet, $\underline{C^*(H)}$CH$_3$), 6.7 (1H, d, ThH, J=4Hz), 7.0 (2H, d, ThH, J=4Hz), 7.2 (4H, m, ArH), 7.4 (2H, d, ArH, J=9Hz), 7.6 (1H, d, ThH, J=4Hz), 7.7 (1H, d, ThH, J=4Hz), 7.9 (1H, d, ThH, J=4Hz), 8.1 (2H, d, ArH, J=9Hz) ppm.

i.r. ν_{max} (KBr): 2954, 2925, 2849, 1715 (C=O str.), 1604, 1279, 657 cm^{-1}.

2.6 SYNTHESIS OF ESTER (60) [Series XI] DERIVED FROM 5'-(4-n-DECYLOXYPHENYL)-2',2-BITHIENYL-5-CARBOXYLIC ACID (59) (Scheme 6)

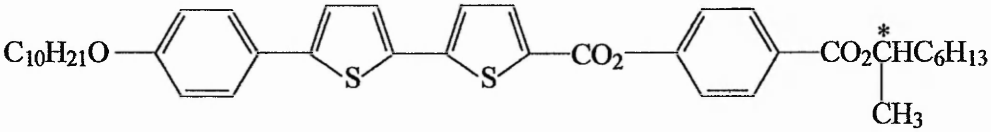

(60) [Series XI]

The synthesis of ester **(60)** **[Series XI]** derived from 5'-(4-n-decyloxyphenyl)-2',2-bithienyl-5-carboxylic acid **(59)** and (*S*)-1-methylheptyl 4-hydroxybenozate **(25)** is depicted in **Scheme 6.**

It was initially envisaged to use the boronic acid methodology proposed in **Scheme 6a** (p. 106) to make the desired final ester. However, severe difficulties were encountered in attempting to synthesise pure and adequate amounts of the 5-bromo-2,2'-bithienyl despite several literature reports.[108,109] For example, the reaction of 2,2'-bithienyl with *N*-bromosuccinimide (NBS) in carbon tetrachloride and NBS in dimethylformamide at -20°C in the dark, as reported by Bauerle *et al.*,[108] resulted in an inseparable mixture of isomers being formed. Carpita *et al.*[109] report the synthesis of 5-bromo-2,2'-bithienyl in 53% yield by cross-coupling the Grignard reagent of 2-bromothiophene with 2,5-dibromothiophene in the presence of $PdCl_2$ as catalyst. However, when this procedure was repeated, 2,2':5,2''-terthienyl was recovered as the main product along with small amounts of unreacted starting material and other inseparable isomers. Due to the

SCHEME 6

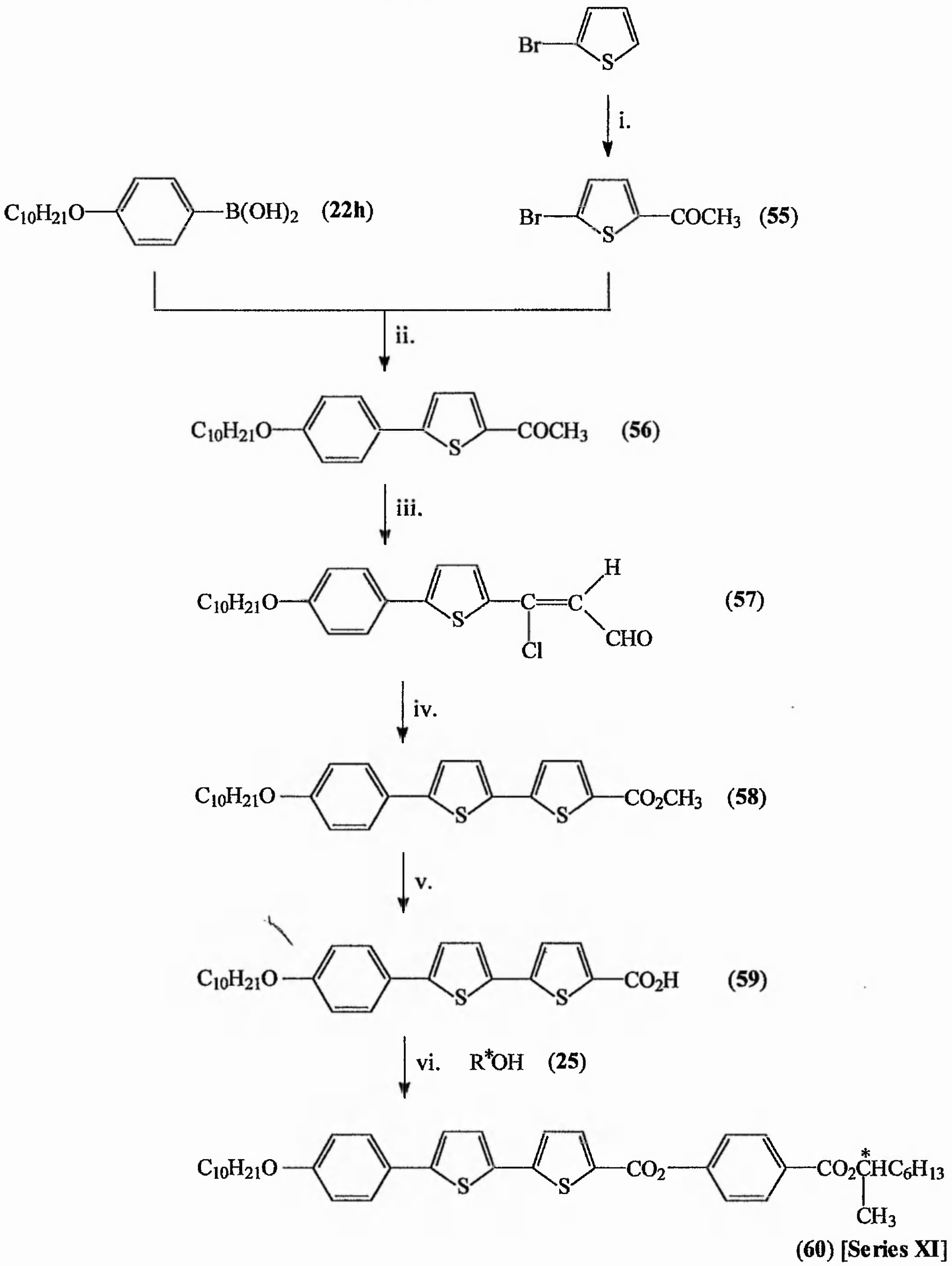

i. CH_3COCl, $TiCl_4$, DCM.
ii. 2M Na_2CO_3, DME, $Pd(PPh_3)_4$, reflux.
iii. $POCl_3$, DMF, 35°C.
iv. a) Na/EtOH; b) methyl thioglycollate.
v. KOH, 80% aq. EtOH.
vi. DCC, DCM, DMAP.

difficulties encountered, this route was finally abandoned in favour of using classical ring closure methods as shown in **Scheme 6**.

SCHEME 6a

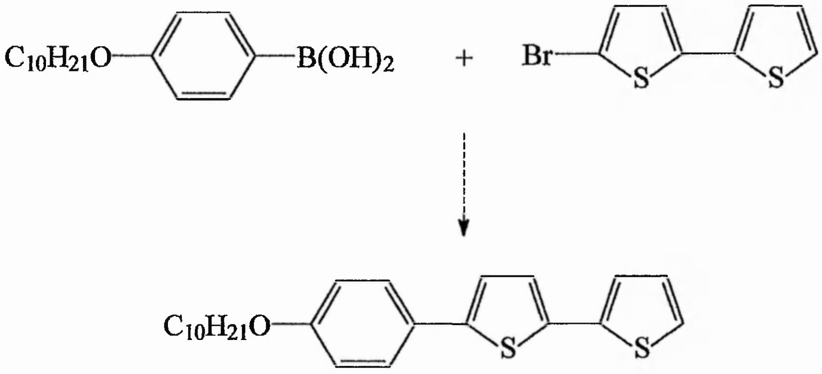

Friedel-Crafts acylation of commercial 2-bromothiophene using acetyl chloride, in the presence of titanium(IV) chloride as catalyst, afforded 2-acetyl-5-bromothiophene (**55**) in excellent yield (89%). 4-n-Decyloxyphenylboronic acid (**22h**) was cross-coupled with (**55**) in the presence of *tetrakis*(triphenylphosphine)palladium(0) as catalyst to afford the desired 2-acetyl-5-(4-n-decyloxyphenyl)thiophene (**56**) in good yield (69%). Reaction of compound (**56**) with *N,N*-dimethylformamide-phosphorus oxychloride, followed by work-up with sodium acetate gave the desired 3-chloro-3-(5-(4-n-decyloxyphenyl)thienyl-2-yl)propenal (**57**). Brettle *et al.*[110] have recently adopted a similar strategy to synthesis several thiophene-based compounds, however, the initial discovery of this methodology is attributed to Arnold and Zemlicka.[111]

Condensation of compound (**57**) with methyl thioglycollate afforded methyl 5'-(4-n-decyloxyphenyl)-2',2-bithienyl-5-carboxylate (**58**) in good yield (62%). Subsequent base hydrolysis of compound (**58**) gave 5'-(4-n-decyloxyphenyl)-2',2-bithienyl-5-carboxylic acid (**59**), which was esterified with (*S*)-1-methylheptyl 4-hydroxybenzoate (**25**) in the presence of DMAP as catalyst to furnish (*S*)-4-(1-methylheptyloxycarbonyl)phenyl 5'-(4-n-decyloxyphenyl)-2',2-bithienyl-5-carboxylate (**60**) [**Series XI**].

2.6.1 *2-Acetyl-5-bromothiophene* (**55**)

Friedel-Crafts acylation of 2-bromothiophene (15.0 g, 0.092 mol) using acetyl chloride (6.5 ml, 0.092 mol) in the presence of titanium(IV) chloride (10.1 ml, 0.092 mol) in dry dichloromethane (100 ml) was carried out as described by the method reported on p. 72 for compounds (**30a-i**). After work-up, the crude product was recrystallised from methylated spirits to afford 2-acetyl-5-bromothiophene (**55**), 16.8 g (89%), as an off-white crystalline solid, m.p. 96-97°C (lit.[102] m.p. 94-95°C). Product purity checked by TLC (silica gel, one spot).

^{1}H n.m.r. δ ($CDCl_3$): 2.5 (3H, s, $COCH_3$), 7.1 (1H, d, ThH, J=4Hz), 7.4 (1H, d, ThH, J=4Hz) ppm.

i.r. ν_{max} (KBr): 3093, 1646 (C=O str.), 1409, 1274, 981, 925, 805 cm^{-1}.

2.6.2 *2-Acetyl-5-(4-n-decyloxyphenyl)thiophene* (**56**)

4-n-Decyloxyphenylboronic acid (**22h**) (4.0 g, 0.014 mol) was cross-coupled with 2-acetyl-5-bromothiophene (**55**) (2.9 g, 0.014 mol) with *tetrakis*(triphenylphosphine)-

palladium(0) (0.3 mol%) as catalyst under similar conditions to those reported on p. 63 for compounds (**23a-i**). After work-up purification was achieved by recrystallisation from ethanol to afford the desired 2-acetyl-5-(4-n-decyloxyphenyl)thiophene (**56**), 3.6 g (69%), as a yellow crystalline solid, m.p. 102-104°C. Product purity confirmed by TLC (silica gel, one spot).

^{1}H n.m.r. δ ($CDCl_3$): 0.9 (3H, t, CH_3), 1.2-1.4 (14H, m, alkyl), 1.8 (2H, quint., $ArOCH_2\underline{CH_2}$), 2.6 (3H, s, $COCH_3$), 4.0 (2H, t, $ArO\underline{CH_2}$), 6.9 (2H, d, ArH, J=9Hz), 7.2 (1H, d, ThH, J=4Hz), 7.6 (2H, d, ArH, J=9Hz), 7.70 (1H, d, ThH, J=4Hz) ppm.

i.r. ν_{max} (KBr) 2956, 2917, 2849, 1656 (C=O str.), 1448, 1284, 1258, 799 cm^{-1}.

2.6.3 *3-Chloro-3-(5-(4-n-decyloxyphenyl)thienyl-2-yl)propenal* (**57**)

In an atmosphere of nitrogen, phosphorus oxychloride (1.87 ml, 0.020 mol) was added, dropwise, with stirring to ice cold *N,N*-dimethylformamide (1.87 ml, 0.024 mol) and then allowed to warm to room temperature. The reaction mixture was re-cooled to 0°C and a solution of 2-acetyl-5-(4-n-decyloxyphenyl)thiophene (**56**) (3.0 g, 0.0084 mol) in dry DMF was added, dropwise, and the reaction mixture was heated at 35°C for 3 h. with stirring. Thereafter, the reaction mixture was poured onto ice-cold 10% aqueous sodium acetate solution (100 ml), heated to 40°C for 30 min. and then cooled to room temperature. The crude product was extracted with dichloromethane (3 x 50 ml), washed with water, dried ($MgSO_4$) and the solvent removed under reduced pressure. The crude residue was then purified using column chromatography eluting with DCM followed by recrystallisation from methylated spirits to afford the desired 3-chloro-3-(5-(4-n-decyloxyphenyl)thienyl-2-yl)propenal (**57**), 2.4 g (76%), as a pale yellow crystalline solid, m.p. 61-63°C. Product purity checked by TLC (silica gel, one spot).

^{1}H n.m.r. δ ($CDCl_3$): 0.9 (3H, t, CH_3), 1.2-1.4 (14H, m, alkyl), 1.8 (2H, quint., $\mathrm{ArOCH_2\underline{CH_2}}$), 4.0 (2H, t, $\mathrm{ArO\underline{CH_2}}$), 6.6 (1H, d, C=CH, J=6Hz), 6.9 (2H, d, ArH, J=9Hz), 7.2 (1H, d, ThH, J=4Hz), 7.5 (2H, d, ArH, J=9Hz), 7.6 (1H, d, ThH, J=4Hz), 10.2 (1H, d, CHO, J=6Hz) ppm.

i.r. ν_{max} (KBr): 2918, 2850, 1677 (C=O str.), 1589, 1448, 1289, 1116, 797 cm^{-1}.

2.6.4 *Methyl 5'-(4-n-decyloxyphenyl)-2',2-bithienyl-5-carboxylate* (**58**)

In an atmosphere of nitrogen, a solution of 3-chloro-3-(5-4-n-decyloxyphenyl)thienyl-2-yl)propenal (**57**) (1.9 g, 0.0047 mol) in dry ethanol (20 ml) was added, dropwise, to a cooled (0°C), stirred mixture of methyl thioglycollate (0.42 ml, 0.0047 mol) and sodium ethoxide (prepared from sodium metal (0.12 g, 0.0052 mol) in dry ethanol) at 0°C. After stirring at 0°C for 1 h., the reaction mixture was allowed to warm to room temperature and carefully poured into water. The organic product was extracted with DCM (2 x 50 ml), washed with water (2 x 50 ml), dried ($MgSO_4$) and the solvent removed *in vacuo*. The crude product was then purified by flash chromatography on silica gel eluting with 4:1 DCM:petroleum ether (b.p. 40-60°C), followed by recrystallisation from toluene to furnish the desired methyl 5'-(4-n-decyloxyphenyl)-2',2-bithienyl-5-carboxylate (**58**), 1.3 g (62%), as a pale yellow crystalline solid, m.p. and transition temperatures: K-S_A 126.2°C; I 167.7°C S_A 124.6°C CrX/K. Product purity confirmed by TLC (silica gel, one spot).

Found: C, 68.62; H, 7.30%. $C_{26}H_{32}O_3S_2$ requires C, 68.39; H, 7.06%.

^{1}H n.m.r. δ ($CDCl_3$): 0.9 (3H, t, CH_3), 1.2-1.4 (14H, m, alkyl), 1.8 (2H, quint., $ArOCH_2\underline{CH_2}$), 3.9 (3H, t, CO_2CH_3), 4.0 (2H, t, $ArO\underline{CH_2}$), 6.9 (2H, d, ArH, J=9Hz), 7.1 (2H, d, ThH, J=4Hz), 7.2 (1H, d, ThH, J=4Hz), 7.5 (2H, d, ArH, J=9Hz), 7.7 (1H, d, ThH, J=4Hz) ppm.

i.r. ν_{max} (KBr): 2918, 2850, 1708 (C=O str.), 1463, 1289, 1261, 1106, 798 cm^{-1}.

2.6.5 *5'-(4-n-Decyloxyphenyl)-2',2-bithienyl-5-carboxylic acid* (**59**)

5'-(4-n-Decyloxyphenyl)-2',2-bithienyl-5-carboxylic acid (**59**) was prepared according to the method reported on p. 83 for compounds (**39a-f**). Quantities: methyl 5'-(4-n-decyloxyphenyl)-2',2-bithienyl-5-carboxylate (**58**) (1.1 g, 0.0024 mol); potassium hydroxide (1.2 g, 0.022 mol) and; 80% aqueous ethanol (50 ml). After work-up, the crude acid was used in the next step of the reaction without further purification.

^{1}H n.m.r. δ (DMSO/$CDCl_3$): 0.9 (3H, t, CH_3), 1.2-1.4 (14H, m, alkyl), 1.8 (2H, quint., $ArOCH_2\underline{CH_2}$), 3.2 (1H, s, CO_2H, disappears on D_2O shake), 4.0 (2H, t, $ArO\underline{CH_2}$), 6.9 (2H, d, ArH, J=9Hz), 7.2 (2H, t, ThH), 7.25 (1H, d, ThH, J=4Hz), 7.5 (2H, d, ArH, J=9Hz), 7.70 (1H, d, ThH, J=4Hz) ppm.

i.r. ν_{max} (KBr): 3300-3100 (O-H str.), 2954, 1661 (C=O str.), 1466, 1254, 794 cm^{-1}.

2.6.6 (S)-*4-(1-Methylheptyloxycarbonyl)phenyl 5'-(4-n-decyloxyphenyl)-2',2-bithienyl-5-carboxylate* (**60**) **[Series XI]**

Compound (**60**) **[Series XI]** was prepared according to the procedure outlined on p. 65 for compounds (**27a-f**). Quantities: 5'-(4-n-decyloxyphenyl)-2',2-bithienyl-5-carboxylic acid (**59**) (0.31 g, 0.00068 mol); (*S*)-1-methylheptyl 4-hydroxybenzoate (**25**)

(0.17 g, 0.00068 mol); DCC (0.17 g, 0.00082 mol) and; DMAP (2-3 crystals). After work-up, purification was achieved by flash chromatography on silica gel eluting with 1:2 DCM:petroleum ether (b.p. 40-60°C), followed by repeated recrystallisation from ethanol/toluene to afford the (*S*)-4-(1-methylheptyloxycarbonyl)phenyl 5'-(4-n-decyloxyphenyl)-2',2-bithienyl-5-carboxylate **(60)**, 0.26 g (63%), as a pale yellow crystalline solid. Product purity confirmed by TLC (silica gel, one spot) and HPLC (>99%).

The melting points and transition temperatures for compound **(60)** **[Series XI]** are listed in **Table 14** (p. 187) of the results and discussion section.

Found: C, 71.36; H, 7.52%. $C_{40}H_{50}O_5S_2$ requires C, 71.18; H, 7.47%.

MS (*m/z*) 674 (M+), 623, 461.

^{1}H n.m.r. δ ($CDCl_3$): 0.9 (6H, t, 2 x CH_3), 1.2-1.4 (27H, m, alkyl + C*(H)$\underline{CH_3}$), 1.8 (2H, quint., $ArOCH_2\underline{CH_2}$), 4.0 (2H, t, $ArO\underline{CH_2}$), 5.2 (1H, sextet, $\underline{C^*(H)}CH_3$), 6.9 (2H, d, ArH, J=9Hz), 7.15 (1H, d, ThH, J=4Hz), 7.2 (1H, d, ThH, J=4Hz), 7.3 (3H, m, ThH/ArH), 7.5 (2H, d, ArH, J=9Hz), 7.9 (1H, d, ThH, J=4Hz), 8.1 (2H, d, ArH, J=9Hz) ppm.

i.r. ν_{max} (KBr) 2925, 2851, 1720 (C=O str.), 1460, 1278, 795 cm^{-1}.

2.7 SYNTHESIS OF ESTER (70) [Series XII] DERIVED FROM 5-(4'-n-DECYLOXYBIPHENYL-4-YL)THIOPHENE-2-CARBOXYLIC ACID (69) (Scheme 7)

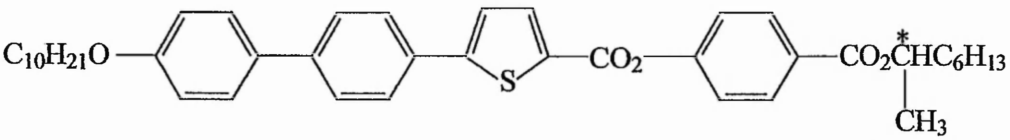

(70) [Series XII]

The synthesis of ester (**70**) [**Series XII**] derived from 5-(4'-n-decyloxybiphenyl-4-yl)thiophene-2-carboxylic acid (**69**) and (*S*)-1-methylheptyl 4-hydroxybenzoate (**25**) is depicted in **Scheme 7**.

The Grignard reagent prepared from 4-bromoanisole was treated with an excess of trimethyl borate at -78°C to afford 4-methoxyphenylboronic acid (**61**) in excellent yield (83%). Palladium-catalysed cross-coupling of (**61**) with commercial 1-bromo-4-iodobenzene afforded 4-bromo-4'-methoxybiphenyl (**62**). The ease of formation of compound (**62**) relies on the synthetic versatility of 1-bromo-4-iodobenzene as an important bifunctional precursor. The iodo-substituent is a better leaving group than the bromo-substituent and the boronic acid (**61**) reacts selectively at the iodo-site to give a two-ring intermediate (**62**) which still possesses a reactive bromo-substituent.

Compound (**62**) was subsequently dealkylated using hydrobromic acid to yield 4'-bromo-4-hydroxybiphenyl (**63**). *O*-Alkylation of (**63**) with 1-bromodecane in the presence of anhydrous potassium carbonate afforded the intermediate 4-bromo-4'-n-

SCHEME 7

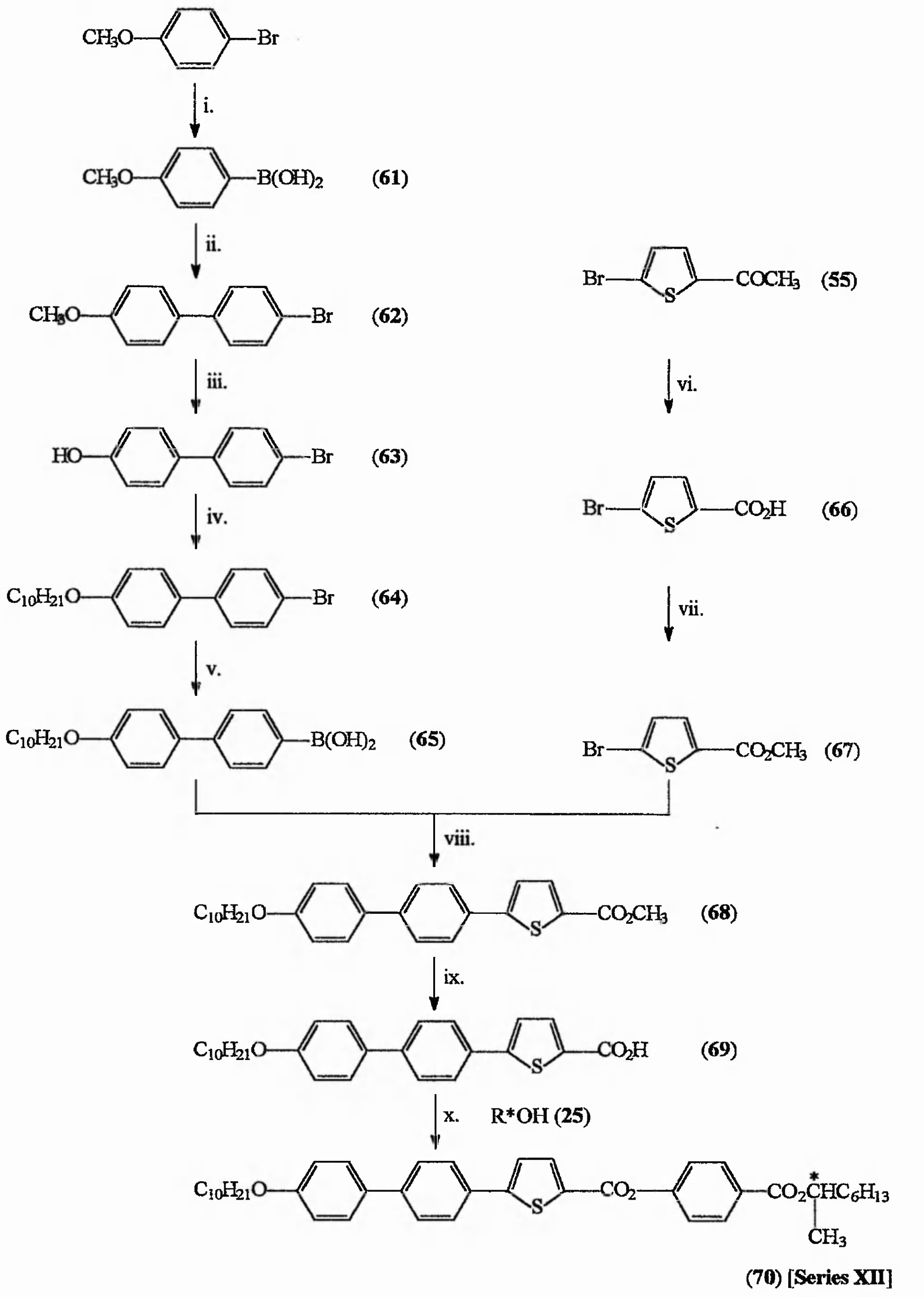

i.	$B(OMe)_3$, -78°C.	vi.	NaOH, Br_2.
ii.	C_6H_4BrI, DME, reflux.	vii.	Me_2SO_4, K_2CO_3, reflux.
iii.	Br, glacial acetic acid, reflux.	viii.	DME, Na_2CO_3, $Pd(PPh_3)_4$.
iv.	$C_{10}H_{21}Br$, K_2CO_3, reflux.	ix.	KOH, 80% aq. EtOH.
v.	a) 1.6M n-BuLi, -78°C, N_2. b) $B(OMe)_3$, 4M HCl.	x.	DCC, DCM, DMAP.

decyloxybiphenyl (**64**). Lithiation of (**64**) followed by quenching with an excess of trimethyl borate generated the corresponding 4'-n-decyloxybiphenyl-4-boronic acid (**65**). Hypobromite oxidation of (**65**) gave 5-bromothiophene-2-carboxylic acid (**66**) which was subsequently methylated in the presence of dimethyl sulphate to afford the corresponding methyl 5-bromothiophene-2-carboxylate (**67**). Suzuki coupling between compounds (**65**) and (**67**) yielded methyl 5-(4'-n-decyloxybiphenyl-4-yl)thiophene-2-carboxylate (**68**) which on base hydrolysis (ethanolic KOH) afforded the 5-(4'-n-decyloxybiphenyl-4-yl)thiophene-2-carboxylic acid (**69**). Esterification of (**69**) with (*S*)-1-methylheptyl 4-hydroxybenzoate (**25**) furnished the desired chiral ester (**70**) **[Series XII]**.

2.7.1 *4-Methoxyphenylboronic acid* (**61**)

In an atmosphere of nitrogen, a solution of 4-bromoanisole (80.0 g, 0.43 mol) in dry THF (200 ml) was added, dropwise, to a mixture of magnesium turnings (12.4 g, 0.516 mol), iodine (single crystal) and dry THF (50 ml) at such a rate that the solvent boiled gently. After the addition was complete, the reaction mixture was heated under reflux for 1 h., and the resultant Grignard reagent was transferred to a pressure equalising funnel and added, dropwise, to a vigorously stirred solution of trimethyl borate (95.6 ml, 0.86 mol) in dry THF (100 ml) at -78°C at such a rate that the temperature did not exceed -70°C. The ensuing white suspension was then allowed to warm to room temperature overnight with stirring. 4M-Aqueous hydrochloric acid (100 ml) was added, dropwise, at 0°C and the solution left to stir at room temperature for 1 h. The crude product was extracted with diethyl ether (3 x 100 ml), washed with water (100 ml), dried ($MgSO_4$) and the solvent removed under reduced pressure. The crude residue was recrystallised from water to afford the pure 4-methoxyphenylboronic acid **(61)**, 53.8 g (83%), as a white solid. Product purity confirmed by TLC (silica gel, one spot).

^{1}H n.m.r. δ ($CDCl_3$): 3.9 (3H, t, CH_3O), 6.9 (2H, d, ArH, J=9Hz), 7.8 (2H, d, ArH, J=9Hz) ppm. OH protons not observed.

i.r. ν_{max} (KBr): 3320-3100 (O-H str.), 2998, 2838, 1604, 1570, 1166, 1024, 751 cm^{-1}.

2.7.2 *4-Bromo-4'-methoxybiphenyl* (**62**)

A solution of 4-methoxyphenylboronic acid **(61)** (16.1 g, 0.107 mol) in 1,2-dimethoxyethane (30 ml) was cross-coupled with 1-bromo-4-iodobenzene (30.2 g, 0.107 mol) in the presence of *tetrakis*(triphenylphosphine)palladium(0) (0.3 mol%) as catalyst, using similar conditions to those reported on p. 63 for compounds (**23a-i**). After work-up, the crude product was recrystallised from ethanol to afford the pure 4-bromo-4'-methoxybiphenyl (**62**), 18.4 g (69%), m.p. 143-145°C [lit.[112] 146°C], as a buff crystalline solid. Product purity confirmed by TLC (silica gel, one spot).

^{1}H n.m.r. δ ($CDCl_3$): 3.9 (3H, t, CH_3O), 7.0 (2H, d, ArH, J=9Hz), 7.4 (2H, d, ArH, J=9Hz), 7.5 (2H, d, ArH, J=9Hz), 7.61 (2H, d, ArH, J=9Hz) ppm.

i.r. ν_{max} (KBr): 3008, 2960, 2836, 1603, 1481, 1288, 1036, 810 cm^{-1}.

2.7.3 *4'-Bromo-4-hydroxybiphenyl* (**63**)

A mixture of 4-bromo-4'-methoxybiphenyl (**62**) (25.0 g, 0.095 mol), glacial acetic acid (30 ml) and 48% aqueous hydrobromic acid (25.8 ml, 0.475 mol) was heated under reflux for 14 h. Thereafter, the reaction mixture was allowed to cool and transferred to a separating funnel where the crude product was extracted with ethyl acetate (3 x 100 ml). The combined organic extract was washed with saturated sodium hydrogen carbonate solution (2 x 100 ml), dried ($MgSO_4$) and the solvent was removed *in vacuo.* The crude product was purified by recrystallisation from glacial acetic acid to furnish the desired 4'-bromo-4-hydroxybiphenyl (**63**), 17.5 g (74%), as a white solid, m.p. 163-165°C (lit.[113] 164-166°C). Product purity checked by TLC (silica gel, one spot).

^{1}H n.m.r. δ ($CDCl_3$): 6.9 (2H, d, ArH, J=9Hz), 7.4 (2H, d, ArH, J=9Hz), 7.45 (2H, d, ArH, J=9Hz), 7.5 (2H, d, ArH, J=9Hz) ppm. OH proton not observed.

i.r. ν_{max} (KBr): 3410-3200 (O-H str.), 1480, 1262, 1082, 813 cm^{-1}.

2.7.4 *4-Bromo-4'-n-decyloxybiphenyl* (**64**)

O-Alkylation of 4'-bromo-4-hydroxybiphenyl (**63**) (8.0 g, 0.032 mol) with 1-bromodecane (8.4 g, 0.038 mol) in the presence of anhydrous potassium carbonate (7.0 g, 0.064 mol) was undertaken using the method described on p. 60 for compounds (**21a-i**). After work-up, the crude product was recrystallised from acetone to yield the desired 4-bromo-4'-n-decyloxybiphenyl (**64**), 9.3 g (75%), as a white crystalline solid, m.p. 120-121°C [lit.[114] 122°C]. Product purity confirmed by TLC (silica gel, one spot).

^{1}H n.m.r. δ ($CDCl_3$): 0.9 (3H, t, CH_3), 1.2-1.4 (14H, m, alkyl), 1.8 (2H, quint., $ArOCH_2\underline{CH_2}$), 4.0 (2H, t, $ArO\underline{CH_2}$), 6.9 (2H, d, ArH, J=9Hz), 7.4 (2H, d, ArH, J=9Hz), 7.45 (2H, d, ArH, J=9Hz), 7.5 (2H, d, ArH, J=9Hz) ppm.

i.r. ν_{max} (KBr): 2957, 2918, 2849, 1605, 1474, 1288, 1255, 811 cm^{-1}.

2.7.5 *4'-n-Decyloxybiphenyl-4-boronic acid* (**65**)

4'-n-Decyloxybiphenyl-4-boronic acid (**65**) was prepared from 4-bromo-4'-n-decyloxybiphenyl (**64**) (6.6 g, 0.017 mol), 1.6M n-BuLi (13.0 ml, 0.020 mol) and trimethyl borate (7.6 ml, 0.068 mol) using the method reported on p. 62 for compounds (**22a-i**). After work-up, the crude boronic acid (**65**), 4.8 g (60%), was obtained as a white waxy solid, which was used in the next step of the reaction without further purification.

^{1}H n.m.r. δ ($CDCl_3$): 0.9 (3H, t, CH_3), 1.2-1.4 (14H, m, alkyl), 1.8 (2H, quint., $ArOCH_2\underline{CH_2}$), 4.0 (2H, t, $ArO\underline{CH_2}$), 4.8 (2H, s, OH, disappears on D_2O shake), 6.9 (2H, d, ArH, J=9Hz), 7.4 (4H, d, ArH, J=9Hz), 7.9 (2H, d, ArH, J=9Hz) ppm.

i.r. ν_{max} (KBr): 3360-3320 (O-H str.), 2917, 2850, 1605, 1394, 816 cm^{-1}.

2.7.6 *5-Bromothiophene-2-carboxylic acid* (**66**)

A cooled (0°C) solution of sodium hypobromite [prepared at 0°C by adding bromine (16.7 ml, 0.32 mol) to a solution of sodium hydroxide (38.4 g, 0.96 mol) in water (100 ml)] was added, dropwise, to a stirred solution of 2-acetyl-5-bromothiophene (**55**) (26.5 g, 0.13 mol) in dioxan (85 ml) ensuring that the temperature did not exceed 50°C. When the addition was complete, the reaction mixture was heated to 60°C for 30 min., allowed to cool to room temperature and transferred to a separating funnel where the unreacted starting material and bromoform, was removed by extraction with chloroform. The aqueous layer was acidified (4M HCl), and the ensuing white suspension was extracted into chloroform (3 x 100 ml), treated with sodium metabisulphite solution, washed with brine (2 x 100 ml), water (2 x 100 ml) and dried

($MgSO_4$). The solvent was then removed *in vacuo* and the crude residue was recrystallised from petroleum ether (b.p. 40-60°C) to furnish the desired 5-bromothiophene-2-carboxylic acid (**66**), 16.1 g (60%), as a white crystalline solid, m.p. 142-143°C (lit.[115] m.p. 142°C). Product purity confirmed by TLC (silica gel, one spot).

^1H n.m.r. δ ($CDCl_3$): 7.1 (1H, d, ThH, J=4Hz), 7.6 (1H, d, ThH, J=4Hz), 8.4 (1H, s, CO_2H, disappears on D_2O shake) ppm.

i.r. ν_{max} (KBr): 3420-3300 (O-H str.), 2922, 2852, 1691 (C=O str.), 1426, 814 cm^{-1}.

2.7.7 *Methyl 5-bromothiophene-2-carboxylate* (67)

A mixture of 5-bromothiophene-2-carboxylic acid (**66**) (14.0 g, 0.068 mol), anhydrous powdered potassium carbonate (18.5 g, 0.136 mol), dimethyl sulphate (6.4 ml, 0.068 mol) and dry acetone (100 ml) was heated under reflux for 8 h. After cooling, the reaction mixture was filtered to remove the inorganic salts and the filtrate was evaporated to dryness. The crude residue was recrystallised from aqueous methanol to furnish methyl 5-bromothiophene-2-carboxylate (**67**), 9.0 g (60%), as a white crystalline solid, m.p. 62-64°C (lit.[78] m.p. 62-63°C). Product purity confirmed by TLC (silica gel, one spot).

^1H n.m.r. δ ($CDCl_3$): 4.0 (3H, s, CO_2CH_3), 7.4 (1H, d, ThH, J=4Hz), 7.7 (1H, d, ThH, J=4Hz) ppm.

i.r. ν_{max} (KBr): 2944, 2841, 1714 (C=O str.), 1532, 1414, 1332, 1261, 1094, 742 cm^{-1}.

2.7.8 *Methyl 5-(4'-n-decyloxybiphenyl-4-yl)thiophene-2-carboxylate* (**68**)

The cross-coupling reaction between 4'-n-decyloxybiphenyl-4-boronic acid (**65**) (3.2 g, 0.009 mol) and methyl 5-bromothiophene-2-carboxylate (**67**) (2.0 g, 0.009 mol) was carried out under similar conditions reported to those on p. 63 for compounds (**23a-i**) in the presence of *tetrakis*(triphenylphosphine)palladium(0) (0.3 mol%). Purification was achieved by flash chromatography on silica gel eluting with DCM, followed by recrystallisation from toluene to afford the desired methyl 5-(4'-n-decyloxybiphenyl-4-yl)thiophene-2-carboxylate (**68**), 2.2 g (54%), as an off-white crystalline solid, m.p. and transition temperatures: K-S_A 162.8°C; I 231.5°C S_A 162.6°C CrX 90.0°C K. Product purity confirmed by TLC (silica gel, one spot).

Found: C, 74.38; H, 7.54%. $C_{28}H_{34}O_3S$ requires C, 74.63; H, 7.60%.

^{1}H n.m.r. δ ($CDCl_3$): 0.9 (3H, t, CH_3), 1.2-1.4 (14H, m, alkyl), 1.8 (2H, quint., $ArOCH_2\underline{CH_2}$), 3.9 (3H, s, CO_2CH_3), 4.0 (2H, t, $ArO\underline{CH_2}$), 7.0 (2H, d, ArH, J=9Hz), 7.3 (1H, d, ThH, J=4Hz), 7.5 (2H, d, ArH, J=9Hz), 7.6 (2H, d, ArH, J=9Hz), 7.7 (2H, d, ArH, J=9Hz), 7.8 (1H, d, ThH, J=4Hz) ppm.

i.r. ν_{max} (KBr): 2954, 2917, 2848, 1723 (C=O str.), 1453, 1273, 809 cm^{-1}.

2.7.9 *5-(4'-n-Decyloxybiphenyl-4-yl)thiophene-2-carboxylic acid* (**69**)

5-(4'-n-Decyloxybiphenyl-4-yl)thiophene-2-carboxylic acid (**69**) was prepared according to the method reported on p. 83 for compounds (**39a-f**). Quantities: methyl 5-(4'-n-decyloxybiphenyl-4-yl)thiophene-2-carboxylate (**68**) (1.8 g, 0.004 mol); potassium hydroxide (2.0 g, 0.036 mol) and; 80%-aqueous ethanol (40 ml). After work-up, the crude acid was used in the next step of the reaction without further purification.

^{1}H n.m.r. δ ($CDCl_3$): 0.9 (3H, t, CH_3), 1.2-1.4 (14H, m, alkyl), 1.8 (2H, quint., $ArOCH_2\underline{CH_2}$), 4.0 (2H, t, $ArO\underline{CH_2}$), 7.0 (2H, d, ArH, J=9Hz), 7.4 (1H, d, ThH, J=4Hz), 7.61 (2H, d, ArH, J=9Hz), 7.6 (2H, d, ArH, J=9Hz), 7.7 (2H, d, ArH, J=9Hz), 7.8 (1H, d, ThH, J=4Hz) ppm. No OH proton detected.

i.r. ν_{max} (KBr): 3440-3320 (O-H str.), 2952, 2848, 1663 (C=O str.), 1456, 810 cm^{-1}.

2.7.10 (S)-*4-(1-Methylheptyloxycarbonyl)phenyl 5-(4'-n-decyloxybiphenyl-4-yl) thiophene-2-carboxylate* (**70**) **[Series XII]**

Ester (**70**) **[Series XII]** was prepared using the method described on p. 65 for compounds (**27a-f**). Quantities: 5-(4'-n-decyloxybiphenyl-4-yl)thiophene-2-carboxylic acid (**69**) (0.28 g, 0.00064 mol); (*S*)-1-methylheptyl 4-hydroxybenzoate (**25**) (0.16 g, 0.00064 mol); DCC (0.16 g, 0.00077 mol) and; DMAP (2-3 crystals). Purification was achieved by flash chromatography on silica gel eluting with 1:1 DCM:petroleum ether (b.p. 40-60°C), followed by repeated recrystallisation from ethanol to afford the desired (*S*)-4-(1-methylheptyloxycarbonyl)phenyl 5-(4'-n-decyloxybiphenyl-4-yl)thiophene-2-carboxylate (**70**), 0.25g (54%), as a pale yellow crystalline solid.

The melting point and transition temperatures are reported in **Table 15** of the results and discussion section on p. 189.

Found: C, 75.38; H, 7.98%. $C_{42}H_{52}O_5S$ requires C, 75.41; H, 7.84%.

MS (*m/z*) 668 (M+), 419.

^{1}H n.m.r. δ ($CDCl_3$): 0.9 (6H, t, 2 x CH_3), 1.2-1.4 (27H, m, alkyl + $C^*(H)\underline{CH_3}$), 1.8 (2H, quint., $ArOCH_2\underline{CH_2}$), 4.0 (2H, t, $ArO\underline{CH_2}$), 5.1 (1H, sextet, $\underline{C^*(H)}CH_3$), 7.0 (2H, d, ArH, J=9Hz), 7.3 (2H, d, ArH, J=9Hz), 7.4 (1H, d, ThH, J=4Hz), 7.61 (2H, d, ArH, J=9Hz), 7.6 (2H, d, ArH, J=9Hz), 7.7 (2H, d, ArH, J=9Hz), 8.0 (1H, d, ThH, J=4Hz), 8.1 (2H, d, ArH, J=9Hz) ppm.

i.r. ν_{max} (KBr): 2953, 2922, 2852, 1719 (C=O str.), 1448, 1274, 691 cm^{-1}.

2.8 SYNTHESIS OF ESTER (77) [Series XIII] DERIVED FROM 5-(4'-n-DECYLOXY-3'-FLUOROBIPHENYL-4-YL)THIOPHENE-2-CARBOXYLIC ACID (76) (Scheme 8)

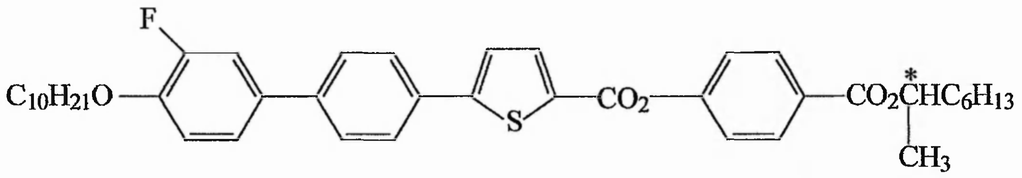

(77) **[Series XIII]**

The synthesis of ester (77) **[Series XII]** derived from 5-(4'-n-decyloxy-3'-fluorobiphenyl-4-yl)thiophene-2-carboxylic acid **(76)** and (*S*)-1-methylheptyl 4-hydroxybenzoate **(25)** is shown in **Scheme 8.**

O-Alkylation of commercial 4-bromo-2-fluorophenol with 1-bromodecane afforded the 4-n-decyloxy-3-fluoro-1-bromobenzene **(71)**. Lithiation of **(71)** at -78°C with 2.5M n-butyllithium followed by trimethyl borate quench gave the desired 4-n-decyloxy-3-fluorophenylboronic acid **(72)**, which was subsequently cross-coupled with 1-bromo-4-iodobenzene to generate 4'-n-decyloxy-3'-fluoro-4-bromobiphenyl **(73)**. Compound **(73)** was then subjected to a second lithiation reaction followed by quenching with trimethyl borate to afford 4'-n-decyloxy-3'-fluorobiphenyl-4-boronic acid **(74)**. Palladium-catalysed cross-coupling of compound **(74)** with methyl 5-bromothiophene-2-carboxylate **(67)** gave the desired methyl 5-(4'-n-decyloxy-3'-fluorobiphenyl-4-yl)thiophene-2-carboxylate **(75)**, which on subsequent hydrolysis gave the desired 5-(4'-n-decyloxy-3'-fluorobiphenyl-4-yl)thiophene-2-carboxylic acid **(76)**. DCC

SCHEME 8

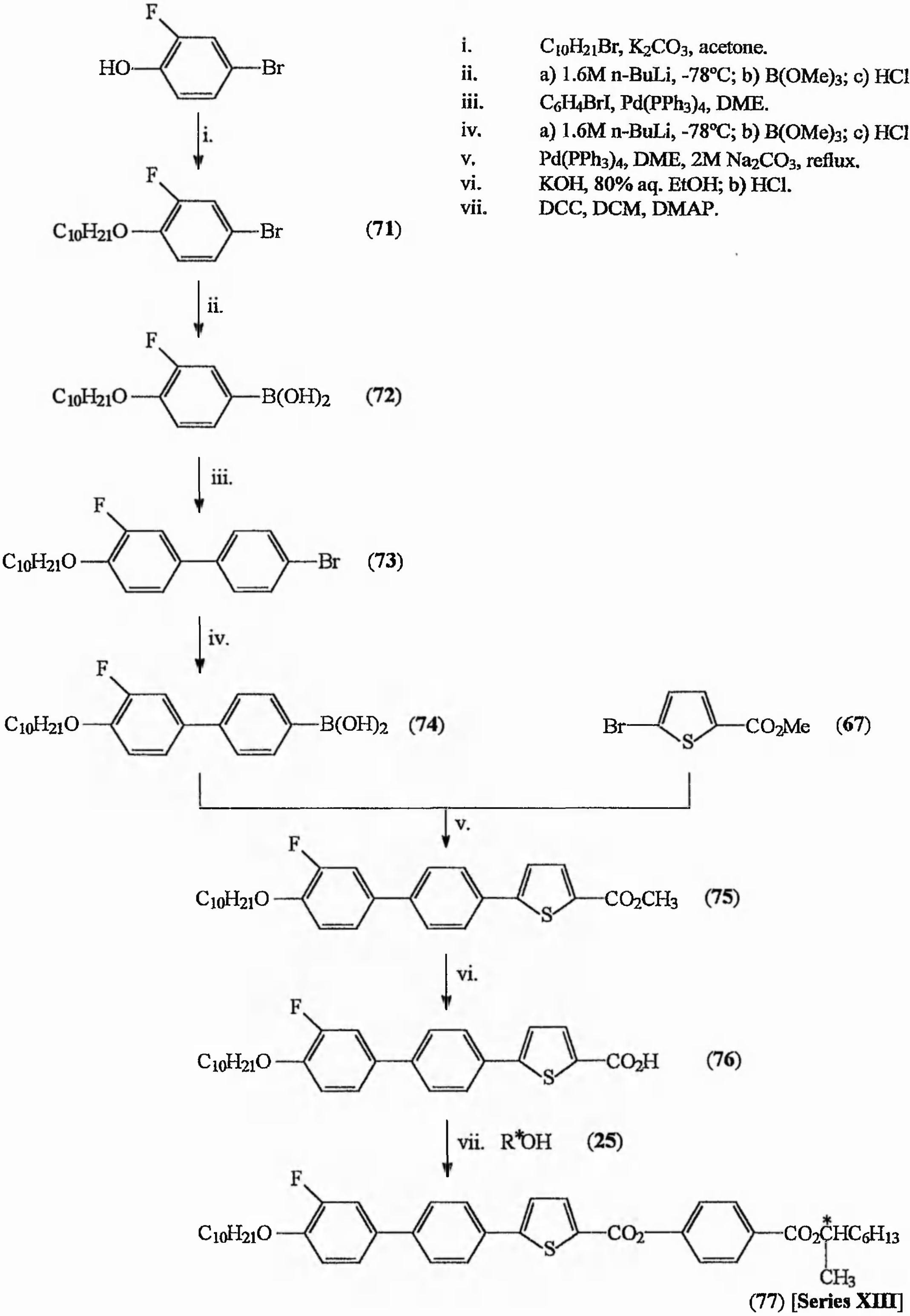

- i. $C_{10}H_{21}Br$, K_2CO_3, acetone.
- ii. a) 1.6M n-BuLi, -78°C; b) $B(OMe)_3$; c) HCl.
- iii. C_6H_4BrI, $Pd(PPh_3)_4$, DME.
- iv. a) 1.6M n-BuLi, -78°C; b) $B(OMe)_3$; c) HCl.
- v. $Pd(PPh_3)_4$, DME, 2M Na_2CO_3, reflux.
- vi. KOH, 80% aq. EtOH; b) HCl.
- vii. DCC, DCM, DMAP.

esterification of (**76**) with (*S*)-1-methylheptyl 4-hydroxybenzoate (**25**) using DMAP as catalyst afforded the desired chiral ester (**77**) **[Series XIII]**.

2.8.1 *4-n-Decyloxy-3-fluoro-1-bromobenzene* (**71**)

O-Alkylation of 4-bromo-2-fluorophenol (10.1 g, 0.053 mol) with 1-bromodecane (14.1 g, 0.064 mol) in the presence of anhydrous potassium carbonate (14.6 g, 0.106 mol) in dry acetone (100 ml) was carried out by using the method shown on p. 60 for compounds (**21a-i**). After work-up, purification was achieved by vacuum distillation (Kugelrohr) to afford the pure 4-n-decyloxy-3-fluoro-1-bromobenzene (**71**), 15.7 g (92%), b.p. 150°C/0.05 mm Hg (Lit.[80] 169°C/0.1 mm Hg), as a colourless liquid. Product purity checked by TLC (silica gel, one spot).

^{1}H n.m.r. δ ($CDCl_3$): 0.9 (3H, t, CH_3), 1.2-1.4 (14H, m, alkyl), 1.8 (2H, quint., $ArOCH_2\underline{CH_2}$), 4.0 (2H, t, $ArO\underline{CH_2}$), 6.8-7.2 (3H, unresolved multiplet, ArH) ppm.

i.r. ν_{max} (Thin film): 2924, 2854, 1503, 1264, 1129, 798 cm^{-1}.

2.8.2 *4-n-Decyloxy-3-fluorophenylboronic acid* (**72**)

Compound (**72**) was prepared using a similar method to that reported on p. 114 for compound (**61**). Quantities: 4-n-decyloxy-3-fluoro-1-bromobenzene (**71**) (11.6 g, 0.035 mol); magnesium turnings (1.0 g, 0.042 mol) and; trimethyl borate (15.6 ml, 0.14 mol). After work-up, the crude product obtained was used in the next step of the reaction without further purification.

^1H n.m.r. δ ($CDCl_3$): 0.9 (3H, t, CH_3), 1.2-1.4 (14H, m, alkyl), 1.8 (2H, quint., $ArOCH_2\underline{CH_2}$), 4.0 (2H, t, $ArO\underline{CH_2}$), 6.8-7.2 (3H, unresolved multiplet, ArH) ppm. OH protons not detected.

i.r. ν_{max} (KBr): 3460-3220 (O-H str.), 2954, 2919, 1614, 1470, 1310, 1022, 816 cm^{-1}.

2.8.3 *4'-n-Decyloxy-3'-fluoro-4-bromobiphenyl* (**73**)

1-Bromo-4-iodobenzene (6.4 g, 0.023 mol) was cross-coupled with 4-n-decyloxy-3-fluorophenylboronic acid (6.8 g, 0.023 mol) (**72**), in the presence of *tetrakis*-(triphenylphosphine)palladium(0) (0.3 mol%), using a similar method to the one reported on p. 63 for compounds (**23a-i**). After work-up, purification of the crude product was achieved by flash chromatography, eluting with 1:20 DCM:petroleum ether (b.p. 40-60°C) followed by recrystallisation from aqueous methanol to afford the 4'-n-decyloxy-3'-fluoro-4-bromobiphenyl (**73**), 6.3 g (67%), as a white crystalline solid, m.p. 62-64°C. Product purity confirmed by TLC (silica gel, one spot).

^1H n.m.r. δ ($CDCl_3$): 0.9 (3H, t, CH_3), 1.2-1.4 (14H, m, alkyl), 1.8 (2H, quint., $ArOCH_2\underline{CH_2}$), 4.0 (2H, t, $ArO\underline{CH_2}$), 7.0-7.3 (3H, unresolved multiplet, ArH), 7.4 (2H, d, ArH, J=9Hz), 7.5 (2H, d, ArH, J=9Hz) ppm.

i.r. ν_{max} (KBr): 2954, 2921, 2851, 1532, 1488, 1134, 807 cm^{-1}.

2.8.4 *4'-n-Decyloxy-3'-fluorobiphenyl-4-boronic acid* (**74**)

4'-n-Decyloxy-3'-fluorobiphenyl-4-boronic acid (**74**) was prepared using similar conditions to those reported on p. 62 for compounds (**22a-i**). Quantities: 4'-n-decyloxy-3'-fluoro-4-bromobiphenyl (**73**) (6.1 g, 0.015 mol); 1.6M n-BuLi (11.0 ml, 0.018 mol) and; trimethyl borate (6.7 ml, 0.06 mol). After work-up, the crude boronic acid was recrystallised from aqueous methanol to give the desired 4'-n-decyloxy-3'-fluorobiphenyl-4-boronic acid (**74**), 4.8 g (86%), as a white solid. Product purity confirmed by TLC (silica gel, one spot).

^{1}H n.m.r. δ ($CDCl_3$): 0.9 (3H, t, CH_3), 1.2-1.4 (14H, m, alkyl), 1.8 (2H, quint., $ArOCH_2\underline{CH_2}$), 4.0 (2H, t, $ArO\underline{CH_2}$), 7.0-7.3 (3H, unresolved multiplet, ArH), 7.4 (2H, d, ArH, J=9Hz), 7.5 (2H, d, ArH, J=9Hz) ppm. OH proton not observed.

i.r. ν_{max} (KBr): 3300-3100 (O-H str.), 2954, 2920, 2851, 1605, 1303, 1135, 809 cm^{-1}.

2.8.5 *Methyl 5-(4'-n-decyloxy-3'-fluorobiphenyl-4-yl)thiophene-2-carboxylate* (**75**)

The cross-coupling reaction between the 4'-n-decyloxy-3'-fluorobiphenyl-4-boronic acid (**74**) (3.4 g, 0.0092 mol) and methyl 5-bromothiophene-2-carboxylate (**67**) (2.0 g, 0.0092 mol) was carried out according to the method described on p. 63 for compounds (**23a-i**) in the presence of *tetrakis*(triphenylphosphine)palladium(0) (0.3 mol%). After work-up, purification was achieved using flash chromatography eluting with 1:1 DCM:petroleum ether (b.p. 40-60°C), followed by recrystallisation from toluene to afford the desired methyl 5-(4'-n-decyloxy-3'-fluorobiphenyl-4-yl)thiophene-2-carboxylate (**75**), 2.7 g (62%), as a pale yellow crystalline solid, m.p. and transition temperatures: K-S_A 125.2°C; I 199.6°C S_A 110.0°C K. Product purity confirmed by TLC (silica gel, one spot).

Found: C, 71.73; H, 7.12%. $C_{28}H_{33}O_3FS$ requires C, 71.76; H, 7.10%

^{1}H n.m.r. δ ($CDCl_3$): 0.9 (3H, t, CH_3), 1.2-1.5 (14H, m, alkyl), 1.8 (2H, quint., $ArOCH_2\underline{CH_2}$), 3.9 (3H, s, CO_2CH_3), 4.0 (2H, t, $ArO\underline{CH_2}$), 7.0-7.4 (4H, unresolved multiplet, ThH/ArH), 7.7 (2H, d, ArH, J=9Hz), 7.7 (2H, d, ArH, J=9Hz), 7.8 (1H, d, ThH, J=4Hz) ppm.

i.r. ν_{max} (KBr): 2917, 2849, 1705 (C=O str.), 1528, 1454, 1298, 1133, 803 cm^{-1}.

2.8.6 *5-(4'-n-Decyloxy-3'-fluorobiphenyl-4-yl)thiophene-2-carboxylic acid* (76)

Hydrolysis of methyl 5-(4'-n-decyloxy-3'-fluorobiphenyl)thiophene-2-carboxylate **(75)** (1.9 g, 0.004 mol) was carried out according to the procedure described on p. 83 for compounds **(39a-f)**, using potassium hydroxide (2.0 g, 0.036 mol) in 80% aqueous ethanol (50 ml). After work-up, the crude residue was used in the next step of the reaction without further purification.

^{1}H n.m.r. δ ($CDCl_3$): 0.9 (3H, t, CH_3), 1.2-1.5 (14H, m, alkyl), 1.8 (2H, quint., $ArOCH_2\underline{CH_2}$), 4.0 (2H, t, $ArO\underline{CH_2}$), 7.0-7.4 (4H, unresolved multiplet, ThH/ArH), 7.7 (2H, d, ArH, J=9Hz), 7.7 (2H, d, ArH, J=9Hz), 7.8 (1H, d, ThH, J=4Hz) ppm. OH proton not observed.

i.r. ν_{max} (KBr): 3450-3320 (O-H str.), 2918, 2850, 1702 (C=O str.), 1460, 807 cm^{-1}.

2.8.7 (S)-*4-(1-Methylheptyloxycarbonyl)phenyl 5-(4'-n-decyloxy-3'-fluorobiphenyl-4-yl)thiophene-2-carboxylate* (77) **[Series XIII]**

The ester (77) was prepared using the method described on p. 65 for compounds **(27a-f)**. Quantities: 5-(4'-n-decyloxy-3'-fluorobiphenyl-4-yl)thiophene-2-carboxylic acid **(76)** (0.28 g, 0.00062 mol); (*S*)-1-methylheptyl 4-hydroxybenzoate **(25)** (0.16 g, 0.00062 mol); DCC (0.15 g, 0.00074 mol) and; DMAP (2-3 crystals). Purification was achieved by flash chromatography on silica gel eluting with 1:1 DCM:petroleum ether (b.p. 40-60°C), followed by recrystallisation from ethanol to afford the desired (*S*)-4-(1-methylheptyloxycarbonyl)phenyl 5-(4'-n-decyloxy-3'-fluorobiphenyl-4-yl)thiophene-2-carboxylate (77) [**Series XIII**], 0.23g (54%), as a pale yellow crystalline solid.

The melting point and transition temperatures are reported in **Table 16** of the results and discussion section on p. 190.

Found: C, 73.38; H, 7.54%. $C_{42}H_{51}O_5FS$ requires C, 73.44; H, 7.48%.

MS (*m/z*) 686 (M+), 409.

^{1}H n.m.r. δ ($CDCl_3$): 0.9 (6H, t, 2 x CH_3), 1.2-1.4 (27H, m, alkyl + C*(H)$\underline{CH_3}$), 1.8 (2H, quint., $ArOCH_2\underline{CH_2}$), 4.0 (2H, t, $ArO\underline{CH_2}$), 5.2 (1H, sextet, $\underline{C^*(H)}CH_3$), 7.0-7.4 (6H, unresolved multiplet, ThH/ArH), 7.6 (2H, d, ArH, J=9Hz), 7.7 (2H, d, ThH, J=9Hz), 8.0 (1H, d, ThH, J=4Hz), 8.1 (2H, d, ArH, J=9Hz) ppm.

i.r. ν_{max} (KBr): 2953, 2922, 1722 (C=O str.), 1448, 1279, 1082, 804 cm^{-1}.

2.9 SYNTHESIS OF ESTER (80) [Series XIV] DERIVED FROM 4-(4'-n-DECYLOXYBIPHENYL-4-YL)THIOPHENE-2-CARBOXYLIC ACID (79) (Scheme 9)

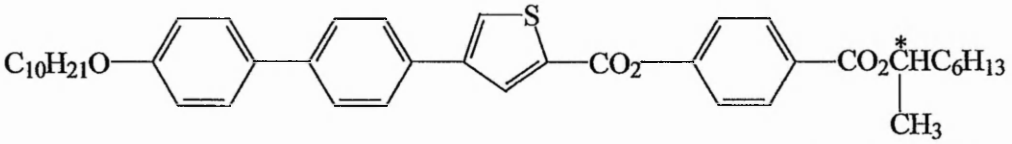

(80) **[Series XIV]**

The synthetic route leading to the preparation of ester **(80)** [**Series XIV**] derived from 4-(4'-n-decyloxybiphenyl-4-yl)thiophene-2-carboxylic acid **(79)** and (*S*)-1-methylheptyl 4-hydroxybenzoate **(25)** is shown in **Scheme 9**.

Palladium-catalysed cross-coupling of 4'-n-decyloxybiphenyl-4-boronic acid **(65)** with methyl 4-bromothiophene-2-carboxylate **(37)** afforded methyl 4-(4'-n-decyloxybiphenyl-4-yl)thiophene-2-carboxylate **(78)**. Subsequent base hydrolysis of compound **(78)** gave the desired 4-(4'-n-decyloxybiphenyl-4-yl)thiophene-2-carboxylic acid **(79)**. DCC esterification of compound **(79)** with (*S*)-1-methylheptyl 4-hydroxybenzoate **(25)** using DMAP as catalyst afforded the desired chiral ester **(80)** [**Series XIV**].

2.9.1 *Methyl 4-(4'-n-decyloxybiphenyl-4-yl)thiophene-2-carboxylate* **(78)**

4'-n-Decyloxybiphenyl-4-boronic acid **(60)** (3.2 g, 0.0091 mol) in 1,2-dimethoxyethane (30 ml) was cross-coupled with methyl 4-bromothiophene-2- carboxylate **(37)** (2.0 g, 0.0091 mol) in the presence of *tetrakis*(triphenylphosphine)palladium(0) (0.3 mol%) under conditions similar to those reported p. 63 for compounds **(23a-i)**. After work-

SCHEME 9

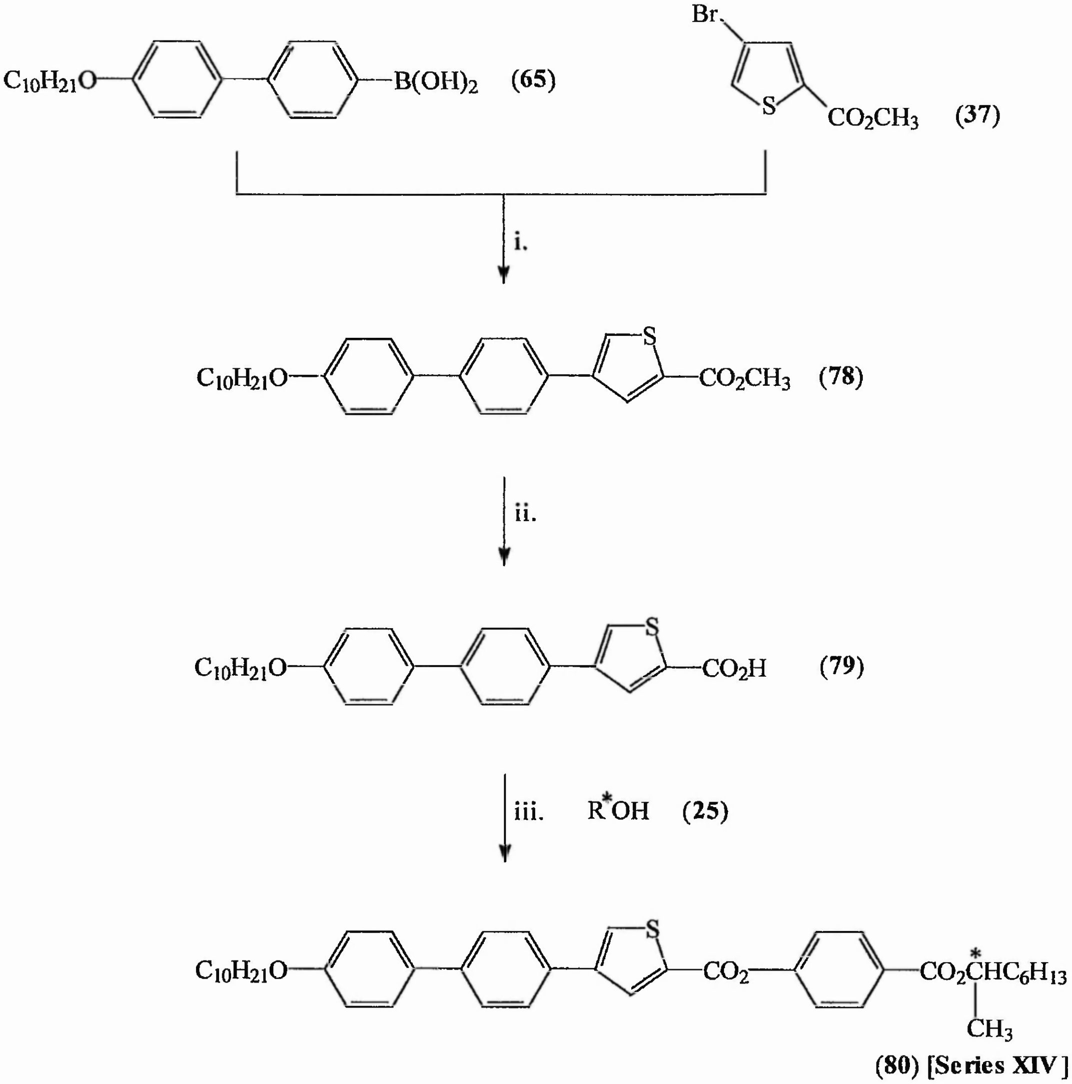

i. 2M Na_2CO_3, DME, $Pd(PPh_3)_4$, reflux.
ii. KOH, 80% aq. EtOH.
iii. DCC, DCM, DMAP.

up, product purification was carried out by flash chromatography on silica gel eluting with 2:1 DCM:petroleum ether (b.p. 40-60°C), followed by recrystallisation from toluene to afford the desired methyl 4-(4'-n-decyloxybiphenyl-4-yl)thiophene-2-carboxylate (**78**), 2.5 g (62%), as a white crystalline solid, m.p. and transition temperatures: K-S_A 143.7°C; I 186.1°C S_A 127.7°C K. Product purity confirmed by TLC (silica gel, one spot).

Found: C, 74.67; H, 7.66%. $C_{28}H_{34}O_3S$ requires C, 74.63; H, 7.60%.

^{1}H n.m.r. δ ($CDCl_3$): 0.9 (3H, t, CH_3), 1.2-1.4 (14H, m, alkyl), 1.8 (2H, quint., $ArOCH_2\underline{CH_2}$), 3.9 (3H, s, CO_2CH_3), 4.0 (2H, t, $ArO\underline{CH_2}$), 7.0 (2H, d, ArH, J=9Hz), 7.5 (2H, d, ArH, J=9Hz), 7.6 (2H, d, ArH, J=9Hz), 7.7 (2H, d, ArH, J=9Hz), 7.8 (1H, d, ThH, J=2Hz), 8.1 (1H, d, ThH, J=2Hz) ppm.

i.r. ν_{max} (KBr): 2954, 2918, 1715 (C=O str.), 1443, 1289, 1086, 774 cm^{-1}.

2.9.2 *4-(4'-n-Decyloxybiphenyl-4-yl)thiophene-2-carboxylic acid* (**79**)

4-(4'-n-Decyloxybiphenyl-4-yl)thiophene-2-carboxylic acid (**79**) was prepared according to the method reported on p. 83 for compounds (**39a-f**). Quantities: methyl 4-(4'-n-decyloxybiphenyl-4-yl)thiophene-2-carboxylate (**78**) (1.8 g, 0.004 mol); potassium hydroxide pellets (2.0 g, 0.036 mol) and; 80% aqueous ethanol (50 ml). After work-up, the crude acid was used in the next step of the reaction without further purification.

^{1}H n.m.r. δ ($CDCl_3$): 0.9 (3H, t, CH_3), 1.2-1.4 (14H, m, alkyl), 1.8 (2H, quint., $ArOCH_2\underline{CH_2}$), 2.9 (1H, s, CO_2H, disappears on D_2O shake), 4.0 (2H, t, $ArO\underline{CH_2}$), 7.0

(2H, d, ArH, J=9Hz), 7.5 (2H, d, ArH, J=9Hz), 7.6 (2H, d, ArH, J=9Hz), 7.7 (2H, d, ArH, J=9Hz), 7.8 (1H, d, ThH, J=2Hz), 8.1 (1H, d, ThH, J=2Hz) ppm.

i.r. ν_{max} (KBr): 3430-3200 (O-H str.), 2952, 2848, 1677 (C=O str.), 1275, 810 cm^{-1}.

2.9.3 (S)-*4-(1-Methylheptyloxycarbonyl)phenyl 4-(4'-n-decyloxybiphenyl-4-yl)-thiophene-2-carboxylate* (**80**) [**Series XIV**]

Ester (**80**) [**Series XIV**] was prepared according to the method reported on p. 65 for compounds (**27a-f**). Quantities: 4-(4'-n-decyloxybiphenyl-4-yl)thiophene-2-carboxylic acid (**74**) (0.28 g, 0.00062 mol); (*S*)-1-methylheptyl 4-hydroxybenzoate (**25**) (0.16 g, 0.00062 mol); DCC (0.15 g, 0.00074 mol) and; DMAP (2-3 crystals). After work-up, the crude ester was purified by flash chromatography on silica gel eluting with 1:2 DCM:petroleum ether (b.p. 40-60°C), followed by repeated recrystallisation from ethanol to give the desired (*S*)-4-(1-methylheptyloxycarbonyl)phenyl 4-(4'-n-decyloxybiphenyl-4-yl)thiophene-2-carboxylate (**80**) [**Series XIV**], 0.24 g (52%), as a white crystalline solid. Product purity confirmed by TLC (silica gel, one spot) and HPLC (>99%).

The melting point and transition temperatures for compound (**80**) [**Series XIV**] are reported in **Table 17** (p. 191) of the results and discussion section.

Found: C, 75.21; H, 7.74%. $C_{42}H_{52}O_5S$ requires C, 75.41; H, 7.84%.

MS (*m/z*) 668 (M+), 419.

^{1}H n.m.r. δ ($CDCl_3$): 0.9 (6H, t, 2 x CH_3), 1.2-1.4 (27H, m, alkyl + C*H($\underline{CH_3}$), 1.8 (2H, quint., $ArOCH_2\underline{CH_2}$), 4.0 (2H, t, $ArO\underline{CH_2}$), 5.2 (1H, sextet, $\underline{C^*H}(CH_3)$), 7.0 (2H, d, ArH, J=9Hz), 7.3 (2H, d, ArH, J=9Hz), 7.61 (2H, d, ArH, J=9Hz), 7.6 (2H, d, ArH, J=9Hz), 7.70 (2H, d, ArH, J=9Hz), 7.8 (1H, d, ThH, J=2Hz), 8.1 (2H, d, ArH, J=9Hz), 8.3 (1H, d, ThH, J=2Hz) ppm.

i.r. ν_{max} (KBr): 2923, 2853, 1742 (C=O str.), 1284, 1238, 1161, 777 cm^{-1}.

2.10 SYNTHESIS OF ESTER (84) [Series XV] DERIVED FROM 4"-n-DECYLOXY-1",1':4',1-TERPHENYL-4-CARBOXYLIC ACID (83) (Scheme 10)

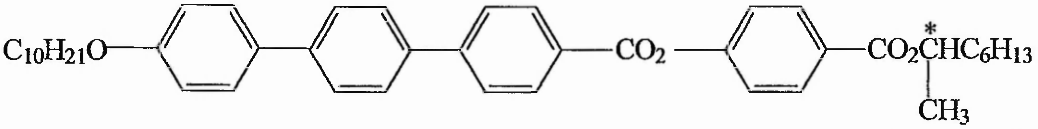

(84) [Series XV]

The synthesis of ester (**84**) derived from 4"-n-decyloxy-1",1':4',1-terphenyl-4-carboxylic acid (**83**) and (*S*)-1-methylheptyl 4-hydroxybenzoate (**25**) was prepared as outlined in **Scheme 10.**

Palladium-catalysed cross-coupling between 4'-n-decyloxybiphenyl boronic acid (**65**) and methyl 4-bromobenzoate (**81**) yielded methyl 4"-n-decyloxy-1",1':4',1-terphenyl-4-carboxylate (**82**) in good yield. Subsequent base hydrolysis (ethanolic KOH) of compound (**82**) gave the desired 4"-n-decyloxy-1",1':4',1-terphenyl-4-carboxylic acid (**83**). DCC esterification of compound (**83**) with (*S*)-1-methylheptyl 4-hydroxybenzoate (**25**) using DMAP as catalyst afforded the (*S*)-4-(1-methylheptyloxycarbonyl)phenyl 4"-n-decyloxy-1",1':4',1-terphenyl-4-carboxylate (**84**) [**Series XV**].

2.10.1 *Methyl 4-bromobenzoate* (**81**)

Commercial 4-bromobenzoic acid (10.0 g, 0.05 mol), dimethyl sulphate (4.7 ml, 0.05 mol), anhydrous potassium carbonate (6.9 g, 0.05 mol) and dry acetone (100 ml) was reacted according to the procedure outlined on p. 60 for compounds (**21a-i**). After work-up, the crude product was purified by recrystallisation from acetone to afford the

SCHEME 10

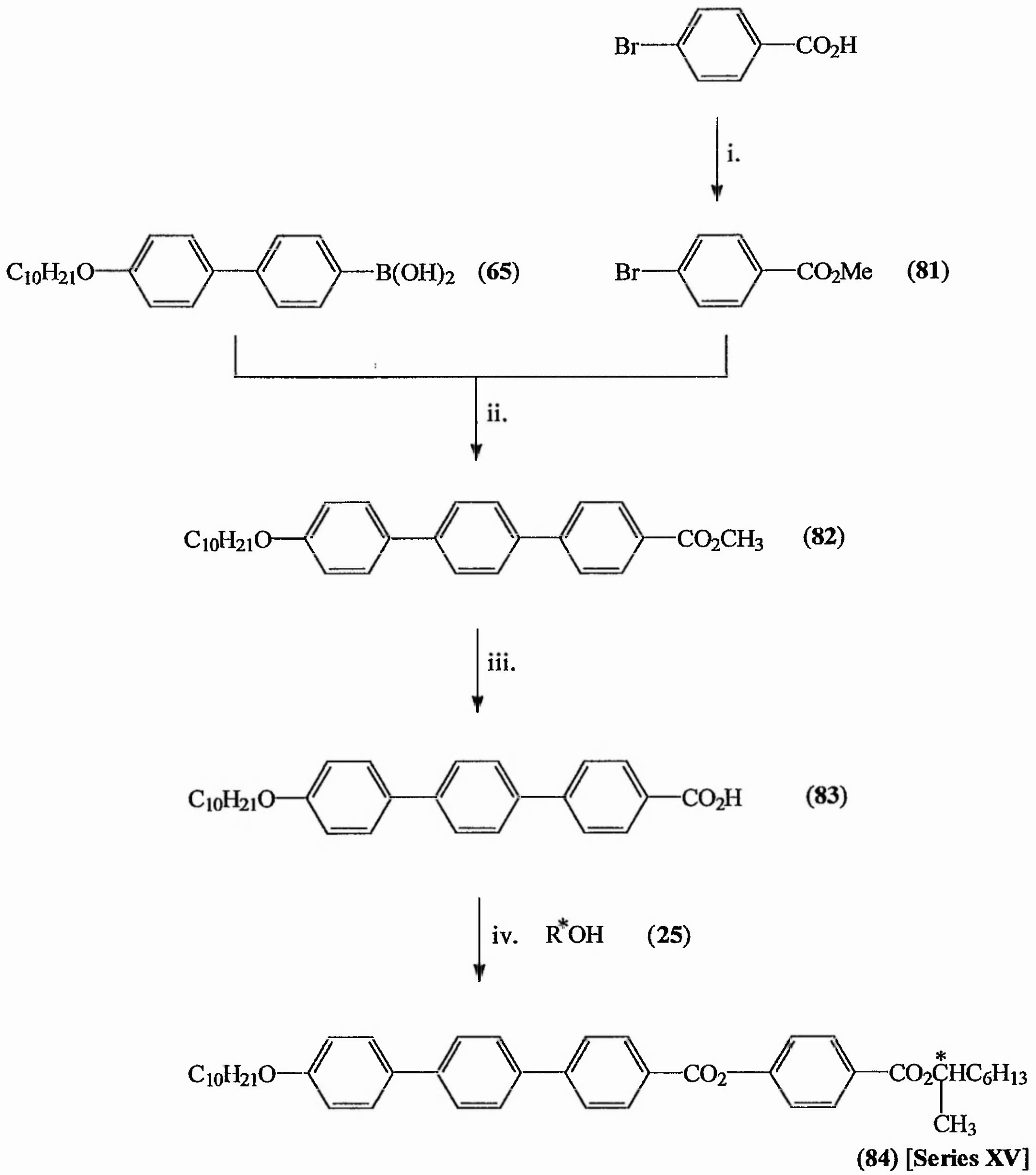

i. K_2CO_3, Me_2SO_4, acetone, reflux.
ii. 2M Na_2CO_3, DME, $Pd(PPh_3)_4$, reflux.
iii. KOH, 80% aq. EtOH.
iv. DCC, DCM, DMAP.

methyl 4-bromobenzoate (**81**), 7.8 g (73%), as a white crystalline solid, m.p. 78-80°C. Product purity confirmed by TLC (silica gel, one spot).

^{1}H n.m.r. δ ($CDCl_3$): 4.0 (3H, s, CO_2CH_3), 7.6 (2H, d, ArH, J=9Hz), 7.8 (2H, d, ArH, ppm.

i.r. ν_{max} (KBr): 2950, 2849, 1715 (C=O str.), 1589, 1277, 1115, 1010, 759 cm^{-1}.

2.10.2 *Methyl 4"-n-decyloxy-1",1':4',1-terphenyl-4-carboxylate* (**82**)

4'-n-Decyloxybiphenyl-4-boronic acid (**65**) (3.2 g, 0.0091 mol) and methyl 4-bromobenzoate (**81**) (1.9 g, 0.0091 mol) were coupled in the presence of *tetrakis*(triphenylphosphine)palladium(0) (0.3 mol%) using the conditions reported on p. 63 for compounds (**23a-i**). After work-up purification was achieved by recrystallisation from toluene to give the methyl 4"-n-decyloxy-1",1':4',1-terphenyl-4-carboxylate (**82**), 2.5 g (62%), as a white crystalline solid, m.p. and transition temperatures: K-S_A 252.8°C; I 281.5°C S_A 253.6°C CrX 102.9°C K. Product purity confirmed by TLC (silica gel, one spot).

Found: C, 79.82; H, 8.13%. $C_{30}H_{36}O_3$ requires C, 81.04; H, 8.16%.

^{1}H n.m.r. δ ($CDCl_3$): 0.9 (3H, t, CH_3), 1.2-1.4 (14H, m, alkyl), 1.8 (2H, quint., $ArOCH_2\underline{CH_2}$), 3.9 (3H, s, CO_2CH_3), 4.0 (2H, t, $ArO\underline{CH_2}$), 7.0 (2H, d, ArH, J=9Hz), 7.6 (2H, d, ArH, J=9Hz), 7.7 (6H, m, ArH), 8.1 (2H, d, ArH, J=9Hz) ppm.

i.r. ν_{max} (KBr): 2604, 2918, 2849, 1724 (C=O str.), 1291, 1112, 822, 771 cm^{-1}.

2.10.3 4"-n-Decyloxy-1",1':4',1-terphenyl-4-carboxylic acid (**83**)

4"-n-Decyloxy-1",1':4',1-terphenyl-4-carboxylic acid (**83**) was prepared according to the procedure described on p. 83 for compounds (**39a-f**). Quantities: methyl 4"-n-decyloxy-1",1':4',1-terphenyl-4-carboxylate (**82**) (1.3 g, 0.003 mol); potassium hydroxide pellets (1.5 g, 0.027 mol) and; 80% aqueous ethanol (50 ml). After work-up the 4"-n-decyloxy-1",1':4',1-terphenyl-4-carboxylic acid (**83**) was used in the next step of the reaction without further purification.

^{1}H n.m.r. δ ($CDCl_3$): 0.9 (3H, t, CH_3), 1.2-1.4 (16H, m, alkyl), 1.8 (2H, quint., $ArOCH_2\underline{CH_2}$), 4.0 (2H, t, $ArO\underline{CH_2}$), 7.0 (2H, d, ArH, J=9Hz), 7.6 (2H, d, ArH, J=9Hz), 7.7 (6H, m, ArH), 8.1 (2H, d, ArH, J=9Hz) ppm. OH proton not detected.

i.r. ν_{max} (KBr): 3440-3220 (O-H str.), 2849, 1686 (C=O str.), 1290, 823 cm^{-1}.

2.10.4 *(S)-4-(1-Methylheptyloxycarbonyl)phenyl 4"-n-decyloxy-1",1':4',1-terphenyl-4-carboxylate* (**84**) [**Series XV**]

Ester (**84**) [**Series XV**] was prepared according to the procedure outlined on p. 65 for compounds (**27a-f**). Quantities: 4"-n-decyloxy-1",1':4',1-terphenyl-4-carboxylic acid (**83**) (0.30 g, 0.0007 mol); (*S*)-1-methylheptyl 4-hydroxybenzoate (**25**) (0.18 g, 0.0007 mol); DCC (0.17 g, 0.00084 mol) and; DMAP (2-3 crystals). After work-up, purification was achieved by flash chromatography on silica gel eluting with 1:1 DCM:petroleum ether (b.p. 40-60°C), followed by repeated recrystallisation from ethanol to afford the (*S*)-4-(1-methylheptyloxycarbonyl)phenyl 4"-n-decyloxy-1",1':4',1-terphenyl-4-carboxylate (**84**), 0.24 g (52%), as a white crystalline solid. Product purity confirmed by TLC (silica gel, one spot) and HPLC (>99%).

The melting point and transition temperatures for compound **(84)** [**Series XV**] are listed in **Table 18** (p. 192) of the results and discussion section.

Found: C, 79.55; H, 8.29%. $C_{44}H_{54}O_5$ requires C, 79.72; H, 8.21%.

MS (*m/z*) 662 (M+), 452.

^{1}H n.m.r. δ ($CDCl_3$): 0.9 (6H, t, 2 x CH_3), 1.2-1.4 (27H, m, alkyl + C*H($\underline{CH_3}$), 1.8 (2H, quint., $ArOCH_2\underline{CH_2}$), 4.0 (2H, t, $ArO\underline{CH_2}$), 5.2 (1H, sextet, $\underline{C^*H}(CH_3)$, 7.0 (2H, d, ArH, J=9Hz), 7.3 (2H, d, ArH, J=9Hz), 7.6 (2H, d, ArH, J=9Hz), 7.7 (4H, quadruplet, ArH), 7.8 (2H, d, ArH, J=9Hz), 8.1 (2H, d, ArH, J=9Hz), 8.3 (2H, d, ArH, J=9Hz) ppm.

i.r. ν_{max} (KBr): 2922, 2852, 1731 (C=O str.), 1465, 1291, 822 cm^{-1}.

RESULTS AND DISCUSSION

3. RESULTS AND DISCUSSION

This chapter reports and discusses the mesomorphic data, which was determined by thermal optical microscopy (sandwich cell and free-standing film, where appropriate), DSC and miscibility for each series prepared (**Series I-XV**). In order to evaluate the mesomorphic data in terms of a meaningful structure-property relationship, this chapter has been sub-divided into the following sections:

i. section 3.1-3.8 contains the mesomorphic data for **Series I-VIII**, respectively. These compounds all contain two-rings in the central molecular core, at least one of which is thiophene, either 2,4- or 2,5-disubstituted;

ii. section 3.9 contains a comparative study of **Series I-VIII**, *i.e.*, two-ring molecular core containing compounds;

iii. sections 3.10-3.16 contains mesomorphic data for **Series IX-XV**, respectively. These compounds all comprise three-rings in the central molecular core of which at least one ring is thiophene except for **Series XV** which serves as a non-heterocyclic model compound.

iv. section 3.17 details a comparative study of three-ring molecular core containing compounds, *i.e.*, **Series IX-XV** and the influence of lateral fluorination is also considered and finally;

v. section 3.18 presents a global summary of all the four-ring containing esters.

3.1 LIQUID CRYSTALLINE PROPERTIES OF (*S*)-4-(1-METHYLHEPTYLOXYCARBONYL)PHENYL 5-(4-n-ALKOXYPHENYL)-THIOPHENE-2-CARBOXYLATES (27a-f) [Series I]

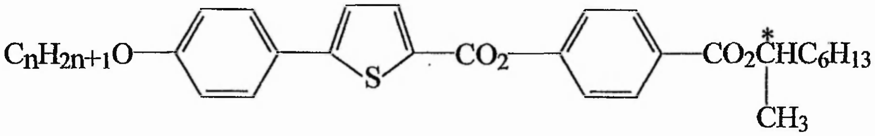

(27a-f)

Six members, n=6-10 and 12, of an homologous series of (*S*)-4-(1-methylheptyloxycarbonyl)phenyl 5-(4-n-alkoxyphenyl)thiophene-2-carboxylates **(27a-f)** **[Series I]** were prepared. Their mesophase transition temperatures are listed in **Table 1** and represented graphically in **Plot 1** against the number of carbon atoms, n, in the alkoxy chain.

On cooling from the isotropic liquid, all the homologues (n=6-10 and 12) exhibit an enantiotropic S_A phase which appears initially as rod-like protrusions termed bâtonnets. These then coalesce rapidly to give the classical focal-conic fan texture interspersed with homeotropic areas (**Plate 1**, p. 203). The points for I-S_A transition temperatures lie on two smooth curves which show an alternating odd-n even-n effect, *i.e.*, the curve for the even-n homologues occurs uppermost. Both curves fall gradually as n increases and tend to converge at the n=12 homologue. The n=6 homologue exhibits no other phase change prior to the onset of crystallisation.

Except for the n=7 homologue, the remaining homologues (n=8-10 and 12) exhibit the S_C*ferro-, ferri- and antiferro-electric phase types on cooling from the S_A phase. The

Table 1: Transition temperatures[a] (°C) and enthalpy values[b] (kJ mol^{-1}) for an homologous series of (*S*)-4-(1-methylheptyloxycarbonyl)phenyl 5-(4-n-alkoxyphenyl)thiophene-2-carboxylates (**27a-f**) [**Series I**].

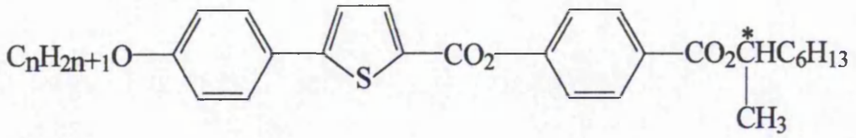

(**27a-f**)

n-alkyl	K-S_A/S_C*$_{FERRI}$/ S_C*$_{ANTI}$	I-S_A	S_A-S_C*$_{FERRO}$	S_A/S_C*-S_C*$_{FERRI}$	S_C*$_{FERRI}$-S_C*$_{ANTI}$	S_A/S_C*$_{ANTI}$ -K
C_6H_{13} (**27a**)	78.3[a] [24.91][b]	116.0 [6.90]	-	-	-	41.5 [6.72]
C_7H_{15} (**27b**)	76.9 [29.97]	108.7 [5.94]	-	(76.6)[c] [-][d]	(75.5) [-]	54.9 [28.03]
C_8H_{17} (**27c**)	71.0 [25.69]	107.7 [6.58]	87.5 [0.47]	86.0 [-]	83.1 [-]	32.4 [17.49]
C_9H_{19} (**27d**)	75.0 [41.82]	102.8 [5.69]	90.3 [0.19]	79.6 [-]	(72.6) [-]	38.5 [21.92]
$C_{10}H_{21}$ (**27e**)	66.4 [29.97]	100.9 [5.89]	92.3 [0.26]	86.7 [-]	84.1 [-]	45.2 [27.77]
$C_{12}H_{25}$ (**27f**)	60.3 [27.39]	96.5 [5.35]	92.0 [0.37]	80.2 [-]	77.7 [-]	38.8 [13.63]

( )[c] - denotes monotropic transition

[-][d] - enthalpy of transition too small to be evaluated

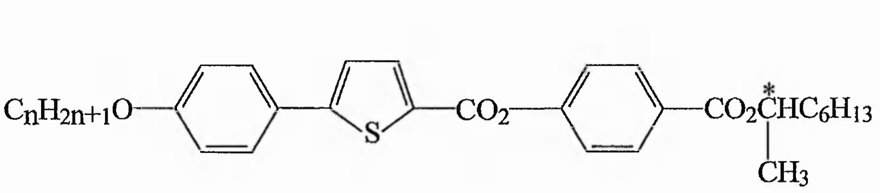

(27a-f)

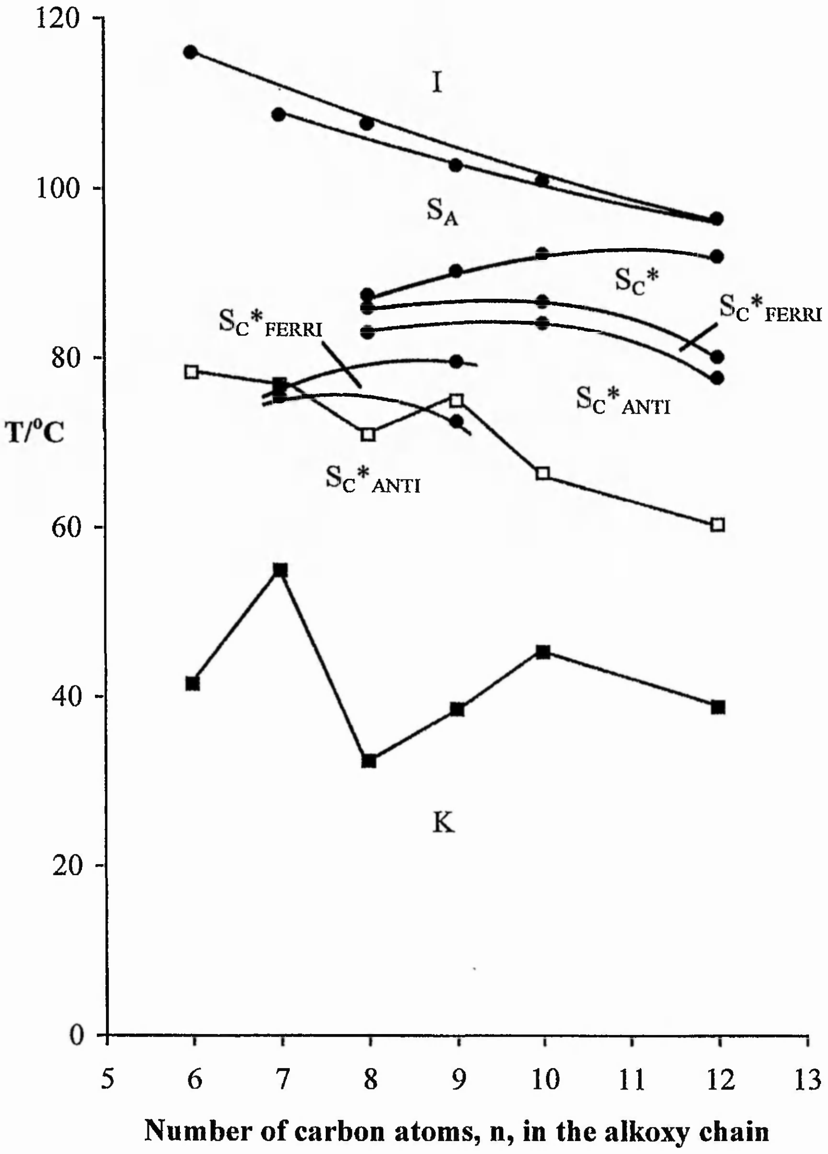

Plot 1: Transition temperature plot for members of an homologous series of (*S*)-4-(1-methylheptyloxycarbonyl)phenyl 5-(4-n-alkoxyphenyl)-thiophene-2-carboxylates (**27a-f**) [**Series I**].

S_C*ferroelectric phase is not observed for the n=7 homologue and it passes directly to the S_C*ferrielectric phase from the S_A phase.

On cooling from the S_A phase of homologues n=8-10 and 12, the focal-conic fans developed a series of fine arcs across their backs whereas the homeotropic region developed an intense blue or red coloration (pseudohomeotropic) marking the onset of the S_C*ferroelectric phase (**Plate 2**, p. 203). The colour in the pseudohomeotropic area changed as the temperature was either increased or decreased and is indicative of an helical structure, *i.e.*, the temperature dependence of the pitch of the $S_C{}^*{}_{FERRO}$ phase. On further cooling of the $S_C{}^*{}_{FERRO}$ phase, an intense mobile milky-white schlieren texture developed in the pseudohomeotropic region thus marking the onset of the $S_C{}^*{}_{FERRI}$ phase (**Plate 3**, p. 204). The $S_C{}^*{}_{ANTI}$ phase replaced the $S_C{}^*{}_{FERRI}$ phase as the shimmering ceased and the 'pseudohomeotropic' region reformed (**Plate 4**, p. 204).

Differential Scanning Calorimetry (DSC) was used as a complimentary technique to further assist with phase identification. The I-S_A transition generated an enthalpy value in the region of 5.71-8.55 kJ mol^{-1} which is characteristic of a first order transition. The enthalpy of the S_A-$S_C{}^*{}_{FERRO}$ transition was not detected easily and corresponded to a weak second order transition with enthalpies ranging from 0.19 and 0.47 kJ mol^{-1}. The transitions from $S_C{}^*{}_{FERRO}$-$S_C{}^*{}_{FERRI}$ and $S_C{}^*{}_{FERRI}$-$S_C{}^*{}_{ANTI}$ were very difficult to monitor due to the very small enthalpy changes involved.

3.2 LIQUID CRYSTALLINE PROPERTIES OF (*S*)-4'-(1-METHYLHEPTYLOXYCARBONYL)BIPHENYL-4-YL 5-(4-n-ALKOXYPHENYL)-THIOPHENE-2-CARBOXYLATES (28a-i) [Series II]

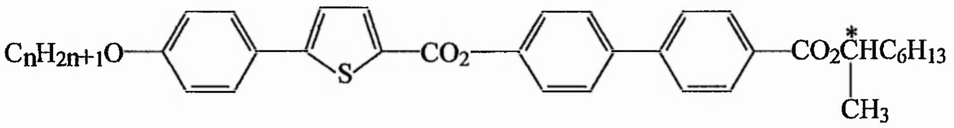

(28a-i)

Nine members, n=3-10 and 12, of an homologous series of (*S*)-4'-(1-methylheptyloxycarbonyl)biphenyl-4-yl 5-(4-n-alkoxyphenyl)thiophene-2-carboxylates **(28a-i) [Series II]** were prepared. Their mesophase transition temperatures are listed in **Table 2** and represented graphically in **Plot 2** against the number of carbon atoms, n, in the alkoxy chain.

On cooling from the isotropic liquid, all the homologues (n=3-10 and 12) exhibit an enantiotropic S_A phase with an enthalpy value in the region of 5.71-8.55 kJ mol^{-1} characteristic of a first order transition. The points for the I-S_A transition temperatures lie on two smooth curves with the even-n homologues lying uppermost. Both curves fall gradually as n increases and tend to converge at the n=8 homologue. The n=3 homologue exhibits no other phase type prior to the onset of crystallisation.

On cooling the n=4 homologue, the fan texture becomes arced or banded and an unfocusable golden-yellow schlieren-mosaic texture develops in the previously homeotropic regions indicative of either the S_I* phase or a high order smectic crystal

Table 2: Transition temperatures[a] (°C) and enthalpy values[b] (kJ mol^{-1}) for an homologous series of (*S*)-4'-(1-methylheptyloxycarbonyl)biphenyl-4-yl 5-(4-n-alkoxyphenyl)thiophene-2-carboxylates (**28a-i**) [**Series II**].

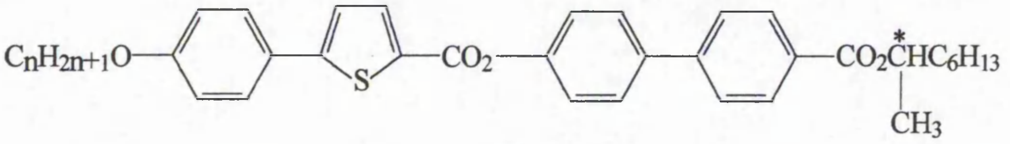

(**28a-i**)

n-alkyl	K-S_A/S_I*	I-S_A	S_A-S_C*$_{FERRO}$	S_C*$_{FERRO}$-S_C*$_{FERRI}$	S_C*$_{FERRO}$-S_C*$_{ANTI}$	S_C*$_{FERRI}$-S_C*$_{ANTI}$	S_A/S_C*$_{ANTI}$-S_I*	S_A/S_I*-K
C_3H_7 (**28a**)	135.4[a] [22.95][b]	220.9 [7.08]	-	-	-	-	-	130.9 [22.24]
C_4H_9 (**28b**)	94.1 [14.45]	223.8 [8.55]	-	-	-	-	104.1 [0.57]	67.2 [9.12]
C_5H_{11} (**28c**)	86.8 [15.08]	214.0 [8.19]	135.0 [0.04]	-	124.5 [-][c]	-	111.2 [0.49]	54.1 [9.29]
C_6H_{13} (**28d**)	63.6 [11.46]	211.0 [7.50]	151.3 [-]	-	131.1 [-]	-	109.3 [0.52]	26.1 [4.77]
C_7H_{15} (**28e**)	87.4 [22.41]	204.4 [5.78]	169.6 [0.10]	-	148.6 [-]	-	101.4 [0.34]	52.1 [7.62]
C_8H_{17} (**28f**)	88.1 [23.14]	200.8 [7.90]	178.1 [0.11]	-	158.5 [-]	-	106.0 [0.65]	55.9 [17.82]
C_9H_{19} (**28g**)	94.5 [21.40]	196.6 [6.30]	181.7 [0.04]	156.1 [-]	-	154.1 [-]	107.6 [0.90]	57.5 [18.60]
$C_{10}H_{21}$ (**28h**)	88.1 [23.90]	193.2 [7.69]	183.2 [0.62]	159.6 [0.05]	-	158.3 [-]	108.9 [1.38]	46.1 [4.84]
$C_{12}H_{25}$ (**28i**)	85.6 [22.48]	186.6 [5.71]	181.2 [0.88]	149.0 [-]	-	145.9 [-]	94.0 [0.92]	33.4 [4.90]

[-][c] - enthalpy of transition too small to be evaluated

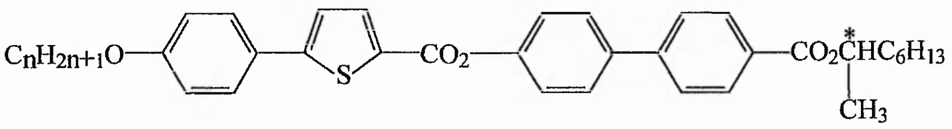

(28a-i)

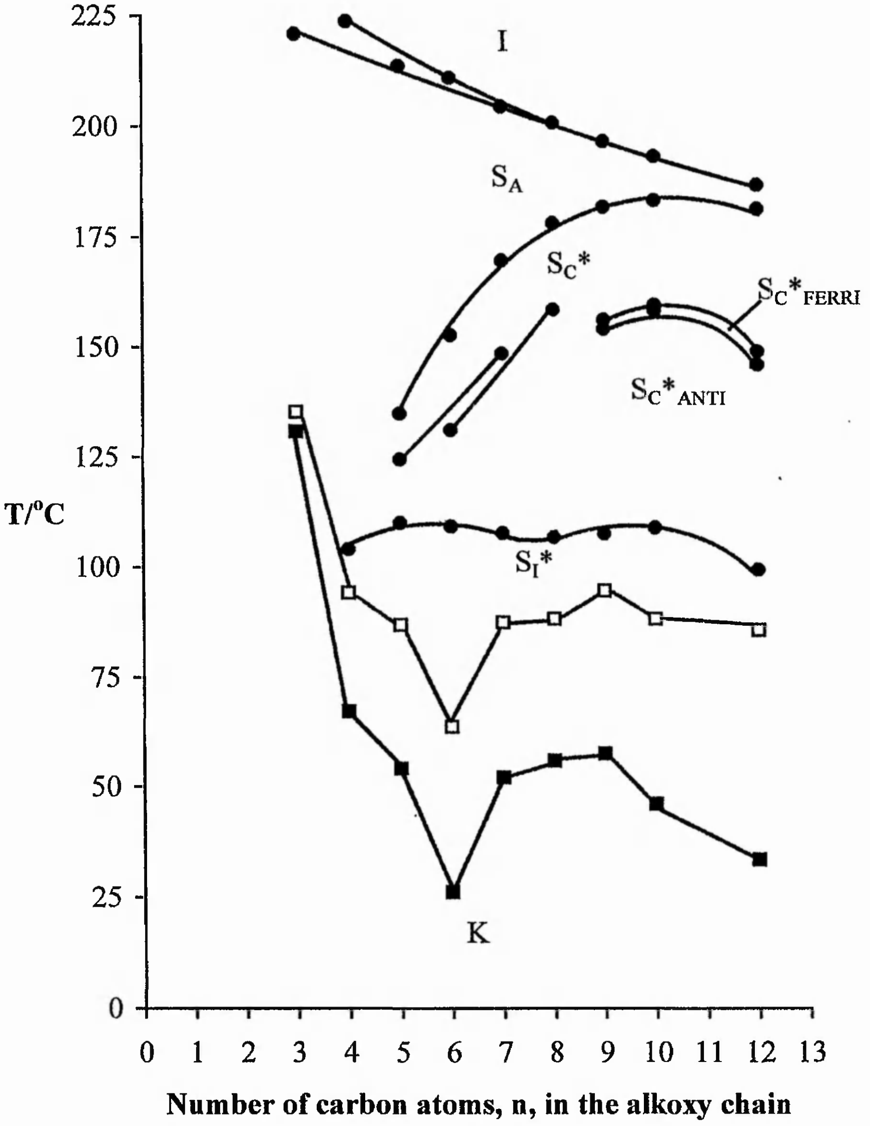

Plot 2: Transition temperature plot for members of an homologous series of (*S*)-4'-(1-methylheptyloxycarbonyl)biphenyl-4-yl 5-(4-n-alkoxyphenyl)-thiophene-2-carboxylates (**28a-i**) [**Series II**].

phase. The true identity of this phase was ascertained by miscibility study as reported below.

The n=5-8 homologues do not exhibit the S_C*_{FERRI} phase, but pass directly from the S_C*_{FERRO} to the S_C*_{ANTI} phase which on further cooling also exhibit this unusual unfocusable schlieren-mosaic texture. On cooling the S_C*_{FERRO} phase of homologues n=9-12, the S_C*_{FERRI} and S_C*_{ANTI} phase types are observed as characterised earlier on p. 143. On further cooling of the S_C*_{ANTI} phase the unfocusable texture was again observed and the true identity of this phase type was determined by miscibility with (*S*)-4-(1-methylheptyloxycarbonyl)phenyl 4'-nonyloxybiphenyl-4-carboxylate as the standard (**85**).[116]

An elaborate and pain-staking free-standing film miscibility study was performed rather than the conventional sandwich cell study, *i.e.*, between glass slide and coverslip, because it is well known that the ferri- and antiferro-electric phase types are influenced by strong boundary forces. Also, the identification of either the S_I* or high order smectic crystal phases will be easier since the latter will form as a mosaic texture with strong grain boundaries in the film, whereas a *soft* schlieren-mosaic texture will be observed for the S_I* phase.

A series of binary mixtures of the n=10 homologue (**28h**) were prepared with the standard compound (**85**) and mesomorphic properties were determined and represented graphically in **Plot 2a** which shows complete miscibility across the entire

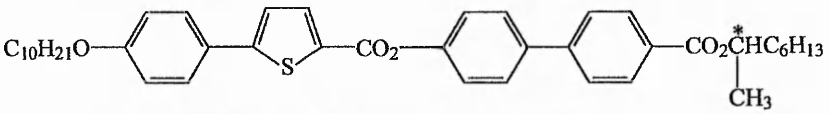

(28h)

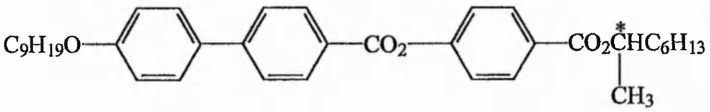

(85)

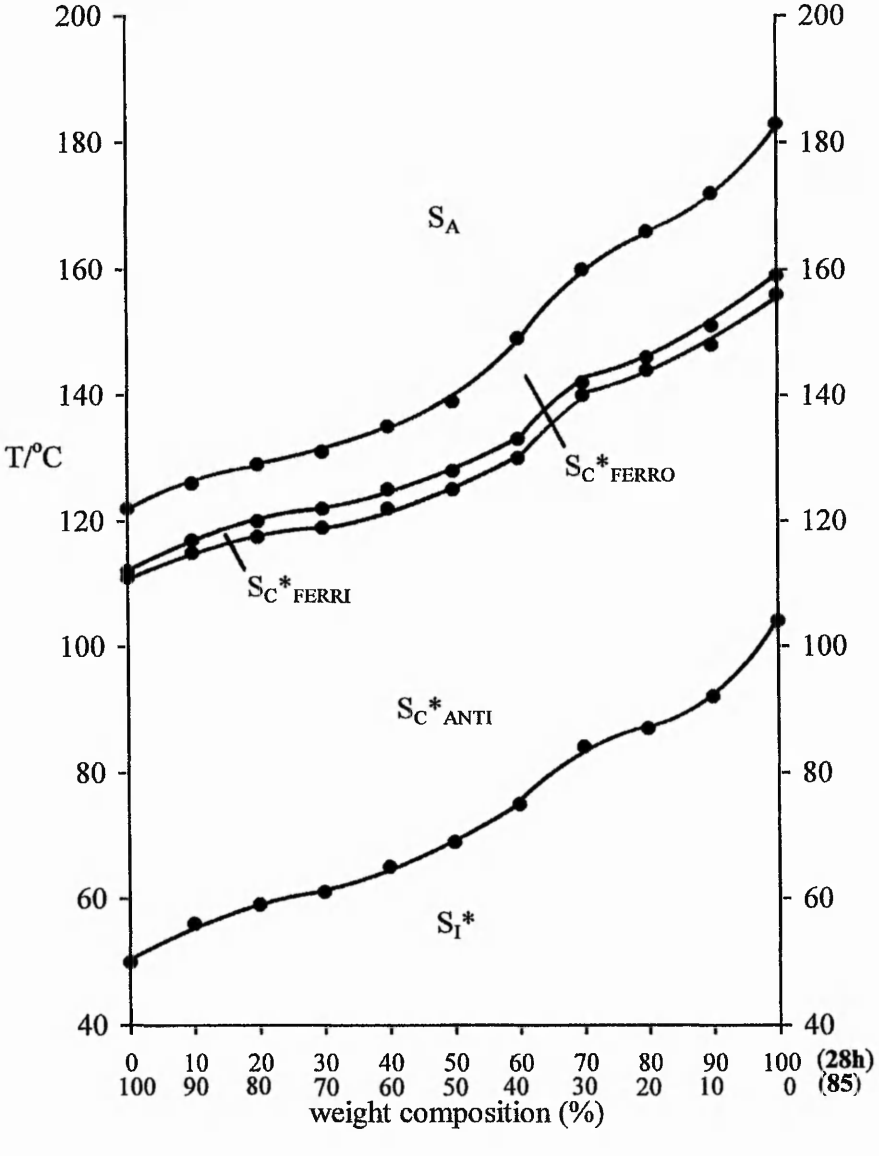

Plot 2a: Miscibility study for various compositions of (*S*)-4'-(1-methylheptyloxycarbonyl)biphenyl-4-yl 5-(4-n-decyloxyphenyl)thiophene-2-carboxylate (**28h**) with the standard (*S*)-4-(1-methylheptyloxycarbonyl)phenyl 4'-nonyloxybiphenyl-4-carboxylate (**85**).

range for the S_C*ferro-, ferri-, antiferro-electric and S_I* phase types. Such a study provides spectacular optical textures for each phase type as evidenced by **Plates 5-9.** For the 50:50 composition, the S_A-S_C*_{FERRO} transition was detected by the onset of a spectacular blue-green colour (**Plate 5**, p. 205) in the previously dark film. The onset of the S_C*_{FERRI} phase gives rise to a shimmering milky-white texture (**Plate 6**, p. 205) which is in constant motion and as this ceases an almost clear film develops (**Plate 7**, p. 206) in the film characteristic of the S_C*_{ANTI} phase. Transition to the S_I* phase was rather spectacular as a fabulous finger-print texture[117] (**Plate 8**, p. 206) developed in the film which then cleared to give a schlieren mosaic-like texture (**Plate 9**, p. 207) characteristic of the S_I* phase.

The identity of these phase types has been further ascertained by complimentary electro-optic studies undertaken by Professor Komitov, Chalmers University, Gothenburg, Sweden. The synthesis and characterisation of the liquid crystalline properties of the n=10 homologue (**28h**) has been accepted for publication to the Journal of Materials Chemistry and a copy of the abstract is included in the appendices.

3.3 LIQUID CRYSTALLINE PROPERTIES OF (*S*)-4-(1-METHYLHEPTYLOXYCARBONYL)PHENYL 5'-n-ALKYL-2',2-BITHIENYL-5-CARBOXYLATES (33a-f) [Series III]

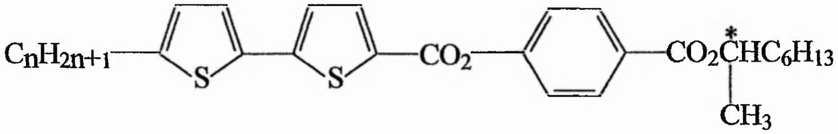

(33a-f)

Six members, n=6-10 and 12, of an homologous series of (*S*)-4-(1-methylheptyloxycarbonyl)phenyl 5'-n-alkyl-2',2-bithienyl-5-carboxylates **(33a-f)** **[Series III]** were prepared. Their mesophase transition temperatures are listed in **Table 3** and represented graphically in **Plot 3** against the number of carbon atoms, n, in the alkyl chain.

None of the homologues (n=6-10 and 12) exhibit enantiotropic phases. All homologues exhibit a monotropic S_A phase with enthalpy values ranging from 8.03-11.38 kJ mol^{-1}. A smooth curve can be drawn for the points correlating to the I-S_A transition temperatures (odd-n above even-n). Both curves decline gradually as n increases and tend to converge at the n=12 homologue. The n=6-8 homologues show no further mesophases prior to the onset of crystallisation.

Occurrence of the S_C*ferro-, ferri- and antiferro-electric phase types is dependent upon the homologue. The n=9 homologue exhibits an additional S_C*ferrielectric phase prior to the onset of crystallisation whereas the n=10 homologue exhibits S_C*ferro-, ferri- and antiferro-electric phase types. The n=12 homologue does not exhibit a $S_C{*}_{FERRO}$

Table 3: Transition temperatures[a] (°C) and enthalpy values[b] (kJ mol^{-1}) for an homologous series of (*S*)-4-(1-methylheptyloxycarbonyl)phenyl 5'-n-alkyl-2',2-bithienyl-5-carboxylates (**33a-f**) [**Series III**].

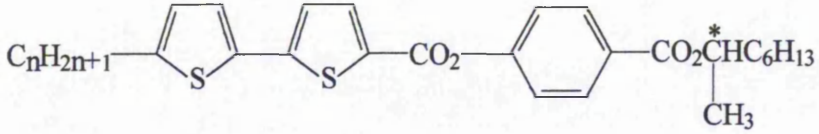

(**33a-f**)

n-alkyl	K-I	I-S_A	S_A-$S_C^*{}_{FERRO}$	S_A/$S_C^*{}_{FERRO}$-$S_C^*{}_{FERRI}$	$S_C^*{}_{FERRI}$-$S_C^*{}_{ANTI}$	S_C^*/$S_C^*{}_{FERRI}$ $S_C^*{}_{ANTI}$-K
C_6H_{13} (**33a**)	79.8[a] [34.43][b]	(62.5)[c] [8.03]	-	-	-	(52.6) [22.18]
C_7H_{15} (**33b**)	64.7 [36.84]	(63.7) [8.10]	-	-	-	(32.4) [14.75]
C_8H_{17} (**33c**)	63.4 [39.42]	(59.9) [10.40]	-	-	-	(45.4) [24.96]
C_9H_{19} (**33d**)	61.5 [34.93]	(59.2) [9.80]	-	(46.0) [-][d]	-	(31.0) [5.60]
$C_{10}H_{21}$ (**33e**)	59.0 [39.33]	(56.1) [10.58]	(50.9) [0.06]	(48.5) [-]	(47.6) [-]	(42.3) [11.10]
$C_{12}H_{25}$ (**33f**)	57.1 [45.86]	(55.4) [11.38]	-	(54.4) [-]	(49.4) [-]	(20.7) [13.75]

( )[c] -denotes monotropic transition

[-][d] - enthalpy of transition too small to be evaluated

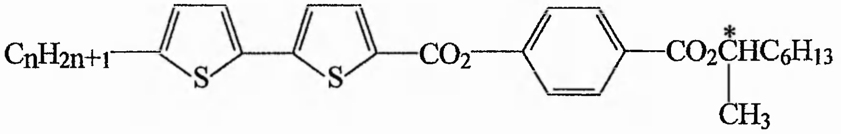

(33a-f)

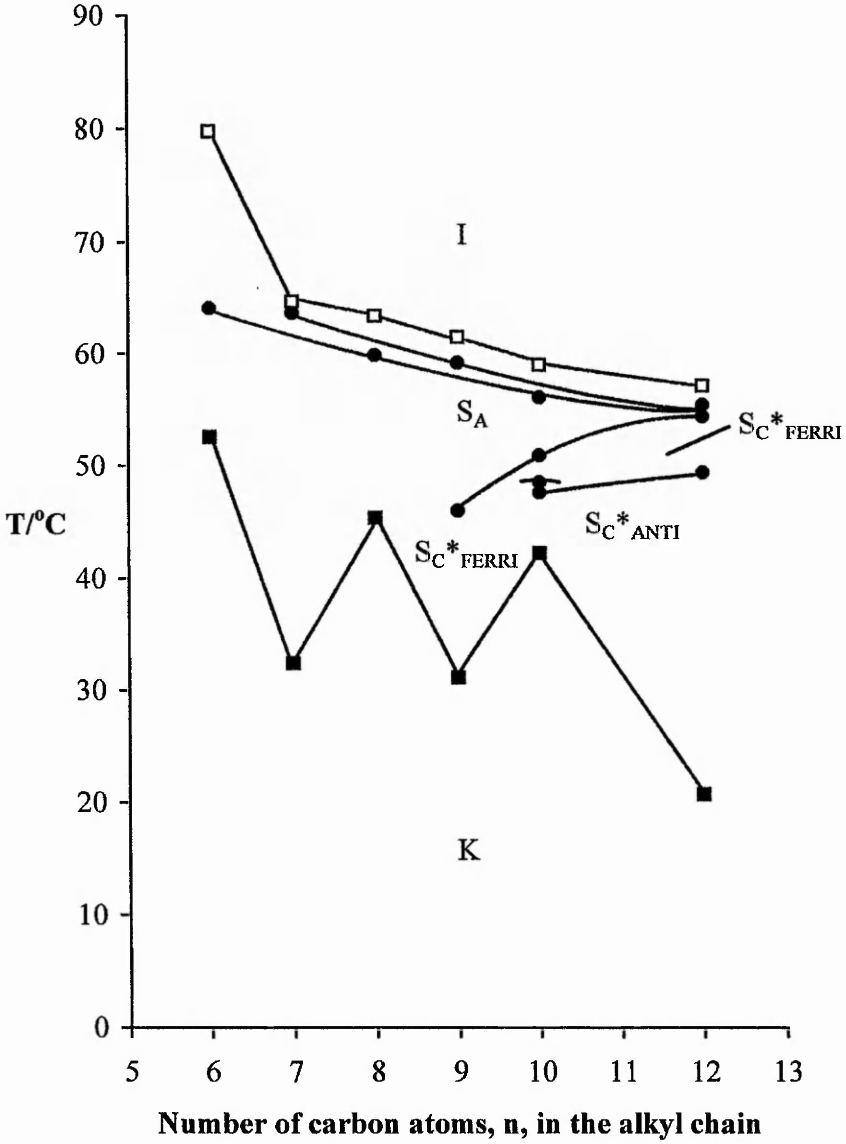

Plot 3: Transition temperature plot for members of an homologous series of (*S*)-4-(1-methylheptyloxycarbonyl)phenyl 5'-n-alkyl-2',2-bithienyl-5-carboxylates (**33a-f**) [**Series III**].

phase on cooling from the S_A phase but coverts directly into the $S_C{}^*{}_{FERRI}$ phase which on further cooling exhibits the $S_C{}^*{}_{ANTI}$ phase. No other phases are observed prior to the onset of crystallisation.

3.4 LIQUID CRYSTALLINE PROPERTIES OF (*S*)-4'-(1-METHYLHEPTYLOXYCARBONYL)BIPHENYL-4-YL 5'-n-ALKYL-2',2-BITHIENYL-5-CARBOXYLATES (34a-i) [Series IV]

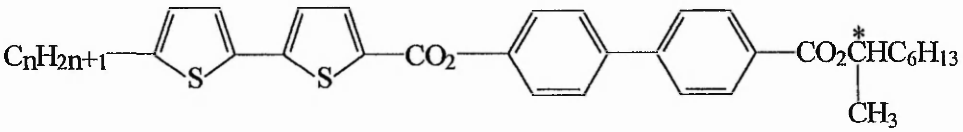
(34a-i)

Nine members, n=3-10 and 12, of an homologous series of (*S*)-4'-(1-methylheptyloxycarbonyl)biphenyl-4-yl 5'-n-alkyl-2',2-bithienyl-5-carboxylates **(34a-i)** **[Series IV]** were prepared. Their mesophase transition temperatures are listed in **Table 4** and represented graphically in **Plot 4** against the number of carbon atoms, n, in the alkyl chain.

All the homologues (n=3-10 and 12) exhibit a S_A phase which appears initially as bâtonnets on cooling from the isotropic liquid with enthalpy values ranging from 5.37-7.01 kJ mol^{-1}. The points for the I-S_A transition lie on two smooth curves which shown an alternating odd-n (upper curve) even-n (lower curve) effect. Both curves decrease gradually as n increases and tend to converge at the n=10 homologue. The n=3 and n=4 homologues exhibit no other phases prior to the onset of crystallisation.

On cooling the S_A phase, homologues n=5-12 exhibit the S_C*_{FERRO} phase which is characterised by arcs across the fans coupled with a coloured pseudohomeotropic region. Further cooling of homologues n=5-7 produces the S_I* phase which is characterised by an unfocusable schlieren mosaic texture and also by DSC which

Table 4: Transition temperatures[a] (°C) and enthalpy values[b] (kJ mol^{-1}) for an homologous series of (*S*)-4'-(1-methylheptyloxycarbonyl)biphenyl-4-yl 5'-n-alkyl-2',2-bithienyl-5-carboxylates (**34a-i**) [**Series IV**].

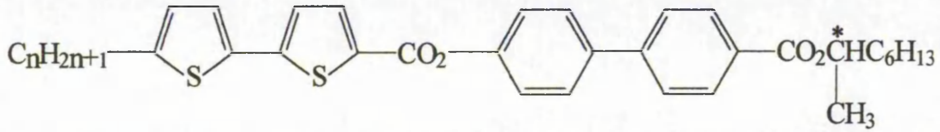

(34a-i)

n-alkyl	K-S_A/S_C*$_{FERRO}$/S_C*$_{FERRI}$/S_I*	I-S_A	S_A-S_C*$_{FERRO}$	S_C*$_{FERRO}$-S_C*$_{FERRI}$	S_C*$_{FERRI}$-S_C*$_{ANTI}$	S_C*$_{FERRO}$-S_C*$_{FERRI/ANTI}$	S_C*$_{FERRO}$/S_C*$_{ANTI}$-S_I*	S_A/S_I*-K
C_3H_7 **(34a)**	109.7 [23.42]	162.7 [5.37]	-	-	-	-	-	95.4 [22.56]
C_4H_9 **(34b)**	114.8 [30.84]	155.6 [5.65]	-	-	-	-	-	103.4 [29.46]
C_5H_{11} **(34c)**	83.6 [25.66]	158.4 [6.43]	(71.3)[c] [-][d]	-	-	-	(64.9) [-]	39.2 [3.65]
C_6H_{13} **(34d)**	65.2 [25.87]	152.2 [6.16]	91.3 [-]	-	-	-	(63.0) [0.34]	23.8 [13.65]
C_7H_{15} **(34e)**	81.9 [25.43]	152.7 [6.72]	102.4 [-]	-	-	-	(80.0) [0.24]	23.6 [6.17]
C_8H_{17} **(34f)**	96.3 [30.02]	148.2 [6.92]	117.6 [0.13]	-	-	(90.6) [-]	(78.6) [1.02]	33.8 [12.04]
C_9H_{19} **(34g)**	100.4 [28.70]	148.6 [6.75]	125.2 [-]	-	-	109.1 [-]	(90.1) [2.31]	35.3 [3.40]
$C_{10}H_{21}$ **(34h)**	86.7 [29.02]	146.1 [7.01]	133.6 [0.31]	-	-	116.3 [-]	95.1 [4.51]	49.0 [6.46]
$C_{12}H_{25}$ **(34i)**	44.8 [7.23]	142.0 [6.71]	135.0 [0.34]	116.3 [-]	110.7 [-]	-	94.8 [5.63]	36.9 [5.25]

( )[c] - denotes monotropic transition
[-][d] - enthalpy of transition too small to be evaluated

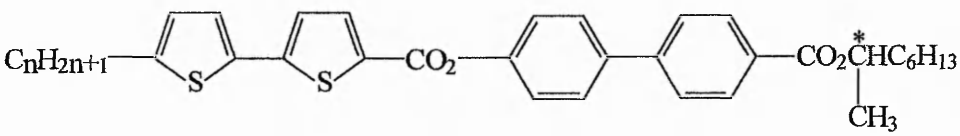

(34a-i)

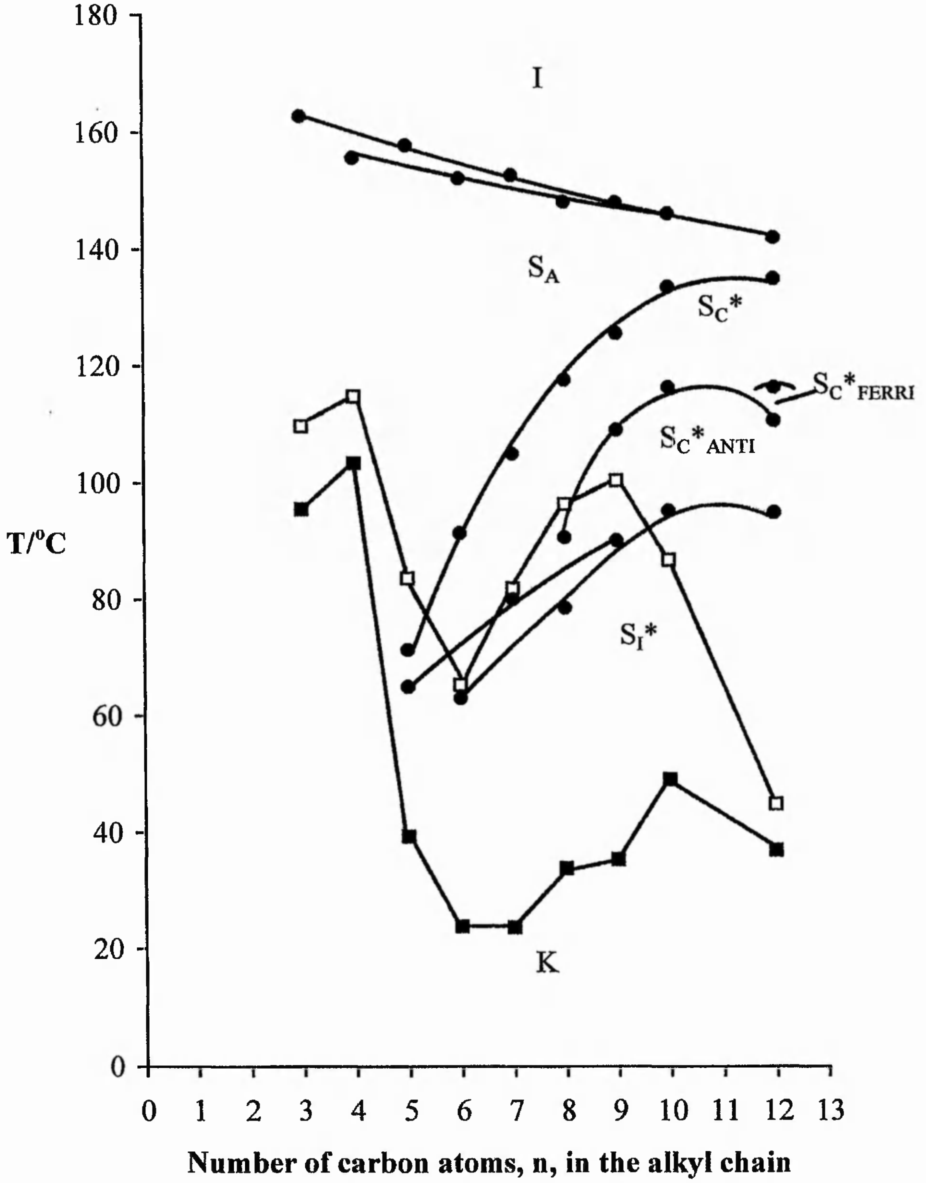

Plot 4: Transition temperature plot for members of an homologous series of (*S*)-4'-(1-methylheptyloxycarbonyl)biphenyl-4-yl 5'-n-alkyl-2',2-bithienyl-5-carboxylates (**34a-i**) [**Series IV**].

indicates a weakly first order transition which corresponds to a smectic-smectic transition.

On cooling the S_C*_{FERRO} phase of homologues n=8-10, a very short-lived S_C*_{FERRI} phase was detected, characterised by a very intense shimmering texture, which then almost immediately converted to the S_C*_{ANTI} phase. The n=12 homologue on cooling from the S_C*_{FERRO} phase shows a more stable S_C*_{FERRI} phase (5.6°C) which on further cooling develops into the S_C*_{ANTI} phase. On further cooling, homologues n=8-10 and 12 exhibit a texture which is reminiscent of the S_I* phase but also has characteristics of the CrJ phase, *i.e.*, chunky fan texture. DSC data for homologues n=8-12 equates to a first order transition which verifies the presence of a highly ordered phase (CrJ) rather than a weakly ordered smectic liquid crystal phase (S_I*). However, it may be that either both the S_I* phase and the CrJ phase co-exist or a very short-lived S_I* phase is present. Again to ascertain the true identity of this phase type, further optical work was undertaken on the n=12 homologue (**34i**). Initially, the mesophase types were investigated using free-standing film technique. The S_C*ferro-, ferri- and antiferroelectric phase types were clearly discernible as described earlier on p. 143, *i.e.*, blue-green coloration for the S_C*ferroelectric phase followed by intense shimmering (S_C*ferrielectric) and loss of shimmering (S_C*antiferroelectric). Transition of the S_C*antiferroelectric phase to the next phase gave a schlieren-mosaic-like texture (**Plate 9**, p. 207) which was indicative of an S_I* phase. The absence of a mosaic texture with strong grain boundaries ruled out the CrJ phase. Thereafter, a miscibility study was undertaken with (*R*)-4-(1-methylheptyloxycarbonyl)phenyl 4'-nonyloxybiphenyl-4-

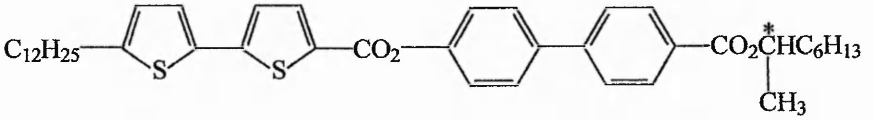

(34i)

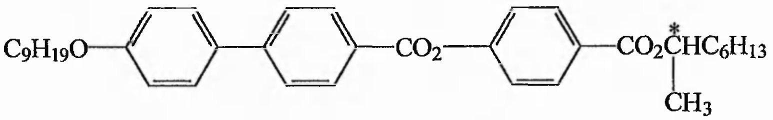

(85)

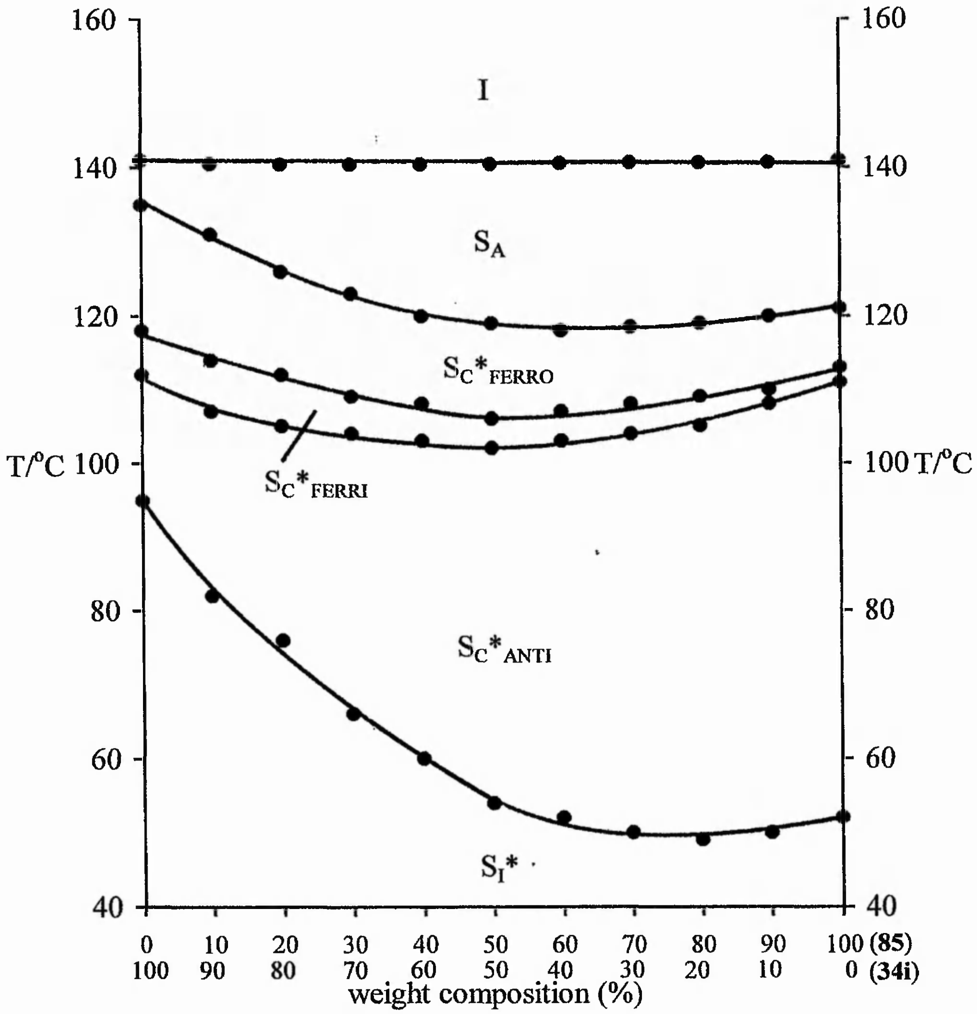

Plot 4a: Miscibility study for various compositions of (*S*)-4'-(1-methylheptyloxycarbonyl)biphenyl-4-yl 5'-n-dodecyl-2',2-bithienyl-5-carboxylate **(34i)** with the standard (*S*)-4-(1-methylheptyloxycarbonyl)phenyl 4'-nonyloxybiphenyl-4-carboxylate **(85)**.

carboxylate (**85**) as the standard. As shown by **Plot 4a**, there is continuous miscibility across the entire temperature range for the S_A, S_C*ferro-, S_C*ferri-, S_C*antiferroelectric and S_I* phase types. However, despite the seemingly continuous miscibility, the co-existence of the CrJ phase cannot be ignored and further elaborate electro-optical studies are currently being undertaken by our collaborators in Sweden. The results of this investigation were presented at the 17th International Liquid Crystal Conference, 1998, Strasbourg, France and subsequently published in Molecular Crystals and Liquid Crystals, 1999, Vol. 332, pp. 303-311. A copy of the abstract is appended.

3.5 LIQUID CRYSTALLINE PROPERTIES OF (*S*)-4-(1-METHYLHEPTYLOXYCARBONYL)PHENYL 4-(4-n-ALKOXYPHENYL)-THIOPHENE-2-CARBOXYLATES (40a-f) [Series V]

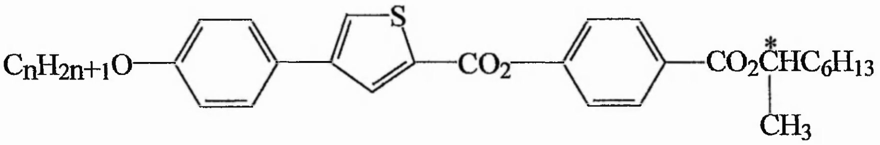

(40a-f)

Six members, n=6-10 and 12, of an homologous series of (*S*)-4-(1-methylheptyloxycarbonyl)phenyl 4-(4-n-alkoxyphenyl)thiophene-2-carboxylates were prepared. Their mesophase transition temperatures are listed in **Table 5** and plotted against, n, the number of carbon atoms in the alkoxy chain, as shown in **Plot 5.**

All homologues (n=6-10 and 12) exhibit a monotropic S_A phase alone with enthalpy values in the region of 3.88-5.73 kJ mol^{-1}. The points for the I-S_A transition temperatures lie on two smooth curves, showing the odd-even effect, with the curve for the even-n homologues lying above those for the odd-n homologues. Both curves increase gradually as n increases with the two lines converging at the n=12 homologue.

Table 5: Transition temperatures[a] (°C) and enthalpy values[b] (kJ mol^{-1}) for an homologous series of (*S*)-4-(1-methylheptyloxycarbonyl)phenyl 4-(4-n-alkoxyphenyl)thiophene-2-carboxylates (**40a-f**) [**Series V**].

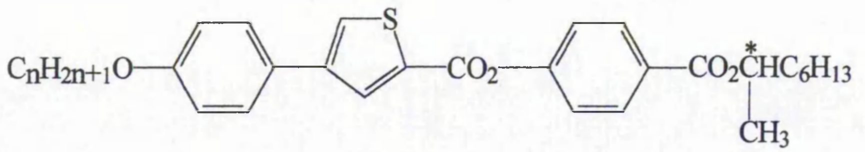

(**40a-f**)

n-alkyl	K-I	I-S_A	S_A-K
C_6H_{13} (**40a**)	58.2[a] [37.50][b]	(44.3)[c] [3.88]	(44.2) [17.68]
C_7H_{15} (**40b**)	64.8 [31.49]	(43.5) [29.24][†]	(43.4) [29.24]
C_8H_{17} (**40c**)	49.6 [29.17]	(46.7) [4.42]	(28.1) [18.62]
C_9H_{19} (**40d**)	59.3 [48.51]	(46.1) [5.73]	(29.9) [13.70]
$C_{10}H_{21}$ (**40e**)	53.1 [29.71]	(47.7) [4.43]	(33.1) [18.74]
$C_{12}H_{25}$ (**40f**)	49.5 [4.94]	(48.0) [4.92]	(27.3) [30.11]

( )[c] - denotes monotropic transition

[ ][†] - due to transitions I-S_A and S_A-K being very close together only one peak is observed on the DSC trace and hence the value quoted is for both phase changes.

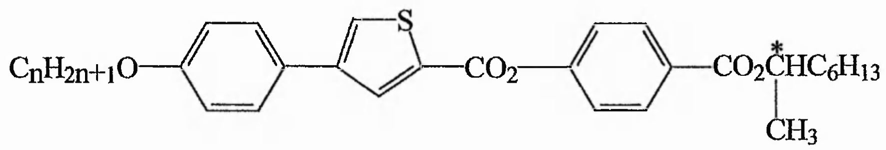

(40a-f)

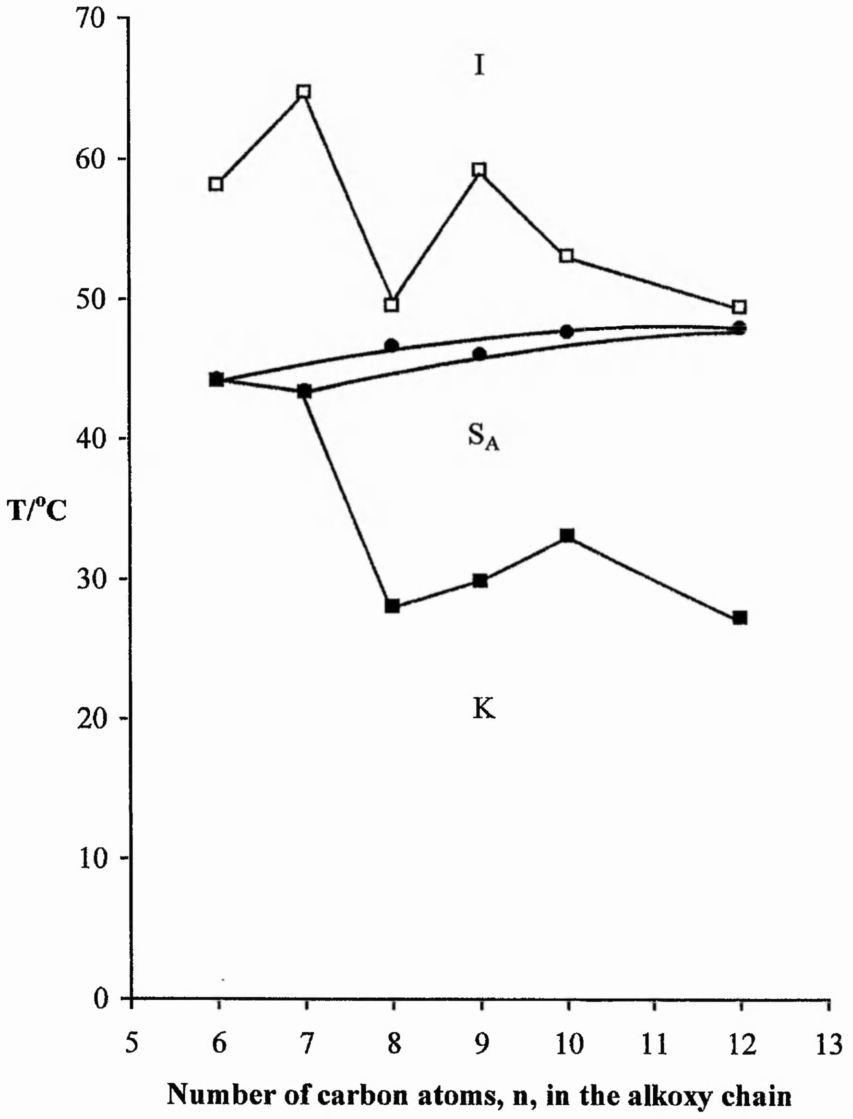

Plot 5: Transition temperature plot for members of an homologous series of (*S*)-4-(1-methylheptyloxycarbonyl)phenyl 4-(4-n-alkoxyphenyl)-thiophene-2-carboxylates (**40a-f**) [**Series V**].

3.6 LIQUID CRYSTALLINE PROPERTIES OF (*S*)-4'-(1-METHYLHEPTYLOXYCARBONYL)BIPHENYL-4-YL 4-(4-n-ALKOXYPHENYL)-THIOPHENE-2-CARBOXYLATES (41a-f) [Series VI]

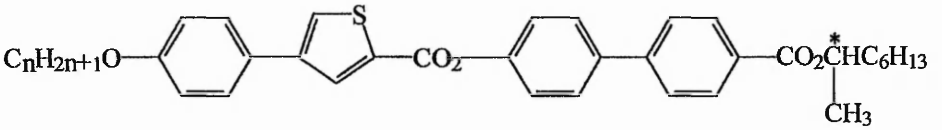

(41a-f)

Six members, n=6-10 and 12, of an homologous series of (*S*)-4'-(1-methylheptyloxycarbonyl)biphenyl-4-yl 4-(4-n-alkoxyphenyl)thiophene-2-carboxylates **(41a-f) [Series VI]** were prepared. Their mesophase transition temperatures are listed in **Table 6** and represented graphically in **Plot 6** against the number of carbon atoms, n, in the alkoxy chain.

On cooling from the isotropic liquid, all homologues (n=6-10 and 12) exhibit a S_A phase (enthalpy values range between 6.01-7.41 kJ mol^{-1}) which appear initially as bâtonnets and then coalesce to give the focal-conic fan texture interspersed with homeotropic regions. The points for the I-S_A transition lie on two smooth curves which show the odd-even effect (even-n above odd-n homologues). Both curves fall gradually as n increases with convergence at the n=10 homologue. The n=6 homologue exhibits no other phase prior to the onset of crystallisation.

The n=7 homologue exhibits a monotropic $S_C{}^*{}_{FERRO}$ and $S_C{}^*{}_{FERRI}$ phase prior to crystallisation whereas the higher homologues, n=8-10 and 12, exhibit $S_C{}^*$ ferro-, ferri- and antiferro-electric phase types.

Table 6: Transition temperatures[a] (°C) and enthalpy values[b] (kJ mol^{-1}) for an homologous series of (*S*)-4'-(1-methylheptyloxycarbonyl)biphenyl-4-yl 4-(4-n-alkoxyphenyl)thiophene-2-carboxylates (**41a-f**) [**Series VI**].

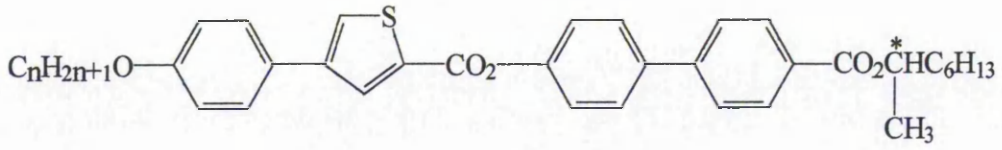

(**41a-f**)

n-alkyl	K-S_A/ S_C*_{FERRI}/ S_C*_{ANTI}	I-S_A	S_A-S_C*_{FERRO}	S_C*_{FERRO}-S_C*_{FERRI}	S_C*_{FERRI}-S_C*_{ANTI}	S_C*_{ANTI}-K
C_6H_{13} (**41a**)	132.1[a] [31.79][b]	145.5 [7.41]	-	-	-	111.1 [27.00]
C_7H_{15} (**41b**)	125.0 [37.37]	140.1 [6.74]	(105.7)[c] [-][d]	(101.4) [-]	-	96.1 [27.99]
C_8H_{17} (**41c**)	108.2 [31.13]	139.1 [6.85]	114.6 [-]	112.9 [-]	110.6 [-]	92.2 [27.11]
C_9H_{19} (**41d**)	110.8 [30.38]	136.5 [6.01]	120.4 [-]	117.6 [-]	(107.5) [-]	90.2 [29.43]
$C_{10}H_{21}$ (**41e**)	107.9 [31.02]	134.8 [6.36]	124.0 [0.15]	119.4 [-]	113.7 [-]	84.5 [26.03]
$C_{12}H_{25}$ (**41f**)	107.8 [30.87]	133.5 [6.50]	126.1 [0.26]	108.0 [-]	(102.7) [-]	78.5 [25.71]

( )[c] - denotes monotropic transition

[-][d] - enthalpy of transition too small to be evaluated

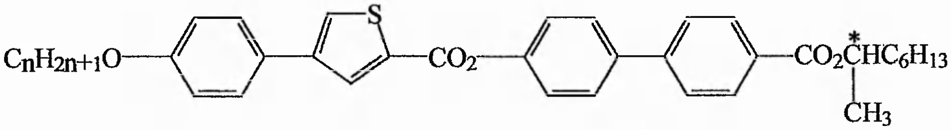

(41a-f)

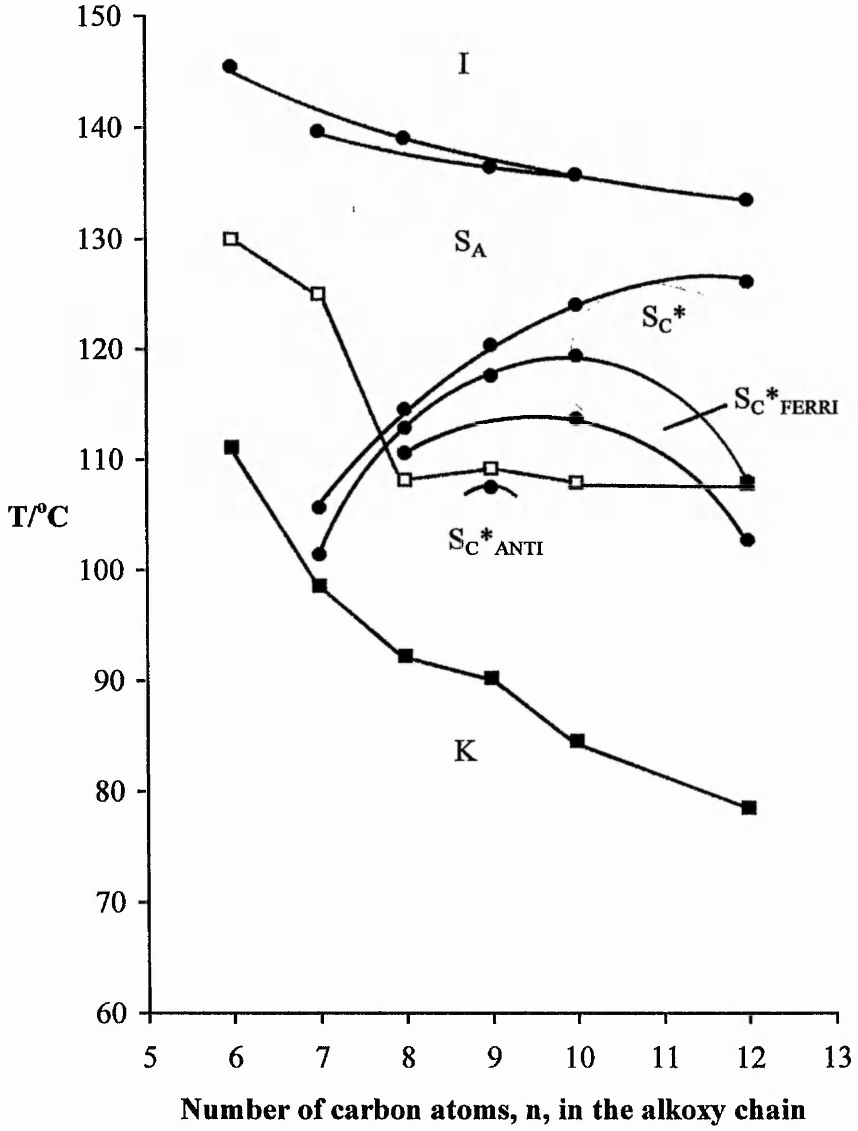

Plot 6: Transition temperature plot for members of an homologous series of (*S*)-4'-(1-methylheptyloxycarbonyl)biphenyl-4-yl 4-(4-n-alkoxyphenyl)-thiophene-2-carboxylates (**41a-f**) [**Series VI**].

3.7 LIQUID CRYSTALLINE PROPERTIES OF (*S*)-4-(1-METHYLHEPTYLOXYCARBONYL)PHENYL 5'-n-ALKYL-2',4-BITHIENYL-2-CARBOXYLATES (47a-f) [Series VII]

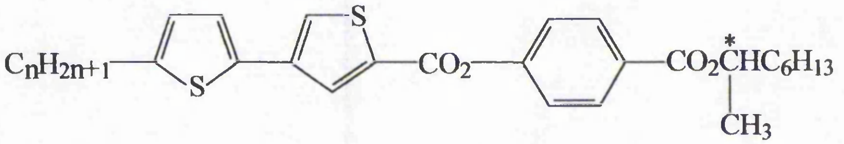

(47a-f)

Six members, n=6-10 and 12, of an homologous series of (*S*)-4-(1-methylheptyloxycarbonyl)phenyl 5'-n-alkyl-2',4-bithienyl-2-carboxylates (**47a-f**) were prepared and the thermal properties of **Series VII** are listed in **Table 7**. Unfortunately none of these homologues are mesomorphic.

Table 7: Transition temperatures[a] (°C) and enthalpy values[b] (kJ mol^{-1}) for an homologous series of (*S*)-4-(1-methylheptyloxycarbonyl)phenyl 5'-n-alkyl-2',4-bithienyl-5-carboxylates (**47a-f**) [**Series VII**].

n-alkyl	K-I	I-K
C_6H_{13} **(47a)**	67.9 [38.04]	30.0 [29.29]
C_7H_{15} **(47b)**	59.5 [34.95]	35.5 [29.67]
C_8H_{17} **(47c)**	64.2 [45.68]	38.4 [44.48]
C_9H_{19} **(47d)**	56.0 [35.15]	38.3 [32.25]
$C_{10}H_{21}$ **(47e)**	45.9 [30.97]	47.5 [29.71]
$C_{12}H_{25}$ **(47f)**	38.1 [35.94]	31.1 [36.05]

3.8 LIQUID CRYSTALLINE PROPERTIES OF (*S*)-4'-(1-METHYLHEPTYLOXYCARBONYL)BIPHENYL-4-YL 5'-n-ALKYL-2',4-BITHIENYL-2-CARBOXYLATES (48a-f) [Series VIII]

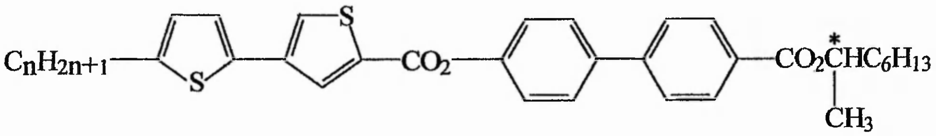

(48a-f)

Six members, n=6-10 and 12, of an homologous series of (*S*)-4'-(1-methylheptyloxycarbonyl)biphenyl-4-yl 5'-n-alkyl-2',4-bithienyl-2-carboxylates **(48a-f)** were prepared. Their mesophase transition temperatures are listed in **Table 8** and represented graphically in **Plot 7** against the number of carbon atoms, n, in the alkyl chain.

All the homologues (n=6-10 and 12) exhibit a monotropic S_A phase alone with enthalpy values ranging from 5.24-8.33 kJ mol^{-1}. The points for the I-S_A transition lie on a decreasing continuous smooth curve.

Table 8: Transition temperatures[a] (°C) and enthalpy values[b] (kJ mol^{-1}) for an homologous series of (S)-4'-(1-methylheptyloxycarbonyl)biphenyl-4-yl 5'-n-alkyl-2',4-bithienyl-thiophene-2-carboxylates (**48a-f**) [**Series VIII**].

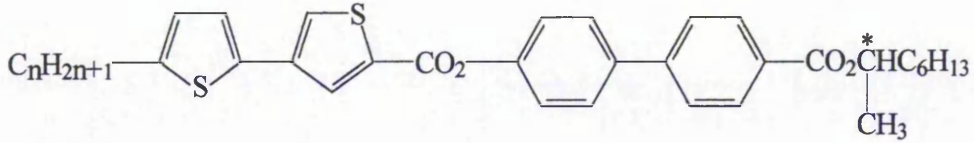

(**48a-f**)

n-alkyl	K-S_A	I-S_A	S_A-K
C_6H_{13} (**48a**)	125.8[a] [37.37][b]	(111.0)[c] [37.82][†]	110.1 [37.82]
C_7H_{15} (**48b**)	120.0 [44.36]	(109.3) [5.24]	104.3 [18.41]
C_8H_{17} (**48c**)	116.0 [41.07]	(107.6) [37.56]	104.1 [37.56]
C_9H_{19} (**48d**)	114.8 [48.24]	(105.6) [8.33]	99.7 [11.24]
$C_{10}H_{21}$ (**48e**)	113.8 [41.78]	(104.6) [7.17]	103.9 [25.98]
$C_{12}H_{25}$ (**48f**)	114.5 [32.71]	(103.4) [6.94]	95.4 [22.00]

( )[c] - denotes monotropic transition

[†] Transitions I-S_A and S_A-K very close together and hence only one peak is observed on the DSC trace and the value shown is for both phase changes

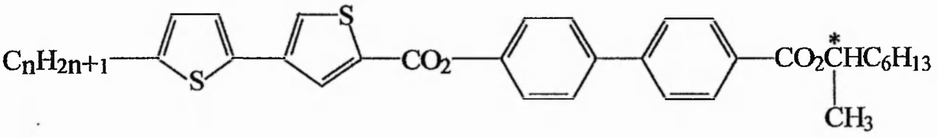

(48a-f)

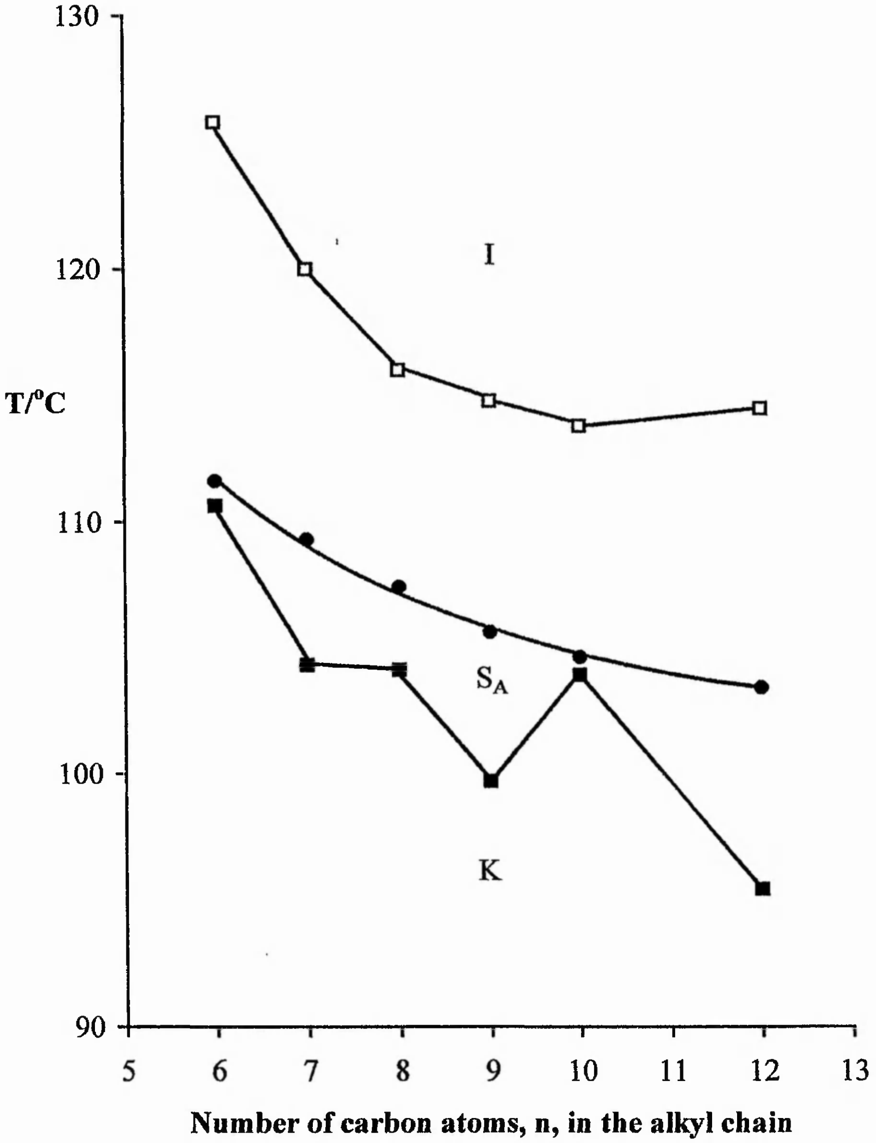

Plot 7: Transition temperature plot for members of an homologous series of (*S*)-4'-(1-methylheptyloxycarbonyl)biphenyl-4-yl 5'-n-alkyl-2',4-bithienyl-2-carboxylates (**48a-f**) [**Series VIII**].

3.9 COMPARATIVE STUDY OF COMPOUNDS COMPRISING TWO RINGS IN THE CENTRAL MOLECULAR CORE, *i.e.*, SERIES I-VIII

It is now an appropriate stage to compare the mesomorphic data for chiral thiophene-based esters comprising two rings in the central molecular core, *i.e.*, members of **Series I-VIII**, in order to assess:

i. the influence of altering the central molecular core on mesophase type and thermal stability, *i.e.*, systematically altering the central molecular core from 'phenyl-phenyl' (biphenyl) to 'phenyl-thiophene' to 'thiophene-thiophene' (bithienyl);

ii. the influence of altering the substitution geometry on mesophase type and thermal stability, *i.e.*, from '1,5-phenyl-thiophene' to '1,4-phenyl-thiophene' and from '2',2-bithienyl' to '2',4-bithienyl' and;

iii. the influence of increasing the overall molecular length with the introduction of an additional 1,4-phenylene unit in the phenolic moiety on mesophase type and mesophase thermal stability.

3.9.1 INFLUENCE OF ALTERING THE TWO-RING CENTRAL MOLECULAR CORE ON MESOMORPHIC PROPERTIES

In order to undertake a meaningful comparative study of the influence of changing the two-ring central molecular core on mesomorphic properties it was decided to compare the same homologue for several series. The n=9 homologue was chosen because literature data for the non-heterocyclic counterpart is readily available, *i.e.*, (*S*)-4-(1-methylheptyloxycarbonyl)phenyl 4'-n-nonyloxybiphenyl-4-carboxylate (**85**).[116]

However, compound **(85)** was re-synthesised using the same batch of chiral phenol **(25)** used for the preparation of thiophene-based esters reported in the thesis to maintain consistency. **Table 9** shows the m.p. and clearing point (cl.p.) temperatures for the n=9 homologue for (*S*)-4-(1-methylheptyloxycarbonyl)phenyl 4'-n-decycloxybiphenyl-4-carboxylate **(85)**, **Series I** and **Series III**.

Table 9: Mesomorphic data (°C) for compounds **(85)**, **(27d)** **[Series I]** and **(33d)** **[Series III]**.

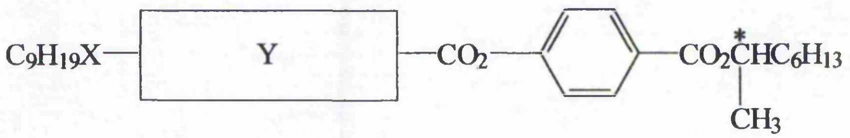

Compound Series	X	Y	m.p.	cl.p.	Phase Range	Phase Types
(85)	O	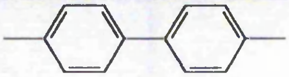	59.0	141.9	82.9	S_A, $S_C{}^*{}_{FERRO}$, $S_C{}^*{}_{FERRI}$, $S_C{}^*{}_{ANTI}$, $S_I{}^*$
(27d) **[Series I]**	O	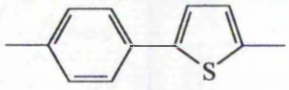	75.0	102.8	27.8	S_A, $S_C{}^*{}_{FERRO}$, $S_C{}^*{}_{FERRI}$, $S_C{}^*{}_{ANTI}$
(33d) **[Series III]**	-	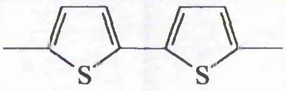	61.5	59.2	2.2	S_A, $S_C{}^*{}_{FERRI}$

From a comparison of the clearing point temperatures listed in **Table 9**, the following thermal stability order may be deduced.

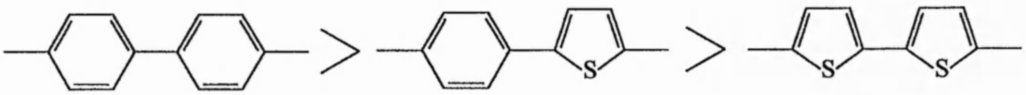

(85) **(27d) [Series I]** **(33d) [Series III]**

As expected, it can be concluded that the biphenyl core (**85**) is the most thermally stable compound, inferring that this system has the highest efficiency of packing. Replacement of the right-hand centrally disposed phenyl ring with a thiophene ring to yield 'phenyl-thiophene' introduces a bend in the molecular core. The molecules can no longer pack efficiently and hence the thermal stability is reduced by approximately 40°C. Surprisingly, despite the non-linear geometry, the melting point of compound (**27d**) is higher than compound (**85**) by a magnitude of 17°C.

Replacement of both phenyl rings in compound (**85**) with thiophene rings to give the corresponding 'thiophene-thiophene' molecular core, *i.e.*, (**33d**) [**Series III**], introduces a severe bend in the core which further reduces the linear packing efficiency of the molecules. Hence, as evidenced, both the thermal stability and the melting point is reduced.

Replacement of the left-hand terminally disposed phenyl ring in phenyl-thiophene [**Series I**] with a thiophene ring to yield thiophene-thiophene [**Series III**] reduces the melting point by approximately 13°C and the clearing point by a further 43.6°C. As shown overleaf, there appears to be an additive effect whereby successive replacement of the 1,4-phenylene ring with a 2,5-thienyl moiety lowers the thermal stability by approximately 40°C.

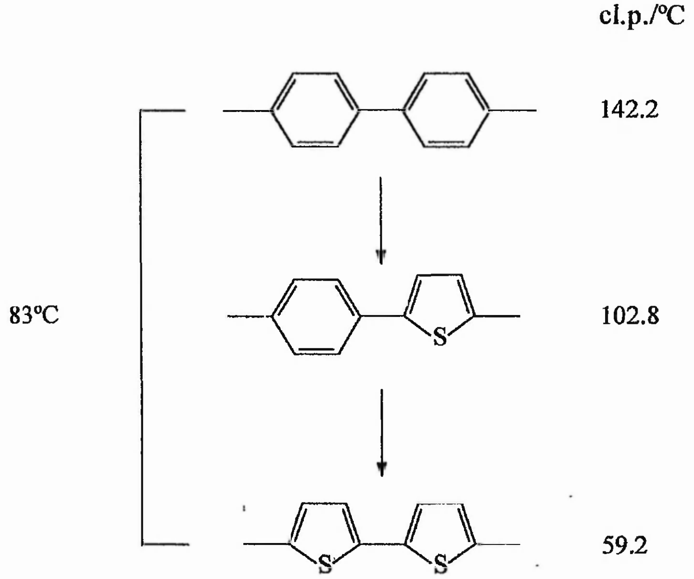

In addition, the lack of an ether oxygen atom between the terminal alkyl group and the molecular core in compound **(33d)** will tend to reduce both molecular polarisability and mesomeric relay. The alkoxy terminal substituent is well known to enhance thermal stability with respect to the alkyl terminal substituent because of the ability of the lone pair of electrons on the oxygen atom to conjugate with the ester moiety in the central molecular core. Hence, compounds **(85)** and **(27d)**, which contain terminal alkoxy substituents are thermally more stable than compound **(33d)**.

(85)

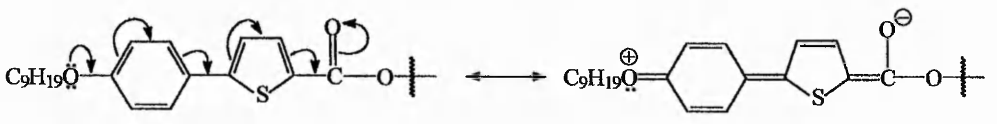

(27d)

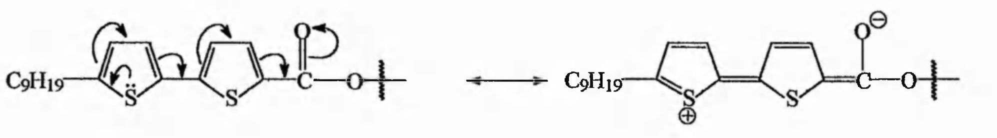

(33d)

3.9.2 INFLUENCE OF ALTERING THE SUBSTITUTION GEOMETRY OF THE TWO-RING CENTRAL MOLECULAR CORE ON MESOMORPHIC PROPERTIES

In order to compare the influence of altering the substitution geometry within the two-ring thiophene-containing molecular core, the mesomorphic data for members of **Series I**, **III**, **V** and **VII** was compared. The central core was systematically altered from '1,5-phenyl-thiophene' (**Series I**) to '1,4-phenyl-thiophene' (**Series V**) and from '2',2-bithienyl' (**Series III**) to '2',4-bithienyl' (**Series VII**). **Table 10** shows the average m.p. and cl.p. temperatures for the n=6-10 and 12 homologues of **Series I**, **III**, **V** and **VII**.

Table 10: Average mesomorphic data (°C) for members of **Series I**, **III**, **V** and **VII** (n=6-10 and 12).

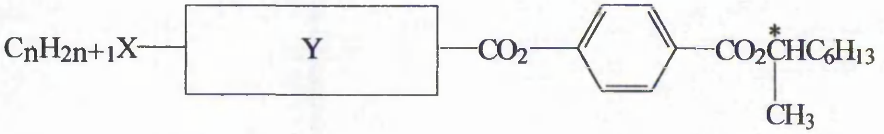

Series	X	Y	m.p.	cl.p.	Phase Range	Phase Types
I	O	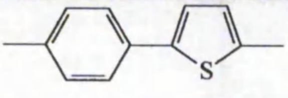	71.3	105.4	34.1	S_A, $S_C^*{}_{FERRO}$, $S_C^*{}_{FERRI}$, $S_C^*{}_{ANTI}$
III	-	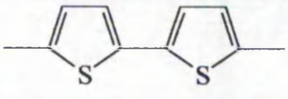	63.2	59.5[a]	4.9	S_A, $S_C^*{}_{FERRO}$, $S_C^*{}_{FERRI}$, $S_C^*{}_{ANTI}$
V	O	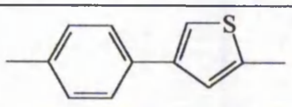	55.8	46.1[a]	9.7	S_A
VII	-	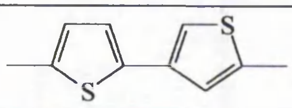	57.9	-	-	-

[a] monotropic transitions

From the results shown in **Table 10**, the following mesophase thermal stability order may be deduced based on the average clearing point temperatures.

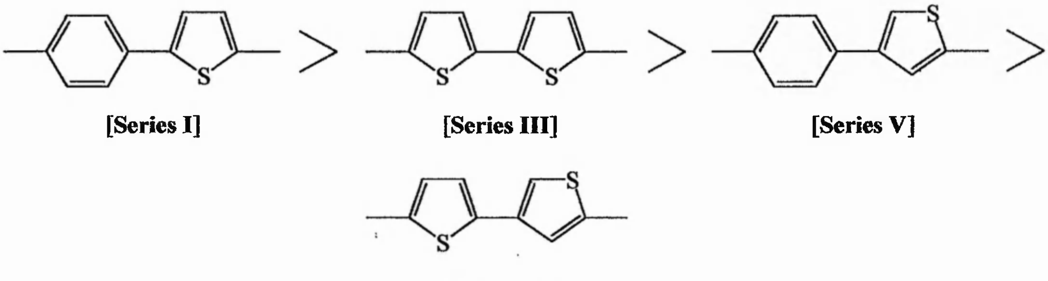

[Series I] **[Series III]** **[Series V]**

[Series VII]

Altering the substitution pattern of the thiophene moiety from a '1,5-phenyl-thiophene' linkage **[Series I]** to a '1,4-phenyl-thiophene' linkage **[Series V]** drastically reduces the mesophase thermal stability by 59.3°C and has the effect of eliminating ferro-, ferri- and antiferro-electric phase types. A monotropic S_A phase alone is observed.

However, altering the substitution pattern from a 2',2-bithienyl linkage **[Series III]** to 2',4-bithienyl linkage **[Series VII]** has a very dramatic effect on mesophase thermal stability and type. The latter are non-mesomorphic which is probably due to a combination of poor molecular geometry and poor anisotropy of molecular polarisability ($\Delta\alpha$). Although molecular modelling and X-ray studies were not performed due to lack of facilities and time constraints it is envisaged that the disposition of the sulphur atom and directionality of the dipole moment plays a vital role in explaining its non-mesomorphic nature. It is well known that the two sulphur atoms in 2',2-bithienyl are disposed in a *trans*-fashion.[118,119] The very poor mesomorphic properties in 2',4-bithienyl may be due to a *cis*-arrangement of the two sulphur atoms which may by non-conducive for mesophase formation.

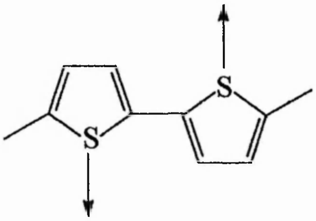

2',2-bithienyl
Trans-configuration

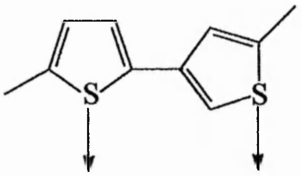

2',4-bithienyl
Cis-configuration

3.9.3 INFLUENCE OF INCREASING THE OVERALL MOLECULAR LENGTH ON MESOMORPHIC PROPERTIES

The influence of increasing the overall molecular length on mesophase thermal stability may be investigated by comparing three-ring containing compounds *i.e.*, **Series I, III, V** and **VII**, with their four-ring counterparts *i.e.*, **Series II, IV, VI** and **VIII**, respectively. All the homologues comprise a two-ring central molecular core and the overall molecular length is increased by including an extra 1,4-phenylene ring in the terminal 'chiral moiety'. **Table 11** shows the average m.p. and cl.p. temperatures for the n=6-10 and 12 homologues of **Series I-VIII**.

Comparison of the average clearing points for **Series I-VIII** as expressed in **Table 11**, reveals the thermal stability order shown on p. 178. Comparing any three-ring series with its four-ring counterpart reveals that the inclusion of an extra 1,4-phenyl ring in the terminal chiral moiety increases the mesophase thermal stability by approximately 90°C. This increase may be attributed to an increase in the overall molecular length coupled with extended or enhanced conjugation, both of which are conducive to increased thermal stability.

Table 11: Average mesomorphic data (°C) for compounds **Series I-VIII** (n=6-10 and 12).

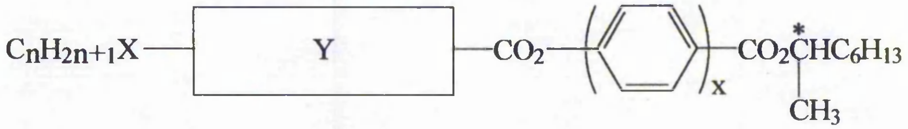

Series	X	Y	x	m.p.	cl.p.	Phase Range	Phase Types
I	O	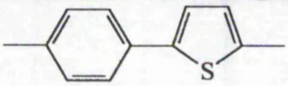	1	71.3	105.4	34.1	S_A, S_C^*, $S_C^*{}_{FERRI}$, $S_C^*{}_{ANTI}$
II	O	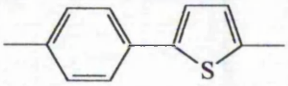	2	84.6	198.8	114.2	S_A, S_C^*, $S_C^*{}_{FERRI}$, $S_C^*{}_{ANTI}$, S_I^*
III	-	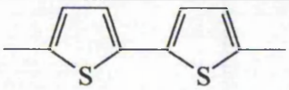	1	63.2	59.5	4.9	S_A, S_C^*, $S_C^*{}_{FERRI}$, $S_C^*{}_{ANTI}$,
IV	-	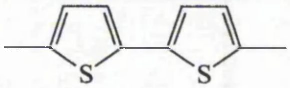	2	79.2	148.3	69.1	S_A, S_C^*, $S_C^*{}_{FERRI}$, $S_C^*{}_{ANTI}$
V	O	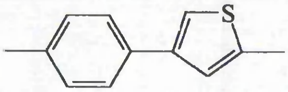	1	55.8	46.1	9.7	S_A
VI	O	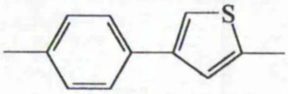	2	115.3	138.3	23.0	S_A, S_C^*, $S_C^*{}_{FERRI}$, $S_C^*{}_{ANTI}$
VII	-	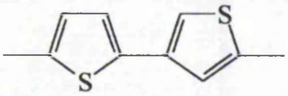	1	55.3	-	-	-
VIII	-	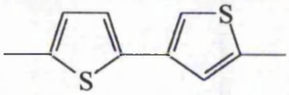	2	117.5	106.9	10.6	S_A

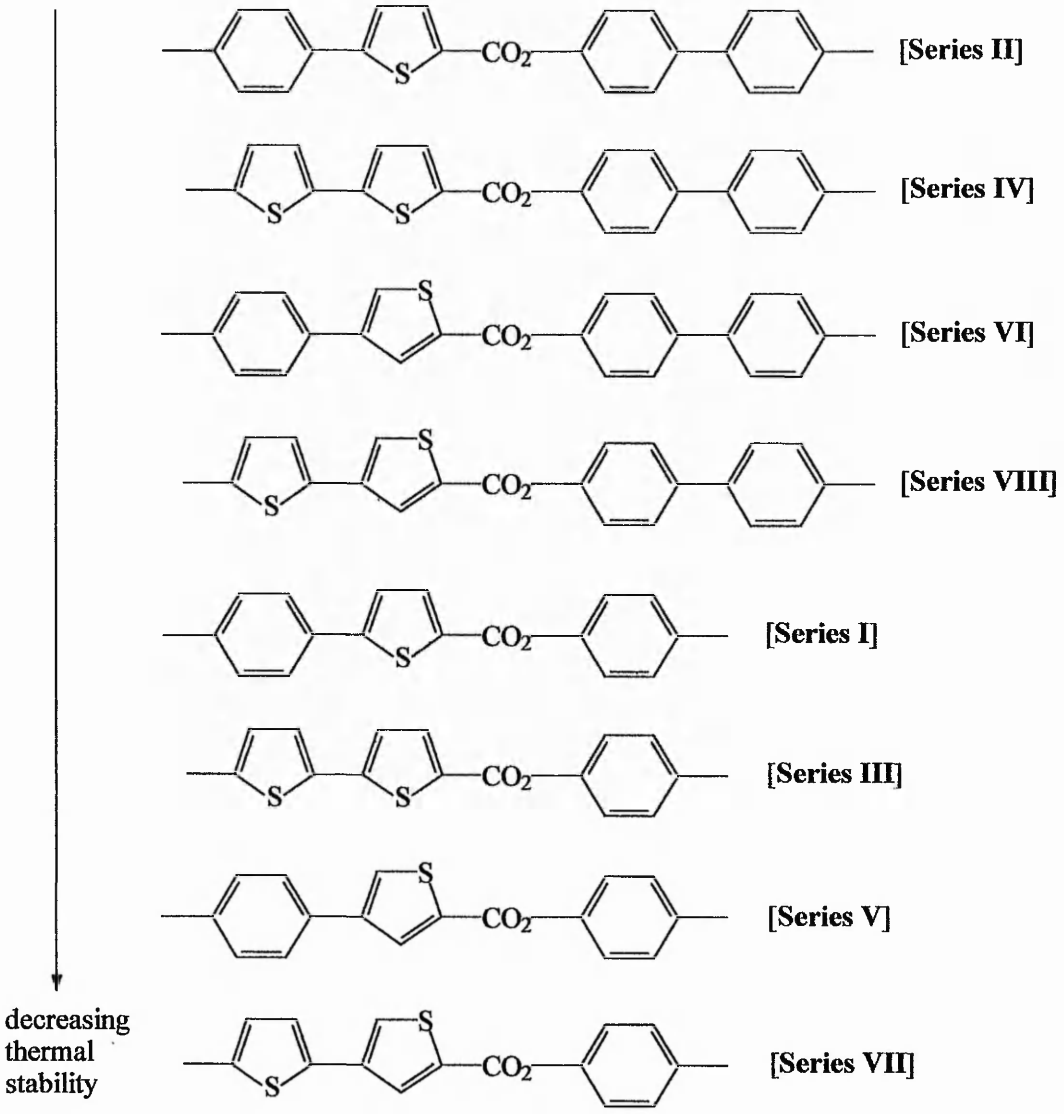

Increasing the molecular length also enhances mesophase formation as evidenced by comparing members of **Series V** with **Series VI**. The former exhibit a monotropic S_A phase alone, whereas the latter (four-ring) exhibit S_A, S_C*ferro-, ferri- and antiferroelectric phase types. Similarly, members of **Series VII** (three-ring) are non-mesomorphic whilst their four-ring counterparts [**Series VIII**] exhibit a S_A phase, albeit monotropic.

3.10 LIQUID CRYSTALLINE PROPERTIES OF (*S*)-4-(1-METHYLHEPTYLOXYCARBONYL)PHENYL 5''-n-ALKYL-2'',2':5',2-TERTHIENYL-5-CARBOXYLATES (53a-f) [Series IX]

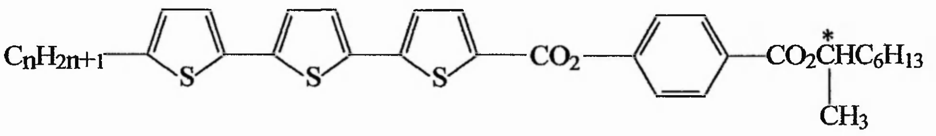

(53a-f)

Six members, n=6-10 and 12, of an homologous series of (*S*)-4-(1-methylheptyloxycarbonyl)phenyl 5''-n-alkyl-2'',2':5',2-terthienyl-5-carboxylates **(53a-f)** were prepared. Their mesophase transition temperatures are listed in **Table 12** and represented graphically in **Plot 8** against the number of carbon atoms, n, in the alkyl chain.

On cooling from the isotropic liquid, all the members (n=6-10 and 12) exhibit a classical S_A phase with enthalpy values in the region of 4.08-9.17 kJ mol^{-1}. Two smooth curves can be drawn for the points correlating to the I-S_A transition temperatures with the odd-n homologues lying uppermost. The curves decline gradually as n increases and tend to converge at the n=10 homologue. The n=6 and 7 homologues exhibit a high order smectic crystal phase on cooling from the S_A phase. The appearance of concentric arcs and a 'ghost-like' mosaic texture suggests the CrE phase **(Plate 10**, p. 207). No other phase is detected prior to the onset of crystallisation.

Table 12: Transition temperatures[a] (°C) and enthalpy values[b] (kJ mol^{-1}) for an homologous series of (*S*)-4-(1-methylheptyloxycarbonyl)phenyl 5''-n-alkyl-2'',2':5',2-terthienyl-5-carboxylates (**53a-f**) [**Series IX**].

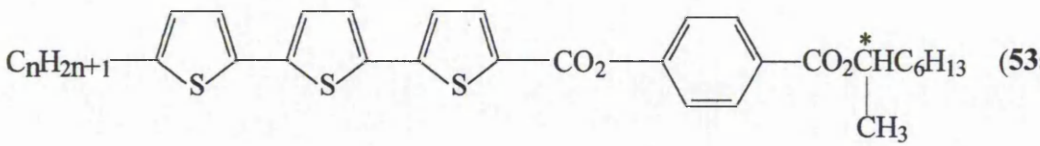

(**53a-f**)

n-alkyl	K- S_A/S_C*_{ANTI}	I-S_A	S_A-CrE	S_A-S_C*	S_A/S_C*- S_C*_{FERRI}	S_C*_{FERRI}- S_C*_{ANTI}	S_C*_{ANTI}-S_I*	S_C*_{ANTI}/CrE /S_I*-K
C_6H_{13} (**53a**)	111.3[a] [13.30][b]	164.1 [9.10]	(109.6)[c] [10.30][†]	-	-	-	-	109.6 [10.30]
C_7H_{15} (**53b**)	113.0 [38.50]	161.1 [9.17]	(111.3) [11.26]	-	-	-	-	67.4 [6.61]
C_8H_{17} (**53c**)	126.9 [39.78]	154.2 [8.26]	-	-	130.2 [-][d]	129.1 [-]	-	101.9 [8.53]
C_9H_{19} (**53d**)	118.0 [31.28]	149.9 [6.88]	-	132.7 [0.20]	131.5 [-]	130.5 [-]	(93.7) [1.17]	93.5 [10.08]
$C_{10}H_{21}$ (**53e**)	98.4 [29.10]	145.5 [6.66]	-	133.2 [0.22]	125.7 [-]	123.5 [-]	(79.6) [0.84]	76.7 [4.92]
$C_{12}H_{25}$ (**53f**)	53.0 [5.41]	138.8 [4.08]	-	131.5 [0.16]	119.2 [-]	117.6 [-]	(64.3) [0.82]	55.9 [2.60]

( )[c] - denotes monotropic transition

[-][d] - enthalpy of transition too small to be evaluated

[ ][†] - transitions S_A-CrE and CrE-K occur very close together and hence only one peak is observed on DSC trace and hence, value quoted is for both phase changes

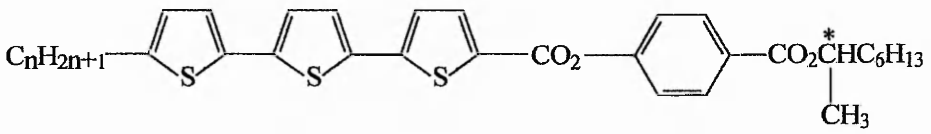

(53a-f)

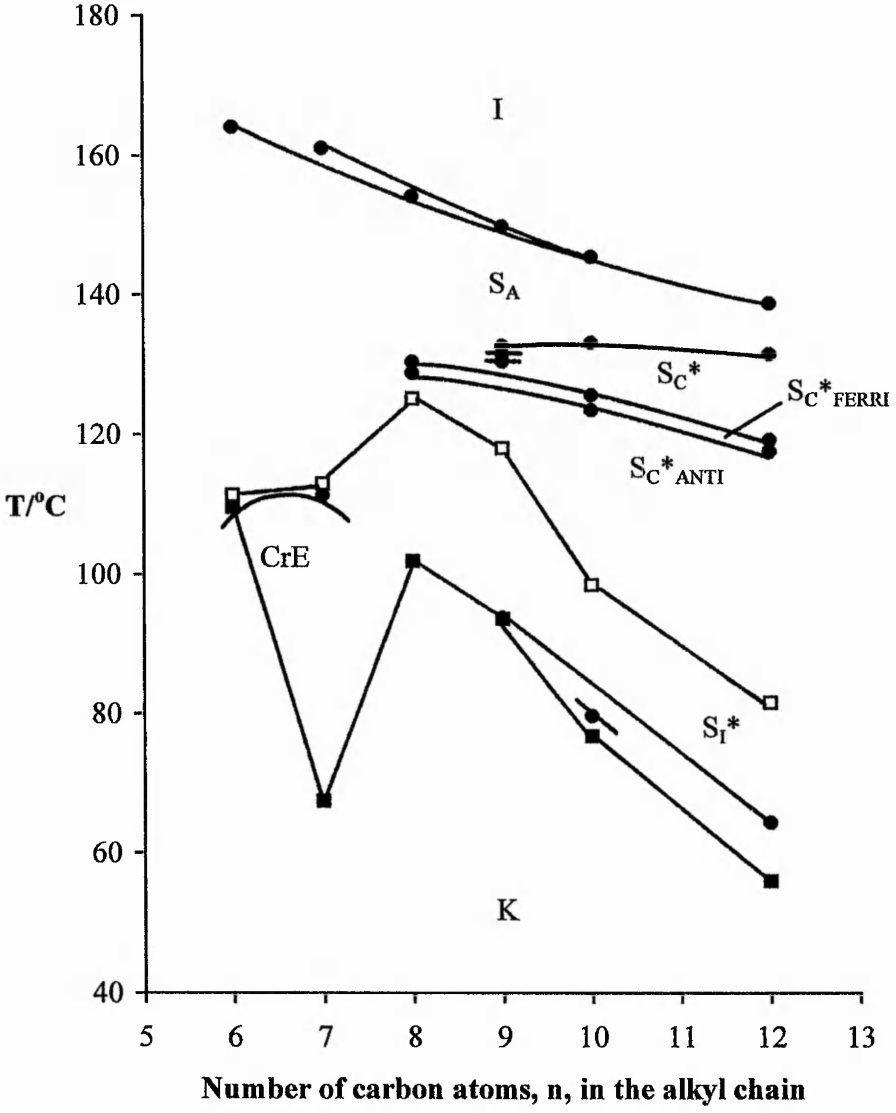

Plot 8: Transition temperature plot for members of an homologous series of (*S*)-4-(1-methylheptyloxycarbonyl)phenyl 5''-n-alkyl-2'',2':5',2-terthienyl-5-carboxylates (**53a-f**) [**Series IX**].

The n=8 homologue on cooling from the S_A phase exhibits a very short-lived S_C* ferri- and antiferro-electric phase just before the onset of crystallisation.

The remaining homologues, n=9-10 and 12, exhibit S_C*ferro-, ferri-, antiferro-electric and S_I* phase types prior to crystallisation as described previously on p. 143.

3.11 LIQUID CRYSTALLINE PROPERTIES OF (*S*)-4'-(1-METHYLHEPTYLOXYCARBONYL)BIPHENYL-4-YL 5"-n-ALKYL-2",2':5',2-TERTHIENYL-5-CARBOXYLATES (54a-f) [Series X]

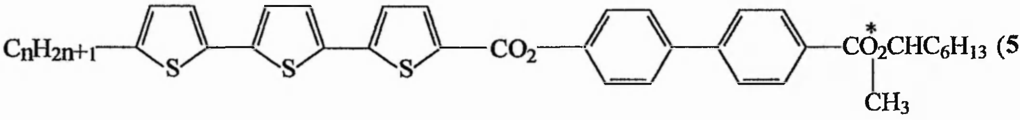

(54a-f)

Six members, n=6-10 and 12, of an homologous series of (*S*)-4'-(1-methylheptyloxycarbonyl)biphenyl-4-yl 5"-n-alkyl-2",2':5',2-terthienyl-5-carboxylates **(54a-f)** were prepared. Their mesophase transition temperatures are listed in **Table 13** and represented graphically in **Plot 9** against the number of carbon atoms, n, in the alkyl chain.

All the homologues (n=6-10 and 12), exhibit the S_A phase (enthalpy values range from 5.91 to 7.84 kJ mol^{-1}) which appears initially as bâtonnets and then gradually coalesce to give the focal-conic fan texture along with areas of homeotropic. The points for the I-S_A transition temperatures lie on a smooth decreasing curve.

On cooling from the S_A phase all the homologues (n=6-10 and 12) exhibit the S_C* ferro-, ferri-/antiferro-electric phase types as characterised earlier on p. 143. On further cooling from the S_C*_{ANTI} phase, homologues n=6 and 7 exhibit a S_I* phase which is characterised by an unfocusable schlieren-mosaic texture in the previously homeotropic area. The n=6 homologue exhibits no other phase prior to the onset of crystallisation.

Table 13: Transition temperatures[a] (°C) and enthalpy values[b] (kJ mol^{-1}) for an homologous series of (*S*)-4'-(1-methylheptyloxycarbonyl)biphenyl-4-yl 5"-n-alkyl-2",2':5',2-terthienyl-5-carboxylates (**54a-f**) [**Series X**].

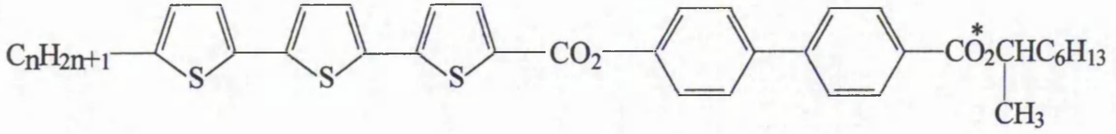

(**54a-f**)

n-alkyl	K-S_I*/CrX	I-S_A	S_A-S_C*	S_C*-S_C*$_{FERRI/ANTI}$	S_C*$_{FERRI/ANTI}$-S_I*	S_I*-CrX	S_C*$_{FERRI/ANTI}$-CrX	S_I*/CrX-K
C_6H_{13} (**54a**)	60.4[a] [9.25][b]	245.4 [6.82]	173.8 [-][d]	147.7 [-]	116.0 [0.82]	-	-	49.9 [4.38]
C_7H_{15} (**54b**)	80.6 [17.45]	240.8 [7.84]	192.8 [0.06]	170.4 [-]	120.2 [1.55]	110.0 [1.55]	-	78.1 [4.08]
C_8H_{17} (**54c**)	112.0 [25.97]	236.1 [7.42]	207.1 [0.19]	179.4 [-]	-	-	124.9 [2.71]	73.2 [4.29]
C_9H_{19} (**54d**)	108.6 [13.45]	232.1 [7.40]	212.0 [0.43]	187.8 [-]	-	-	131.0 [3.83]	102.0 [7.33]
$C_{10}H_{21}$ (**54e**)	112.4 [15.00]	228.4 [5.91]	214.3 [0.10]	182.5 [-]	-	-	129.8 [3.66]	109.5 [12.66]
$C_{12}H_{25}$ (**54f**)	129.8 [41.16]	222.0 [7.32]	214.0 [0.71]	174.5 [-]	-	-	(123.4)[c] [4.76]	105.6 [5.42]

( )[c] – denotes monotropic transition

[-][d] - enthalpy of transition too small to be evaluated

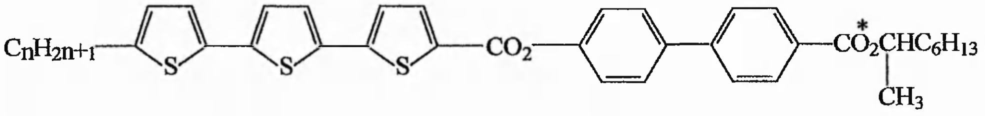

(54a-f)

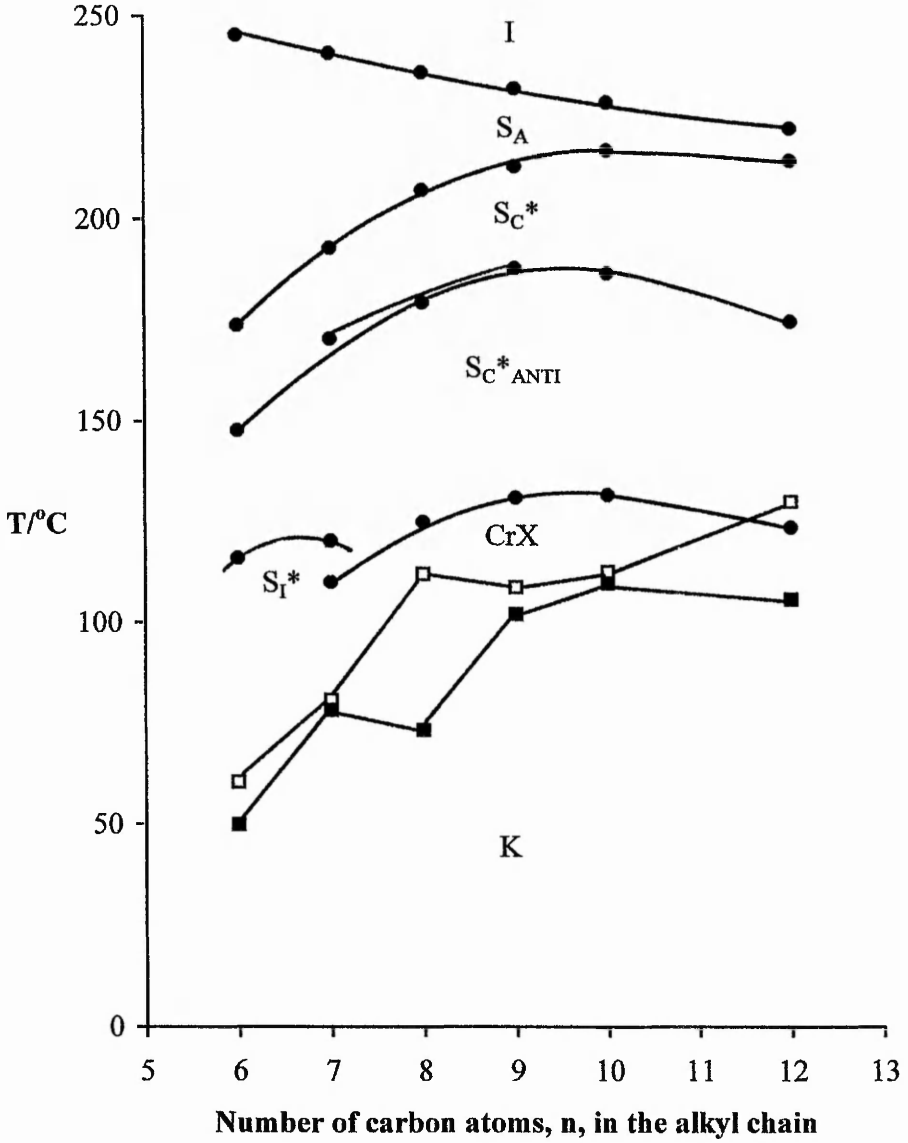

Plot 9: Transition temperature plot for members of an homologous series of (*S*)-4'-(1-methylheptyloxycarbonyl)biphenyl-4-yl 5''-n-alkyl-2'',2':5',2-terthienyl-5-carboxylates **(54a-f)** **[Series X]**.

The n=7 homologue on cooling from the S_I* phase shows a high order crystal phase which has been assigned as CrX as different parts of the slide show characteristics of different phases.

The remaining homologues, n=8-10 and 12, on cooling from the S_C*_{ANTI} phase do not show the S_I* phase like homologues n=6 and 7 but instead exhibit a high order smectic crystal phase which again has been assigned as CrX due to the reasons described previously. No other phases are observed prior to the onset of crystallisation.

3.12 LIQUID CRYSTALLINE PROPERTIES OF (*S*)-4-(1-METHYLHEPTYLOXYCARBONYL)PHENYL 5'-(4-n-DECYLOXYPHENYL)-2',2-BITHIENYL-5-CARBOXYLATE (60) [Series XI]

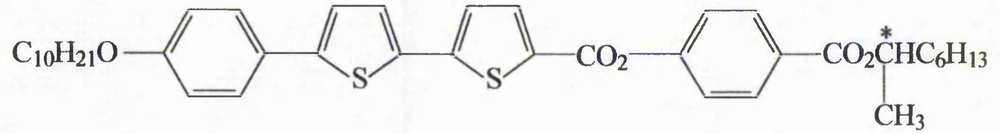

(60)

The mesomorphic and enthalpy data for (*S*)-4-(1-methylheptyloxycarbonyl)phenyl 5'-(4-n-decyloxyphenyl)-2',2-bithienyl-5-carboxylate **(60)** **[Series XI]** is listed in **Table 14**.

On cooling from the isotropic liquid, a classical S_A phase was exhibited followed by the $S_C{}^*{}_{FERRO}$ phase which was characterised by arcs across the fans coupled with a blue coloration in the previously homeotropic areas. Cooling of the $S_C{}^*{}_{FERRO}$ phase gave the $S_C{}^*{}_{FERRI}$ phase, which was immediately preceded by the $S_C{}^*{}_{ANTI}$ phase. No other phases were observed prior to crystallisation.

Table 14: Transition temperatures[a] (°C) and enthalpy values[b] (kJ mol^{-1}) of (*S*)-4-(1-methylheptyloxycarbonyl)phenyl 5'-(4-n-decyloxyphenyl)-2',2-bithienyl-5-carboxylate **(60)** **[Series XI]**.

K-S_A	I-S_A	S_A- $S_C{}^*$	$S_C{}^*$-$S_C{}^*{}_{FERRI/ANTI}$	$S_C{}^*{}_{FERRI/ANTI}$-K
104.4[a] [35.51][b]	188.0 [6.22]	172.1 [0.36]	155.2 [0.02]	76.0 [12.11]

3.13 LIQUID CRYSTALLINE PROPERTIES OF (*S*)-4-(1-METHYLHEPTYLOXYCARBONYL)PHENYL 5-(4'-n-DECYLOXYBIPHENYL-4-YL)-THIOPHENE-2-CARBOXYLATE (70) [Series XII]

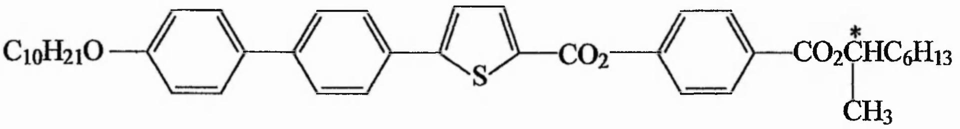

(70)

The mesomorphic and enthalpy data for (*S*)-4-(1-methylheptyloxycarbonyl)phenyl 5-4'-n-alkoxybiphenyl-4-yl)thiophene-2-carboxylate **(70)** **[Series XII]** is listed in **Table 15.**

On cooling from the isotropic liquid, the S_A phase was exhibited which appeared initially as bâtonnets which then coalesced to form the focal-conic fan texture along with homeotropic regions. Cooling of the S_A phase gave the $S_C{}^*{}_{FERRO}$ phase which was characterised by the appearance of arcs across the fans coupled with a blue or red coloration in the previously homeotropic regions. Cooling of the $S_C{}^*{}_{FERRO}$ phase gave the $S_C{}^*{}_{FERRI}/S_C{}^*{}_{ANTI}$ phase which then developed into the $S_I{}^*$ phase on cooling and was characterised by an unfocusable yellow schlieren-mosaic texture in the homeotropic areas. Further cooling of the $S_I{}^*$ phase gave a high order crystal phase tentatively assigned as CrX phase which was characterised by the appearance of chunky fans coupled with a mosaic texture in the homeotropic regions.

Table 15: Transition temperatures[a] (°C) and enthalpy values[b] (kJ mol^{-1}) of (*S*)-4-(1-methylheptyloxycarbonyl)phenyl 5-(4'-n-decyloxybiphenyl-4-yl)-thiophene-2-carboxylate (**70**) [**Series XII**].

K-S_A	I-S_A	S_A-S_C*	S_C*-S_C*$_{FERRI/ANTI}$	S_C*$_{FERRI/ANTI}$-S_I*	S_I*-CrX	CrX-K
72.4[a] [4.74][b]	221.3 [5.83]	207.8 [-]	181.2 [-]	128.5 [1.06]	81.1 [1.41]	65.1 [5.25]

[-] - enthalpy of transition too small to be evaluated

3.14 LIQUID CRYSTALLINE PROPERTIES OF (*S*)-4-(1-METHYLHEPTYLOXYCARBONYL)PHENYL 5-(4'-n-DECYLOXY-3'-FLUOROBIPHENYL-4-YL)THIOPHENE-2-CARBOXYLATE (77) [Series XIII]

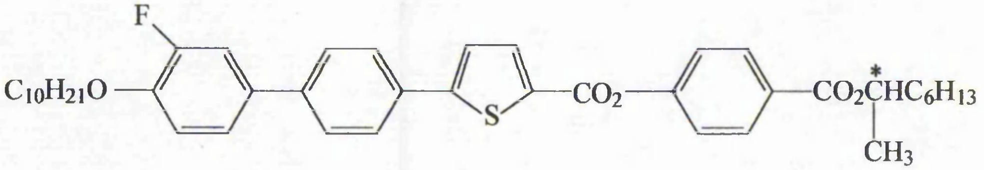

(77)

The mesomorphic data for (*S*)-4-(1-methylheptyloxycarbonyl)phenyl 5-(4'-n-decyloxy-3'-fluorobiphenyl-4-yl)thiophene-2-carboxylate (77) [**Series XIII**] is listed in **Table 16.**

On cooling from the isotropic liquid, a classical S_A phase was exhibited which on cooling gave the $S_C{}^*$ phase which was characterised by arcs across the fans coupled with an intense blue coloration in the previously homeotropic areas. The $S_C{}^*{}_{\mathrm{FERRI}}$ phase appeared on cooling from the $S_C{}^*$ phase, which then was immediately preceded by the $S_C{}^*{}_{\mathrm{ANTI}}$ phase. No other phases were observed prior to crystallisation.

Table 16: Transition temperatures[a] (°C) and enthalpy values[b] (kJ mol^{-1}) of (*S*)-4-(1-methylheptyloxycarbonyl)phenyl 5-(4'-n-decyloxy-3'-fluorobiphenyl-4-yl)thiophene-2-carboxylate (77) [**Series XIII**].

K-S_A	I-S_A	S_A- $S_C{}^*$	$S_C{}^*$-$S_C{}^*{}_{\mathrm{FERRI/ANTI}}$	$S_C{}^*{}_{\mathrm{FERRI/ANTI}}$-K
79.3[a] [15.90][b]	196.3 [4.98]	182.3 [0.76]	151.2 [-]	70.3 [6.08]

[-] - enthalpy of transition too small to be evaluated

3.15 LIQUID CRYSTALLINE PROPERTIES OF (*S*)-4-(1-METHYLHEPTYLOXYCARBONYL)PHENYL 4-(4'-n-DECYLOXYBIPHENYL-4-YL)-THIOPHENE-2-CARBOXYLATE (80) [Series XIV]

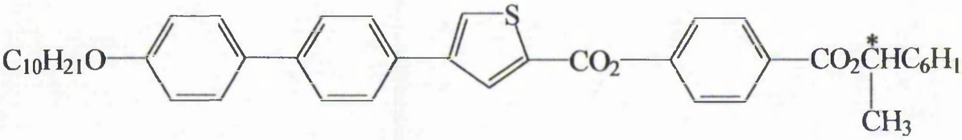

(80)

The mesomorphic and enthalpy data for (*S*)-4-(1-methylheptyloxycarbonyl)phenyl 4-(4'-n-decyloxybiphenyl-4-yl)thiophene-2-carboxylate (**80**) [**Series XIV**] is listed in **Table 17**.

On cooling from the isotropic liquid, the S_A phase was exhibited which appeared initially as bâtonnets which then slowly formed the focal-conic fan texture along with areas of homeotropic. The S_C* phase appeared on cooling the S_A phase and was characterised by the presence of arcs across the focal-conic fans coupled with very faint schlieren in the pseudohomeotropic areas. On further cooling of the S_C* phase, the pseudohomeotropic region exhibited a red coloration indicative of a helical structure. No other phases were exhibited prior to crystallisation.

Table 17: Transition temperatures[a] (°C) and enthalpy values[b] (kJ mol^{-1}) of (*S*)-4-(1-methylheptyloxycarbonyl)phenyl 4-(4'-n-decyloxybiphenyl-4-yl)-thiophene-2-carboxylate (**80**) [**Series XIV**].

K-S_A	I-S_A	S_A-S_C*	S_C*-K
120.2[a] [16.87][b]	173.0 [5.75]	158.5 [0.34]	121.8 [15.95]

3.16 LIQUID CRYSTALLINE PROPERTIES OF (*S*)-4-(1-METHYLHEPTYLOXYCARBONYL)PHENYL 4"-n-DECYLOXY-1",1':4',1-TERPHENYL-4-CARBOXYLATE (84) [Series XV]

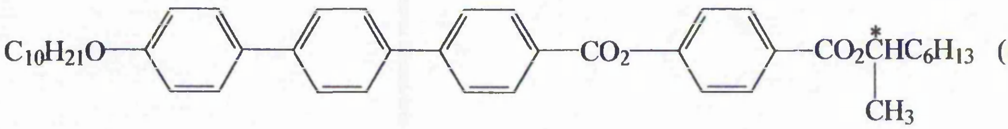

(84)

The mesomorphic and enthalpy data for (*S*)-4-(1-methylheptyloxycarbonyl)phenyl 4"-n-decyloxy-1",1':4',1-terphenyl-4-carboxylate **(84)** **[Series XV]** is listed in **Table 18**.

On cooling from the isotropic liquid, the S_A phase appeared as bâtonnets which coalesced to form the focal-conic fan texture along with areas of homeotropic. Once again, on cooling of the S_A phase, the S_C* phase was detected which then converted to the S_C*_{ANTI} phase via a very short-lived S_C*_{FERRI} phase. On further cooling of the S_C*_{ANTI} phase the S_I* phase was observed which was characterised by an unfocusable yellow schlieren-mosaic texture. No other phases were observed prior to crystallisation.

Table 18: Transition temperatures[a] (°C) and enthalpy values[b] (kJ mol^{-1}) of (*S*)-4-(1-methylheptyloxycarbonyl)phenyl 4"-n-decyloxy-1",1':4',1-terphenyl-4-carboxylate **(84)** **[Series XV]**.

K-S_A	I-S_A	S_A-S_C*	S_C*-S_C*_{FERRI}/ S_C*_{ANTI}	S_C*_{ANTI}-S_I*	S_I*-K
94.6 [15.46]	258.2 [6.08]	235.0 [0.22]	211.0 [-]	145.0 [1.12]	81.0 [7.98]

[-] - enthalpy of transition too small to be evaluated

3.17 COMPARATIVE STUDY OF COMPOUNDS COMPRISING THREE-RINGS IN THE CENTRAL MOLECULAR CORE, *i.e.*, SERIES IX-XV

It is now an appropriate stage to undertake a second comparative study but this time of compounds containing three-rings in the central molecular core. Such a study may also be cross-referenced with respect to the two-ring molecular core containing compounds mentioned earlier.

This comparative study can involve numerous permutations and combinations and it was decided to focus on the following areas:

i. influence of increasing the overall molecular length by introducing aromatic moieties in the central molecular core;

ii. influence of sequential replacement of 1,4-phenyl by 2,5-thienyl moieties in the central molecular core and;

iii. influence of introducing a lateral fluoro-substituent in the central three-ring molecular core.

3.17.1 INFLUENCE OF INCREASING THE OVERALL MOLECULAR LENGTH ON MESOMORPHIC PROPERTIES

In this situation, the overall molecular length was increased by introducing an additional aromatic moiety into a two-ring central molecular core to generate a three-ring central molecular core. The aromatic moiety was either 1,4-phenylene or 2,5-thienyl and as reported overleaf the mesophase thermal stability is dependent upon the nature of the aromatic moiety.

The influence of introducing an extra 1,4-phenylene ring into a two-ring central molecular core which contains one thiophene ring on mesomorphic properties is summarised in **Table 19**. The n=10 homologue of **Series I** and **V** may be compared with **Series XII** and **XIV**, respectively.

Table 19: Mesomorphic data (°C) for the n=10 homologue of **Series I**, **V**, **XII** and **XIV**.

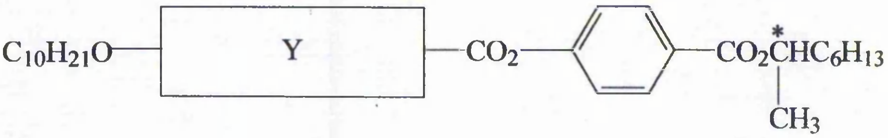

Series	Y	m.p.	cl.p.	Phase Range	Phase Types
I	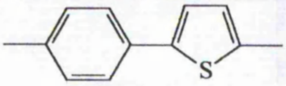	66.4	100.9	34.5	S_A, S_C*, $S_C{*}_{FERRI}$, $S_C{*}_{ANTI}$
V	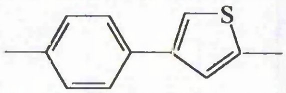	53.1	47.7	5.4	S_A
XII	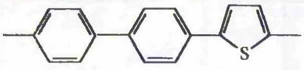	72.4	221.3	148.9	S_A, S_C*, $S_C{*}_{FERRI}$, $S_C{*}_{ANTI}$, S_I*, CrX
XIV	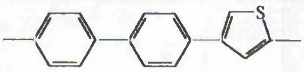	120.2	173.0	52.8	S_A, S_C*

From the results listed in **Table 19**, the following average thermal stability order may be quoted.

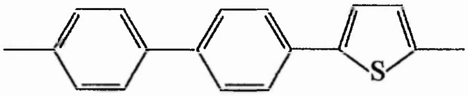

[Series XII]

>

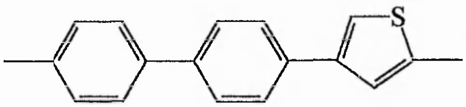

[Series XIV]

>

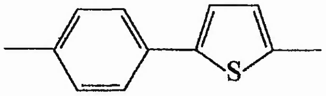

[Series I]

>

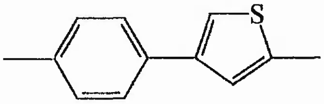

[Series V]

As evidenced by the data in **Table 19**, the inclusion of an additional 1,4-phenylene ring in the molecular core of either **Series I** or **Series V** increases mesophase thermal stability by a magnitude of 120.4°C and 125.3°C, respectively.

Interestingly, four-ring thiophene-based liquid crystals which contain three-rings in the central molecular core are more stable than their corresponding isomeric counterparts which contain two rings in the central molecular core. For example, on comparing the thermal stability data of the n=10 homologue of **Series XII** (cl.p. 221.3°C) with its isomeric four-ring counterpart [**Series II**] (cl.p. 193.2°C) and **Series XIV** (cl.p. 173.0°C) with **Series VI** (cl.p. 134.8°C) reveals that **Series XII** and **XIV** are thermally more stable than **Series II** and **VI** by a magnitude of 28.1°C and 38.2°C. Once again, this may be attributed to enhanced conjugation, as shown overleaf, and possibly improved geometry whereby the thiophene ring occupies a more central position.

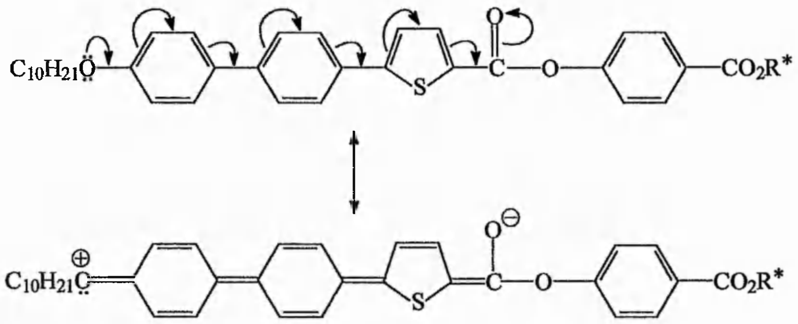

(70)
[Series XII]

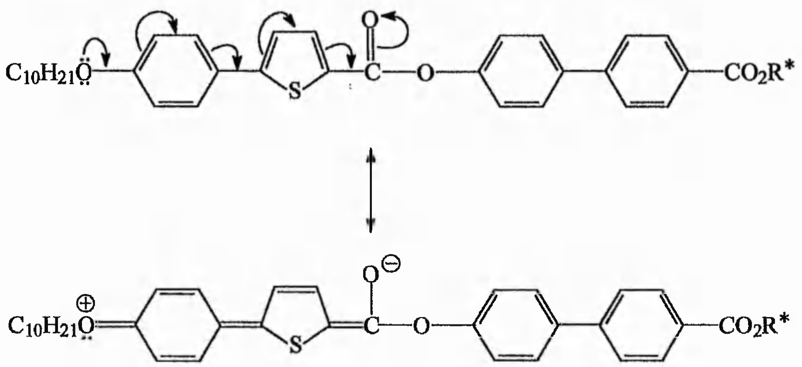

(28h)
[Series II]

A comparative study to investigate the influence of introducing an extra 1,4-phenylene ring in the molecular core of two-ring compounds which contains two thiophene rings may also be considered. **Table 20** shows the m.p. and cl.p. temperatures for **Series III** and **XI**.

As shown in **Table 20**, inclusion of an extra 1,4-phenylene ring, terminally disposed, increases the mesophase thermal stability by 131.9°C suggesting considerable improvement in molecular polarisability and molecular geometry. **Series III** exhibits short-lived monotropic phases whereas **Series XI** exhibits a multitude of stable phases.

Table 20: Mesomorphic data (°C) for the n=10 homologue of **Series III** and **XI**.

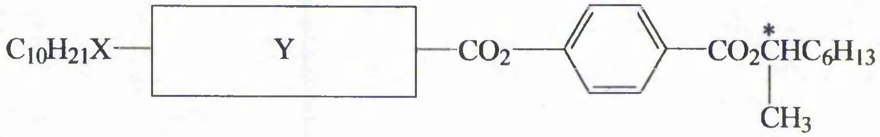

Series	X	Y	m.p.	cl.p.	Phase Range	Phase Types
III	-	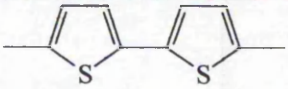	59.0	56.1	2.9	S_A, S_C*, S_C*_{FERRI}, S_C*_{ANTI}
XI	O	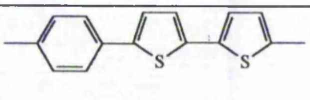	104.4	188.0	83.6	S_A, S_C*, $S_C*_{FERRI/ANTI}$

It is also appropriate to investigate the influence of including an extra 2,5-thiophene ring, terminally disposed, into the central molecular core of **Series III** to generate terthiophene [**Series IX**]. In this situation, as shown by the data in **Table 21**, the inclusion of an extra thiophene moiety increases mesophase thermal stability by 89.4°C.

Table 21: Mesomorphic data (°C) for n=10 homologue of **Series III** and **IX**.

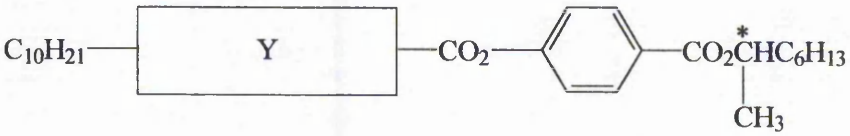

Series	Y	m.p.	cl.p.	Phase Range	Phase Types
III	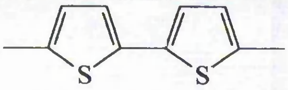	59.0	56.1	2.9	S_A, S_C*, S_C*_{FERRI}, S_C*_{ANTI}
IX	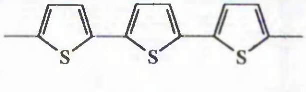	98.4	145.5	47.1	S_A, S_C*, S_C*_{FERRI}, S_C*_{ANTI}, S_I*

Summarising the data from **Tables 20** and **21**, shows that the inclusion of either an extra 1,4-phenyl- or 2,5-thienyl-ring in the molecular core increases mesophase thermal stability. As shown below, the addition of an extra 1,4-phenyl ring in comparison with an extra 2,5-thienyl ring is by far superior by a magnitude of 42.5°C.

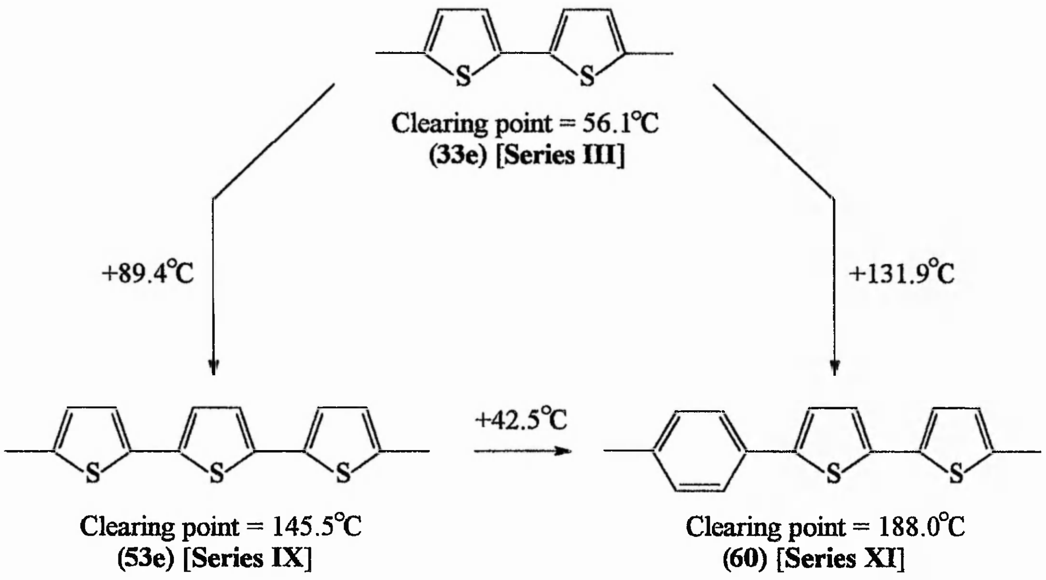

3.17.2 INFLUENCE OF SEQUENTIAL REPLACEMENT OF 1,4-PHENYL BY 2,5-THIENYL ON MESOPHASE THERMAL STABILITY

In order to assess the influence of successively replacing 1,4-phenylene moieties with 2,5-thienyl moieties in the central molecular core on mesomorphic properties, **Series IX**, **XI**, **XII** and **XV** were compared. The central three-ring molecular core was systematically altered from 'terthienyl' [**Series IX**] to 'phenyl-bithienyl' [**Series XI**] to 'biphenyl-thiophene' [**Series XII**] and finally to 'terphenyl' [**Series XV**]. The mesomorphic data for **Series IX**, **XI**, **XII** and **XV** is reported in **Table 23**.

Table 23: Mesomorphic data (°C) for the n=10 homologue of **Series IX**, **XI**, **XII** and **XV**.

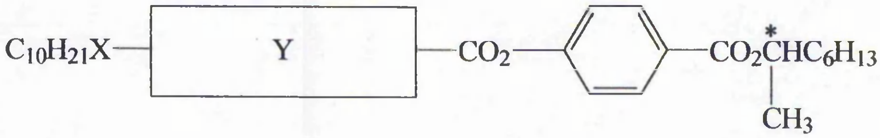

Series	X	Y	m.p.	cl.p.	Phase Range	Phase Types
IX	-	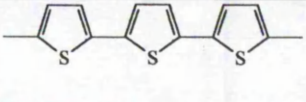	98.4	145.5	47.1	S_A, $S_C{}^*$, $S_C{}^*{}_{\text{FERRI/ANTI}}$, $S_I{}^*$
XI	O	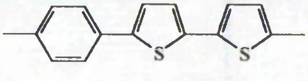	104.4	188.0	83.6	S_A, $S_C{}^*$, $S_C{}^*{}_{\text{FERRI/ANTI}}$
XII	O	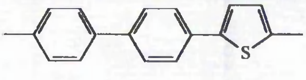	72.4	221.3	148.9	S_A, $S_C{}^*$, $S_C{}^*{}_{\text{FERRI/ANTI}}$ $S_I{}^*$, CrX
XV	O		94.6	258.2	163.6	S_A, $S_C{}^*$, $S_C{}^*{}_{\text{FERRI/ANTI}}$ $S_I{}^*$

From the results displayed in **Table 23**, the following average thermal stability order may be reported.

 > 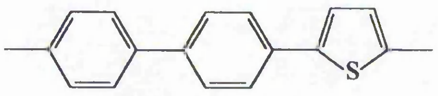 >

[Series XV] **[Series XII]**

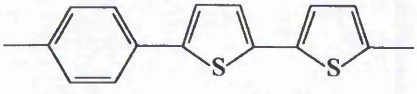 > 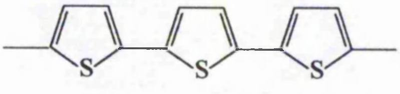

[Series XI] **[Series XI]**

As expected, the most thermally stable compound is the non-heterocyclic terphenyl compound [**Series XV**]. Replacement of the right-hand, centrally disposed, phenyl ring for thiophene to generate **Series XII**, introduces a bend into the previously linear molecule which results in the packing efficiency being reduced and hence the mesophase thermal stability is decreased by approximately 40°C.

Replacement of a second 1,4-phenyl ring by a second thiophene moiety to generate **Series XI** further reduces the thermal stability by a magnitude of approximately 30°C.

Replacement of all three 1,4-phenyl rings with 2,5-thiophene rings to give terthiophene [**Series IX**] drastically reduces the mesophase thermal stability. The disposition of three thiophene rings and non-linear geometry is detrimental to mesophase thermal stability.

3.17.3 INFLUENCE OF LATERAL FLUORINATION

A lateral fluoro substituent was introduced in the 3'-position of the left-hand, terminally disposed, phenyl ring of **Series XII** to give **Series XIII**. The mesomorphic data for **Series XII** and **XIII** are reported in **Table 24.**

From the data listed in **Table 24**, the introduction of a lateral fluoro-susbstituent lowers the mesophase thermal stability of [**Series XII**] by a magnitude of 25.0°C when compared with its non-fluorinated analogue, *i.e.*, [**Series XIII**]. Another advantage of lateral fluorination is the ability to suppress high order smectic crystal phases and this is evidenced clearly by [**Series XIII**] which no longer exhibits the CrX phase upon lateral fluorination.

Table 24: Mesomorphic data (°C) for the n=10 homologue of **Series XII** and **XIII**.

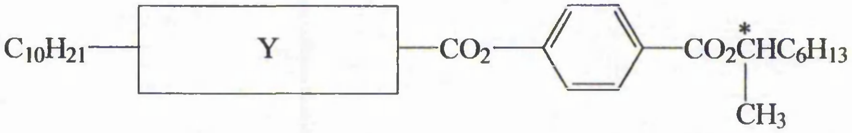

Series	Y	m.p.	cl.p.	Phase Range	Phase Types
XII	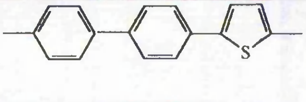	72.4	221.3	148.9	S_A, S_C*, $S_C*_{FERRI/ANTI}$, S_I*, CrX
XIII	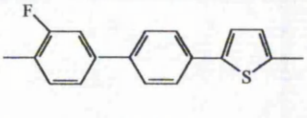	79.3	196.3	117.0	S_A, S_C*, $S_C*_{FERRI/ANTI}$

3.18 SUMMARY OF COMPARATIVE STUDY

Combining the data for the n=10 homologue reported in the first comparative study which deals primarily with compounds containing two-rings in the central molecular core (p. 170) with the second comparative study on compounds containing three-rings in the central molecular core (p. 193), the following thermal stability order can be proposed.

The thermal stability may be rationalised in terms of molecular geometry, extent of molecular polarisability and conjugation. However, it is notable that four-ring compounds comprising three rings in the central molecular core and one ring in the terminal ‘chiral phenol’ are thermally more stable than their isomeric four-ring compounds which contain two-rings in the central molecular core and two rings in the ‘chiral phenol’.

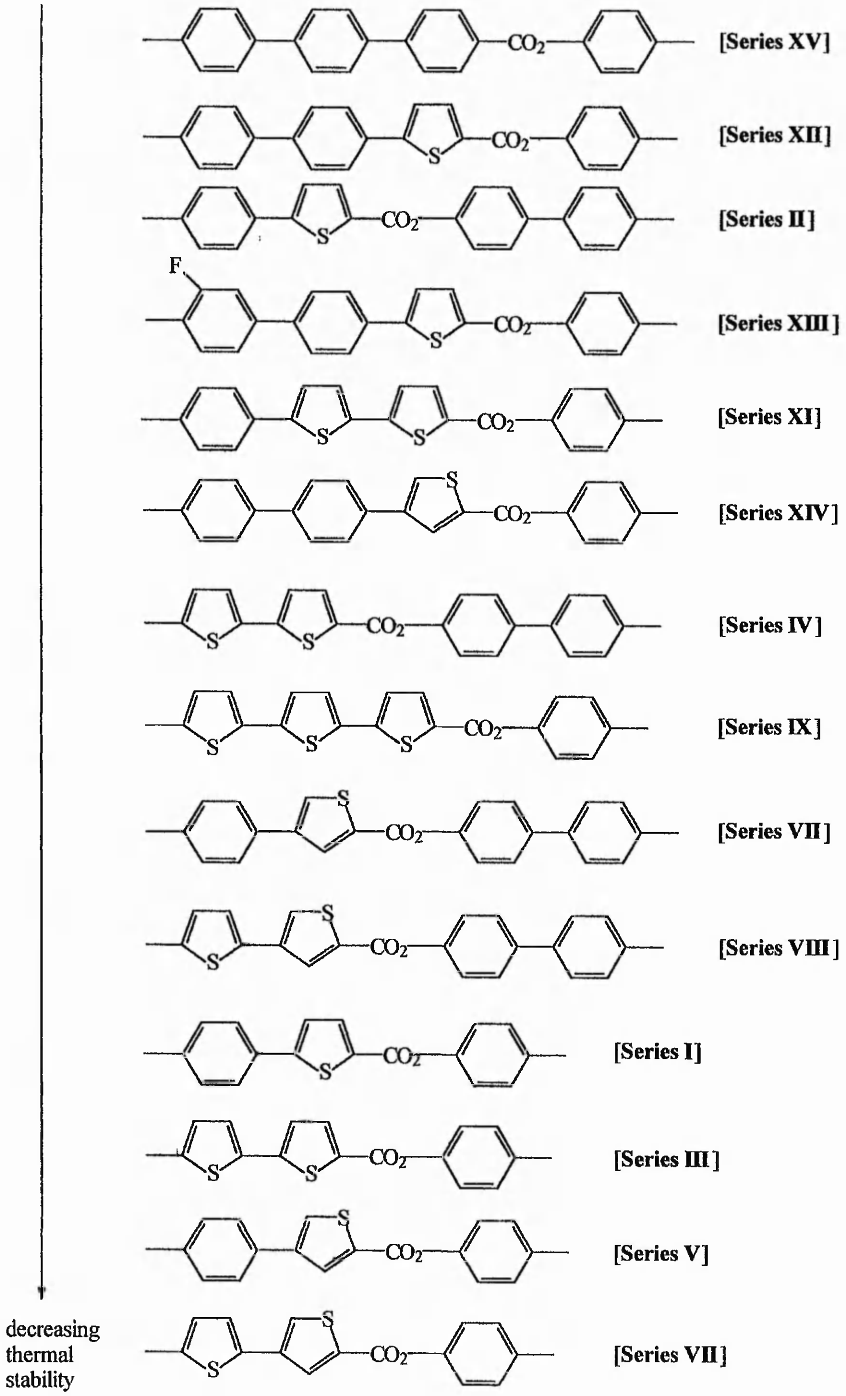

PHOTOGRAPHIC PLATES

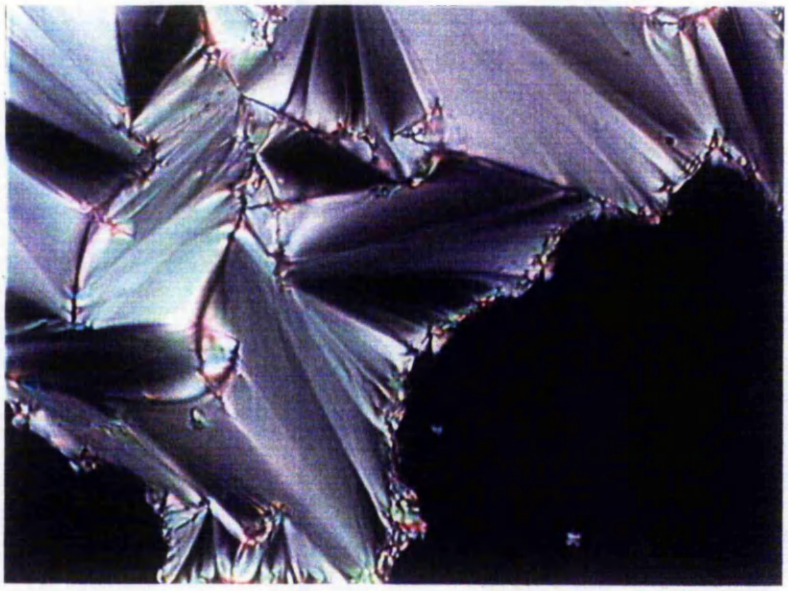

Plate 1. The focal-conic fan texture interspersed with homeotropic areas (dark) of the S_A phase for compound (**27e**) of **Series I**.

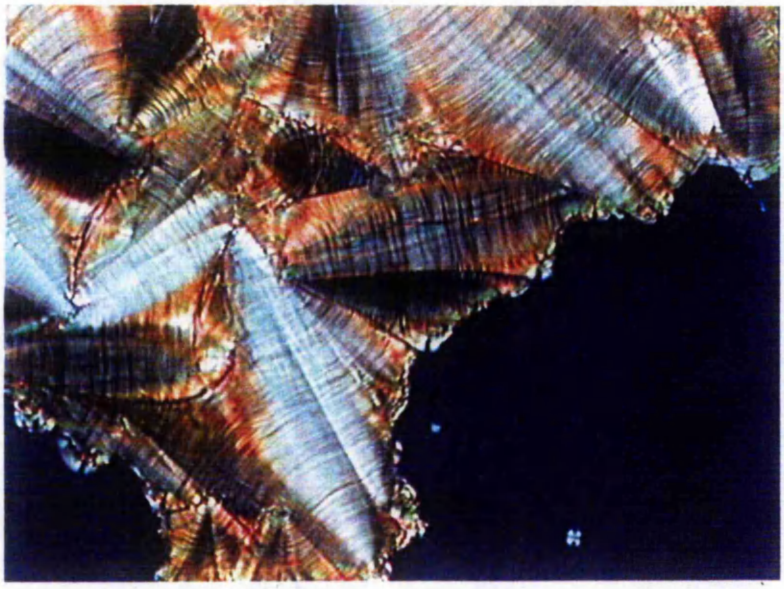

Plate 2. The arced or broken focal-conic fan and ‘pseudohomeotropic’ (appears blue) texture of the S_C*ferroelectric phase for compound (**27e**) of **Series I**. Same area as Plate 1.

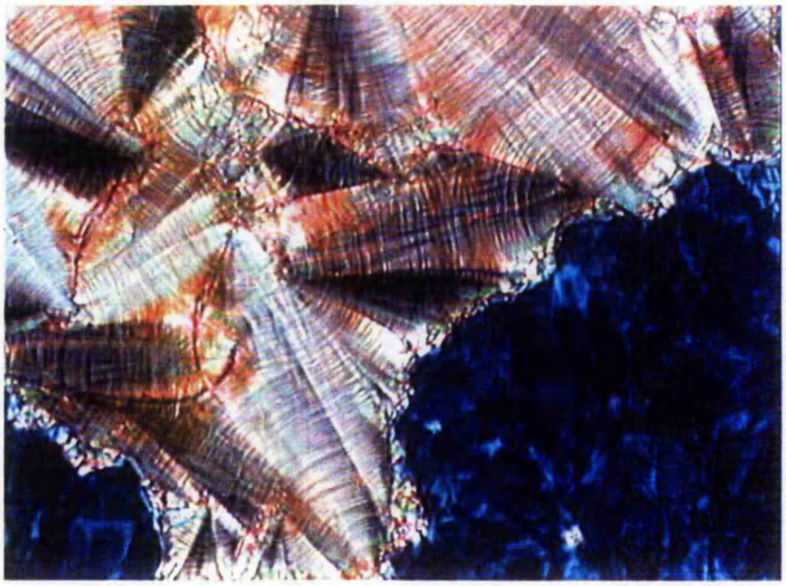

Plate 3. Onset of milky-white shimmering texture of the S_C*ferrielectric phase for compound (**27e**) of **Series I**. Same area as Plate 2.

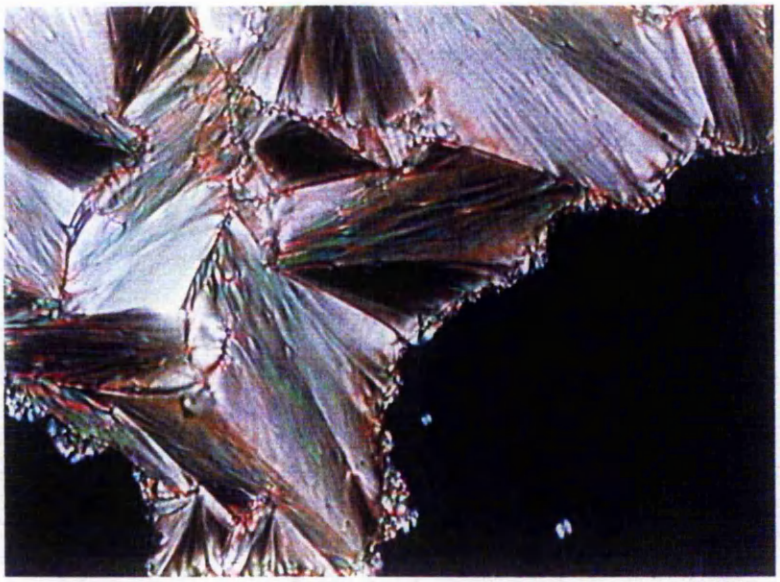

Plate 4. The arced focal-conic fan texture almost showing wish-bone defects interspersed with 'pseudohomeotropic' texture of the S_C*antiferroelectric phase for compound (**27e**) of **Series I**. Same area as Plate 3.

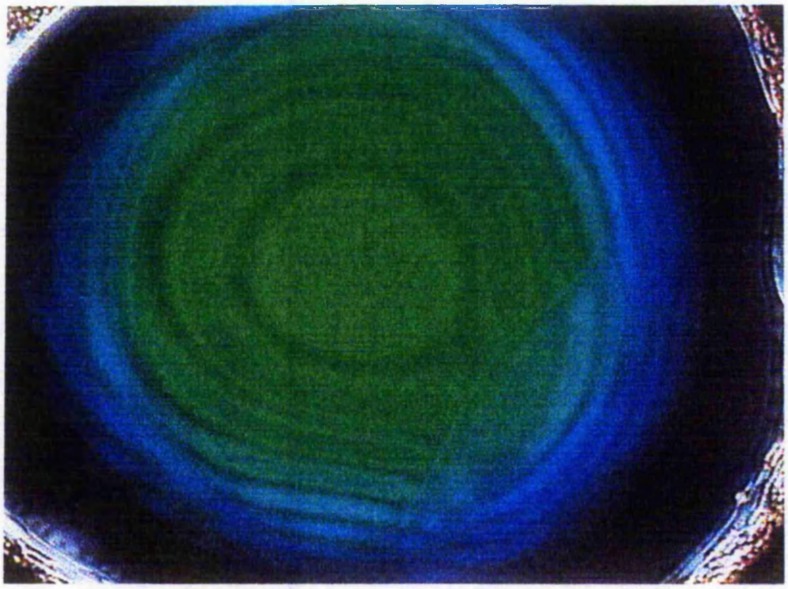

Plate 5. Free-standing film texture marking the onset of the S_C*ferroelectric phase (blue-green colour) for compound (**28h**) of **Series II**.

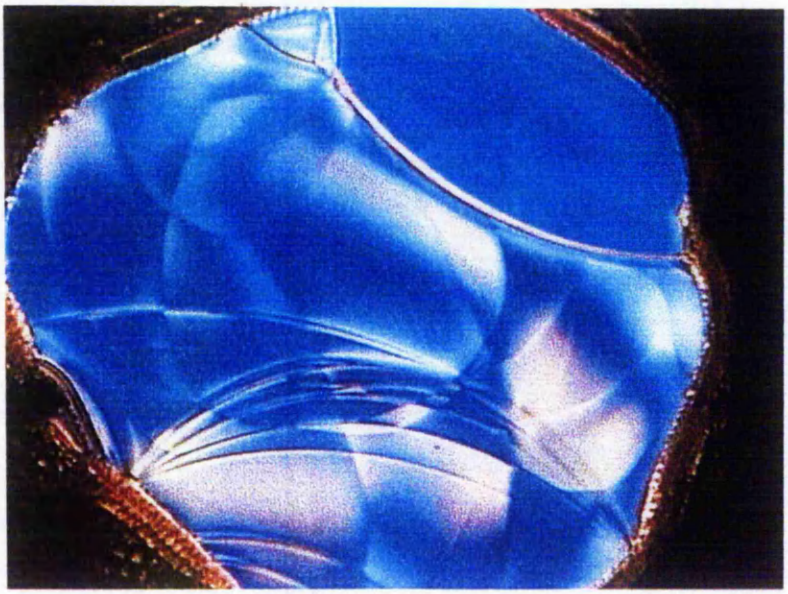

Plate 6. Free-standing film texture exhibiting a milky-white turbulent texture characteristic of the S_C*ferrielectric phase of compound (**28h**) of **Series II**.

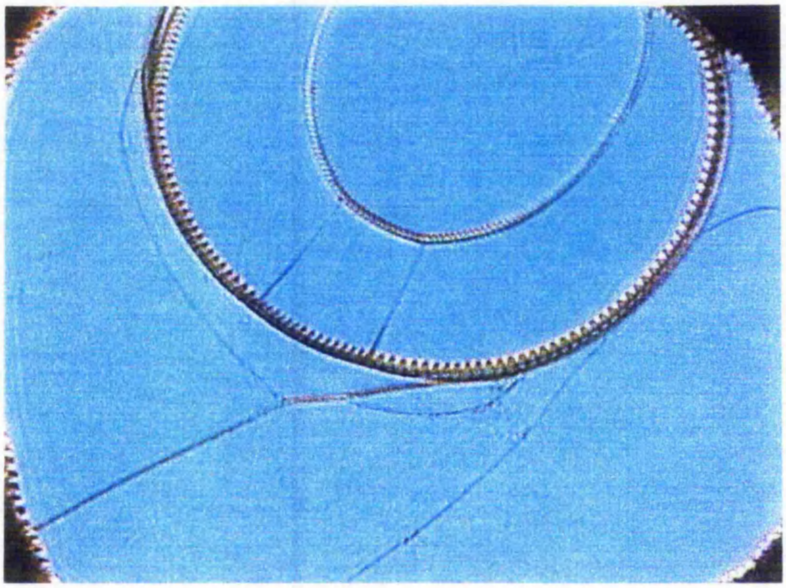

Plate 7. Free-standing film texture of the S_C*antiferroelectric phase from the previous S_C*ferrielectric phase of compound (**28h**) of **Series II**. Same area as Plate 6, loss of intense shimmering.

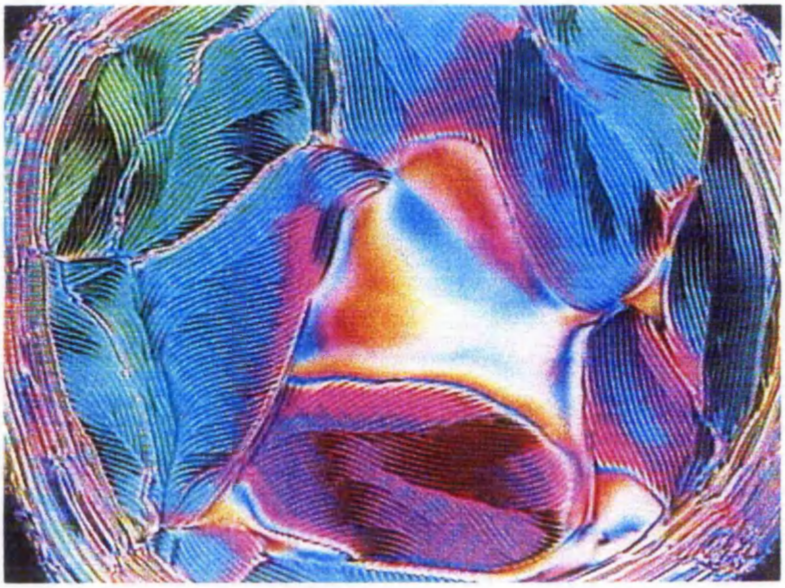

Plate 8. Free-standing film texture marking the onset of the S_I* phase from the S_C*antiferroelectric phase exhibiting an unusual fingerprint texture for compound (**28h**) of **Series II**.

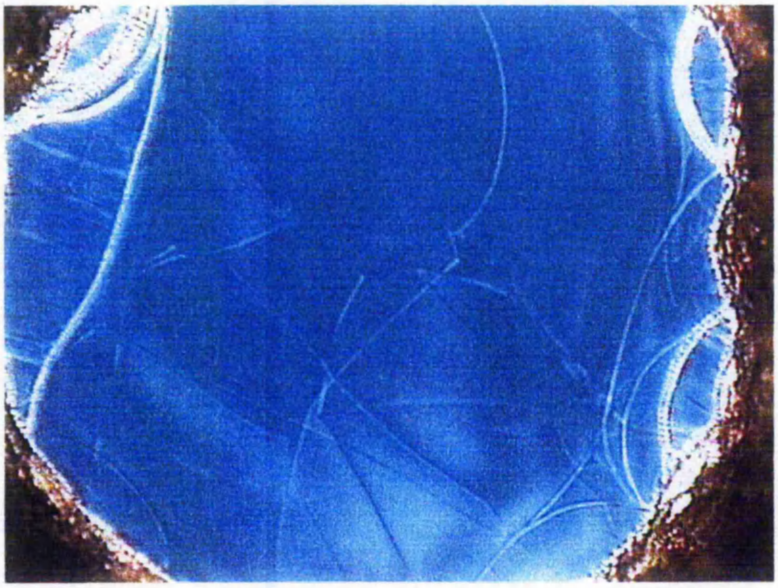

Plate 9. Free-standing film texture exhibiting the fully developed S_I* phase for compound (**28h**) of **Series II**. Same area as Plate 8.

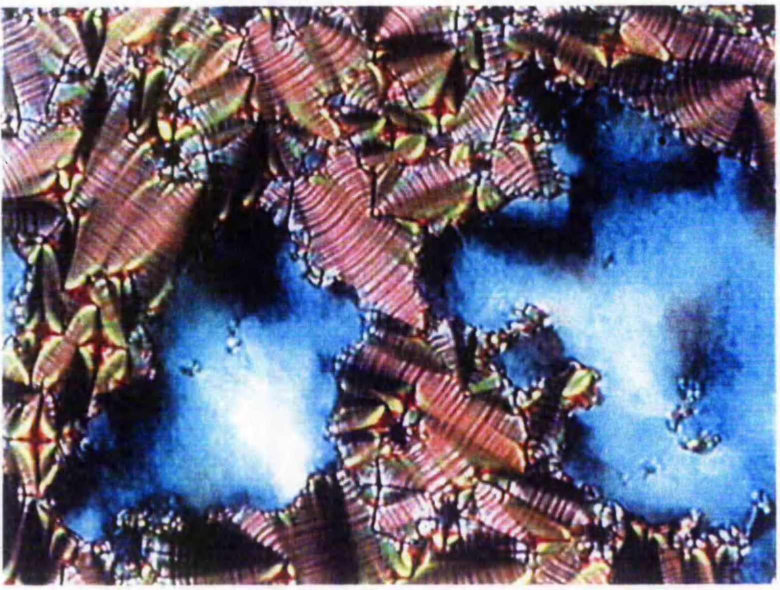

Plate 10. The arced (continuous) and 'ghost-like' mosaic/platelet texture reminiscent of the CrE phase as exhibited by compound (**53a**) of **Series IX**.

REFERENCES

REFERENCES

1. Reinitzer, F., *Monatsh. Chem.*, **9**, 421 (1888); *Liquid Crystals*, **5**, 7 (1989).

2. Lehmann, O., *Z. Krist.*, **18**, 464 (1890).

3. Tammann, G., *Ann. Physik*, **4**, 524 (1901); **8**, 103 (1902); **19**, 421 (1906).

4. Nernst, W., *Z. Elecktrochem.*, **12**, 431 (1906).

5. Vorländer, D., *'Kristallinisch-flussige Substanzen'*, Enke, Stuttgart (1908); *Ber. Dtsch. Chem. Ges.*, **41**, 2033 (1908).

6. Friedel, G., *Ann. Physique*, **18**, 273 (1922).

7. Vorländer, D. and Wilke, R., *Z. Physik. Chem.*, **57**, 361 (1906).

8. Bose, E., *Z. Phys.*, **10**, 32 (1909); **10**, 230 (1909).

9. Ornstein, L.S. and Zernicke, F., *Z. Phys.*, **19**, 134 (1918).

10. Zocher, H., *Z. Phys.*, **28**, 790 (1927).

11. Oseen, C.W., *Trans. Faraday Soc.*, **29**, 833 (1933).

12. Brown, G.H. and Shaw, W.G., *Chemical Reviews*, **57**(6), 1049 (1957).

13. Gray, G.W., 'Molecular Structure and the Properties of Liquid Crystals', Academic Press, London and New York (1962).

14. Gray, G.W., Harrison, K.J. and Nash, J.A., *Electron Lett.*, **9**, 130 (1973).

15. Schadt, M., and Helfrich, W., *Appl. Phys Lett.*, **18**, 127 (1971).

16. Clark, N.A. and Lagerwall, S.T., *Appl. Phys. Lett.*, **36**, 899 (1980).

17. Meyer, R.B., Liébert, L., Strzelecki, L. and Keller, P., *J. Phys. Paris Lett.*, **36**, L69 (1975).

18. Chandani, A.D.L., Gorecka, E., Ouchi, Y., Takezoe, H., Fukuda, A., Terashima, K., Furukawa, K. and Kishi., *Jpn. J. Appl. Phys.*, **28**, L1261 (1989).

19. Chandani, A.D.L., Gorecka, E., Ouchi, Y., Takezoe, H. and Fukuda, A., *Jpn. J. Appl. Phys.*, **28**, L1265 (1989). For review; Fukada, A., Takanishi, Y., Isozaki, T., Ishikawa, K. and Takezoe, H., *J. Mater. Chem.*, **4**, 997 (1994).

20. Collings, P.J. and Patel, J.S. (eds.), 'Handbook of Liquid Crystal Research' Oxford University Press, Oxford (1997).

21. Demus, D., Goodby, J.W. and Gray, G.W., Spiess H.-W. and Vill V. (eds.), 'Handbook of Liquid Crystals, Vols. I-IV', Wiley - VCH, Federal Republic of Germany (1998).

22. Goodby, J.W, *Liquid Crystals*, **24**, 25 (1998).

23. Chandrasekhar, S., Sadashiva, B.K. and Suresh, K.A., *Pranama*, **9**, 471 (1977).

24. Malthête, J., Canceill, J., Gabard, J. and Jacques, J., *Tetrahedron*, **37**, 2823 (1981).

25. Nguyen, H.T., Destrade, C. and Malthête, J., *Liquid Crystals*, **8**, 797 (1990).

26. Nguyen, H.T., Destrade, C. Allouchi, H., Bideau, J.P., Cotrait, M., Guillon, D., Weber, P. and Malthête, J., *Liquid Crystals*, **15**, 435 (1993).

27. Andersch, J. and Tschierske, C., *Liquid Crystals*, **21**, 51 (1996).

28. Bernal, J.D. and Crowfoot, D., *Trans. Faraday Soc.*, **29**, 1032 (1933).

29. Leadbetter, A.J., Durrant, J.L.A. and Rugman, M., *Mol. Cryst. Liq. Cryst. Lett.*, **34**, 231 (1977).

30. Crooker, P.P., *Liquid Crystals*, **5**, 751 (1989).

31. Goodby, J.W., Waugh, M.A., Stein, S.M., Chin, E., Pindak, R. and Patel, J.S., *J. Am. Chem. Soc.*, **111**, 8119 (1989).

32. Hückel, E., *Physik. Z.*, **22**, 561 (1921).

33. Slaney, A.J., Nishiyama, I., Styring, P. and Goodby, J.W., *J. Mater. Chem.*, **2**, 805 (1992).

34. Sackmann, H. and Demus, D., *Mol. Cryst. Liq. Cryst.*, **21**, 239 (1973).

35. Cladis, P.E., *Phys. Rev. Lett.*, **35**, 48 (1975).

36. Byron, D.J., Matharu, A.S., Shirazi, S.N.R., Tajbakhsh, A.R. and Wilson, R.C., *Liquid Crystals*, **14**, 645 (1993).

37. de Vries, A., *Mol. Cryst. Liq. Cryst.*, **11**, 361 (1970).

38. Levelut, A.M. and Lambert, M., *Compt. Rend. Acad. Sci. (Paris)*, **272**, 1018 (1971).

39. Goodby, J.W., *Mol. Cryst. Liq. Cryst.*, **75A**, 91 (1979).

40. Doucet, J. and Levelut, A.M., *J.Phys. (Paris)*., **38**, 1163 (1977).

41. Goodby, J.W., *Mol. Cryst. Liq. Cryst. Lett.*, **92**, 171 (1983).

42. Bowden, C.J., Herrington, T.M., Moseley, A.M. and Richardson, R., *Liquid Crystals*, **18**, 825 (1995).

43. Gray, G.W., Jones, B. and Marson, F., *J. Chem. Soc.*, 393 (1957).

44. Demus, D., Kunicke, G., Neelson. J. and Sackmann, H., *Z. Naturforsch.*, **23a**, 84 (1968).

45. Diele, S., Brant, P. and Sackmann, H., *Mol. Cryst. Liq. Cryst.*, **17**, 163 (1972).

46. Lydon, J.E., *Mol. Cryst. Liq. Cryst. Lett.*, **72**, 79 (1981).

47. Levelut, A. and Clerc, M., *Liquid Crystals*, **24**, 105 (1998).

48. Coates, D. and Gray, G.W., *Phys. Lett.*, **45A**, 115 (1973).

49. Coates, D. and Gray, G.W., *Phys. Lett.*, **51A**, 335 (1975).

50. Collings, P.J. and Hird, M., 'Introduction to Liquid Crystals', Taylor and Francis Limited, London (1997)

51. Toyne, K.J., 'Thermotropic Liquid Crystals - (Critical reports on Applied Chemistry)', ed. Gray, G.W., John Wiley and Sons, Chichester, Vol. 22, Chap. 2 (1987).

52. Gray, G.W., 'Liquid Crystals and Plastic Crystals', eds. Gray, G.W. and Winsor, P.A., Ellis Horwood Ltd., Chichester, Vol. 1, Chap. 2 (1974).

53. Gray, G.W., Hartley, J.B. and Jones, B., *J. Chem. Soc.*, 1412 (1955).

54. Gray, G.W. and McDonnell, D.G., *Mol. Cryst. Liq. Cryst.*, **53**, 147 (1979).

55. Gray, G.W. and Worrall, B.M., *J. Chem. Soc.*, 1545 (1959).

56. Gray, G.W. and Jones, B., *J. Chem. Soc.*, 683 (1954).

57. Gray, G.W., Hird, M., Lacey, D. and Toyne, K.J., *J. Chem. Soc. Perkin Trans. II*, 2041 (1989).

58. Gray, G.W., Hird, M., Lacey, D. and Toyne, K.J., *Mol. Cryst. Liq. Cryst.*, **172**, 165 (1989).

59. Gray, G.W., Hird, M. and Toyne, K.J., *Mol. Cryst. Liq. Cryst.*, **204**, 43 (1991).

60. Goulding, M.J. and Greenfield, S., *Liquid Crystals*, **13**, 345 (1993).

61. Hird, M., Toyne, K.J., Gray, G.W., McDonnell, D.G. and Sage, I.C., *Liquid Crystals*, **18**, 1 (1985).

62. Hird, M. and Toyne, K.J., *Mol. Cryst. Liq. Cryst.*, **323**, 1 (1998).

63. Carr, N., Gray, G.W. and McDonnell, D.G., *Mol. Cryst. Liq. Cryst.*, **97**, 13, (1983).

64. Kelly, S.M., *Liquid Crystals*, **5**, 171 (1989).

65. Gray, G.W., Hird, M. and Toyne, K.J., *Mol. Cryst. Liq. Cryst.*, **195**, 221 (1991).

66. Valasek, J., *Phys. Rev.*, **17**, 475 (1921).

67. Yoshino, K., Ozaki, M., Sakurai, T., Sakamoto, K. and Honma, M., *Jpn. J. Appl. Phys. Lett.*, **23**, 175 (1984).

68. Nishiyama, I., and Goodby, J.W., *J. Mater. Chem.*, **2**, 1015 (1992).

69. Ouchi, Y., Yoshioka, Y., Ishii, H., Seki, K., Kitamura, M., Noyori, R., Takanishi, Y. and Nishiyama., *J. Mater. Chem.*, **5**, 2297 (1995).

70. Isozaki, T., Hiraoka, K., Takanishi, Y., Takezoe, H., Fukuda, A., Suzuki, Y. and Kawamura, I., *Liquid Crystals*, **12**, 59 (1992).

71. Hiji, N., Chandani, A.D.L., Nishiyama, I., Ouchi, Y., Takezoe, H. and Fukuda, A., *Ferroelectrics*, **85**, 99 (1988).

72. Nishiyama, I., Yoshizawa, A., Fukumasa, M. and Hirai, T., *Jpn. J. Appl. Phys. Lett.*, **28**, 2288 (1989).

73. Inui, S., Kawano, S., Saito, M., Iwane, H., Takanishi, Y., Hiraoka, K., Ouchi, Y., Takezoe, H. and Fukuda, A., *Jpn. J. Appl. Phys. Lett.*, **29**, 987 (1990).

74. Suzuki, Y., Hagiwara, T., Aihara, Y., Sadamure, Y. and Kawamura, I., *Proceedings of the Fifteenth Japanese Liquid Crystal Conference [Osaka]: Abstracts*, **302** (1989).

75. Takeda, H.and Suzuki, Y., *Proceedings of the Sixteenth Japanese Liquid Crystal Conference [Hiroshima]: Abstracts.*, **134** (1990).

76. Brown, J.W., Trent Polytechnic, Ph.D Thesis (1986).

77. Butcher, J.L., Nottingham Polytechnic, Ph.D Thesis (1991).

78. Shirazi, S.N.R., The Nottingham Trent University, Ph.D Thesis (1993).

79. McSherry, I., The Nottingham Trent University, Ph.D Thesis (1996).

80. Kiryanov, A.A, Sampson, P. and Seed, A.J., *Mol. Cryst. Liq. Cryst.*, **329**, 237 (1999).

81. Byron, D.J., Komitov, L., Matharu, A.S., McSherry, I. and Wilson, R.C., *J. Mater. Chem.*, **6**, 1871 (1996).

82. Miyaura, N., Yanagi, T. and Suzuki, A., *Synth. Comm.*, **11**, 513 (1981).

83. Hawkins, R.T., Lennarz, W.J. and Snyder, H.R., *J. Am. Chem. Soc.*, **82**, 3053 (1960).

84. Hird, M., Gray, G.W. and Toyne, K.J., *Mol. Cryst. Liq. Cryst.*, **206**, 187 (1991).

85. Thompson, W.J. and Gaudino, J., *J. Org. Chem.*, **49**, 5237 (1984).

86. Martin, A.R. and Yang, Y., *Acta. Chem. Scand.*, **47**, 221 (1993).

87. Hassner, A. and Alexanian, V., *Tetrahedron Lett.*, **46**, 4475 (1978).

88. Chin, E. and Goodby, J.W., *Mol. Cryst. Liq. Cryst.*, **141**, 311 (1986).

89. Booth, C.J., Dunmur, D.A., Goodby, J.W., Kang, J.S. and Toyne, K.J., *J. Mater. Chem.*, **4**, 747 (1994).

90. Tamao, K., Kodama, S., Nakajima, I., Kumada, M., Minato, A. and Suzuki, K., *Tetrahedron*, **38**, 3347 (1982).

91. Huang-Minlon, *J. Am. Chem. Soc.*, **68**, 2487 (1946).

92. Khor, E., Ng, S.C., Li, H.C. and Chai, S., *Heterocycles*, **32**(9), 1805 (1991).

93. Wright, G., The Nottingham Trent University, PhD Thesis (1996).

94. Goldfarb, Y.L., Fabrichnyi, B.P. and Rogovik, V.I., *Chem. Abstr.*, **61**, 629 (1964).

95. Chadwick, D.J., Chambers, G., Meakins, D. and Snowden, R.L., *J. Chem. Soc. Perkin Trans. I.*, 1766 (1973).

96. Ladd, D.L., Harrsch, P.B. and Kruse, L.I., *J. Org. Chem.*, **53**, 417 (1988).

97. Goldfarb, Y.L., Volkenstein, Y.B. and Lopatin, B.V., *Zh. Obshch. Khim.*, **60**, 9227 (1964).

98. Gronowitz, S., Moses, P., Hörnfeldt, A.B. and Hakannson, R., *Ark. Kemi.*, **17**, 165 (1961).

99. Seed, A.J., Toyne, K.J. and Goodby, J,W., *J. Mater. Chem.*, **5**, 653 (1995).

100. Gronowitz, S. and Lawitz, K., *Chemica Scripta.*, **22**, 265 (1983).

101. Stille, J.K., *Angew. Chem. Int. Ed. Engl.* **25**, 508 (1986).

102. Duncton, M.A.J. and Pattenden, G., *J. Chem. Soc., Perkin Trans. I.*, 1235 (1999).

103. Uhlenbroek, J.H. and Bijoo, J.D., *Rec. Trav. Chim. Pays-Bas.*, **79**, 1181 (1960).

104. Asano, T., Ito, S., Saito, N. and Hatakeda, K., *Heterocycles*, **6**, 317 (1977).

105. Jayasuriya, N. and Kagan, J., *Heterocycles*, **24**(10), 2901 (1986).

106. Crisp, G.T., *Synth. Commun.*, **19**, 307 (1989).

107. Seed, A.J., Toyne, K.J. and Goodby, J.W., *J. Mater. Chem.*, **5**, 653-661 (1995).

108. Bäuerle, P., Würthner, F., Götz, G. and Effenberger, F., *Synthesis*, 1099 (1993).

109. Carpita, A. and Rossi, R., *Gazz. Chim. Ital.*, **115**, 575 (1985).

110. Brettle, R., Dunmur, D.A., Marson, C.M., Pinol, M. and Toriyama, K., *Liquid Crystals*, **13**, 515 (1993).

111. Arnold, Z. and Zemlicka, J., *Proc. Chem. Soc.*, 227 (1958).

112. Gray, G.W. and Mosley, A., *J. Chem. Soc., Perkin Trans II.*, 97 (1976).

113. Drapala, T., *Rocz. Chem.*, **44**(1), 61 (1970).

114. Andersch, J., Tschierske, A., Diele, S. and Lose, D., *J. Mater. Chem.*, **6**(8), 1297 (1996).

115. Fournari, P., Guilard, R. and Person, M., *Bull. Soc. Chem. Fr.*, 4121 (1967).

116. Robinson, W.K., Gleeson, H,F., Hird, M., Seed, A.J. and Styring, P., *Ferroelectrics*, **178**, 249 (1996).

117. Gorecka, E., Glogarova, M., Sverenyaka, H. and Lejcek, L., *Ferroelectrics*, **178**, 101 (1996).

118. Berardi, R., Spinozzi, F. and Zannoni, C., *Liquid Crystals*, **16**, 381 (1994).

119. Caldarelli, S., Catalano, D., DiBari, L., Lumetti, M., Ciofalo, M. and Veracini, C.A., *J. Mol. Struct.*, **323**, 181 (1994).

APPENDICES

APPENDIX 1: SYNTHESIS OF (*S*)-1-METHYLHEPTYL 4-HYDROXYBENZOATE (25) AND (*S*)-1-METHYLHEPTYL 4'-HYDROXYBIPHENYL-4-CARBOXYLATE (26).

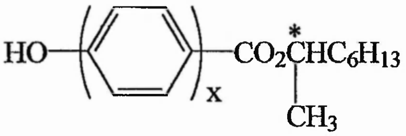

where x=1, (**25**); x=2 (**26**)

The synthetic route leading to the preparation of the appropriate chiral phenol either (*S*)-1-methylheptyl 4-hydroxybenzoate (**25**) or (*S*)-1-methylheptyl 4'-hydroxybiphenyl-4-carboxylate (**26**) is depicted in **Scheme 1a**.

The appropriate carboxylic acid was protected by treatment with methyl chloroformate in aqueous sodium hydroxide at 0°C and then subsequently esterified using (*R*)-2-octanol, diethylazodicarboxylate and triphenylphosphine to give the (*S*)-protected esters as colourless liquids. The reaction proceeds with inversion of the absolute configuration at the chiral centre. The esters were then deprotected using an ethanol-ammonia solution at room temperature to give the corresponding chiral phenol either (*S*)-1-methylheptyl 4-hydroxybenzoate (**25**) or (*S*)-1-methylheptyl 4'-hydroxybiphenyl-4-carboxylate (**26**) in excellent yield.

SCHEME 1a

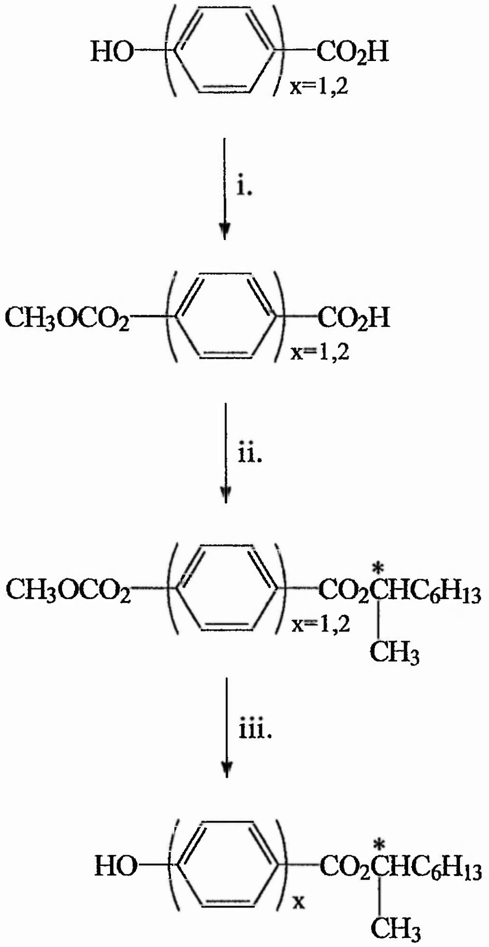

where x=1, (**25**); x=2 (**26**)

i. Methyl chloroformate, NaOH, 0°C.
ii. (*R*)-2-octanol, $Pd(PPh_3)_4$, diethylazodicarboxylate.
iii. Ammonia, ethanol.

4-Methoxycarbonyloxyphenyl-4-carboxylic acid

4-Hydroxy-4-benzoic acid (25.0 g, 0.181 mol) was added slowly to a vigorously stirred solution of sodium hydroxide (21.7 g, 0.543 mol) in water (300 ml) at 0°C. Methyl chloroformate (34.2 g, 0.362 mol) was added dropwise, and the temperature maintained at 0°C. The resulting white slurry was then stirred under these conditions for a further 4 h. The pH was adjusted to 5 using concentrated hydrochloric acid solution (1:1, concentrated HCl:water) and the voluminous white precipitate was filtered off and washed with water. The resulting white solid was then dried and recrystallised from glacial acetic acid to yield 25.5 g (72%) of a white crystalline product, m.p. 178-180°C.

^{1}H n.m.r. δ ($CDCl_3$): 4.0 (3H, s, CH_3O), 7.3 (2H, d, ArH, J=9Hz), 8.2 (2H, d, ArH, J=9Hz) ppm. No OH signal observed.

i.r. ν_{max} (KBr): 2840, 1680, 1605, 1428, 1290, 1186, 1065, 930, 819 cm^{-1}.

4-Methoxycarbonyloxybiphenyl-4-carboxylic acid

4-Methoxycarbonyloxybiphenyl-4-carboxylic acid was prepared according to the method described above. Quantities: 4-hydroxybiphenyl-4-carboxylic acid (34.5 g, 0.161 mol), methyl chloroformate (30.4 g, 0.322 mol), sodium hydroxide (19.3 g, 0.484 mol). Work-up of the crude product gave 33.3 g (76%) of a white crystalline solid, m.p. 258-260°C.

^{1}H n.m.r. δ ($CDCl_3$): 4.0 (3H, s, CH_3O), 7.3 (2H, d, ArH, J=9Hz), 7.7 (4H, m, ArH), 8.1 (2H, d, ArH, J=9Hz) ppm. No OH signal observed.

i.r. ν_{max} (KBr): 2840, 1675, 1608, 1430, 1295 1185, 1065, 930, 820 cm^{-1}.

(S)-1-Methylheptyl-4-methoxycarbonylphenyl-4-carboxylate

Triphenylphosphine (29.8 g, 0.115 mol) and (*R*)-2-octanol (15.0 g, 0.115 mol) in dry THF (150 ml) were added dropwise, to a stirred mixture of 4-methoxycarbonyloxyphenyl-4-carboxylic acid (22.5 g, 0.115 mol) and diethylazodicarboxylate (20.0 g, 0.115 mol) in dry THF (150 ml) under nitrogen. The reaction was stirred for a further 24 h. at room temperature where TLC indicated that the reaction had gone to completion. The white precipitate was removed by filtration through a pad of Hyflosupercel, the filtrate was washed with brine (50 ml), dried ($MgSO_4$) filtered and the solvent removed under reduced pressure. The resulting white solid was purified by flash chromatography on silica gel eluting with 5% v/v ethyl acetate:petroleum ether (b.p. 40-60°C) to give the desired (*S*)-1-methylheptyl-4-methoxycarbonylphenyl-4-carboxylate, 24.8 g (70%) as a colourless oil. Product purity checked by TLC (silica gel, one spot).

^{1}H n.m.r. δ ($CDCl_3$): 0.9 (3H, t, CH_3), 1.3 (13H, m, CH_2), 4.0 (3H, s, CH_3O), 5.2 (1H, sextet, $C^*\underline{H}(CH_3)$), 7.3 (2H, d, ArH, J=9Hz), 7.7 (4H, m, ArH), 8.1 (2H, d, ArH, J=9Hz) ppm.

i.r. ν_{max} (KBr): 2957, 2871, 1771, 1718, 1440, 1260, 1111, 938, 774 cm^{-1}.

(S)-1-Methylheptyl-4-methoxycarbonylbiphenyl-4-carboxylate

(*S*)-1-Methylheptyl-4-methoxycarbonylphenyl-4-carboxylate was prepared according to the method described previously. Quantities: triphenylphosphine (29.8 g, 0.115 mol); (*R*)-2-octanol (15.0 g, 0.115 mol); 4-methoxycarbonyloxyphenyl-4-carboxylic acid (31.3 g, 0.115 mol) and; diethylazodicarboxylate (20.0 g, 0.115 mol). Work-up of the crude mixture gave the desired (*S*)-1-methylheptyl-4-methoxycarbonylphenyl-4-carboxylate as a colourless oil, 28.3 g (64%).

^{1}H n.m.r. δ ($CDCl_3$): 0.9 (3H, t, CH_3), 1.3 (13H, m, CH_2), 4.0 (3H, s, CH_3O), 5.2 (1H, sextet, C*$\underline{\underline{H}}$($CH_3$), 7.3 (2H, d, ArH, J=9Hz), 7.7 (4H, d ArH, J=9Hz), 8.1 (2H, d, ArH, J=9Hz) ppm.

i.r. ν_{max} (KBr): 2958, 2928, 1766, 1714, 1440, 1260, 1222, 1109, 934, 774 cm^{-1}.

(S)-1-Methylheptyl 4-hydroxybenzoate (**25**)

A solution of (*S*)-1-methylheptyl-4-methoxycarbonylphenyl-4-carboxylate (23.5 g, 0.076 mol) in ethanol (30 ml) was added dropwise, to a stirred mixture of ammonia (120 ml, 35% solution) and ethanol (150 ml) at room temperature. TLC analysis showed complete reaction after a period of 1 h. The ethanol was reduced under reduced pressure and the product extracted into diethyl ether (3 x 100 ml) and the solvent removed to yield a colourless oil, 16.2 g (85%).

^{1}H n.m.r. δ ($CDCl_3$): 0.9 (3H, t, CH_3), 1.3 (13H, m, CH_2), 5.2 (2H, m, C*$\underline{\underline{H}}$($CH_3$) and OH, disappears on D_2O shake), 6.9 (2H, d, ArH, J=9Hz), 7.9 (2H, d, ArH, J=9Hz) ppm.

i.r. ν_{max} (KBr): 2929, 1710, 1592, 1453, 1281, 1165, 1113, 773 cm^{-1}.

(S)-1-Methylheptyl 4'-hydroxybiphenyl-4-carboxylate (**26**)

(*S*)-1-Methylheptyl 4'-hydroxybiphenyl-4-carboxylate (**26**) was prepared according to the method reported previously. Quantities: (*S*)-1-methylheptyl-4-methoxycarbonylphenyl-4-carboxylate (27.8 g, 0.072 mol) and; ammonia (120 ml, 35%

solution) to afford the desired product as a white crystalline solid (**26**), 18.6 g (79%), m.p. 85-87°C.

^{1}H n.m.r. δ ($CDCl_3$): 0.9 (3H, t, CH_3), 1.3 (13H, m, CH_2), 5.2 (2H, m, C*$\underline{\underline{H}}$($CH_3$) and OH, disappears on D_2O shake), 6.9 (2H, d, ArH, J=9Hz), 7.5 (2H, d, ArH, J=9Hz), 7.6 (2H, d, ArH, J=9Hz), 8.1 (2H, d, ArH, J=9Hz) ppm.

i.r. ν_{max} (KBr): 2956, 2847, 1683, 1563, 1354, 1294, 1195, 834, 774 cm^{-1}.

APPENDIX 2: COPY OF ABSTRACT OF PAPER ACCEPTED FOR PUBLICATION TO JOURNALS OF MATERIALS CHEMISTRY

Ferro-, ferri- and antiferro-electric behaviour in a bent-shaped mesogen

Avtar S Matharu,[a*] Chrissie Grover,[a] Lachezar Komitov[b] and Gunnar Andersson[b]

[a]Department of Chemistry and Physics, The Nottingham Trent University, Clifton Lane, Nottingham, England NG11 8NS.

[b]Department of Microelectronics and Nanoscience, Chalmers Institute of Technology, S-412 96, Göteborg, Sweden.

Abstract

The synthesis of a novel bent-shaped, four-ring thiophene-based chiral liquid crystalline ester derived from 5-(4-*n*-decyloxyphenyl)thiophene-2-carboxylic acid and (*S*)-1-methylheptyl 4'-hydroxybiphenyl-4-carboxylate is reported, *i.e.*, (*S*)-4'-(1-methylheptyloxycarbonyl)biphenyl-4-yl 5-(4-*n*-decyloxyphenyl)thiophene-2-carboxylate. Optical microscopy, differential scanning calorimetry, miscibility study, and complimentary electro-optical and current response studies reveal the existence of the SmA*, SmC*ferroelectric, SmC*ferrielectric, SmC*antiferroelectric and SmI*antiferroelectric phase types. Another mesophase type possibly exists below SmI*antiferroelectric which generates a rapid electro-optic response. Comparison with the analogous three-ring compound, *i.e.*, (*S*)-4-(1-methylheptyloxycarbonyl)phenyl 5-(4-*n*-decyloxyphenyl)thiophene-2-carboxylate increases the thermal stability by 95.8°C and the SmI*antiferroelectric phase is observed in addition.

---

[*] Author for correspondence

APPENDIX 3: COPY OF ABSTRACT OF MANUSCRIPT PUBLISHED IN MOLECULAR CRYSTALS AND LIQUID CRYSTALS

Mol. Cryst. Liq. Cryst., 1999, Vol. 332, pp. 303-311
Reprints available directly from the publisher
Photocopying permitted by license only

Printed in Malaysia

Novel Bi- and Ter-Thiophenes Exhibiting Ferri- and Antiferro-Electric Behaviour

AVTAR MATHARU, ROBERT WILSON and CHRISSIE GROVER

Department of Chemistry and Physics, The Nottingham Trent University,
Clifton Lane, Nottingham NG11 8NS. England

Preliminary results of the synthesis and liquid crystalline properties of suitably substituted bi- and ter-thiophene-based chiral esters, derived from the appropriate thiophene-based carboxylic acid and either (*S*)-4-(1-methylheptyloxycarbonyl)phenol or (*S*)-1-methylheptyl-4'-hydroxybiphenyl-4-carboxylate are reported. The bithiophene ester comprising one phenyl ring exhibits monotropic smectic A, smectic C* ferro-, ferri- and antiferro-electric phase types. Increasing the number of rings, either thienyl or phenyl, increases both the melting point and thermal stability. The four ring compounds exhibit enantiotropic smectic A, smectic C* ferro-, ferri- and antiferro-electric phases together with underlying unknown phase type (S_X). The identity of the S_X phase is tentatively assigned as S_I* following free-standing film characterisation and miscibility study.

Keywords: thiophene; bithienyl; terthienyl; ferroelectric; ferrielectric; antiferroelectric

INTRODUCTION

Since the reported occurrence of the ferri- and antiferro-electric phase types in 1989, there has been a rapid upsurge in this area of work primarily because the antiferroelectric phase participates in tristate switching via a